Polyethers

Edwin J. Vandenberg, *Editor*

A symposium sponsored by the

Division of Polymer Chemistry

at the 167th Meeting of the

American Chemical Society,

Los Angeles, Calif.,

April 2, 1974.

ACS SYMPOSIUM SERIES **6**

Polyethers

ACS Symposium Series

Robert F. Gould, *Series Editor*

FOREWORD

The ACS SYMPOSIUM SERIES was founded in 1974 to provide a medium for publishing symposia quickly in book form. The format of the SERIES parallels that of its predecessor, ADVANCES IN CHEMISTRY SERIES, except that in order to save time the papers are not typeset but are reproduced as they are submitted by the authors in camera-ready form. As a further means of saving time, the papers are not edited or reviewed except by the symposium chairman, who becomes editor of the book. Papers published in the ACS SYMPOSIUM SERIES are original contributions not published elsewhere in whole or major part and include reports of research as well as reviews since symposia may embrace both types of presentation.

PREFACE

This book is based largely on the papers presented at a "Polyether" Symposium in honor of Dr. Charles C. Price, Benjamin Franklin Professor of Chemistry at the University of Pennsylvania, on the occasion of his receiving the Creative Invention Award of the American Chemical Society for his pioneering U.S. Patent 2,866,774 on elastomeric polyether urethanes. One of the symposium papers by N. Doddi, W. C. Forsman, and C. C. Price has already been published in *J. Polymer Sci.*, Polym. Phys. Ed. (1974) **12**, 1395. In addition, two papers are included from P. Dreyfuss and T. Saegusa with S. Kobayashi, outstanding polyether researchers who were not able to participate in the symposium.

The Price Award patent covers elastomeric polyurethanes made from the reaction of diisocyanates with the propylene oxide adducts of polyols. These polyether urethanes have proved to be of great commercial value as foamed rubber products, which have contributed greatly to the comfort and well-being of mankind. Approximately 1 billion lbs of these superior foamed products are used each year in the United States, particularly in cushioning for furniture and cars.

In addition to the Award patent, Dr. Charles C. Price has played a broad, pioneering role in the polyether field. In organizing the symposium, the editor sought new contributions on polyethers which generally related to Dr. Price's work which is described in part in his Award address at the beginning of this book.

The editor thanks Dr. Charles C. Price and the other contributors for their outstanding papers and for their cooperation in organizing, presenting, and publishing this symposium.

<div align="right">EDWIN J. VANDENBERG</div>

November 11, 1974
Wilmington, Del.

Polyethers

CHARLES C. PRICE

Department of Chemistry, University of Pennsylvania, Philadelphia, Penn. 19174

A. Introduction

Several inherent characteristics of the ether linkage have
stimulated extensive research and development of linear polymers
with ether links in the polymer backbone (1,2). The ether link-
age has low polarity and low vander Waals interaction character-
istics (ΔH_{vap} = 87.5 cal/g for pentane vs. 83.9 cal/g for diethyl
ether). The carbon-oxygen bond has a lower barrier to rotation
than the carbon-carbon bond (2.7 kc/m for dimethyl ether vs. 3.3
for propane) and thus provides a lower barrier to coiling and
uncoiling of chains. The ether oxygen has an even lower ex-
cluded volume than a methylene group (vander Waals radii of
1.4 Å vs. 2.1 Å) and thus, of all backbone units, has the
smallest "excluded volume". This also is a factor which permits
greater chain flexibility. The carbon-oxygen bond has as great a
bond energy (85 kc/m) as a carbon-carbon bond (82 kc/m) and much
greater hydrolytic resistance than ester, acetal or amide links.
These useful characteristics have, in the past two decades,
led to extensive commercial development and use of a variety of
polyethers. Poly(propylene oxide) has become the basis of the
large scale, world-wide development of "one-shot" polyurethan
foam rubber, for mattresses, furniture, cushions, padding, etc.
Poly(tetrahydrofuran) has been an important component of Corfam
synthetic leather substitute and of elastic fibres. Linear
poly(2,6-xylenol) is made on a large scale as an engineering
plastic with an important combination of properties, such as
high glass transition temperature, good thermal stability, good
electrical properties, excellent adhesion and ready solubility
in common organic solvents. In each of these polyethers, the
ether link is part of the "backbone" of the polymer chain. In
each, the ether linkage makes an important contribution to the
physical properties and chemical stability on which the utility
is based.
Since the chemistry of the generation of polyethers has been
different from that of the classical vinyl polymerization

1

processes, many academic investigators have also been involved
in studying the mechanism, stereochemistry and other aspects of
polyether formation. It is our purpose here to present some of
the results of these studies for those polyether systems in which
we have been particularly interested, the polyepoxides, the
poly(p-phenylene ethers) and the alternating poly(p-phenylene-
methylene ethers).

B. Polyepoxides

Epoxide polymerization can be described in terms of three
different mechanisms; (1) anionic (base-catalyzed), (2) cationic
(acid-catalyzed), and (3) coordinate. The third actually com-
bines features of the first two extremes, since it involves
coordination of the monomer oxygen at a Lewis acid catalyst
site (L), followed by attack on the thus activated monomer by an
alkoxide already bound to the site.
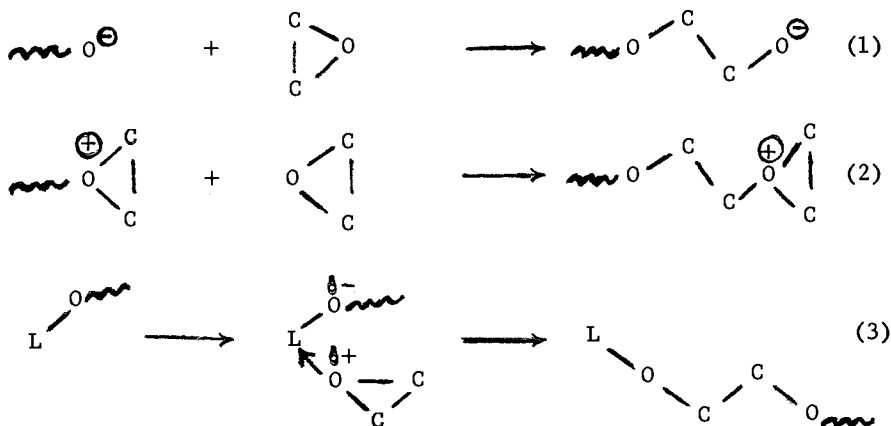
The ring-opening step in each case is a nucleophilic sub-
stitution and, in every case where the stereochemistry has been
established, has been shown to occur with inversion of configu-
ration at the carbon atom undergoing nucleophilic attack (3,4).
The ether-like oxygen in the strained three-membered ring thus
behaves like a good "leaving" group. In the monomer itself, a
strong nucleophile such as alkoxide ion is required for S_N2
attack. However, when the epoxide is converted to an oxonium
state, as in the cationic process, it becomes such a good
"leaving" group that even the weakly nucleophilic oxygen of the
monomer is able to attack effectively.
The characterization of the epoxide oxygen as a good
"leaving" group is supported by the fact that it not only can
undergo S_N2 displacement but E_2 elimination. For example, tetra-

methylethylene oxide, on treatment with a catalytic amount of a
base such as potassium t-butoxide, undergoes "elimination" almost
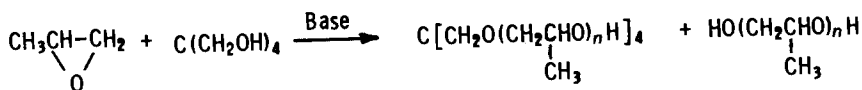quantitatively (5).

(98%)
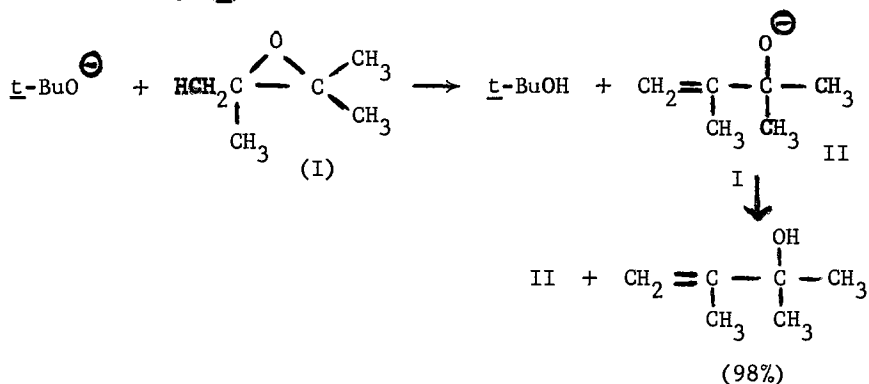
B(1). Anionic. Because of the intervention of the E2
process, only ethylene oxide is readily converted to high-
polymer by base-catalysis. The polymerization can be carried
out so that one polymer molecule forms for each catalyst mole-
cule added (5). With propylene oxide, however, the E2 reaction
intervenes and serves, in effect, as a chain-transfer process.
The alkyloxide ion formed by elimination is, of course, capable
of initiating a new chain, now capped at one-end by an allyl
ether group (6).
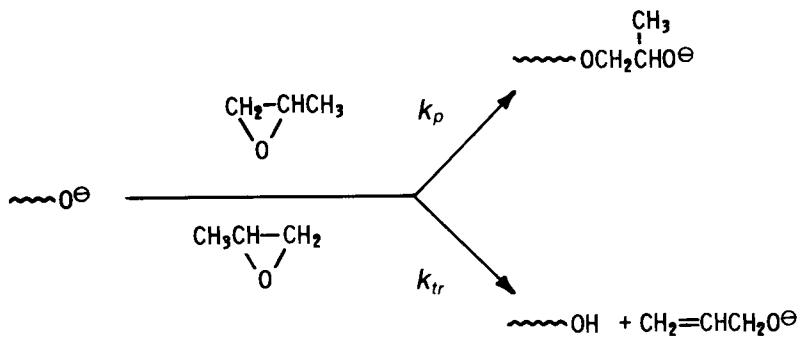
The maximum molecular weight of base-catalyzed propylene oxide
polymer is limited by the ratio of the rates of propagation
(k_p) to transfer (k_{tr}); since at operable temperatures $k_p/k_{tr} \lesssim$
100, this is 6000 awu.
   It was this molecular-weight limiting chain transfer which
led us to seek synthetic approaches to building a crosslinked
rubber structure from poly(propylene oxide) chains. This was
successfully accomplished in 1949 by building branched chain

liquid polymer, followed by conversion into a rubber network
structure by reaction with diisocyanates (7).

$$CH_3\underset{\underset{O}{\diagdown\diagup}}{CH}-CH_2 + C(CH_2OH)_4 \xrightarrow{\text{Base}} C[CH_2O(CH_2\underset{CH_3}{CH}O)_nH]_4 + HO(CH_2\underset{CH_3}{CH}O)_nH$$

The allyl ether end group is preserved only under mild
conditions of polymerization. Studies on its disappearance
under more vigorous conditions led to discovery of the base-
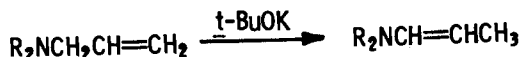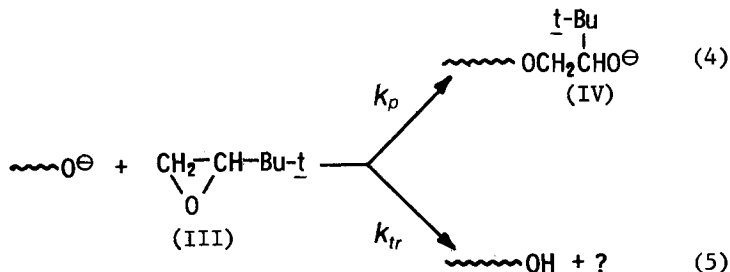catalyzed rearrangement of allyl to cis-propenyl ethers (8,9,10,
11) and postulation of a transition complex involving oxygen-
potassium coordination to explain the cis-stereospecificity.

$$ROCH_2CH{=}CH_2 \xrightarrow{\text{t-BuOK}} \underset{CH{=}CH}{\overset{RO\diagdown \quad \diagup CH_3}{}}$$
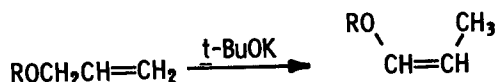
This rearrangement was also found to extend to allyl amines,
although without cis-stereospecificity (12).

$$R_2NCH_2CH{=}CH_2 \xrightarrow{\text{t-BuOK}} R_2NCH{=}CHCH_3$$

t-Butylethylene oxide was studied in the hope that a
structure not permitting E2 elimination to an allyl oxide would
lead to high molecular weight polymer (5). However, the S_N2 dis-
placement is also much slower in this monomer, presumably due to
steric hindrance. Under the more vigorous conditions necessary
for polymerization, another chain transfer process must occur,
although its exact nature has not yet been established. In any
event, the limiting molecular weight for poly(t-butylethylene
oxide) is about 2000.

$$\begin{array}{c}
 \overset{\text{t-Bu}}{\underset{}{\sim\!\!\sim\!\!\sim OCH_2CHO^{\ominus}}} \quad (4) \\
 (IV) \\
{\sim\!\!\sim\!\!\sim O^{\ominus}} + \underset{\underset{O}{\diagdown\diagup}}{CH_2-CH-Bu-\underline{t}} \xrightarrow[\ \ k_{tr}\ \ ]{\ \ k_p\ \ } \\
(III) \\
\sim\!\!\sim\!\!\sim OH + ? \quad (5)
\end{array}$$

It is of interest to note that t-butoxide ion adds to III more
readily than does IV, a neopentyl-type alkoxide (5).

One of the unexpected discoveries in studying base-catalyzed polymerization of III was that, in bulk, it gives a stereoregular, crystalline polymer shown to be different by melting point, X-ray diffraction pattern and solution nmr from the crystalline isotactic polymer. The first guess (13) that it must be syndiotactic was proven to be incorrect and it was shown to be instead regularly alternating isotactic and syndiotactic sequences (abridged to "isosyn") (14). Such a sequence can be explained by a propagation step in which the configuration of the incoming monomer must be opposite to that of the penultimate unit. An hypothesis, illustrated below, was proposed to account for such an unexpected selectivity factor. The main feature of the proposal is the importance of chelation of the ion-paired cation (K^+) with at least the last and next-to-last ether oxygens. The geometry of this chelate is mainly dictated by the requirement that the penultimate t-butyl group be in an equatorial conformation. A few reasonable postulates about the preferred geometry of the transition state (14) then indicate the necessary preference for the configuration of the incoming epoxide to be opposite to that of the penultimate unit.
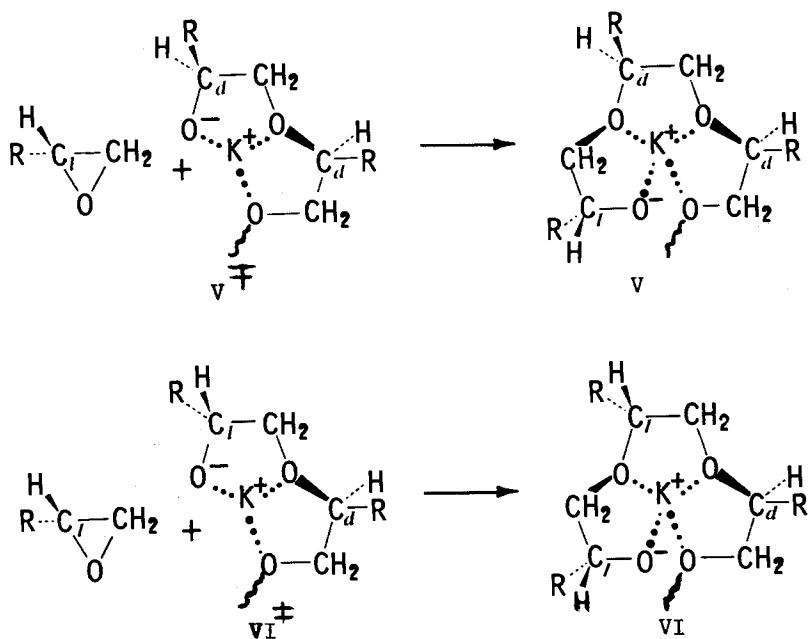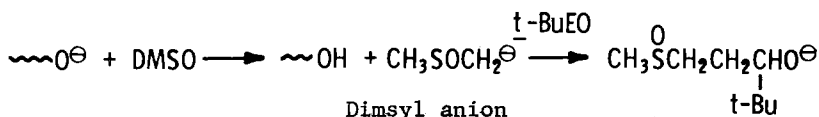

The importance of chelation by K^+ to ether groups in determining the stereoselection is supported by observation on the polymerization of several substituted phenyl glycidyl ethers (14). In this case the stereoselection is for all isotactic

rather than alternating isosyn sequences. This can be accommodated in transition state $V^{\ddagger}$ by the assumption that, in contrast to R = t-Bu, where R prefers to be as far from $K^{\oplus}$ as possible, for R = $ArOCH_2$, the oxygen will seek to coordinate to $K^{\oplus}$ in the transition state. This will require the incoming monomer to have the d-configuration in $V^{\ddagger}$ for R = $ArOCH_2$.

The importance of this particular chelation is supported by the observations that p-methoxy and p-methyl groups increase the yield of crystalline isotactic polymer, while p-chloro or 2,6-dimethyl groups decrease the isotactic fraction (14). The general importance of the chelation in establishing stereochemistry is supported by the observations that addition of dicyclohexyl 18-crown-6 ether in an amount equivalent to catalyst, or of solvents coordinating strongly with K^+, such as dimethylsulfoxide or hexamethylphosphortriamide (HMPT), markedly decrease the crystalline polymer from either t-butylethylene oxide or phenyl glycidyl ether (14).
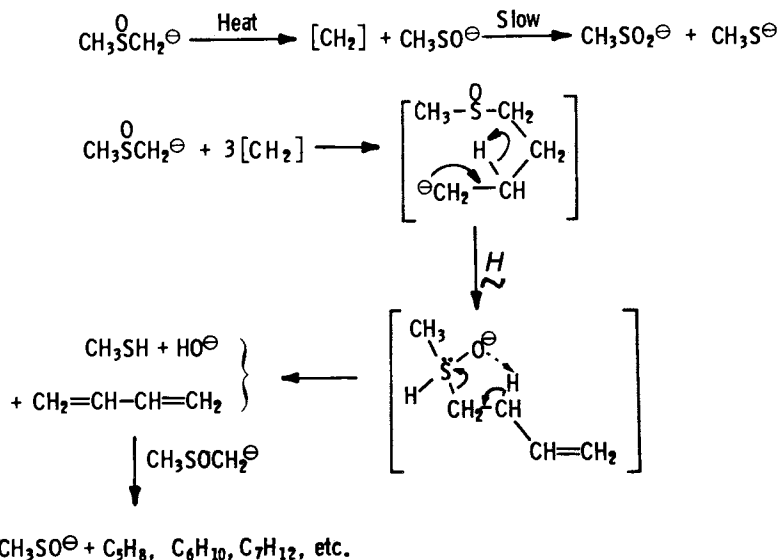
Incidentally, our part in the discovery of the remarkable utility of DMSO as a solvent for base-catalyzed reactions (15,11, 5) was stimulated by our desire to find a solvent suitable for study of base-catalyzed epoxide polymerization under homogeneous conditions. DMSO has one drawback in that it can participate in chain-transfer. This decreases the molecular weight (as compared to comparable conditions in HMPT) and incorporates sulfoxide groups in the polymer from the following transfer process (5).

$$\sim\!\!\sim\!\!O^{\ominus} + DMSO \longrightarrow \ \sim\!\!OH + CH_3SOCH_2^{\ominus} \xrightarrow{t\text{-BuEO}} \overset{O}{\underset{\underset{t\text{-Bu}}{|}}{CH_3\overset{}{S}CH_2CH_2CHO^{\ominus}}}$$

<div align="center">Dimsyl anion</div>

This process then can compete with the unidentified transfer reaction to monomer (reaction (5)).

The use of DMSO also led us to a study of the decomposition of dimsyl ion at elevated temperatures. The identification of methyl mercaptide, methylsulfenate and methylsulfinate ions and a number of methylated butadienes was accounted for by the scheme on the next page.

An interesting and unexpected sidelight of our studies of t-butylethylene oxide arose from the demonstration by Tani (17) that, in the nmr spectrum, the upfield of the three backbone hydrogens in the polymer is the tertiary hydrogen, contrary to normal expectation (13). In isotactic polymer, these three hydrogens appear as double doublets at δ = 3.0, 3.4 and 4.0 ppm. Our assumption that the downfield hydrogen (δ = 4.0 ppm) was the methine (13) was proven incorrect by Tani (17). When he replaced this H by D, it was the upfield absorbance (δ = 3.0) which disappeared, leaving the other two as doublets. A year

$$CH_3\overset{O}{\underset{}{S}}CH_2^{\ominus} \xrightarrow{\text{Heat}} [CH_2] + CH_3SO^{\ominus} \xrightarrow{\text{Slow}} CH_3SO_2^{\ominus} + CH_3S^{\ominus}$$

$$CH_3\overset{O}{\underset{}{S}}CH_2^{\ominus} + 3[CH_2] \longrightarrow \left[\begin{array}{c} CH_3-\overset{O}{\underset{}{S}}-CH_2 \\ H \quad CH_2 \\ {}^{\ominus}CH_2-CH \end{array}\right]$$

$$\Bigg\downarrow \overset{H}{\underset{\sim}{}}$$

$$CH_3SH + HO^{\ominus} \left.\begin{array}{c} \\ \\ \end{array}\right\} \longleftarrow \left[\begin{array}{c} CH_3 \\ S\overset{\ominus}{\underset{}{O}} \\ H \quad CH_2-CH \quad H \\ \qquad CH=CH_2 \end{array}\right]$$
$$+ CH_2{=}CH{-}CH{=}CH_2$$

$$\Bigg\downarrow CH_3SOCH_2^{\ominus}$$

$$CH_3SO^{\ominus} + C_5H_8,\ C_6H_{10}, C_7H_{12},\ \text{etc.}$$

earlier, a similar unexpected upfield nmr shift had been reported for the methylene group in neopentyl methyl ether and neopentyl

$$-\!\!\left(\!CH_2-\overset{R}{\underset{}{C}}H-O\!\right)_{\!n}$$
$$\delta = 3.4,\ 3.0$$
$$4.0$$
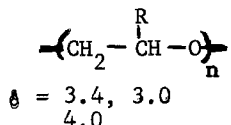
dimethyl amine (18). This led us to the proposal that this "neo-pentyl effect" was due to a preferred conformation of the neo-pentyl methylene hydrogens as far as possible from the lone pairs on oxygen and nitrogen (19). This idea was also shown to explain the downfield chemical shift of methyl ethers, sulfide, selenides, amines, phosphines, arsines, fluoride, chloride and bromide without any "electronegativity" factor but only the very simple postulate that there is no downfield shift of hydrogen by an adjacent lone pair trans to a proton, but by a fixed amount for a lone pair in the skew (or gauche) conformation to the adjacent hydrogen (20).

   B(2). Cationic Polymerization. While alkyl substitutions on the ethylene oxide ring are detrimental to the anionic polymerization process, they are beneficial to the cationic process. Ethylene oxide itself gives only low-molecular weight oils by the usual strong Lewis acid catalysts such as BF_3 or $AlCl_3$. On the other hand, tetramethylethylene oxide, which gives no polymer by base, is readily converted by BF_3 to a solid polymer decomposing

above 300° C and insoluble in all common solvents (21). This
material must be of at least moderately high molecular weight to
exhibit these properties but its insolubility has so far prevented
a molecular weight determination.

The activating effect of electron donor groups, such as
methyl groups, is also shown by the polymerization of cis- and
trans-2-butene oxides. Vandenberg used these monomers to offer
the first proof that the ring opening reaction in cationic polym-
erization proceeded with clean inversion of configuration (22).
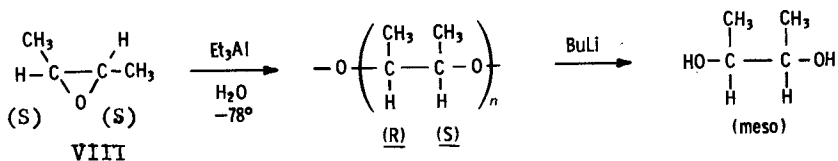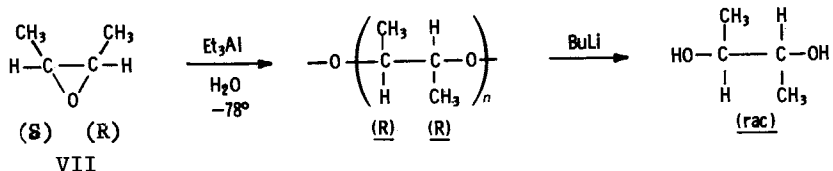
This same stereochemistry for ring opening has been shown
for the case of cis and trans-1,2-dideuterioethylene oxide for
cationic, anionic and coordination polymerization (4,23).

Vandenberg's studies with VII and VIII led to the inter-
esting discovery that, whereas VII gave amorphous polymer, VIII
gave a crystalline polymer, mp ~100°, in 97% yield, even when
rac-VIII was used as starting material. Thus one concludes that
for VII, ring opening of the oxonium intermediate can occur
equally readily at the S-carbon (to give an RR unit) or the R-
carbon (to give an SS unit). In the polymerization of rac-VIII
however, the formation of crystalline polymer must mean that the
reactive oxonium intermediate from an S-unit reacts highly pref-
erentially with S-VIII. This appears to be an excellent example
of "chain end" stereoselection (22). When an S-VIII approaches an
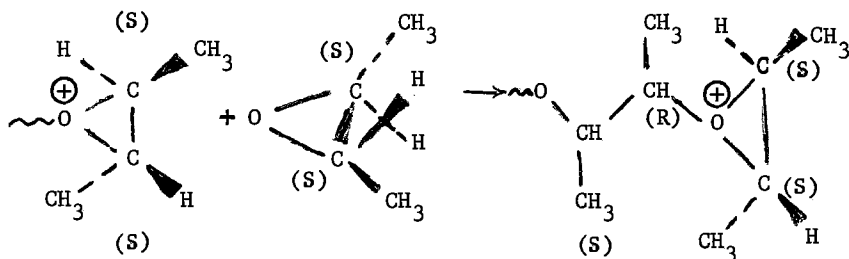
oxonium intermediate derived from S-VIII, as illustrated, with
the two three-membered rings in a favorable right angled orienta-
tion, an H in VIII confronts a methyl in the oxonium ring and
vice versa. If the approaching monomer were R-VIII, then there
would be two highly unfavorable methyl-methyl confrontations.
Thus the stereochemistry of the growing chain end dictates the
stereochemistry of the incoming monomer.

B(3). Coordination Polymerization. Stereoselective polym-
erizations of epoxides have played an important role in devel-
oping the mechanistic concepts for this major development in
polymer chemistry. The first report by Natta of isotactic poly-
propylene (24) appeared a few months before the Pruitt and
Baggett patent issued on the preparation of isotactic poly-
propylene oxide (25). Undoubtedly, the work of Pruitt and Baggett
antedated that of Natta, although it was a year after Natta's
first paper before our work appeared showing that the Pruitt-
Baggett polymer was indeed isotactic (26).
    The chirality (asymmetry) of the methine carbon in propylene
oxide and in its polymer has provided many extra experimental
parameters to use in studies of the mechanism of stereoselective
polymerization by coordination catalysts. The first proposal of
the coordination polymerization scheme to explain stereoselective
α-olefin and olefin oxide polymerization arose from the propylene
oxide studies (26,27).
    There are many effective catalyst systems, such as $FeCl_3$-
propylene oxide, diethylzinc-water and trialkylaluminum-water
acetylacetone reaction products. For none is the exact structure
of the catalyst site established. For all, the number of polymer
molecules formed is small compared to the metal atoms used to
make the catalyst. This suggests that the fraction of metal
atoms at catalyst sites must be at least as small.
    While the detailed structure of a catalyst site remains to
be elucidated, several important features of these catalysts are
now known. Perhaps the most important feature was established
by Tsuruta (28) who proved that the stereoselectivity was not a
feature of the chirality of the growing end but was built into
the catalyst site itself ("catalyst-site" control). The normal
catalyst preparation gives an equal number of R- and S-chiral
catalyst sites which selectively coordinate with R- and S-mono-
mer, respectively. This was demonstrated by starting with 75% R-
and 25% S-monomer. After extensive polymerization, the recovered
monomer was of unchanged optical purity. If the chirality of the
catalyst site were due to the chirality of the growing chain
("chain end" control) one would expect that the growing chains
would assume a 75 to 25 ratio. The preferential reactivity for
R-monomer would then be 9 to 1 (rather than the experimentally
observed 3 to 1) and the recovered monomer should tend toward
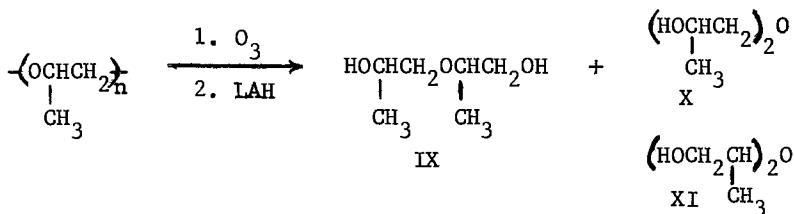a 50:50 mixture with increasing conversion.
    The chirality of the catalyst sites can be influenced in

some cases. For example, Tsuruta (29) has shown that the cata-
lyst made from R-borneol and diethylzinc is stereoelective, i.e.,
it will polymerize RS-propylene oxide giving isotactic polymer
with an excess of R-monomer units and leaving the unreacted
monomer rich in the S-isomer. This behavior can be accounted
for by assuming that R-borneol produces the two chiral catalyst
sites in unequal numbers. A number of other chiral alcohols and
R-monomer failed to give stereoelective catalyst, i.e., they
gave catalyst which behaved as though it had equal numbers of
R- and S-sites (29,30). One possible explanation which has been
offered (31) is that the more hindered bornyl group prevents it
from migrating from the catalyst site L in the propagation step
(reaction (3)). Other simpler groups are known to migrate,
becoming end groups in the polymer (29,32).

    Another effective stereoelective catalyst for both epoxide
and episulfide polymerization is the reaction product of R-(or
S-) t-butylethylene glycol with diethylzinc (33).

    One of the key features of the stereoselective coordination
catalysts for propylene oxide polymerization is that, while they
can give isotactic polymer with a very high ratio of isotactic
to syndiotactic sequences (e.g. > 370) (34), in the same reaction
mixture a large part of the polymer is amorphous. Even when R-
propylene oxide is used as starting material, much of the product
is amorphous polymer of low optical rotation containing many S-
propylene oxide units (30).

    This amorphous polymer has been shown to contain head-to-
head units as the imperfections in structure. This was shown by
degradation and isolation of the dimer glycols (35,36).

$$-\left(OCHCH_2\right)_n \quad \xrightarrow[\text{2. LAH}]{\text{1. } O_3} \quad HOCHCH_2OCHCH_2OH \quad + \quad \begin{array}{c}\left(HOCHCH_2\right)_2O \\ CH_3 \\ X\end{array}$$

$$\begin{array}{ccc} CH_3 && CH_3 \quad CH_3 \\ && IX \end{array} \qquad \begin{array}{c}\left(HOCH_2CH\right)_2O \\ XI \quad CH_3\end{array}$$

    The diprimary (XI) and disecondary (X) dimer glycols will
arise only from head-to-head units in the polymer. Fortunately,
the three isomeric glycols can be separated by glc. For iso-
tactic polymer or amorphous polymer made by base catalysis of
RS-monomer, little if any X and XI were found. The amorphous
polymer separated from isotactic polymer prepared for a variety
of coordination catalysts gave 25 to 40% of X and XI. Further-
more, the correlation of the head-to-head content from such
degradative studies with the optical activity of the amorphous
fraction using R-monomer with the same catalyst shows that for
every head-to-head unit there is one R-monomer converted to an
S-polymer unit. This proves that, at the coordination site

giving amorphous polymer, the abnormal ring opening which occurs at the secondary carbon, to give the head-to-head unit, has done so with inversion of configuration.

A more recent similar study of amorphous polymer accompanying isotactic polymer in the polymerization of RS-t-butylethylene oxide by coordination catalysts has shown that it also contains head-to-head units (14). In this case, the 1^O, 2^O-dimer glycol, which was only 30 to 40% of the dimer mixture, could be separated into its erythro and threo isomers by glc. The isotactic polymer gave, as expected, almost exclusively the erythro-isomer, while the amorphous fractions gave only 40-45% erythro and 55-60% threo.

These data combined indicate that a typical coordination catalyst, such as Et_2Zn-H_2O, contains isotactic catalyst sites and amorphous catalyst sites. The isotactic sites are highly selective in coordinating with either R-(or S-) monomer (reaction (3), step 1) and highly selective in propagating by ring opening only at the primary carbon of the epoxide ring (reaction (3), step 2). The amorphous catalyst site can coordinate equally well with R- or S-monomer in step 1, and has very little preference for attack at the primary or secondary carbon in the ring opening propagation step.

Not much quantitative information is available on the relative reactivities of epoxides in copolymerization. With base in DMSO, phenyl glycidyl ether is 7 times more reactive than propylene oxide, presumably due to the inductive electron-withdrawing effect of the phenoxy group (37). A p-chloro-substituent enhances the reactivity of PGE while a p-methoxy group diminishes it. That coordination catalysts exhibit properties closer to cationic than anionic catalysts is indicated by the opposite influence of p-chloro and p-methoxy groups in PGE, the latter now being the more reactive (38). Furthermore, propylene oxide is 50% more reactive than phenyl glycidyl ether and epichlorohydrin 33% less reactive using Et_3Al-H_2O as a catalyst.

C. Polyphenylene Oxides

The thermal and chemical stability of diphenyl ether has long been recognized as suggesting interesting and useful properties for high polymers built with this structural unit (2). The development of successful methods for preparing such structures has been a challenge to the synthetic chemist. The remarkable chemistry of the processes discovered has also led to significant new facts and hypotheses about the behavior of phenoxy radicals.

The investigations in our laboratory were originally inspired by the work of Hunter and his students (39). They concluded that the amorphous products formed from trihalophenols on treatment with various oxidizing agents were low-molecular weight polymers formed by loss of a halogen atom in either the 2- or 4-

position. We decided to investigate this reaction further, but
with 4-halo-2,6-xylenols as monomers.

        This proved successful when catalysts were used which Cook
(40,41) found useful in converting 2,4,6-tri-t-butylphenol to its
stable blue free radical. Under these conditions, 4-bromo-2,6-
xylenol can be converted to a high-molecular weight polymer in
seconds, liberating the bromine as bromide ion. In the absence
of oxidant catalyst, no bromide ion is liberated even after
months. The polymerization is thus obviously not a nucleophilic
displacement. Furthermore, it has the characteristics of a chain
reaction, since polymer formed even at only 5% conversion is of
high molecular weight (42). While the polymer has a very low
brittle temperature (-150°), its high glass-transition tempera-
ture (> 200°) makes it very hard to crystallize. The polymer is
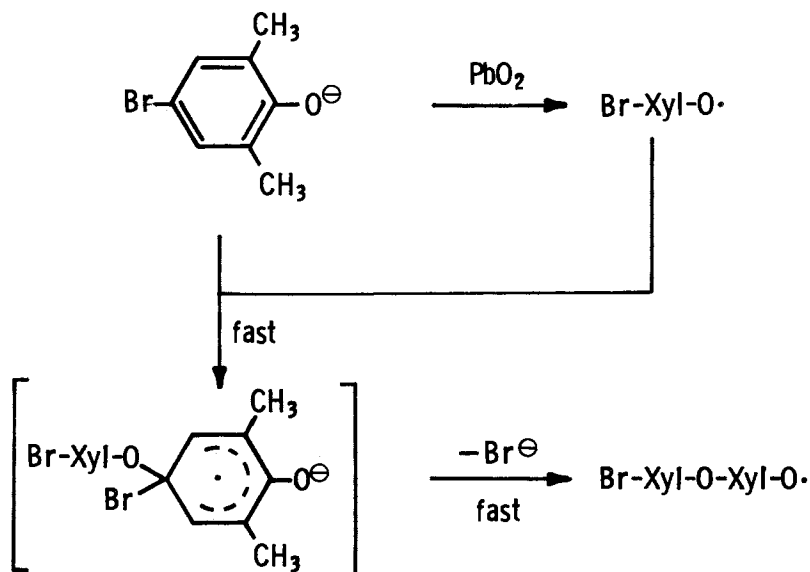
normally amorphous and soluble in the usual organic solvents,
such as benzene. By heating a solution in α-pinene overnight,
it separates as crystalline polymer, mp 275° (43).

        The commercial synthesis of polyxylenol (sometimes referred
to as PPO, poly(phenylene oxide)) is carried out by the oxida-
tive coupling of 2,6-xylenol. This remarkable reaction was dis-
covered by Hay and his coworkers (44). One intriguing feature of
this polymerization is that it is a stepwise condensation. The
product at 50% conversion is a low-molecular weight oil. The
dimer (XIII) and trimer in this material are as easily polymer-
izable as the monomer. The accepted mechanism involves coupling
of aryloxy intermediates to give quinone ketals (45,46,47).

        The Dutch workers in particular studied many simple models
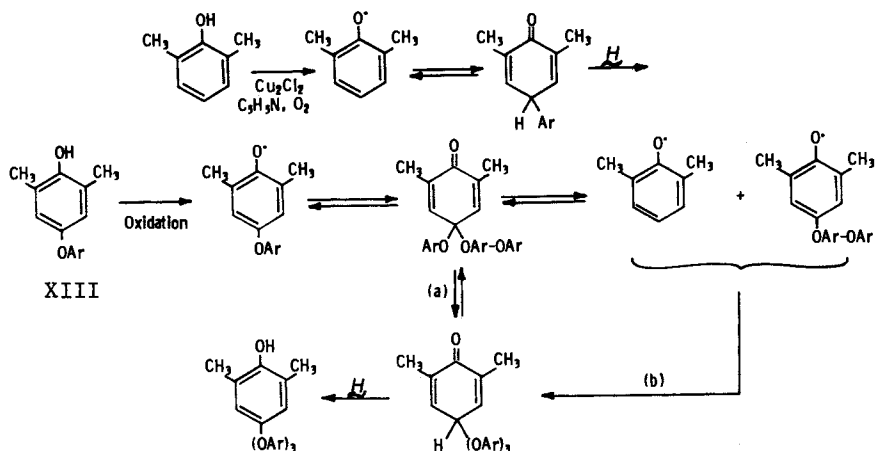
to determine what structural factors and conditions favored con-
version of XIV to XV by direct rearrangement (a) or through dis-
sociation and recombination (b).

One of the intriguing features of the oxidative coupling is
the question of the features dictating C-O coupling to give
dimer XIII vs. C-C coupling to give the diphenoquinone XVI. For
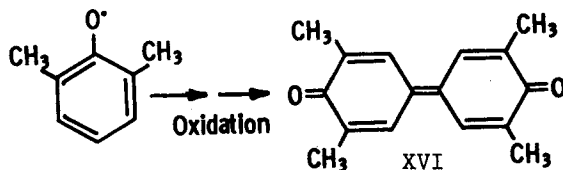
oxidation by Ag_2O (48) or MnO_2 (47), excess oxidant gives poly-
xylenol, while excess xylenol gives XVI. Even under the Hay con-
ditions, replacement of one methyl by t-butyl or both by i-Pr led
to the diphenoquinone as the main product.

The rate of phenol oxidation under the Hay conditions is
first order in catalyst, first order in O_2 pressure and zero
order in phenol, although the magnitude of the rate is quite
sensitive to substitutions in the phenol ring, being favored by
electron-releasing groups (49). We have suggested the scheme on
the next page to account for these observations. The dimer XIII
could arise either by coupling of two free free radicals or by
attack of a radical, liberated in the transformation from B to C
in Scheme I to remove ArO• from D.

Decreased base coordination on Cu (by ligand concentration,
ligand hindrance or ortho hindrance in the phenol) favors C-C
coupling (50). We have proposed the modified Scheme II to ex-
plain this behavior. The essential feature is that decreased
base coordination at Cu increases the affinity of the Cu for the

Scheme I
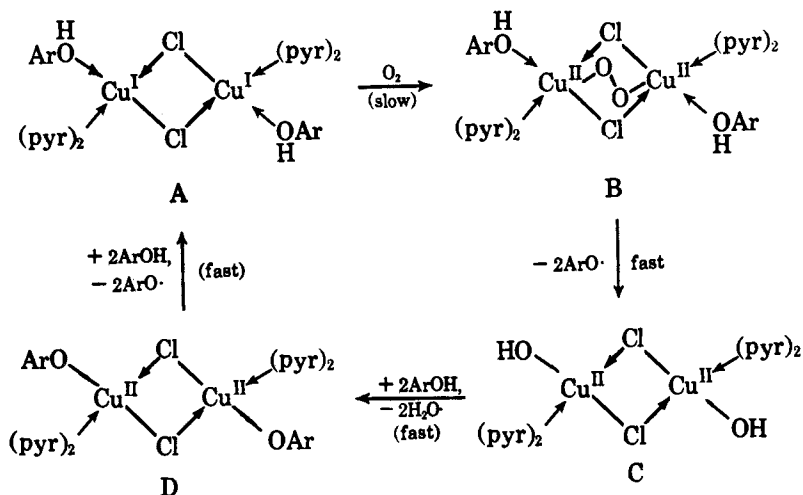
oxygen of the incipient ArO• radical. Since the incipient radical remains bound to Cu at oxygen, it couples at the exposed 4-carbon.

Scheme II

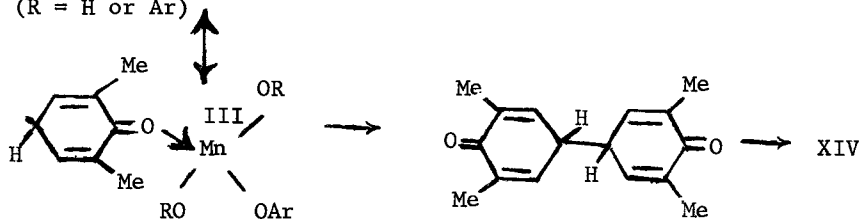2 ArOH (−2H₂O)

D'

+

diphenoquinone
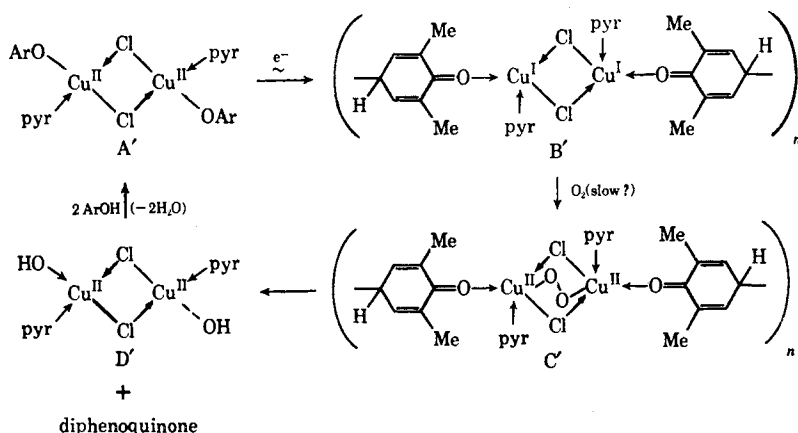
The behavior of Ag$_2$O and freshly-prepared MnO$_2$ can also be fit into this scheme. Using MnO$_2$ as an example, for excess oxidant there might be only one phenol coordinated on manganese (E) while for excess phenol, two (or more) (F).

The manganese in (E), as compared to (F), would be more "neutralized" by hydroxyl groups, would thus be a weaker Lewis
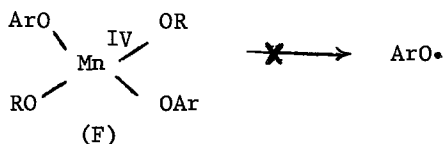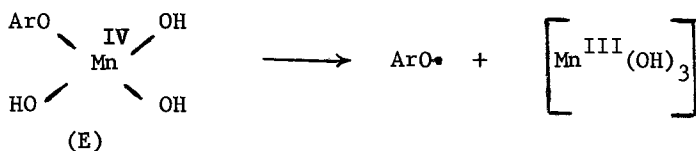
acid and could thus more readily liberate a free aryloxy radical, envisaged as necessary for C-O coupling. In (F), the manganese would be a stronger Lewis acid and, like A', would form a stronger bond to the aryl oxygen, would not liberate the free aryloxy radical and would therefore give C-C coupling.

D. Arylene-Alkylene Copolymers

Dewar has reported that 2,6-dihalo-1,4-diazooxides can be converted by photolysis to poly(2,6-dihalophenylene oxides) (51,52). Dewar has proposed that the role of X = halogen is to promote singlet to triplet interconversion for the intermediate
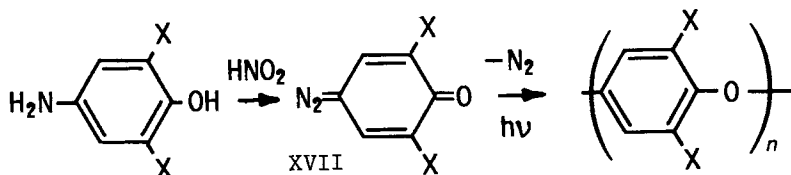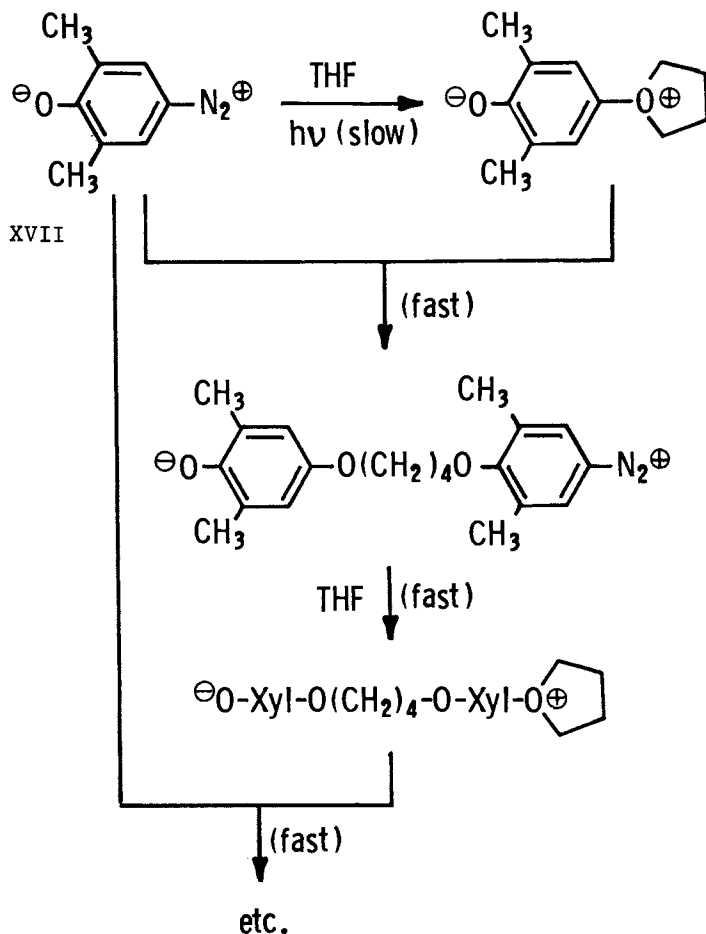

after loss of N_2 (52).

When this reaction was attempted with X = CH_3, no polymer was obtained, unless the reaction was carried out in THF or dioxane. Stille (53) and we (54) discovered concurrently and independently that this polymerization involves incorporation of the cyclic ether solvent.

Scheme III does account for the regular alternating 1:1

Scheme III

polymer obtained. Most of the polymers obtained were low molec-
ular weight, low melting and soluble. Only a small amount (ca.
5%) of high molecular weight crystalline polymer was obtained and
that was deposited as a film on the glass surface of the reac-
tion vessel.

In conclusion, while it is evident that much has been
learned about reactions producing polyethers and important
factors which affect them, there remain intriguing unanswered
questions. While there has been much speculation, it is not
clear that we know in any detail the structural features of
stereoselective and stereoelective coordination catalysts for
epoxide polymerization.

For oxidative coupling of 2,6-xylenol, there has also been much speculation about the nature of the catalyst, but again there is much yet to be learned. In both cases, it seems clear that the central structural questions revolve around the nature of reactive groups coordinated around one or more metal atoms.

In the case of the polymerization of 4-bromo-2,6-xylenol, the free radical chain reaction hypothesis rests on relatively slender evidence. We are in the process of attempting to study the reaction under homogeneous conditions which may provide more substantial evidence for the mechanism involved.

<div align="center">

Literature Cited

</div>

1. National Research Council-Quartermaster Corps Arctic Rubber Conference, Washington, D. C., 30 January-2 February 1949.
2. Quartermaster Corps High Temperature Rubber Conference, Washington, D. C., 3-4 November 1953.
3. Vandenberg, E. J., J. Amer. Chem. Soc. (1961) $\underline{83}$, 3538; J. Polymer Sci. B (1964) $\underline{2}$, 1085.
4. Price, C. C. and Spector, R., J. Amer. Chem. Soc. (1966) $\underline{88}$, 4171.
5. Price, C. C. and Carmelite, D. D., J. Amer. Chem. Soc. (1966) $\underline{88}$, 4039.
6. Price, C. C. and St. Pierre, L. E., J. Amer. Chem. Soc. (1956) $\underline{78}$, 3432.
7. Price, C. C., U. S. Pat. 2,866,744 (30 Dec. 1958); The Chemist (1961) $\underline{38}$, 1.
8. Dege, G. C., Harris, R. L. and MacKenzie, H. S., J. Amer. Chem. Soc. (1959) $\underline{81}$, 3374.
9. Simons, D. M. and Verbanc, J. J., J. Polymer Sci. (1960) $\underline{44}$, 303.
10. Prosser, T. S., J. Amer. Chem. Soc. (1961) $\underline{83}$, 1701.
11. Snyder, W. H. and Price, C. C., J. Amer. Chem. Soc. (1961) $\underline{83}$, 1773.
12. Price, C. C. and Snyder, W. H., Tetrahedron Lett. (1962) 69.
13. Price, C. C. and Fukutani, H., J. Polymer Chem. A-1 (1968) $\underline{6}$, 2653.
14. Price, C. C., Akkapeddi, M. K., deBona, B. T. and Furie, B. C., J. Amer. Chem. Soc. (1972) $\underline{94}$, 3964.
15. Cram, D. J., Richborn, B. and Knox, G. R., J. Amer. Chem. Soc. (1960) $\underline{82}$, 6412.
16. Price, C. C. and Yukuta, Toshio, J. Org. Chem. (1969) $\underline{34}$, 2503.
17. Tani, H. and Oguni, N., Polym. Lett. (1969) $\underline{2}$, 803.
18. Goldberg, S. I., Lam F.-L. and Davis, J. E., J. Org. Chem. (1967) $\underline{32}$, 1648.

19. Price, C. C., Tetrahedron Lett. (1971) 4527.
20. Price, C. C., J. Org. Chem. (1973) 38, 615.
21. Cairns, T. L. and Joyce, R. M., Jr., U. S. Pat, 2,445,912
     (1948); Ishida, S., Bull. Chem. Soc. Japan (1960) 33, 924.
22. Vandenberg, E. J., J. Polymer Sci. (1960) 47, 489.
23. Yokoyama, J. M., Ochi, H., Tadokoro, H. and Price, C. C.,
     Macromolecules (1972) 5, 690.
24. Natta, G., J. Polymer Sci. (1955) 16, 143.
25. Pruitt, M. E. and Baggett, J. M., U. S. Pat. 2,706,182
     (12 April 1955).
26. Price, C. C. and Osgan, M., J. Amer. Chem. Soc. (1956) 78,
     690, 4787.
27. Price, C. C. and Osgan, M., J. Polymer Sci. (1959), 34, 153.
28. Tsuruta, T., Inoue, S., Yoshida, N. and Yokota, Y., Makromol.
     Chem. (1965) 81, 191; see also Tsuruta, T., J. Polymer Sci.
     D (1972) 180.
29. Inoue, S., Tsuruta, T. and Furukawa, J., Makromol. Chem.
     (1962) 53, 215; Inoue, S., Tsuruta, T. and Yoshida, N.,
     Makromol. Chem. (1964) 79, 34.
30. Chu, N. S. and Price, C. C., J. Polymer Sci. A-1 (1963) 1,
     1105.
31. Price, C. C., "The Polyethers", in "The Chemistry of the
     Ether Linkage", Saul Patai, Ed., Interscience, N. Y., N. Y.
     (1967).
32. Ebert, P. E. and Price, C. C., J. Polymer Sci. (1959) 34,
     157.
33. Sepulchre, M., Spassky, N. and Sigwalt, P., Macromolecules
     (1972) 5, 92.
34. Price, C. C. and Tumolo, A. L., J. Polymer Sci. A-1 (1967)
     5, 175.
35. Price, C. C. and Spector, R., J. Amer. Chem. Soc. (1965) 87,
     2069.
36. Price, C. C. and Tumolo, A. L., J. Polymer Sci., A-1 (1967)
     5, 407.
37. Price, C. C., Atarashi, Y. and Yamamoto, R., J. Polymer Sci.
     A-1, (1969) 7, 569.
38. Price, C. C. and Brecker, L., J. Polymer Sci. A-1, (1969) 7,
     575.
39. Hunter, W. H. and Dahlen, M. A., J. Amer. Chem. Soc. (1932)
     54, 2456.
40. Cook, C. D., et al., J. Org. Chem. (1953) 18, 261.
41. Cook, C. D., et al., J. Amer. Chem. Soc. (1956) 78, 2002,
     3797, 4159.
42. Price, C. C. and Staffin, G., Army-Navy-Air Force Elastomer
     Conference, Dayton, Ohio, October 1958; J. Amer. Chem. Soc.
     (1960) 82, 3632; U. S. Pat. 3,382,212 (7 May 1968).
43. Butte, W. A., Price, C. C. and Hughes, R. E., J. Polymer
     Sci. (1962) 61, 528.
44. Hay, A. S., Blanchard, H. S., Endres, G. F. and Eustance, J.
     W., J. Amer. Chem. Soc. (1959) 81, 6335.

45. Cooper, G. D., Blanchard, H. S., Endres, G. F. and
     Finkbeiner, H., J. Amer. Chem. Soc. (1965), 87, 3996.
46. Mijs, W. J., van Lohuizen, O. E., Bussink, J. and Vollbracht
     L., Tetrahedron (1967) 23, 2253.
47. McNelis, E., J. Org. Chem. (1966) 31, 1255.
48. Lindgren, B. O., Acta Chem. Scand. (1960) 14, 1203.
49. Price, C. C. and Nakaoka, K., Macromolecules (1971) 4, 363.
50. Hay, A. S., Fortschr. Hochpolym.-Forsch. (1967) 496.
51. Dewar, M. J. S. and James, A. N., J. Chem. Soc. (1958) 917.
52. Dewar, M. J. S. and Narayanaswami, K., J. Amer. Chem. Soc.,
     (1964), 86, 2422.
53. Stille, J. K., Cassidy, P. and Plummer, L., J. Amer. Chem.
     Soc. (1963) 85, 1318.
54. Kunitake, T. and Price, C. C., J. Amer. Chem. Soc. (1963)
     85, 761.

2

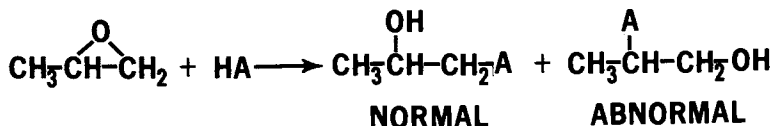# Poly(Propylene Ether) Polyols Prepared With a Zinc Hexacyanocobaltate Complex Catalyst

R. A. LIVIGNI, R. J. HEROLD, O. C. ELMER, and S. L. AGGARWAL

The General Tire and Rubber Co., Research and Development Division, Akron, Ohio 44329
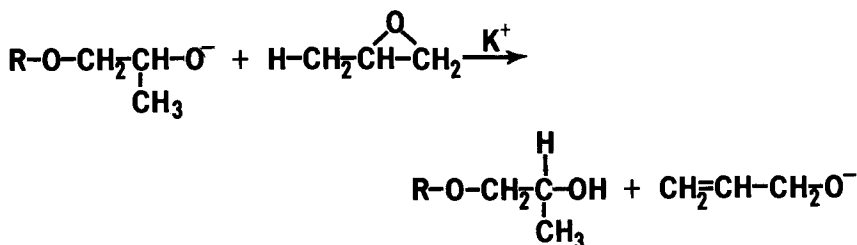
Introduction

A new class of catalysts for the polymerization of 1,2-epoxides was discovered in our laboratories and subsequently patented (1) in 1969. These catalysts consist of complexes containing hexacyanometalate salts. The composition of a typical catalyst can be represented as: $Zn_3[Co(CN)_6]_2 \cdot 2.4(CH_3OCH_2CH_2OCH_3) \cdot 0.85ZnCl_2 \cdot 4.4H_2O$. These complexes are unique as polymerization catalysts for 1,2-epoxides in two respects. First, they are not especially sensitive to the atmosphere and will retain their activity when stored at room temperature in a conventionally capped vial. Second, these catalysts are not only useful for preparing high molecular weight poly(propylene oxide) rubber (2), but they are equally effective when used with certain low molecular weight hydroxyl containing compounds (initiators) to form poly(propylene ether) polyols having good hydroxyl functionality. The latter feature of these catalysts is the topic of this paper.

An unsymmetrically substituted epoxide, such as propylene oxide, can undergo ring opening to give two different products:

$$CH_3\overset{O}{\overset{\frown}{CH-CH_2}} + HA \longrightarrow CH_3\overset{OH}{\underset{|}{CH}}-CH_2A + CH_3\overset{A}{\underset{|}{CH}}-CH_2OH$$

$$\text{NORMAL} \qquad\qquad \text{ABNORMAL}$$

These products have been designated (3) normal and abnormal, with respect to addition of the nucleophile on the unsubstituted or substituted carbon atom of the epoxide. The normal isomer is formed under basic or neutral conditions, via an S_N2 reaction between the nucleophile and the unsubstituted methylenic carbon of the ring. Attack at the unsubstituted carbon atom is favored primarily by steric factors. With more acidic reaction conditions, increasing amounts of the abnormal product are formed, since the substituted carbon atom provides a more stable carbenium ion intermediate.

20

Poly(propylene ether) polyols are important intermediates in the preparation of polyurethane foams and elastomers. They are generally prepared by base catalysis, such as by the use of potassium hydroxide, and consist of almost exclusively the normal product having the secondary hydroxyl group at the terminal unit. St. Pierre and Price (4) found that these polymers contain both allyl and propenyl unsaturation. Dege and coworkers (5) reported that the amount of terminal unsaturation limits the molecular weight of these polymers and decreases their utility in chain extension reactions with diisocyanates. The unsaturation is introduced by a chain transfer reaction to monomer, as suggested by Gee and coworkers (6) and probably occurs at the primary hydrogen of the methyl group (7). A new chain is then formed which contains an allyl ether group at one end.

$$R-O-CH_2\underset{\underset{CH_3}{|}}{CH}-O^- + H-CH_2\overset{\overset{O}{\diagup\diagdown}}{CH}-CH_2 \xrightarrow{K^+}$$

$$R-O-CH_2\underset{\underset{CH_3}{|}}{\overset{\overset{H}{|}}{C}}-OH + CH_2{=}CH-CH_2O^-$$

Some of these terminal allyl groups can undergo rearrangement (8) to propenyl groups in the basic medium.

We have studied, in detail, the formation of poly(propylene ether) diols by the reaction of propylene oxide with 1,5-pentanediol catalyzed by the hexacyanometalate complex: $Zn_3[Co(CN)_6]_2$ $2.4(CH_3OCH_2CH_2OCH_3)0.85$ $ZnCl_2 4.4H_2O$. The hydroxyl type present in the diols, prepared with this catalyst, has been found by Siggia's acetylation method (9) to be almost exclusively secondary, with only 4-10% of the hydroxyls being of the primary type.

Experimental

Kinetic Studies. All chemicals used were rigorously purified. Propylene oxide and 1,5-pentanediol were vacuum distilled from anhydrous calcium sulfate. n-Pentane, n-hexane, and tetrahydrofuran were vacuum distilled from calcium hydride.

The same batch of zinc hexacyanocobaltate (III) complex catalyst was used in all of the kinetic studies. It was prepared by slowly adding a solution of calcium hexacyanocobaltate (III) (6.60 grams) in a mixture of water (48.0 grams) and 1,2-dimethoxyethane (24.0 grams) to a solution of zinc chloride (5.28 grams) in water (6.0 grams). To the resulting combination, a solution containing 1,2-dimethoxyethane (27.5 grams) in water (82.5 grams) was added. The resulting slurry was treated with an aqueous solution containing 25%, 1,2-dimethoxyethane, by weight,

in a Webcell Continuous Dialyzer-Model B, equipped with cello-
phane membranes. Dialysis was discontinued after 16 hours. The
complex was recovered by centrifugation, suspended in dry n-hex-
ane, then collected by vacuum filtration and dried at room temp-
erature under vacuum.

Since the hexacyanometalate complexes can be of variable
composition, it is important to have some means of determining
whether a complex will have sufficient activity in an epoxide
polymerization. This is possible by examining the infrared
absorption spectra (2) of Nujol mulls of these complexes. For
liquid 1,2-dimethoxyethane (glyme), the strong absorption at
851 cm^{-1} has been assigned (10) to the methylenic rocking mode.
In a highly active catalyst consisting of zinc hexacyanocobaltate,
glyme, zinc chloride and water, this absorption is shifted to
838 cm^{-1}, whereas in a catalyst of low activity, the absorption
occurs at 857 cm^{-1}. Kinetic studies in which the poly (propy-
lene ether) diol was prepared directly from the zinc hexacyano-
cobaltate (III) complex catalyst were carried out in capped
bottles under a nitrogen atmosphere. The extent of reaction was
calculated from a measurement of total solids after the propylene
oxide was removed by evaporation. Rate studies on "seeded"
polymerizations were carried out by charging reactants in an all
glass reactor at 10^{-6} Torr, and following the course of the re-
action dilatometrically. Special glass equipment was constructed
for these manipulations, as shown in Figure 1.

Incremental monomer addition studies, bearing on the mechan-
ism of initiation and termination, were done under a nitrogen
atmosphere in bottles. The bottles were fitted with a perforated
cap having a butyl gasket which was extracted using a mixture of
ethanol with 32% by weight of toluene. These polymerizations
were carried out at an initial catalyst concentration of 0.048
weight percent and at 50°C.

Molecular Weight Characterization. Gel permeation chroma-
tography was carried out using a Waters Associates instrument.
Polymers from incremental monomer additions were analyzed in
tetrahydrofuran at room temperature using a 10^6, 10^4, and 10^3 Å
designated column set packed with Styragel. All other polymers
were analyzed in benzene solution. One percent solutions of
polymer were injected for one minute with the instrument operating
at a flow rate of 1 ml/min.

Number-average molecular weights were determined in benzene,
using a Mechrolab Vapor Pressure Osmometer(VPO).

Functionality Determination. Hydroxyl contents were deter-
mined using the phthalic anhydride method and unsaturation was
measured by a methoxymercuration method, both according to ASTM
D2849 (11). Carbonyl contents were obtained using hydroxylamine
hydrochloride, according to S. Siggia (12).

Functionality determinations, using the Williams Plastometer
(13), were carried out on a one gram sample at a force of 5000 ±
5 grams. The polyurethanes were prepared by reacting the poly
(propylene ether) diols with 2,4-tolylene diisocyanate, in the
presence of 0.04% stannous octanoate as a catalyst, for 40 hours
at 120°C. A plug taken from the center of the rubber having a
diameter of 13 mm and weight of one gram was used in the measure-
ment. The Williams plasticity was expressed in mils and taken
as the height of the specimen after a three minute period under
the load specified.

Results and Discussion

Kinetic studies. The rate of formation of poly(propylene
ether) diol using 1,5-pentanediol as an initiator and the zinc
hexacyanocobaltate complex as a catalyst is shown in Figure 2.
The reaction rate curves shown include both a bulk (13.6 mol/l)
monomer polymerization study, as well as a polymerization carried
out in n-pentane (10.7 mol/l). Each of the experimental points
represents a separate run in which the polymerization was termi-
nated at the specified time and residual monomer and solvent re-
moved. The general features of these polymerizations are the
initially slow consumption of monomer extending over three to
four hours followed by the rapid disappearance of monomer to its
total consumption. The catalyst, initially insoluble in either
of the reaction media, is observed to become almost totally dis-
persed when the reaction rate begins to show rapid acceleration.
The solutions, at this time, show only a slight turbidity.
Following the initial slow disappearance of propylene oxide, the
monomer is consumed according to first-order kinetics, as shown
by the straight line plots of log $[M]_0/[M]_t$ versus time, given in
Figure 3.

Gel permeation chromatograms were obtained on the entire
reaction mixture resulting from the polymerization as a function
of the extent of conversion (14) and these are shown in Figure 4.
The peak position at the largest elution volume corresponds to
the lowest molecular weight specie present in the reaction mix-
ture, which is the 1,5-pentanediol. This component is consumed
during the initial stage of the reaction producing a high molecu-
lar weight substance of nearly constant molecular weight. At
23.2% conversion, the gel permeation chromatogram gave no indi-
cation of the presence of 1,5-pentanediol. As discussed above,
there is a rapid increase in the rate of polymerization of the
propylene oxide at 10% to 15% conversion. We attribute the
initially slow rate of polymerization to both the consumption of
the 1,5-pentanediol to form a propylene oxide addition product,
as well as the dispersion of the initially insoluble zinc hexa-
cyanocobaltate complex catalyst. The molecular weight of the
polymer is observed to increase, as noted by the shift of the
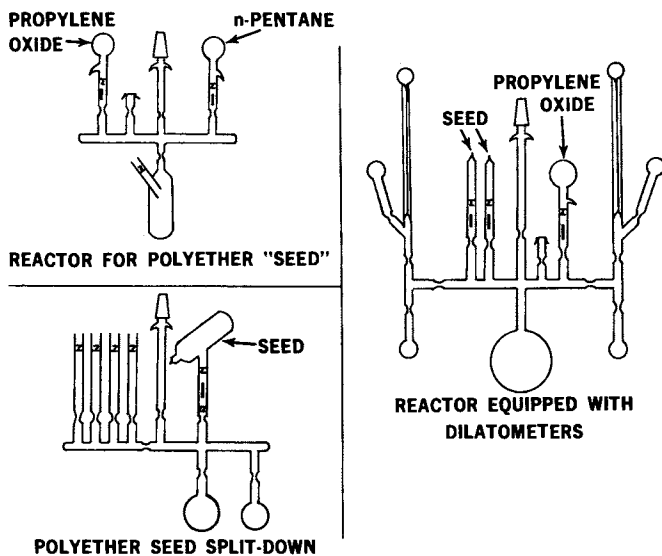peak position towards smaller elution volumes, as the reaction

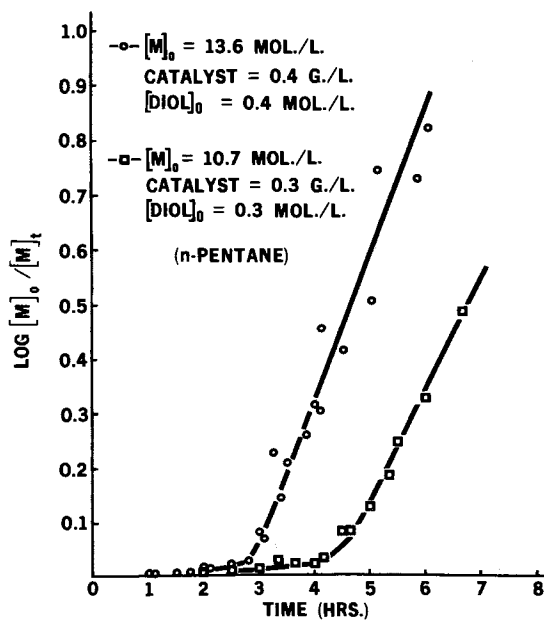Figure 1. Special glass equipment for "seeded" polymerizations

Figure 2. Formation rate of poly(propylene ether) diol in bulk and n-pentane at 50°C
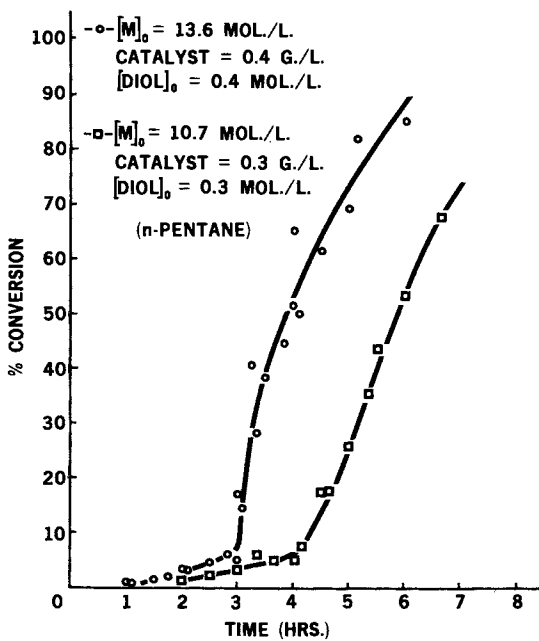
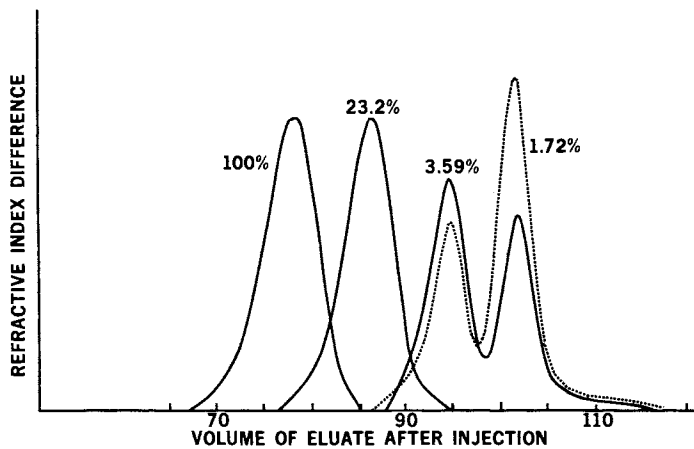*Figure 3.   First-order rate plots for poly(propylene ether) diol formation at 50°C*

Figure 4.   Gel permeation chromatograms of reaction mixture at different extents of polymerization

proceeds. The polymer formed has a narrow molecular weight distribution with some tailing towards the high molecular weight values.

The narrow molecular weight distribution of these poly (propylene ether) diols is similar to that obtained in the so-called "living polymerizations", that is, those proceeding in the absence of a chain termination reaction. The factors which are necessary to produce polymers having a narrow molecular weight distribution have been delineated by Flory (15). These are: (1) chain propagation of each polymer molecule must proceed exclusively by addition of monomers to an active center, (2) all chains must have an equal probability of undergoing growth throughout the course of the reaction, and (3) all chains must be initiated at the beginning of the reaction. Since the poly (propylene ether) diols prepared with the zinc hexacyanocobaltate complex catalyst have a narrow molecular weight distribution, a study was carried out to determine the extent to which the individual steps in this polymerization correspond to the above criteria.

Propylene oxide was polymerized using 1,5-pentanediol as an initiator and zinc hexacyanocobaltate complex as the catalyst. After polymerization was complete, a sample was withdrawn and its number-average molecular weight determined using vapor pressure osmometry. An additional quantity of propylene oxide was added to the system and polymerization of this increment was allowed to go to completion. A sample was once again removed, its number-average molecular weight determined and additional monomer added. This final increment of propylene oxide was polymerized and the number-average molecular weight of the final product determined. The results of this study are given in Table I.

TABLE I
Comparison of Calculated and Measured Molecular Weight of

Poly(Propylene Ether) Diols Prepared by

Sequential Addition of Propylene Oxide

Polymer	$\overline{M}_n$ (Measured by VPO)	$\overline{M}_n$ (Calc.)
From initial polymerization	1690	1783*
From first monomer increment	2350	2209
From second monomer increment	3130	3049

$$*\overline{M}_n = \frac{\text{Weight of Polymer}}{\text{Moles of 1,5-Pentanediol Charged}}$$

The molecular weight of the first sample was calculated from the weight of polymer obtained divided by the moles of 1,5-pentanediol

charged.   The good agreement in the calculated versus measured
molecular weight demonstrates that an insignificant number of
chains result directly from this catalyst, under these conditions.
Indeed, if one calculates the maximum available number of poten-
tial catalyst growth sites, assuming four sites per zinc atom
present, one finds that there are at least 10^2 times more chain
ends per available coordinating site.   This demands that a speci-
fic catalyst site must activate many different chain ends during
polymerization.   Comparing the calculated versus determined
molecular weights of the poly(propylene ether) diol prepared from
the incremental monomer additions, it is concluded that there are
no new polymer chains that are introduced during these polymeri-
zations, either from an initiation reaction or by a chain trans-
fer process with monomer.   Gel permeation chromatograms were
obtained on all three of the poly(propylene ether) diols prepared
in this study and are shown in Figure 5.   A narrow molecular
weight distribution was obtained for all of the polymers with some
tailing towards the high molecular weight region.   As is also
apparent, the increase in the number-average molecular weight
with the polymerization of successive monomer increments is
demonstrated by a shift in the peak position of the chromatograms
towards lower elution volumes.   From these data, it is concluded
that all chains have essentially the same probability of under-
going chain propagation and this polymerization must take place
in the virtual absence of a chain termination reaction.   The
hydroxyl functionality of these poly(propylene ether) diols is
close to the theoretical value of two, as is shown by the values
calculated from the measured hydroxyl number and number-average
molecular weight for the last two polymers; namely, 1.98 $\pm$ 0.2
and 2.10 $\pm$ 0.2, respectively.

Having established that the polymerization of propylene
oxide by the zinc hexacyanocobaltate complex catalyst proceeds
in the absence of a chain termination reaction, it was of interest
to study separately the chain propagation reaction.   A non-termi-
nated polymer "seed" was prepared and its rate of reaction with
propylene oxide was studied.   The results of a series of these
seeded polymerizations carried out at 30°, 40° and 50° are given
in Figure 6, where log $[M]_0/[M]_t$ is plotted against time.
Straight lines are obtained in this plot excepting for an observ-
able increase in the reaction rate in the initial part of the
polymerizations carried out at the two lower temperatures.   It
is concluded from these results that the chain propagation
reaction is first-order in monomer concentration.   An apparent
activation energy of 13.7 $\pm$ 0.8 kcal/mole was calculated for
the chain propagation reaction involving the formation of poly
(propylene ether) diol.   This value compares very well with that
of 14.7 kcal/mole reported by Shigematsu and coworkers (16) for
the sodium hydroxide catalyzed addition of propylene oxide to
isopropyl alcohol.

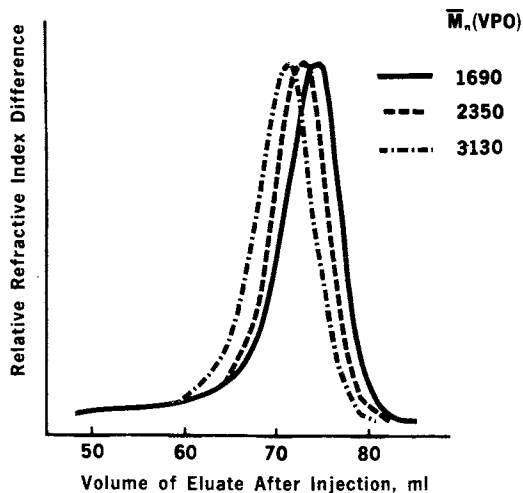The rates of chain propagation of propylene oxide were also

Figure 5.   Gel permeation chromatograms of poly-
(propylene ether) diols prepared by incremental
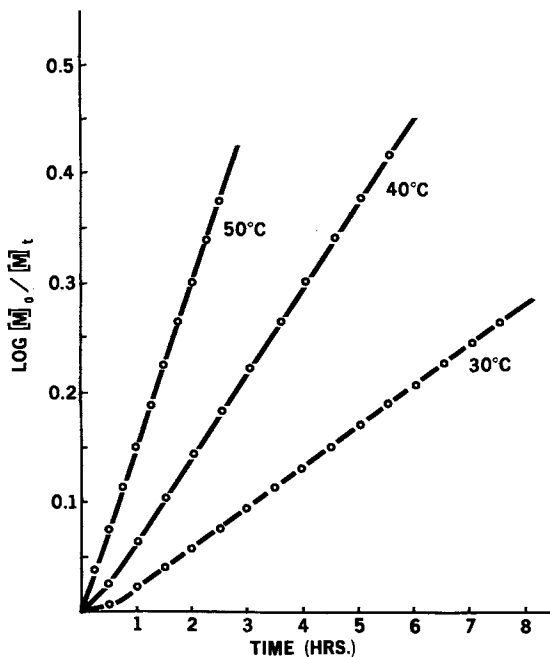monomer addition

Figure 6.   Effect of temperature on propagation rate
during poly(propylene ether) diol formation

measured for the seed, prepared using the zinc hexacyanocobaltate complex catalyst, at two different temperatures in n-hexane and tetrahydrofuran. The results for these polymerizations are given in Figure 7, where log $[M]_o/[M]_t$ is plotted versus time. The results are unexpected in that the rate is faster, at both temperatures, in n-hexane than in tetrahydrofuran. For a typical ionic polymerization, one might expect the opposite result. However, if the solvent could compete with the monomer for coordination sites, this could cause a decrease in the number of active centers growing at any time and result in a decrease in the rate of polymerization. Thus, the slower rate of polymerization in tetrahydrofuran, compared to n-hexane, might be due to the effect caused by coordination of the ether competitively with the monomer, propylene oxide, being more significant than its accelerating the rate of reaction by solvation of the ion pairs.

Functionality Measurements. The approach that was used to characterize the hydroxyl functionality of poly(propylene ether) diols prepared with the zinc hexacyanocobaltate complex catalyst was to compare the equivalents of -OH groups present relative to all other functional groups which might comprise polymer chain ends. The groups which were considered, in addition to -OH, were $>C=C<$ arising from a chain transfer reaction with propylene oxide, and $>C=0$ introduced either by isomerization of propylene oxide followed by an aldol condensation, by chain oxidation, or by the presence of impurities in the monomer (8). A further assumption in this analysis was that there are only two chain ends per chain. Using these assumptions, the number average molecular weight of the polymer was calculated and compared with the fractional amount of this terminal functionality which consists of hydroxyl groups. The number average molecular weight calculated in this manner is in good agreement with values obtained by vapor pressure osmometry, giving validity to this approach. The change in the hydroxyl functionality as the molecular weight of the polymer is increased, calculated in the manner described, is given in Figure 8 for diols prepared experimentally and those available commercially. The abscissa in this plot represents the calculated molecular weight and the ordinate is the hydroxyl functionality calculated from the equivalents of functional groups present. It is observed that there is a much more gradual decrease in the hydroxyl functionality with increasing molecular weight for the polymer prepared with the zinc hexacyanocobaltate complex catalyst than for the commercially available poly(propylene ether) diols, presumably prepared using an alkali metal hydroxide catalyst. For example, at a molecular weight of 3000, 97% of the chain ends are hydroxyl for the diols prepared with the zinc hexacyanocobaltate complex catalyst, whereas only about 90% of the chain ends are hydroxyl in the commercially available diols.

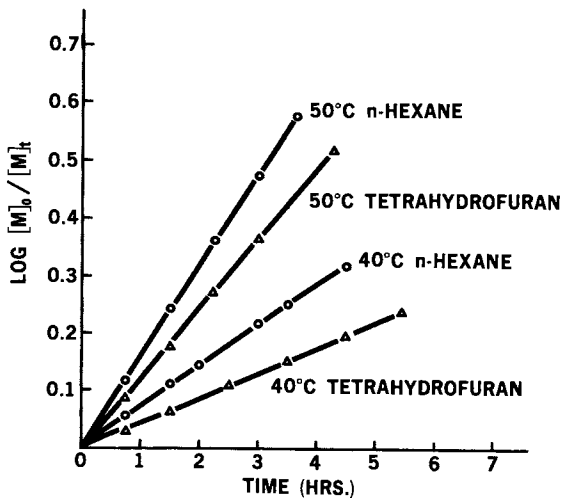Poly(propylene ether) diols are usually chain extended

Figure 7.   Effect of solvent on propagation rate
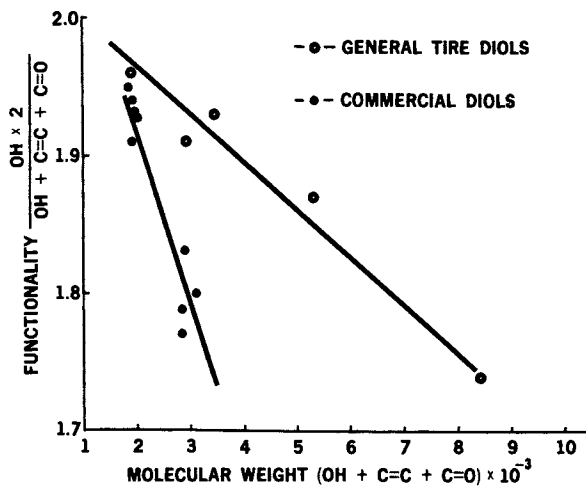during poly(propylene ether) diol formation

Figure 8.   Change in hydroxyl functionality with molec-
ular weight for poly(propylene ether) diols

by reaction with diisocyanates. The polyurethanes resulting from
this reaction were also used to compare the functionality of the
diols prepared with the zinc hexacyanocobaltate complex with
those available commercially. Of course, the extent of reaction
reached, and limitations of measuring reactants, as well as the
functionality will determine the properties of the final product.
Experimental diols were chain extended with 2,4-tolylene diisocya-
nate and the Williams plasticity determined for the resulting
rubbers. Figure 9 shows the plasticity values as a variation
of the 2,4-tolylene diisocyanate equivalents for diols of approxi-
mately 3500 molecular weight. The height of the maxima in this
figure is a relative indication of the functionality of diols of
comparable molecular weight. The Williams plasticity depends
on the molecular weight of the poly(propylene ether) diol (it
governs the amount of polar groups present), as well as the other
factors already mentioned. It can be seen in Figure 9 that the
diols prepared using the zinc hexacyanocobaltate complex have
a higher plasticity, at equivalent molecular weights, than the
commercial diols, again demonstrating the relatively higher
functionality of the experimental diols.

    We have so far been comparing the poly(propylene ether) diols
which result from "KOH catalysis" and the zinc hexacyanocobaltate
complex catalysis with respect to functionality. It is of value
to compare the molecular weight distribution of diols prepared by
these two processes, using the gel permeation chromatograms given
in Figure 10. Generally, the low molecular weight polymers from
both processes have a narrow molecular weight distribution. How-
ever, the molecular weight distribution of the diols prepared with
KOH tail towards the low molecular weight region, whereas those
prepared using the zinc hexacyanocobaltate complex tail towards
the high molecular weight region. As a consequence of this, the
diols prepared with the zinc hexacyanocobaltate complex have a
higher bulk viscosity than the diols prepared with KOH, at the
same number-average molecular weight. The gel permeation chroma-
togram of a diol of molecular weight of 12,000, prepared with the
zinc hexacyanocobaltate complex is given in Figure 10 and demon-
strates the increased breadth in the molecular weight distribu-
tion resulting at higher molecular weights.

    Mechanism. The following scheme is offered to account for
the data presented above. Polymerization probably occurs with
the growing chain coordinated to a zinc atom. The coordination
sites are initially made available by displacement of the 1,2-
dimethoxyethane from the catalyst, either by propylene oxide or
the initiator, 1,5-pentanediol. The 1,5-pentanediol disappears
early in the reaction because of its more acidic nature and
greater ease of coordination than the secondary hydroxyl of the
poly(propylene ether). Coordination of a growing chain would
decrease the free-ion character of the propagating center,
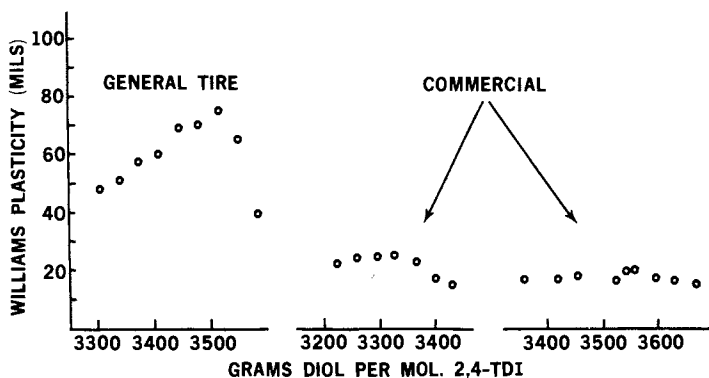compared to catalysis with alkali metal hydroxides. As a result,

Figure 9. *Williams plasticity of polyurethanes prepared from poly-(propylene ether) diols at different ratios of 2,4-tolylene diisocyanate*
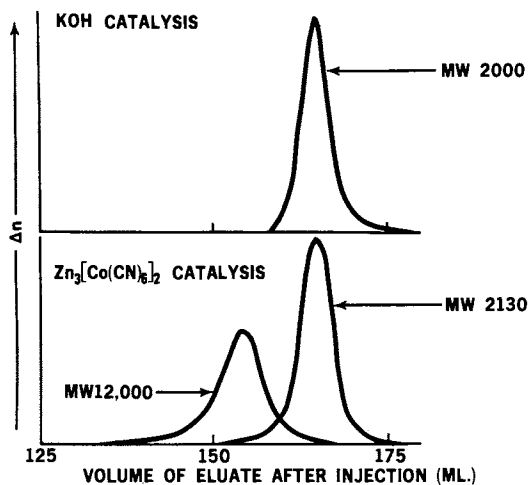

Figure 10. *Gel permeation chromatogram of com-mercial poly(propylene ether) diol and diols pre-pared using zinc hexacyanocobaltate complex catalyst*

chain transfer to propylene oxide should not occur as readily in polymerizations catalyzed with the zinc hexacyanocobaltate complex. This leads to poly(propylene ether) polyols which contain a greater number of terminal hydroxyl groups. Of additional importance is that the zinc hexacyanocobaltate catalyst gives more rapid polymerization rates, therefore, lower polymerization temperatures can be used. This should also reduce the amount of chain transfer to monomer.

Since there are an insufficient number of catalyst sites to be associated with every chain end of the diol and yet the polymers have a narrow molecular weight distribution, a particular catalyst site must activate different chain ends during the course of the reaction. Thus, all chain ends must have approximately the same probability of growth, although only a fraction of chain ends undergo chain propagation at any time during the reaction. This may be represented as follows:

CHAIN PROPAGATION:
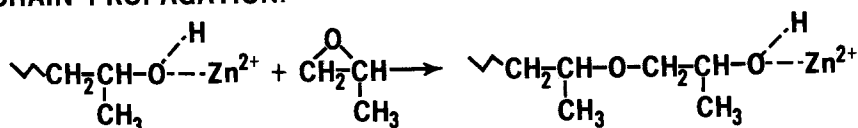
CHAIN ACTIVATION:
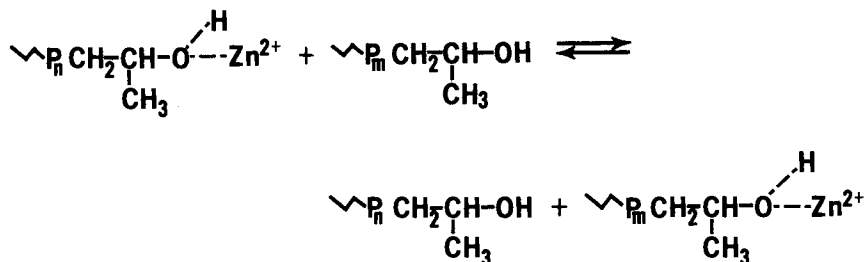
This description is quite similar to that given for the polymerization of ethylene oxide initiated by sodium methoxide in dioxane and methanol, provided by Gee, Higginson and Merrall (17). If the rate of chain end activation proceeded at a very rapid rate relative to chain growth, a narrow, symmetrical distribution would be obtained. If this activation process was very much slower than the rate of monomer addition, a broad distribution would result. In the case of the poly(propylene ether) diols

prepared with the zinc hexacyanocobaltate complex, the rate of chain end activation must be sufficiently different to that of chain growth to give some broadening in the molecular weight distribution. Alternatively, catalyst sites of different activity may be present. If such a mechanism as described above was operating, it would be expected that a more narrow molecular weight distribution could be obtained by: (1) adding monomer slowly to the polymerization, thus increasing the degree of activation of different chain ends prior to chain propagation; and (2) increasing the catalyst concentration, thus increasing the fraction of chains that can undergo growth simultaneously. Partial confirmation of these effects has been obtained for the preparation of poly(propylene ether) triols. The gel permeation chromatograms for such polymers, prepared during conditions where all of the propylene oxide was added initially, and where the propylene oxide is added slowly throughout the polymerization is given in Figure 11. The initiator used in this study was trimethylolpropane. It is apparent that a considerably more narrow molecular weight distribution is obtained for the polymer prepared using slow incremental monomer addition substantiating the mechanism proposed.

Acknowledgment

Summary

Certain complexes of zinc hexacyanocobaltate are effective catalysts in the preparation of poly(propylene ether) polyols from low molecular weight hydroxyl compounds and propylene oxide. The $Zn_3[Co(CN)_6]_2$ 2.4(1,2-dimethoxyethane) 0.85 $ZnCl_2$ 4.4 H_2O catalyzed polymerization of propylene oxide with 1,5-pentanediol was studied. An initially slow rate of polymerization is followed by a rapid rate. The number-average molecular weight of the poly(propylene ether) diol is governed entirely by the weight of the polymer formed and moles of 1,5-pentanediol charged. Using gel permeation chromatography, it was established that the polymer has a narrow molecular weight distribution. The amount of catalyst used in the polymerization is insufficient to have all chain ends growing simultaneously. A mechanism is proposed which involves a catalyst site activating different

ALL P.O. ADDED INITIALLY ------

P.O. ADDED SLOWLY ---------

Δn

MW 7400

MW 6800

125   150   175
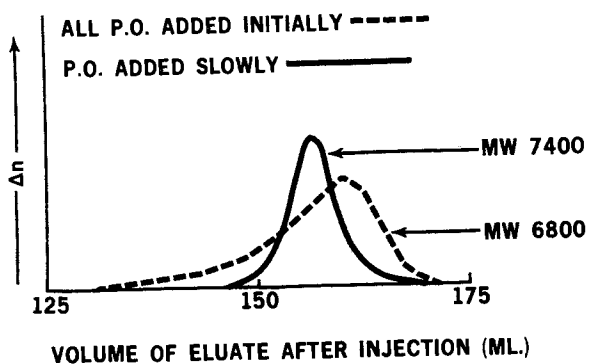
VOLUME OF ELUATE AFTER INJECTION (ML.)

Figure 11.   Effect of monomer addition method on gel permeation chromatogram for poly(propylene ether) triols prepared using zinc hexacyanocobaltate complex catalyst

chains throughout the reaction, giving each an equal chance for growth. The polyols prepared with the zinc hexacyanocobaltate catalyst were found to have better functionality than poly (propylene ether) polyols prepared by conventional methods.

Literature Cited

1. Belner, R. J., Herold, R. J., Milgrom, J., U.S. Patents 3,427,256; 3,427,334; and 3,427,335 to General Tire & Rubber Company (1969).

2. Herold, R. J., Livigni, R. A., Advances in Chemistry Series, Polymerization Kinetics and Technology, Number 128, (1973) 208.

3. Parker, R. E., Isaacs, N. S., Chem. Rev. (1959) 59, 737.

4. St. Pierre, L. E., Price, C. C., J. Am. Chem. Soc. (1956) 78, 3432.

5. Dege, G. J., Harris, R. L., MacKenzie, J. S., J. Am. Chem. Soc., (1959) 81, 3374.

6. Gee, G., Higginson, W. C. E., Taylor, K. J. and Trenholme, H. W., J. Chem. Soc. (1961) 4298.

7. Snyder, W. H., Taylor, K. J., Chu, N. S. and Price, C. C., Trans. N. Y. Acad. of Science Ser. II (1962) 24 (#4) 341.

8. Simons, D. M., Verbanc, J. J., J. Polym. Sci. (1960) 44, 303.

9. Siggia, S., Hanna, J. G., Analy. Chem. (1961) 33, 896.

10. Iwamoto, R., Spectrochim Acta (1971) 27A, 2385.

11. "1973 Annual Book of ASTM Standards", Part 26, p. 888, American Society for Testing and Materials, Philadelphia, Pennsylvania 19103.

12. Siggia, S., "Quantitative Organic Analysis Via Functional Groups", 3rd Edition, 73-75, John Wiley & Sons (1963)

13. "1973 Annual Book of ASTM Standards", Part 28, p. 438 American Society for Testing and Materials, Philadelphia, Pennsylvania 19103.

14. Pavelich, W. A., Livigni, R. A., J. Polym. Sci. (1968) C-21, 215.

15. Flory, P. J., J. Am. Chem. Soc. (1940) <u>62</u>, 1561.

16. Shigematsu, H., Miura, Y. and Ishii, Y., Kogyo Kagaku Zasshi (1962) <u>65</u>, 360. See, for example: Frisch, K. C. ed., "Ring Opening Polymerization", p. 25, Marcel Dekker, N.Y. and London (1969)

17. Gee, G., Higginson, W. C. E. and Merrall, J. Chem. Soc. (1959) 1345.

3

Propylene Oxide Polymers of Varying Stereosequence Distribution

S. L. AGGARWAL and L. F. MARKER

Research and Development Division, The General Tire and Rubber Co., Akron, Ohio 44329

Introduction

In 1956, C. C. Price (1) demonstrated that when l-isomer of propylene oxide is polymerized with potassium hydroxide catalyst, a stereospecific and crystalline polymer is produced. Yet, the racemic monomer polymerized with the same catalyst gave an amorphous product. A ferric chloride catalyst on the other hand produced, from either racemic or optically active monomer, a crystalline high molecular weight fraction having identical crystal structure. These studies demonstrated that long stereoregular sequences having either d or l configuration, necessary for crystallization, can be produced by one catalyst, while another catalyst may lead to amorphous polymers, which may have only short stereoregular sequences of a particular configuration.

Poly(propylene oxide) was unique among stereospecific polymers developed up to that time. The monomer has an optical center which, under appropriate synthesis conditions, can be preserved in the polymer so that d or l forms could be identified at each asymmetric carbon atom. Examination of the crystal structure of isotactic poly(propylene oxide) (2) shows that it crystallizes in a helical form and that the crystals can accommodate only the helices of one optical form and are therefore optically active.

A number of catalyst systems have been developed (3,4,5) which result in propylene oxide polymers of different stereosequence distribution. In the following, we review some of our work on the characterization of stereosequence length in propylene oxide polymers prepared with different catalysts, and more importantly, studies on the effect of the differences in stereosequence length on the crystallization behavior and mechanical properties of the polymers.

Description of Stereosequence Distribution

As in other polymeric systems, both head-to-head and

38

head-to-tail arrangements of consecutive monomer units have been
identified in poly(propylene oxide (6). These arrangements can
be detected by chemical means and have important effects in modi-
fying the crystallization behavior of the polymer (6,7). Another
structural feature that may affect crystallization behavior is
that, for a given configuration (d or l) of the repeating unit in
the isotactic stereoregular polymer chain, two distinct chains
structures are possible depending upon the relative positions of
the oxygen and the asymmetric carbon. These may be designated as
up and down chain structure for each of the d and l configuration
of the isotactic polymer chain. They are superimposable by
turning the polymer chain end-over-end (8). We recognize such
complications as above in the crystallization of stereoregular
poly(propylene oxide). The main interest of our studies, how-
ever, has been in the stereosequence distribution in propylene
oxide polymers prepared with different catalyst systems and the
effect of stereosequence distribution on the properties of these
polymers.

The simplest statistical model which has sufficient gener-
ality to represent the sequence distribution in poly(propylene
oxide) is one in which the configuration of the last three mono-
mer units in the growing chain determine the configuration of
the next unit coming onto the chain. The configuration of the
triad of successive units may take on eight possible arrange-
ments as listed in Table I below. Recent studies have shown that
several types of such triads may be distinguished from ^{1}H and
carbon-13 NMR spectra (9,10,11). We have adopted a shorthand
notation of representing by + the case when two successive units
have the same configuration, and by - when they have opposite
configurations. Triads E_1 are referred to as isotactic, triads
E_4 as syndiotactic, and E_2 and E_3 as heterotactic. The A and B
triads in a polymer made from a racemic monomer cannot be dis-
tinguished from each other by any physical method, and equal pop-
ulations, in any case, of the corresponding A and B triads may
be assumed. Thus, the number of possible triad states of inter-
est in a model for analyzing stereosequence distribution reduces
to four.

TABLE I

Configuration Triads of Three Successive Units

E_1
A) d d d ⎫
B) l l l ⎬ ++

E_2
A) d d l ⎫
B) l l d ⎬ +-

E_3
A) d l l ⎫
B) l d d ⎬ -+

E_4
A) d l d ⎫
B) l d l ⎬ --

We, along with others (12,13,14), have considered a model by
which the stereosequence distribution, i.e., distribution of
triad sequences along the polymer chain, is described as a Markov
chain process (15). Addition of a new repeating unit to a parti-
cular triad leads to a new triad consisting of the last two units
plus the unit added. The transition probabilities associated
with the various possibilities that can thus arise from the four
triads can be defined and are given in Table II.

<div align="center">

TABLE II

Transition Probabilities

FOUR PARAMETER MODEL

</div>

STATE OF CHAIN END	STATE AFTER ADDING MONOMER →			
	E_1	E_2	E_3	E_4
	← TRANSITION PROBABILITIES →			
E_1 : ++ (ddd, lll)	a_1	$(1-a_1)$	0	0
E_2 : +— (ddl, lld)	0	0	a_2	$(1-a_2)$
E_3 : —+ (dll, ldd)	a_3	$(1-a_3)$	0	0
E_4 : —— (dld, ldl)	0	0	a_4	$(1-a_4)$

The above model predicts that the population of state E_2 is
equal to that of the state E_3. Also, the populations of the
triad states depend upon only two parameters: $(1-\alpha_1)/\alpha_3$ and
$(1-\alpha_2)/\alpha_4$. Thus, it would not be possible to determine the four
parameters: $\alpha_1,....\alpha_4$, needed to fully describe the stereose-
quence distribution, from the population of the triad states as
determined, for instance, by NMR. In order to fully character-
ize all the four parameters, one would need populations of
tetrads. No suitable method has evolved to be able to do this.
However, if one is concerned only, as we were, with the
ability of polypropylene oxide to crystallize (16) then since

polypropylene oxide crystallizes only in the isotactic form, we
can restrict our attention to isotactic sequences (i.e., se-
quences of + units). The probability, $P^+(\xi)$, that a given se-
quence of +'s is exactly of length ξ, is given by the equation:

$$P^+(\xi) = P_1 \alpha_1^{(\xi-2)} (1-\alpha_1)^2$$

In this equation, P_1 is the probability that any triad taken at
random be in the configuration ++ and α_1 is the probability that
this triad is followed by a + unit. Thus, the probability $P^+(\xi)$
is based only on two parameters, P_1 and α_1. Qualitatively, we
can associate the equilibrium crystallinity with the concentra-
tion P_1, and the maximum melting point of the polymer with the
probability of forming long sequences which depends on α_1.

Characterization of Sequence Distribution

A number of recent papers describe the use of high resolu-
tion NMR spectroscopy in identifying stereosequence distribution
in polypropylene oxide (9-11,17-20). Using α-deuterated poly-
propylene oxide and 220 HMz NMR, Oguni et al (19) have shown that
the shift in methylene absorbtion can be used to identify the
structures assigned to tail-to-tail linkages and to isotactic and
syndiotactic triads. They showed that the crystalline fraction
of polymer prepared with a diethyl-zinc-water catalyst system did
not contain a measurable amount of tail-to-tail linkages.

Carbon-13 NMR can potentially give more information about
triad distribution. Several workers (10,11,18,20) have made use
of this technique. The three methine peaks observed in the NMR
spectra have been assigned to syndiotactic, isotactic and hetero-
tactic triads. Although theoretically ddl and dll triads should
be non-equivalent, only a single type of heterotactic traid peak
has been found. Since the information obtained from diad and
traid distributions are mutually consistent, we consider only
the existence of only a single heterotactic species.

In our studies (16), we have made use of melting point and
crystallinity as a function of temperature of polypropylene
fractions to obtain the parameters for the statistical model and
for calculation of the average length of isotactic sequences.
Polypropylene oxide prepared by three catalyst systems were
studied. The crystalline fractions were those that were insol-
uble in either acetone at -20°C or in isopropyl alcohol at 25°C.
The melting point and the change in percent crystallinity as a
function of temperature were studied by carefully annealing the
polymer and then measuring dilatometrically the change in density
with temperature. Our calculations, of average isotactic se-
quence length and average length of uncrystallizable sequences
from these data were based on Flory's theory for the crystalli-
zation and fusion of copolymers (21). The details and equations

used for these calculations have been described previously (16).
It is doubtful whether the conditions of Flory's theory are ade-
quately fulfilled but the theory is qualitatively successful in
that (a) its prediction of the shape of crystallization curves is
in good agreement with experiment and (b) the results for similar
polymers are in good agreement with the NMR results of Schaefer
(10,11).

In Table III are given the melting point, the percent crys-
tallinity at room temperature and the average length of crystal-
lizable isotactic sequences and of uncrystallizable sequences,
for the fractions of poly(propylene oxide) prepared with the four
catalyst systems. It should be noted that, even though the aver-
age isotactic sequence length of Sample C and D is about the same,
there is an appreciable difference in percent crystallinity (or
average length of uncrystallizable sequences). Also Sample A has
a much lower degree of crystallinity than would be predicted from
its melting point as compared to that of a sample of very high
crystallinity. Such features as these in the crystalline frac-
tions of polypropylene oxide were the reasons for us to adopt a
probability model requiring that the configuration of the on-
coming unit is governed by the configuration of the previous
three units (4 parameter model) rather than by the configuration
of the last one or two units as has been found to be satisfactory
for other systems, e.g., polymethylmethacrylate (14).

The Effect of Stereosequence Length on Morphology and Crystalli-
zation Kinetics

The effect of stereosequence distribution on crystallization
kinetics is dramatic. We have previously reported our studies on
the important effects of stereosequence length on crystallization
kinetics and morphology of propylene oxide polymers (22). Here
we summarize the main conclusions of this study, so that results
on the time-temperature dependence of mechanical response may be
fully appreciated in the light of these conclusions.

When slowly cooled from the melt, the crystalline fractions
of propylene oxide polymers crystallize in a spherulitic growth
habit. At low degrees of supercooling, rather large spherulites
can be grown. The texture of spherulites grown at the same
degree of supercooling is quite sensitive to the stereosequence
distribution of the polymer. In Figure 1, we show photomicro-
graphs of spherulites of two different poly(propylene oxide)
samples, one of which (Sample A) has long stereosequence length
and the other one (Sample C) has short stereosequence length.
Both spherulites were grown under isothermal conditions and at
the same degree of supercooling. The spherulites grown from
Sample A have a more dense structure and a greater frequency of
fibrillar branching than do spherulites grown from Sample C.
This behavior is in accord with the mechanism of spherulite
growth proposed by Keith and Padden (23) according to which

TABLE III

Melting Temperature, Percent Crystallinity and Stereosequence
Length of Crystalline Fractions of Propylene
Oxide Polymers From Different Catalysts

Homopolymer Sample	Catalyst	% Crystallinity	Melt. Temp. °C	Transition Probability α_1	P1 Probability of ++ States	Average Length	
						Isotactic Sequence	Uncrystallizable Sequence
A	Ferric chloride	49	75	0.992	0.710	122	120
B	$Zn(C_2H_5)2 \cdot 2\text{-}H_2O\text{-}$ cyclohexylamine	34	68	---	---	---	---
C	$Zn(C_2H_5)_2\text{-}H_2O\text{-}$ propylamine	34	68	0.93	0.447	14	28
D	$Zn(C_2H_5)_2\text{-}H_2O$	15	66	0.92	0.196	12.5	70

growth occurs by diffusion of impurities or of material of low tacticity away from the site of crystal growth.

The rate at which these spherulites grow is also affected by tacticity. Measurements were made of the isothermal rate of spherulitic growth on a hot stage of a microscope. For this purpose, a sequence camera was used to photograph automatically the growing spherulites during crystallization. Dilatometric measurements were also made on these polymers in order to determine the rate of isothermal crystallization from the melt. The fraction of the polymer which had crystallized at any time was calculated from the measured density and the known values of the density of crystalline and amorphous poly(propylene oxide) (8,2, 4).

The isothermal dilatometric growth rate data were fitted to the equation predicted by the Avrami theory (25,26,27):

$$1-(X/X_\infty) = \exp. [-(t/\tau_c)^n] \qquad (1)$$

where X is the percent crystallinity at time t, X_∞ is the percent crystallinity at infinite time, and τ_c is a parameter with the dimensions of time, which is a measure of the rate of crystallization. For no value of n could the experimental values be made to fit this equation. The crystallization isotherms could be fitted, however, by making the following assumptions:

1. That the Avrami theory can be written in the form:

$$\ln(1-X/X_\infty) = -(t/\tau_c)^3 [F(t/\tau_n)]/[(1/3!)(t/\tau_n)^3] \qquad (2)$$

where τ_n is the time constant for the nucleation process and

$$F(t/\tau_n) = e^{-t/\tau_n} - 1 + t/\tau_n - (1/2)(t/\tau_n)^2 + (1/3!)(t/\tau_n)^3 \qquad (3)$$

These equations imply that the sperulites are initiated from predetermined nuclei at a rate comparable to the rate of crystallization. This assumption is confirmed by our microscopical measurements.

2. That the Avrami equation in the form of Equation (2) gives the volume fraction occupied by spherulites rather than the percent crystallinity.

We assume that crystallization takes place behind the growing spherulitic boundary at a rate such that the degree of crystallinity in any region is a function, $\Phi(t')$, of the time elapsed after the spherulite front has passed through that region.

Under these conditions, we may write the equation for the the percent crystallinity with time as:

$$(X/X_\infty) = \int_0^t \Phi(t, \tau) \left\{ dV(\tau)/d\tau \right\} d\tau \qquad (4)$$

Here $V(\tau)$, the value of which is given by the Avrami equation, is the volume fraction of the initial melt included in spherulites at time $\underline{t}$; and $\Phi(t, \tau)$ is the percent crystallinity at time τ. There is ample evidence that crystallization in a spherulite continues long after its boundary is formed. Kovacs (28) has shown that there is a slow secondary crystallization in polyethylene which continues to very long times. Tung and Buckser (29) have been able to fit the tail end of the dilatometric curve for the crystallization of polyethylene by assuming that this secondary crystallization has the form of an exponential decay. Stein and his coworkers (30) have observed that even after spherulites have occupied the total volume of the sample, there is a continuing change in the intensity of x-ray scattering.

The crystallization isotherms can then be fitted by assuming that $\Phi(t, \tau)$ can be written in the simple form.

$$\Phi(t, \tau) = 1 - a \exp\left[-(t-\tau)/\tau_s\right]$$

where $\underline{a}$ represents the fraction of crystallization which occurs slowly and τ_s, is the time constant for this secondary crystallization process. In Table IV, we have summarized the results of the crystallization kinetic measurements on poly(propylene oxide) of different stereoregularity. These results lead to the following conclusions.

TABLE IV

Effect of Stereoregularity on Crystallization Kinetics of Propylene Oxide Polymers

Catalyst	Cryst Temp, °C	ΔT °C	Primary Crystallization τ_n min	τ_c min	Spherulitic Growth Rate G (cm/min)	Secondary Crystallization A	τ_s/τ_c
FeCl$_3$	45	30	3.5	12.6	8.2	0.26	1.7
	50	25	15	40.2	4.5	0.26	1.7
	55	20	130	170	0.82	0.26	1.7
Zn(CH$_2$H$_5$)$_2$- H$_2$O Isopropylamine	38	30	10	19	6.0	0.26	7.6
	43	25	22	40	2.5	0.26	7.6
	48	20	70	92	0.90	0.26	7.6

The primary crystallization process is characterized by three parameters. These are the rate of radial growth of the spherulite, $\underline{G}$, the time constant for nucleation, τ_n, and the time constant for the primary crystallization process, τ_c, which is determined from the Avrami equation. All three parameters seem to be dependent on the stereoregularity of the polymer, although the nucleation rate seems to be most strongly dependent.

A more important effect of stereoregularity is found from consideration of the secondary crystallization process. This process is characterized by two parameters. These are: $\underline{a}$, the fraction of the crystallizable material involved in the secondary crystallization process, and τ_s, the time constant for this process. The noteworthy result is that the ratio (τ_s/τ_c) is almost independent of temperature, but very sensitive to the stereoregularity of the polymer. The secondary crystallization process is slower for polymers having short stereosequence lengths than for those having longer stereosequence lengths, even though the primary crystallization process is only slightly affected by stereoregularity.

Mechanical Properties of Vulcanizates of Copolymers of Propylene Oxide

The ability to crystallize has an important effect on the mechanical behavior of rubber vulcanizates. If the rubber has some crystallinity present initially, the crystals act as additional crosslinks in the system resulting in increased stiffness. On the other hand, crystallization induced by strain leads to stress relaxation and increased strength of the vulcanizates.

In order to be able to form crosslinked networks of propylene oxide polymers, a series of copolymers was prepared using allyl glycidal ether as a comonomer. These copolymers were fractionated into stereoregular and amorphous fractions by cooling of acetone or isopropyl alcohol solutions. The density of the soluble fractions was found to vary linearly with the comonomer content. It was assumed that the soluble fractions were completely amorphous and that the deviation of the density of the insoluble fractions from linearity was a measure of their percent crystallinity. The percent crystallinity, X_c, was calculated by assuming that the crystalline portions contained only propylene oxide units, and have the density of crystalline poly-(propylene oxide). In Table V are given the mole percent of comonomer, the density, the calculated value of X_c and the glass transition temperature for the stereoregular (insoluble) fraction of copolymers of propylene oxide made with different catalysts. The designations $\underline{A}$, $\underline{B}$, $\underline{C}$, and $\underline{D}$ represent the catalyst systems which correspond to the ones used for the homopolymers in Table III and are in the order of decreasing stereo-directing influence. The values of X_c increase with the stereo-directing influence of the catalyst. The subscripts 1, 2 in sample codes

in Table V refer to the different comonomer content in the co-
polymers made using the same catalyst system. The glass transi-
tion temperature of the copolymers, as well as that of the cor-
responding homopolymers, was measured using a coated electro-
magnetically driven vibrating reed apparatus (31). Almost all
the soluble (amorphous) fractions had a Tg of about -57°C., the
same as that of the homopolymers with a small average stereo-
sequence length. The Tg of the insoluble fractions given in
Table V varied in the same order as the value of X_c. The gen-
eral effect of the comonomer, however, was to lower the Tg
values.

The copolymers listed in Table V were cured in the form of
0.01" thick films. The cured polymer was cut into strips one
inch wide, and these strips were used for subsequent testing. No
direct measurement was made of the crosslink density of these
polymers, but a relative value could be inferred from Mooney-
Rivlin plots of the stress-strain data.

The following is the summary of the results of the studies
(31) on the effect of stereoregularity on stress-induced crystal-
lization and mechanical properties of the vulcanizates of pro-
pylene oxide copolymers. In the studies on stress-induced cry-
stallization, stress (σ) and birefringence (Δ) were measured as
a function of temperature using an Instron tester fitted with a
thermostatted insulated chamber and an optical system. In an
amorphous rubber, the quantity ($T \cdot \Delta/\sigma$) (where T is absolute tem-
perature) is almost constant. Stress-induced crystallization
leads to the formation of crystals oriented in the stretching
direction which substantially increase the birefringence.

1. Samples, such as D_2, which have short isotactic sequences and
    high comonomer content, display ideal elastomer behavior, in
    that the ratio of birefringence to stress is almost indepen-
    dent of temperature and the stress at constant elongation is
    proportional to absolute temperature. All other samples
    have some critical temperature (e.g., 50°C for Sample A_1)
    above which the vulcanizates behave as an ideal elastomer.
    This suggests that Sample D_2 does not crystallize in either
    the stressed or unstressed state.

2. In a vulcanizate with long isotactic sequences (e.g., A_1) in
    which there is a measurable degree of crystallinity at room
    temperature, the effective crosslink density as determined by
    modulus is largely due to the presence of the crystalline re-
    gions. Such a sample, when stretched 200% and then heated
    slowly, shows a continuous decrease in stress as shown in
    Figure 2, falling almost to one-tenth of its value on heating
    to 100°C. The birefringence change on heating, also shown in
    Figure 2, is somewhat complicated. The birefringence in-
    creases with temperature up to 55°C., then falls off rapidly,
    approaching a constant value at about 75°C. A qualitative

TABLE V

Stereoregular (Insoluble) Fractions of Copolymers of
Propylene Oxide and Allyl Glycidal Ether

Sample Designation	Mole Percent Comonomer	Method of Separation	Wt. Percent Insoluble	Properties of Insoluble Fractions		
				Density, (gm/cc)	Percent Crystallinity	Tg, °C
A_1	1.6	Acetone, 0°C	--	--------	--	-51.3
A_2	3.2	Acetone, 0°C Isopropanol, 0°C	59 74	1.0370 1.0290	32 24	-50.7 -52.2
B_1	2.0	Acetone, -20°C	49	(1.0440)	--	-59.8
B_2	8.6	Isopropanol, -20°C	70	1.0192	5	-58.0
C_1	3.0	Acetone, -20°C	29	1.0126	7	-58.3
C_2	10.0	Isopropanol, -20°C	60	1.0213	6	-58.0
D_1	4.0	Isopropanol, -20°C	20	1.0060	0	-57.0
D_2	7.5	Isopropanol, -20°C	73	1.0112	0	-57.0
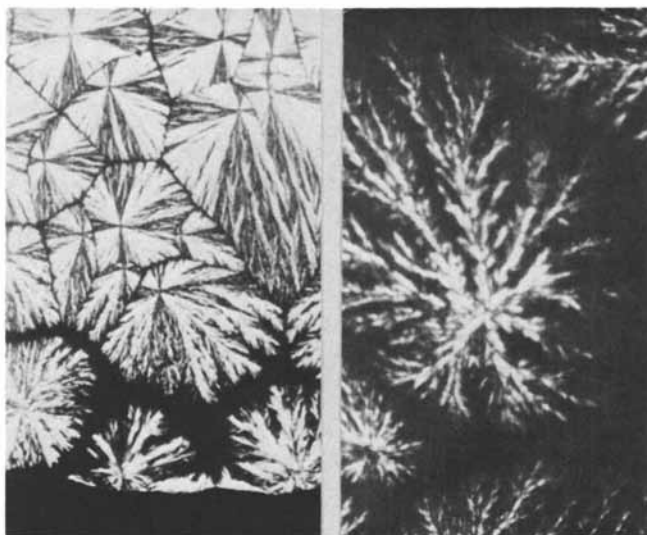
Figure 1.   Effect of stereoregularity on texture of propylene oxide polymers at same degree of supercooling $\Delta T = 30°C$. Sample A (left) with long stereosequence length. Sample C (right) with short stereosequence length.
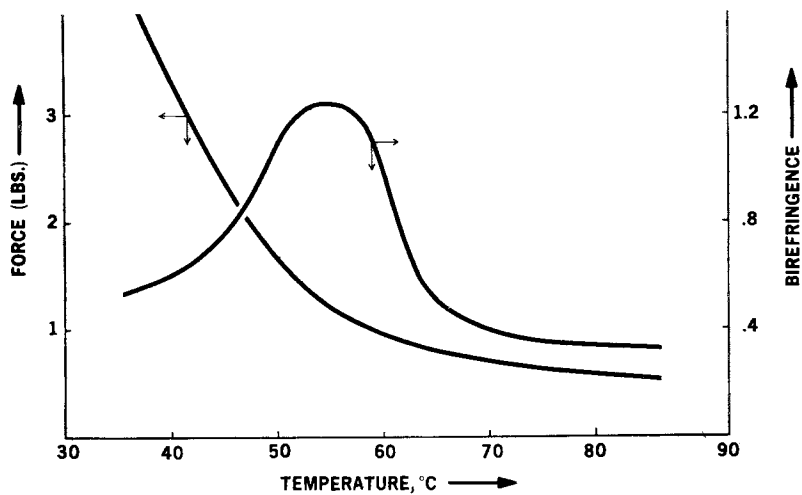
Figure 2.   Force and birefringence changes on heating Sample A_1 from room temperature, after elongating 200%

explanation of this behavior is that as the temperature is raised, unoriented crystalline material present at room temperature starts to melt and is replaced by oriented crystalline material which has a higher melting point and higher birefringence than the unoriented polymer.

3. In some samples, further crystallization occurs on stretching. In Figure 3 are shown the stress optical coefficient [ratio (Δ/σ) of the birefringence Δ and stress σ] as a function of temperature, for three of the samples. These samples were stretched 200%, heated to 100°C and then cooled slowly from this temperature to below -20°C. Measurements of stress and birefringence were made simultaneously in this temperature interval. The stress optical coefficient would be invariant with temperature, if no crystallization occurred such was found to be the case for Sample D, up to -30°C. However, Sample A_1 starts crystallizing at about 50°C and the crystallization is complete by 0°C. Sample B_1 starts crystallizing at about 30°C and the process is not complete until about -30°C. Sample C_1 does not crystallize above 0°C and shows only a slight tendency to crystallize even below this temperature.

4. At room temperature, when stretched 200% and allowed to relax, there is greater change in stress optical coefficient for Sample B_1 than for Sample A_1, even though Sample B_1 has a considerably lower degree of crystallinity. The Sample A_1 with the high degree of crystallinity in the unstressed state at room temperature, allows for little additional stress-induced crystallization. The Sample B_1 with intermediate length of isotactic sequences shows small crystallinity in the unstressed state at room temperature but shows pronounced stress-induced crystallization. The rate of stress-induced crystallization is very much enhanced at high elongations and at lower temperature.

5. Dynamic modulus measurements were made over the temperature range of -50°C to 80°C, and the frequency range of 0.02 to 15 cycles/sec. There was very little dependence of this property on frequency except at temperatures close to the transition temperature of the corresponding homopolymers. This is shown in Figures 4 and 5 which are plots of the frequency dependence of real and imaginary moduli respectively for Sample A_2 at temperatures between -30 and 65°C. This copolymer has a long isotactic stereosequence length and only 3% of comonomer and shows the greatest temperature dependence of dynamic properties of all the copolymers studied. A Williams-Landell-Ferry (WLF) type of time-temperature superposition (32) could be made only by using an unreasonably large shift factor.
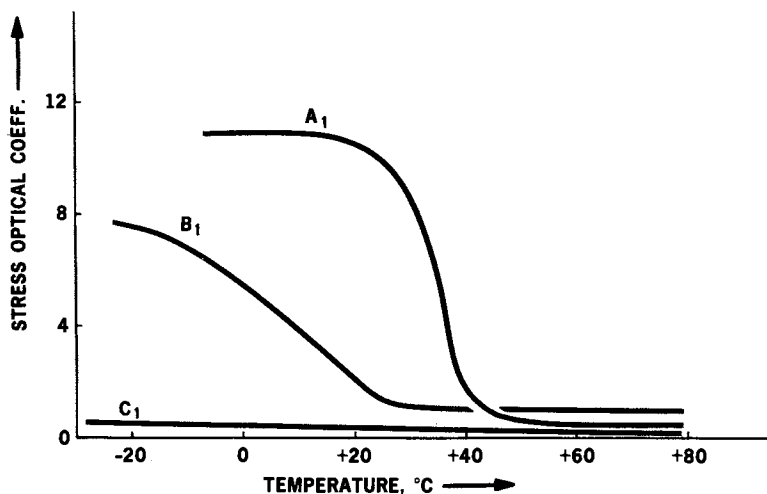
Figure 3. Change in stress optical coefficient of copolymers on cooling from 100°C
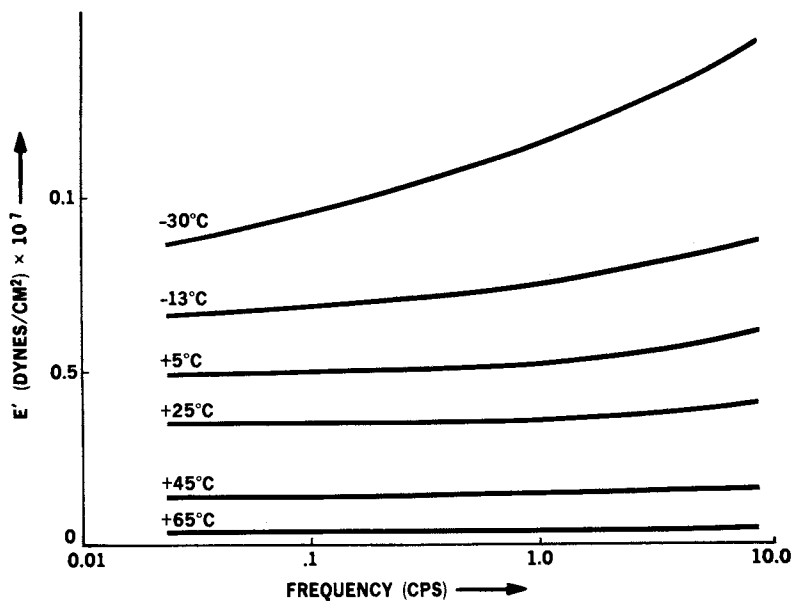

Figure 4. Real component of dynamic modulus vs. frequency for propylene oxide copolymer A₂

Since the temperature dependence of the modulus is much greater than the frequency dependence, it is somewhat more instructive to plot the dynamic modulus at constant frequency as a function of temperature. In Figure 6, we compare the moduli at 0.1 Hz for two copolymers with long stereosequences, but which differ in their comonomer content; copolymer A_1 contains 1.6 mole percent, and copolymer A_2, 3.2 mole percent of comonomer. The moduli are corrected to 80°C by multiplying by the factor $T°(K)/353$, which assumes that the kinetic theory of rubber elasticity is obeyed. The difference in modulus at elevated temperatures reflects the difference in crosslink density. Sample A_2 has the higher comonomer content and hence the higher degree of cure. At lower temperatures, however, A_1 has the higher modulus because of the greater degree of crystallinity. The break in the curve at about 60°C corresponds to the melting of the crystalline portions of the polymer.

In Figure 7, we compare the dynamic moduli at 0.1 cps of a series of copolymers containing 2-4 mole percent of the comonomer and in Figure 8 for the copolymers containing 7-10 mole percent of the comonomer. In these plots, the moduli are corrected to 80°C by multiplying by the factor $T°(K)/353$, which assumes that the kinetic theory of rubber elasticity is obeyed.

The polymers A_2, B_1, C_1 and D_1 are in the order of decreasing stereosequence length. The degree of crystallinity, as indicated by the change in modulus on melting, is in the same order as that determined from the density of the same polymers. The temperature at which crystallinity disappears, as indicated by the break in the curve, decreases with decreasing stereoregularity in the copolymers. This temperature is about 65°C for Sample A_2, 50°C for B_1, about 10°C for C_1 and there is no evidence of crystallinity in copolymer Sample D_1.

For Sample C_1 and D_1 (copolymers that have short isotactic sequences and have 2-4 percent comonomer) and for all the copolymers that have 7-10 mole percent comonomer, the temperature compensated dynamic moduli are almost invariant with temperature. The copolymer with long isotactic sequences (Sample A_2) on the other hand has sigmoidal curve of dynamic modulus versus temperature. The curve for Sample B_1 is similar to that of the Sample A_2, even though on the basis of the comparatively short isotactic sequences in the corresponding homopolymer, we expected its dynamic modulus also to be insensitive to temperature. It seems that this fraction of the polymer had sufficiently long stereosequences and a smaller concentration of the comonomer, which resulted in the observed dynamic modulus versus temperature behavior. In general, the low temperature dynamic modulus (above Tg) at comparable comonomer content is higher, the greater is the stereoregularity, i.e., the content of isotactic triads, in the polymer.
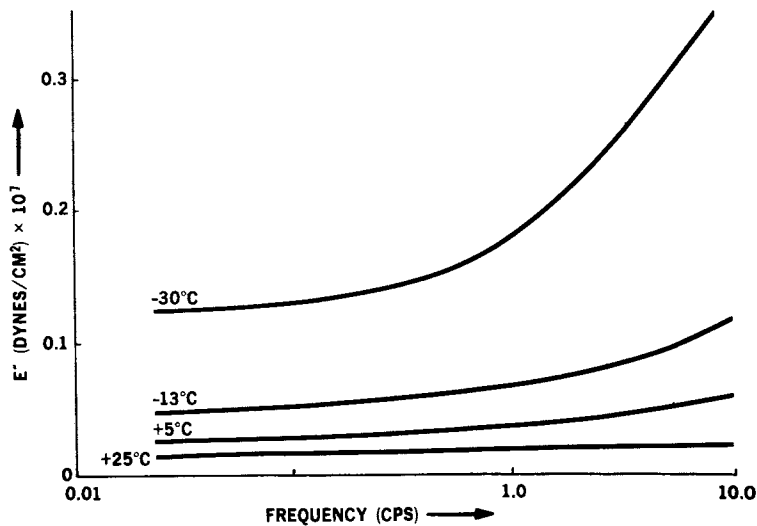
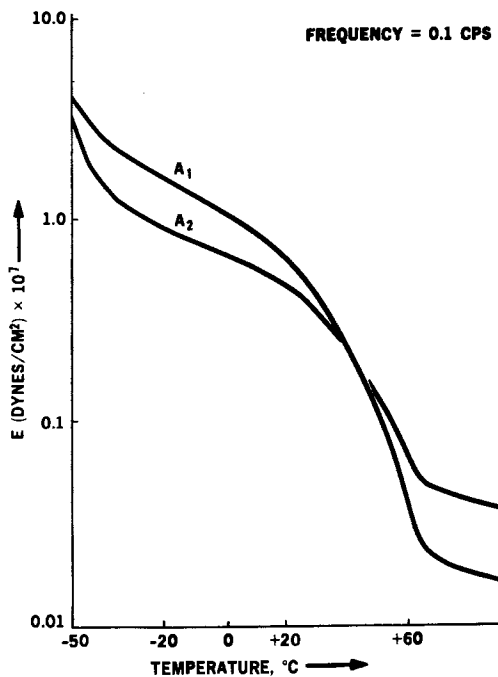Figure 5. *Imaginary component of dynamic modulus* vs. *frequency for propylene oxide copolymer A₂*

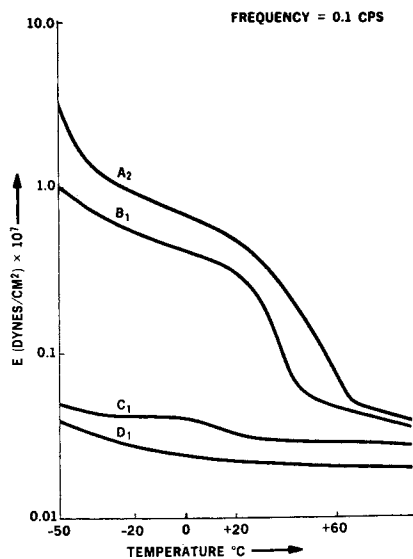Figure 6. *Dynamic modulus* vs. *temperature for propylene oxide copolymers A₁ and A₂*

FREQUENCY = 0.1 CPS

Figure 7. Dynamic modulus vs. tempera-
ture of propylene oxide copolymers. Co-
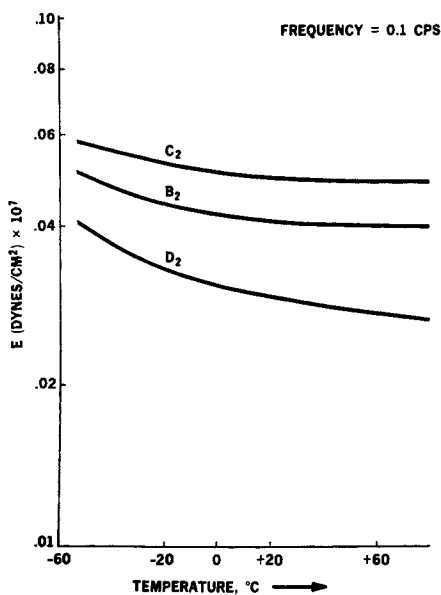monomer 2–4 mole %. Modulus values
corrected to 80°C.

FREQUENCY = 0.1 CPS

Figure 8. Dynamic modulus vs. tempera-
ture of propylene oxide copolymers. Co-
monomer 7–10 mole %. Modulus values
corrected to 80°C.

Summary

1. Stereosequence length of isotactic units in poly(propylene oxide) is determined by the catalyst system used. The stereosequence length of isotactic units in stereoregular poly(propylene oxide) polymers may be characterized from their melting point and degree of crystallinity. The stereosequence length of isotactic units in poly(propylene oxide) from ferric chloride catalyst is considerably longer than those from other catalyst systems such as diethyl zinc-water and diethyl zinc-water-isopropylamine.

2. An important effect of stereosequence length of isotactic units is on crystallization kinetics and morphology of poly(propylene oxide). The spherulites grown from a polymer with long stereosequences have a more dense structure and a greater frequency of fibrillar branching than do the spherulites grown from the polymer that has short stereosequence length. The crystallization kinetic data show that crystallization continues by a secondary crystallization process long after spherulites completely occupy the available volume in the polymer. The ratio of the rate of the secondary crystallization process to that of the primary crystallization process is almost independent of temperature but increases with increasing stereoregularity of the polymer.

3. The mechanical properties of propylene oxide rubbers (copolymers of propylene oxide and allyl glycidal ether) depend both on the catalyst used in preparing the polymer and on the comonomer content. The mechanical properties are very much influenced by the ability of propylene oxide stereosequences in the copolymer to crystallize. The crystalline material can give a substantial increase in modulus and in the strength of the polymer on stretching.

4. One of the most interesting properties shown by copolymers of propylene oxide of low stereoregularity is the invariance of modulus and mechanical loss over a broad range of temperature and frequency.

Literature Cited

1. Price, C. C., and Osgan, M., J. Am. Chem. Soc., (1956) <u>78</u>, 4787.

2. Wunderlich, B., "Macromolecular Physics Vol. 1, Crystal Structure, Morphology Defects", Academic Press, New York, 1973.

3. Pruitt, M., and Bagget, J. M., U.S. Patent 2,706,189 (April

1955).

4. Furukawa, J., Makromol. Chem., (1959) 32, 90.

5. Price, C. C., J. Polymer Sci., (1959) 34, 165.

6. Price, C. C., Spector, R. and Tumolo, A. L., J. Polymer Sci.,
    Part A-1, (1967) 5, 407.

7. Price, C. C., and Spector, R., J. Am. Chem. Soc., (1965) 87,
    2069.

8. Shambelan, C., Ph.D. Thesis, University of Pennsylvania, 1959.

9. Schaefer, Jacob, Katnik, R. J., and Kern, R. J., Macromole-
    cules, (1968) 1 (2), 101.

10. Schaefer, Jacob, Macromolecules, (1969) 2 (5), 533.

11. Schaefer, Jacob, Macromolecules, (1972) 5 (5), 590.

12. Coleman, B., J. Polymer Sci., (1958) 31, 155.

13. Newman, S., J. Polymer Sci., (1960) 47, 111.

14. Miller, R. L., and Nielsen, L. E., J. Polymer Sci., (1960)
    46, 303.

15. Feller, William, "An Introduction to Probability Theory and
    its Applications", 2nd Edition, John Wiley & Sons, New York
    (1957).

16. Aggarwal, S. L., Marker, Leon, Kollar, W. L., and Geroch, R.,
    in Advances in Chemistry Series, Number 52, "Elastomer Stereo-
    specific Polymerization", pp 88-104, American Chemical Soci-
    ety (1966).

17. Bovey, F. A., and Tiers, V. D., Fortshr. Hochpolymer Forsch.,
    (1963) 3, 139.

18. Lapeyre, W., Cheradame, H. Spassky, N., and Sigwalt, P., J.
    de Chim. Phys. (1973) 70, 838.

19. Oguni, N., Watanabee, S., and Tani, H., Polymer Journal (1973)
    4, 664.

20. Oguni, N., Lee, K., Tani, H., Macromolecules, (1972) 5, 819.

21. Flory, P. J., Trans. Faraday Soc., (1955) 51, 848.

22. Aggarwal, S. L., Marker, L., Kollar, W. L., and Geroch, R., J. Polymer Sci., (1966) 4 (A-2), 715.

23. Keith, H. D., and Padden, F. J., J. Appl. Physics., (1964) 35, 1270.

24. Natta, G., Corradani, P., and Dall'Asta, G., Atti Accad. Naz. Lincei Rend., Classe sci. fis. Mat. Nat., (1956) 20, 408.

25. Avrami, M., J. Chem. Phys., (1939) 7, 1103.

26. Avrami, M., J. Chem. Phys., (1940) 8, 212.

27. Avrami, M., J. Chem. Phys., (1941) 9, 177.

28. Kovacs, A. J., "International Symposium on Macromolecules" Milan, Ric. Sic., Suppl. A., (1955) A25, 668.

29. Tung, L. H., and Buckser, J. Phys. Chem., (1959) 63, 763.

30. Hashino, S., Meinecke, E., Powers, J., Stein, R. S., and Newman, S., J. Polymer Sci., (1965) A3, 3041.

31. Marker, Leon, Aggarwal, S. L., Holle, R. E., and Kollar, W. L., Kautschuk und Gummi Kunstoffe, (1966) 19, 377.

32. Williams, M. L., Landel, R. F., Ferry, J. D., J. Appl. Phys., (1963) 26, 359.

4

Heterogeneous Nucleation of Isotactic Poly(Propylene Oxide) Crystallization

J. H. COLE and L. E. ST-PIERRE

Department of Chemistry, McGill University, Montreal, Canada

Introduction

It is known that when crystallising polymers are cooled from the melt, crystallisation usually begins on impurities in the melt, such as dust particles or residual catalyst fragments. Homogeneous nucleation, where crystalline nuclei are believed to be formed by random fluctuations of order and segmental energies in the supercooled melt, usually occurs at higher supercoolings. Controlled addition of heterogeneous nuclei can improve many physical properties of a polymer (1) e.g. clarity, density, impact and tensile strength as well as increasing the crystallisation rates leading to shorter processing cycles.

Numerous attempts have been made to predict the effectiveness of potential nucleating agents with particular attention having been paid to the crystallisation of isotactic polypropylene (1-5), isotactic polystyrene (6), polyethylene (7-9) and poly(ethylene terephthalate) (10,11). However, little can be concluded about the fundamental mechanism of heterogeneous nucleation, or the properties of effective nucleating agents.

Most theories of heterogeneous nucleation require that the foreign nucleus reduces the total interfacial free energy and itself provides part of the interface. There results a lowering of the free energy for nucleation and a decreasing of the degree of supercooling required for nucleation. This reduction in interfacial free energy depends on the geometry of the foreign phase and on its chemical nature.

Hobbs has shown (12) that the abilities of two morphologically different, but chemically identical, graphite fibres to nucleate isotactic polypropylene differed considerably. The same author also showed (13) that a carbon replica of a crystalline isotactic polypropylene surface could increase the nucleation of the polymer during recrystallisation. Thus, the physical, not chemical, nature of the nucleating agent has determined its effectiveness. In the present work we have changed the surface chemistry of a particulate filler, without

58

altering particle size or geometry.

The filler used was a Cab-o-Sil silica with a surface concentration of 6-8 hydroxyl groups/100 A^2. By reacting these hydroxyl groups with various reagents the surface can be modified energetically (14).

The interfacial energies between the silicas of differing chemical surfaces and a crystallising polymer can be characterised using low molecular weight model compounds homologous with the polymer. The isosteric heats of adsorption at approximately zero coverage of the model compounds on the silica surfaces were taken as a measure of the interaction energy. Experimentally these were determined by means of the pulse elution technique of vapour phase chromatography. This has been described previously (15).

The initial investigations using this approach were concerned with the nucleation of the crystallisation of poly(dimethylsiloxane) (16). Silicas with surfaces treated with methoxy, butoxy and trimethylsilyl groups were used as fillers. It was shown that an increase in filler concentration decreased the supercooling required to reach a certain critical nucleation rate; also, at the same filler content, the fillers having the lower surface energies underwent smaller decreases in supercooling. Further work showed (17) that addition of the fillers increased the isothermal crystallisation rate of the poly(dimethyl siloxane), and a semi-quantitative relationship between the nucleation rate and polymer-filler interaction energy was established. Based on the Fisher-Turnbull nucleation equation (18) it was also suggested that there was a linear dependence of the free energy of heterogeneous nucleation on the interaction energy between the polymer and filler.

In the present paper the silica-isotactic poly(propylene oxide) (iPPO) system is examined, with untreated silica and trimethylsilyl coated (1.69 trimethylsilyl groups/100 A^2) silica being the nucleating agents. This system was chosen because: (1) iPPO, as shown in the early work of Price and Osgan (19), can crystallise conveniently at or just above room temperature; (2) the model compound used for iPPO, 1,4 p-dioxane, gives net isosteric heats of adsorption of 8.7 and 1.0 Kcal./mole for the untreated and treated silicas respectively.

The crystallisation behaviour of the pure iPPO and composites was studied using differential scanning calorimetry and dilatometry. Results from these studies will be qualitatively interpreted in terms of the filler-polymer interaction energy.

Experimental

1. Samples.

a. Isotactic poly(propylene oxide). The polymer used was provided by Dr. A.E. Gurgiolo (Dow Chemical Co.). It was prepared

using a $FeCl_3$/propylene oxide catalyst; the fraction insoluble in acetone at $-20°C$ was used in subsequent experiments. According to Aggarwal et al (20) this sample is 49% crystalline, and the melting temperature was found dilatometrically to be 75°C. The molecular weight was estimated from the intrinsic viscosity, $[\eta]$, in benzene solution at 25°C using the relation (21):

$$[\eta] = 1.12 \times 10^{-4} (\overline{M}_V)^{0.77}$$

and was found to be 8.7×10^4 gm/mole.

    b. Silicas. Cab-o-Sil M5, an amorphous thermal silica, particle size 12 mμ, with manufacturers' quoted surface area of 200 m^2/g, was used as received, or after reaction in a high pressure reactor with trimethylchlorosilane (15). Total carbon analysis of the treated sample gave a surface coverage of 1.69 trimethylsilyl groups/100 A^2.

    c. Composites. Known quantities of silica, previously dried at 130°C and 10^{-3} torr pressure were added to a 10% solution of iPPO in CCl_4. The mixture was thoroughly agitated with a stainless steel spatula until the solvent evaporated. When the samples were practically dry, and had become granular in form, they were dried at room temperature under vacuum for 6-8 hours.

    2. Differential Scanning Calorimetry (D.S.C.). The crystallisation of iPPO and composites were studied using the Perkin-Elmer Differential Scanning Calorimeter (DCS-1). Liquid nitrogen was used as coolant, with dry nitrogen the sweeping gas. The temperature read out was calibrated using the trans-ition temperatures of indium (156°C), stearic acid (72°C), distilled water (0°C) and n-decane (-30°C).
    The procedure followed was to first melt the samples at 120°C for 30 minutes to ensure complete melting (22); they were then cooled at a scan speed of 10°C/min. During this time the sample temperature and (dQ/dT) were monitored continuously.

    3. Dilatometry. The isothermal crystallisation rate curves were determined from the dilatometrically measured changes in density. Samples weighing between 1 and 2 gms were sealed under vacuum in glass dilatometers with mercury as the confining liquid. The samples were then melted at 120°C for 30 minutes and then transferred immediately into a water bath controlled to within 0.005°C of the required temperature, using a Hg/toluene thermoregulator. The changes in height of the mercury column were monitored with time until no further change was observable over a period of 24 hours.

Results and Discussion

1. **D.S.C.** Pure iPPO, on cooling at 10°C/min exhibited an exotherm centred at 11.5°C, indicating crystallisation. This exotherm point, reproducible to ±1.0°C, was taken to be the optimum crystallisation temperature (T_{Op}). This interpretation has been discussed by Teilel'baum et al (23) in their work on the crystallisation of natural rubber, and by Beck et al (1) on the crystallisation of isotactic polypropylene.

The silica-filled iPPO samples also exhibited exotherms, but the temperatures at which these isotherms appeared depended on the amount of filler present, and on the surface energy of the filler. From Fig. 1 it can be seen that:

(1) the optimum crystallisation temperature shifts to higher temperatures as the filler content is increased, reaches a maximum, and then decreases;

(2) samples with the same silica content, having different interfacial energies do not exhibit the same crystallisation behaviour. The samples containing the low surface energy silica (1.69 trimethylsilyl groups/100 A^2) underwent lesser shifts in T_{Op} until a loading of approximately 35 parts of silica/100 parts of iPPO. Also the decrease of T_{Op} after the maximum of the low energy surface silica composites is not as great as the high energy surface samples.

These phenomena can be explained by the application of heterogeneous nucleation theory (24,25). Silica powder, as an "extraneous solid" can catalyse the nucleation process. For the pure polymer, the steady-state nucleation rate per unit volume (18), $\dot{N}$ is expressed by:

$$\dot{N} = N_o \cdot \exp\{-[\frac{E_D}{RT} + \frac{\Delta G_o^*}{RT}]\} \qquad (1)$$

where $N_o = \dfrac{n_1 kT}{h}$ (n_1 is the concentration of polymer segments per unit volume and k,T and h are Boltzmann's constant, temperature and Planck's constant respectively). E_D is the free energy of activation for transport across the liquid-nucleus interface, and ΔG_o^* is the free energy for homogeneously forming a nucleus.

Then, in a silica-filled sample:

$$\dot{N}_h = N_o \cdot \exp\{-[\frac{E_D}{RT} + \frac{\Delta G_h^*}{RT}]\} \qquad (2)$$

where ΔG_h^* is the free energy for heterogeneous nucleation, and ΔG_h^* is related to ΔG_o^* by the expression (25):

$$\Delta G_h^* = f(\phi) \Delta G_o^* \qquad (3)$$

with $\qquad f(\phi) = \dfrac{(2+\cos\phi)(1-\cos\phi)^2}{4}$ (Ref. 24) $\qquad (4)$

Here ϕ is the contact angle between the filler particle and the polymer, with $f(\phi)$ increasing as the wetting angle increases. In particular, when

$$\phi \rightarrow 0^{\circ}, \ f(\phi) \rightarrow 0$$

$$\phi \rightarrow 90^{\circ}, \ f(\phi) \rightarrow \tfrac{1}{2}$$

As the interfacial energy between the polymeric liquid and the filler decreases, the wetting decreases, and so ϕ increases, or, as $f(\phi)$ increases the interfacial energy decreases. Thus from equations (3) and (4) it is apparent that the free energy for nucleus formation in the heterogeneous case will always be smaller than that for homogeneous nucleation.

It is reasonable to assume that, in order for a crystallisation exotherm to be detectable by D.S.C., there must exist a critical nucleation rate $\dot{N}_R$. Accordingly, comparison of the temperatures at which these isotherms appear is in effect a measurement of the relative rates of nuclei formation in the various samples. Thus since silica-filled samples are associated with smaller free energies of nucleation, the critical number of nuclei necessary for observation are present at higher temperatures relative to the pure sample. In the pure sample the nucleation is probably heterogeneous, but the number of nucleating species present is relatively small.

Furthermore, with increasing filler content, the number of filler-polymer contacts increases with a resultant increase in the number of nuclei, and an upward shift in the exotherm temperature. In addition to changing the quantity of silica present, it is also possible to change the nature of the interface present between the filler and the iPPO. The trimethylsilyl coated filler has a lower epoxide-silica interfacial energy than that between epoxides and pure silica. Thus the wetting of this sample will be less, and the differences between ΔG_h^* and ΔG_o^* will be diminished (equations (3) and (4)). At lower loadings this results in smaller shifts from the pure iPPO behaviour; $\Delta T = 9^{\circ}C$ for 10 parts pure silica, while $\Delta T = 5.5^{\circ}C$ for 10 parts trimethylsilyl coated silica.

However, as the filler content is increased, the number of silica particles present becomes so large that there is effective crosslinking of polymer segments by adsorption on the silica; this increases the transport term, E_D, in equation (2), and thus the effective number of nuclei is lessened, resulting in a lowering of T_{op}. Also the decrease in the number of effective nuclei at higher loadings is greater for the composites containing pure silica than for the treated silica. This is expected because, as shown by Howard and McConnell, for poly(ethylene oxide) (26), an epoxide polymer adsorbs more strongly on the hydroxyl group-covered surface than on the trimethylsilylated surface.

2. Dilatometry. The kinetics of the isothermal crystallisation of pure and filled iPPO samples from the melt were studied between 45.00 and 55.00°C. The composites contained 10

parts of filler/100 parts of iPPO. The increase in density was taken as a measure of the increase in overall crystallinity. In Fig. 2, $(1 - X_t/X_\infty)$ is plotted against log(time) for the pure polymer; X_t is the weight fraction of polymer crystallised at time t and X_∞ is the weight fraction of polymer crystallised at infinite time.

The sigmoidal isotherms usually found in polymer crystallisation are observed; these represent primary crystallisation i.e. the nucleation and growth of crystalline regions until mutual impingement stops further growth. The second part of curves 2 and 3 as shown in Fig. 3, where the crystallinity increases logarithmically with time, corresponds to secondary crystallisation: this is usually considered to be the crystallisation of any remaining melt, and rearrangement of parts of the crystal regions grown in the primary phase (27).

In Fig. 3 the crystallisation of the high energy surface silica composite is 90% complete while the pure iPPO is only 10% crystallised. A similar but lesser effect is shown in the low energy surface silica composite.

Another parameter characterising the nucleation of the crystallisation is the apparent induction time; this is the time during which there is no apparent change in the height of the mercury column in the dilatometer, when the change in polymer density is too small to be observed. As shown in Fig. 4 there is an appreciable lengthening of the induction period with increasing temperature. At the same crystallisation temperature the induction times vary in the order: Pure iPPO > iPPO + low energy surface silica > iPPO + high energy surface silica. Indeed, at 45.00°C the high energy surface silica composite began to crystallise before the sample reached thermal equilibrium (this was usually reached after 3 minutes). At the same temperature the pure iPPO did not begin to crystallise until 11 minutes had elapsed.

The half-time of primary crystallisation, $t_{\frac{1}{2}}$, shows a similar dependence on temperature and polymer-filler interaction energy (see Fig. 5). To find $t_{\frac{1}{2}}$, it was assumed that the contribution of the slow secondary crystallisation process to the primary portion of the overall crystallisation curve was negligible. Thus $t_{\frac{1}{2}}$ was half the value of the time at the intersection point (see curve 3, Fig. 3), using the extrapolation method of Vidotto et al (28) for the crystallisation of isotactic poly butene-1, and used by Groeninckx et al (11) for the crystallisation of poly(ethylene terephthalate).

These results show that, since the primary crystallisation is composed of two processes, primary nucleation and subsequent crystal growth, and as the crystal growth is independent of the origin of the primary nucleus, the silicas act as heterogeneous nucleating agents for iPPO. Also the high energy surface silica is markedly more effective than the low energy surface silica.

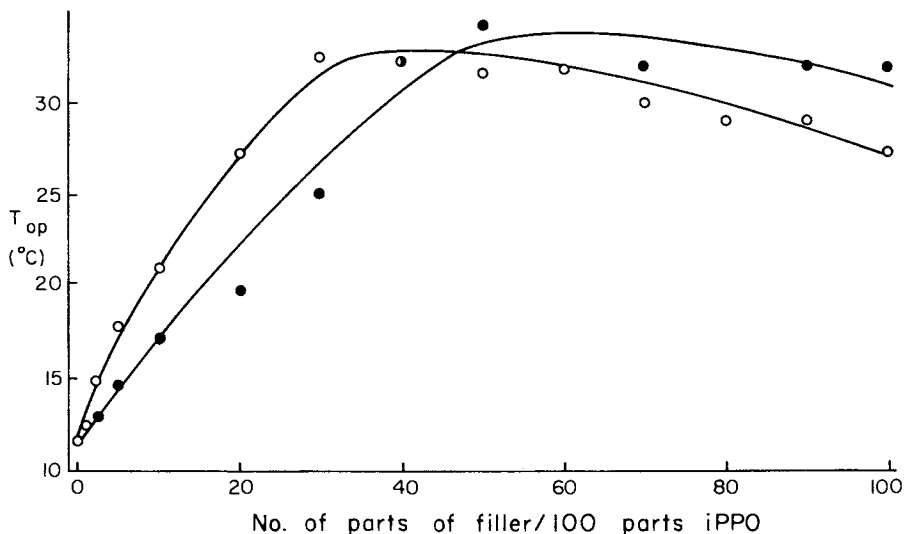A semi-quantitative analysis of the time dependence of the

Figure 1. Plots of T_{op} vs. filler content for treated and untreated silica fillers. ○ = iPPO + untreated silica. ● = iPPO + Me₃SiCl treated silica. ◑ = overlapping point.
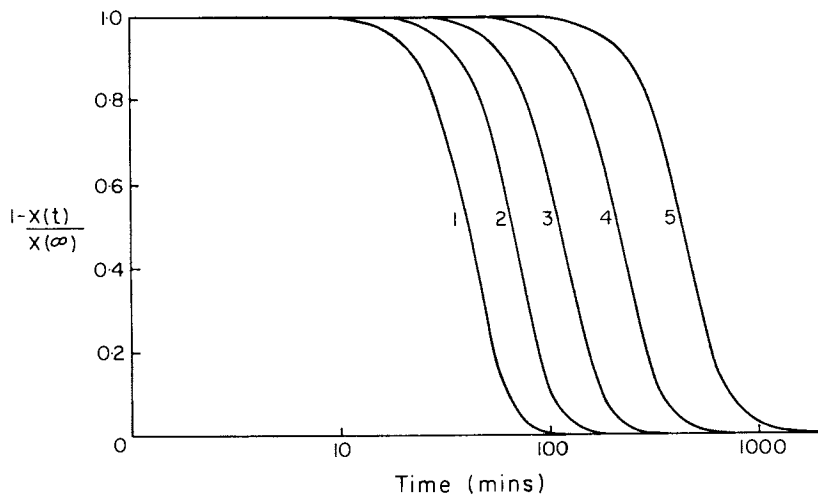

Figure 2. Crystallization isotherms for pure iPPO at crystallization temperatures of 1, 45.00°C; 2, 47.50°C; 3, 50.00°C; 4, 52.50°C; and 5, 55.00°C
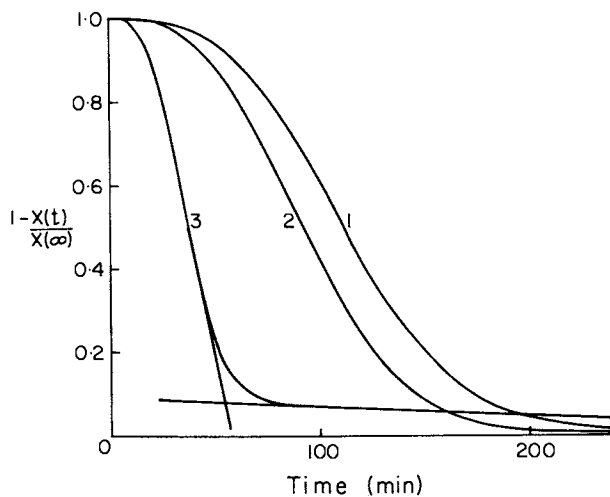
$$\frac{1-X(t)}{X(\infty)}$$

Time (min)

Figure 3. Crystallization isotherms of 1, pure iPPO; 2, iPPO + Me₃SiCl treated silica; and 3, iPPO + untreated silica. Crystallization temperature = 50.00°C.

Crystallisation temp. (°C)

Induction Time (mins)
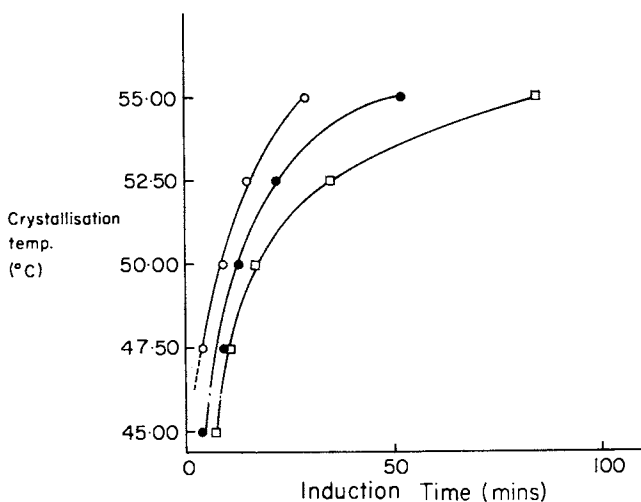
Figure 4. Plots of induction time against crystallization temperature. □ = pure iPPO. ● = iPPO + Me₃SiCl treated silica. ○ = iPPO + untreated silica.

primary crystallisation process was made using the Avrami
relationship (29-31):

$$\theta = \exp(-k_1 t^n) \qquad (5)$$

where $\theta = (d_p-d_t)/(d_p-d_o)$, with d_p being the polymer density at
the end of the primary crystallisation i.e. at the intersection
point as drawn on curve 3 in Fig. 3, and d_o is the density of
the amorphous polymer; d_t is the density of the polymer at time
t. k_1 is the Avrami constant, and n is the Avrami exponent; n
depends on both the type of primary nucleation and the mode of
growth of the crystallising polymer.

Plots of $\log(-\log\theta)$ against $\log(\text{time})$ were drawn for all
samples examined, and typical examples are shown in Fig. 6. From
the slopes of these lines, the Avrami exponent n is obtained.
The average n value for the pure iPPO is 3.20 ± 0.06, and for both
the treated and untreated silica composites is 3.00 ± 0.10 at all
temperatures except for the untreated silica sample at $45.00°C$,
which gave an anomalous n value of 2.50.

The n values of 3.0, according to the simple Avrami theory
suggest either instantaneous nucleation and three-dimensional
crystal growth, or a first order nucleation rate and two-
dimensional crystal growth. However, as Mandelkern has shown
(25), a more general Avrami equation can give non-integral values
for n, as was found in the crystallisation of pure iPPO; thus
it is difficult to attach a quantitative interpretation to a
value of n.

Qualitatively it may be noted that the constant values of n
for both types of silica fillers at all experimental temperature
(with the one exception) indicates a similar crystallisation
mechanism by both the high and low energy surface silica
composites. For the pure polymer, there operates a different
mechanism, showing either a change in heterogeneous nucleation
time dependence or in growth morphology.

Summary

The effectiveness of chemically different, but physically
similar, silica fillers as nucleating agents in the crystal-
lisation of isotactic poly(propylene oxide) was studied using
differential scanning calorimetry and dilatometry. It was found
that varying the epoxide-silica interfacial energy by treating a
silica surface with trimethylchlorosilane caused a change in its
nucleating ability; the greater the interfacial energy, the more
efficiently the silica nucleates.

This effect is interpreted in terms of the Fisher-Turnbull
equation for nucleation, with change in interfacial energy
causing a change in the free energy of heterogeneous nucleation.
Increase in filler content of the composites up to a certain
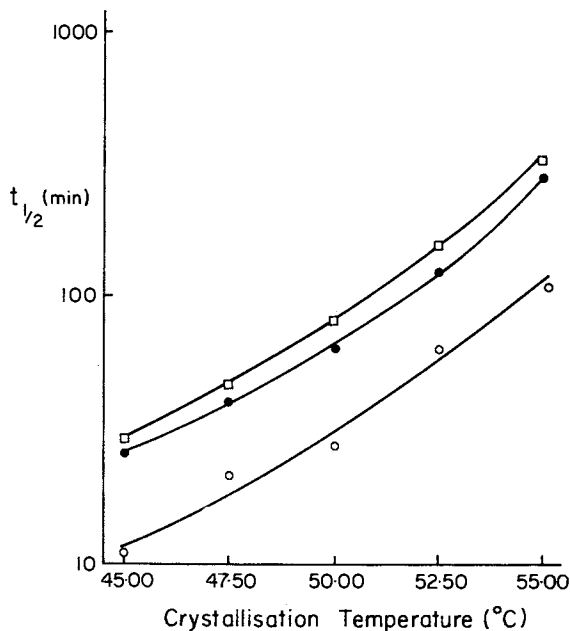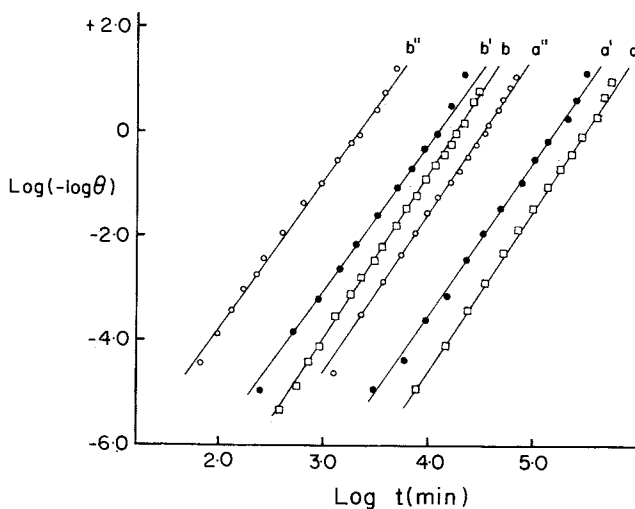loading increased nucleation; additional filler caused effective

Figure 5. Plots of half-time of primary crystallization ($t_{1/2}$) against crystallization temperature. ☐ = pure iPPO. ● = iPPO + Me₃SiCl treated silica. ○ = iPPO + untreated silica. (

Figure 6. Avrami plots of log(−logθ) against log t. ☐ = pure iPPO. ● = iPPO + Me₃SiCl treated silica. ○ = iPPO + untreated silica at different temperatures. a, a′, a″ = 52.50°C. b, b′, b″ = 47.50°C.

cross-linking of polymer segments, thus increasing the free energy of activation for transport across the liquid polymer-filler interface and so decreasing the nucleation rate.

Acknowledgement

I also acknowledge a debt of gratitude to Professor C.C. Price, a great chemist, a great man and a friend of decades. He has been an inspiration to me and to a host of other former students (L.E.St-P.).

Literature Cited

1. Beck, H.N and Ledbetter, H.D., J. Appl. Poly. Sci., (1965), 9, 2131.
2. Beck, H.N., J. Appl. Poly. Sci., (1967), 11, 673.
3. Rybnikar, F., J. Appl. Poly. Sci., (1969), 13, 827.
4. Binsbergen, F.L., Polymer, (1970), 11, 253.
5. Binsbergen F.L. and de Lange, B.G.M., Polymer, (1970), 11, 309.
6. Kargin, V.A., Sogolova, T.I., Rapoport-Molodtsova, N.Ya., Dokl. Akad. Nauk. S.S.S.R., (1964), 156, 1406.
7. Cormia, R.L., Price, F.P. and Turnbull, D., J. Chem. Phys., (1962), 37, 1333.
8. Koutsky, J.A., Walton, A.G. and Baer, E., Polymer Letters, (1967), 5, 185.
9. Mauritz, K.A., Baer, E. and Hopfinger, A.J., J. Poly. Sci., A2, (1973), 11, 2185.
10. Van Antwerpen, F. and van Krevelin, D.W., J. Poly. Sci., A2, (1972), 10, 2423.
11. Groeninckx, G., Berghmans, H., Overbergh, N. and Smets, G., J. Poly. Sci., A2, (1974), 12, 303.
12. Hobbs, S.Y., Nature, Physical Science, (1971), 234, (44), 12.
13. Hobbs, S.Y., Nature, Physical Science, (1972), 239, (89), 28.
14. Chahal, R.S., Ph.D. Thesis, McGill University, (1968).
15. Chahal, R.S. and St-Pierre, L.E., Macromolecules, (1968), 1, 152.
16. Yim, A. and St-Pierre, L.E., Polymer Letters, (1970), 8, 241.
17. Yim, A., Ph.D. Thesis, McGill University, (1971).
18. Turnbull, D. and Fisher, J.C., J. Chem. Phys., (1949), 17, 71.
19. Price, C.C. and Osgan, M., J. Am. Chem. Soc., (1956), 78, 4787.
20. Aggarwal, S.L., Marker, L., Kollar, W.L. and Geroch, R., J. Poly. Sci., A2, (1966), 4, 715.
21. Allen, G., Booth, C. and Jones, M.N., Polymer, (1964), 5, 195.

22. Slonimskii, G.L. and Godovskii, Yu.K., Vysokomol. Soyed., (1967), 9, 863.
23. Teilel'baum, B.Ya and Anoshina, N.P., Vysokomol. Soyed., (1965), 7, 2117.
24. Turnbull, D., Solid State Physics, (1956), 3, 277.
25. Mandelkern, L., "Crystallisation of Polymers", McGraw-Hill Book Co., Inc., New York, 1964.
26. Howard, G.J. and McConnell, P., J. Phys. Chem., (1967), 71, 2974.
27. Keith, H.D., Koll.-Z.Z. Polym., (1969), 231, 421.
28. Vidotto, G., and Kovacs, A.J., Koll.-Z.Z. Polym., (1967), 220, 2.
29. Avrami, M., J. Chem. Phys., (1939), 7, 1103.
30. Avrami, M., J. Chem. Phys., (1940), 8, 212.
31. Avrami, M., J. Chem. Phys., (1941), 9, 177.

5

Applied Crystallization Kinetics. III. Comparison of Polyepichlorohydrins of Different Stereoregularity

P. DREYFUSS

B. F. Goodrich Research and Development Center, Brecksville, Ohio 44141

Introduction

In the course of some of our work on polyethers, we encoun-
tered a series of crystalline polyepichlorohydrins which differed
quite markedly in their processing characteristics but otherwise
seemed quite similar. Differences revealed by the infrared and
nuclear magnetic resonance techniques then available were too
insignificant to be helpful in their characterization. All poly-
mers were shown to be crystalline and isotactic by X-ray analy-
sis. Small differences in optical activity were measurable.
However, these differences were too small to be useful for cor-
relation with physical properties. We found that an examination
of their crystallization behavior and rates of crystallization was
an extremely sensitive and revealing way of characterizing them.

Experimental

Microscopy. Thin films (1-2 mils) were pressed at 150°C
using a Pasedena press fitted with West SCR controllers. Typi-
cally, a small sample was placed between Teflon coated alumi-
num foil sheets, preheated for 30 sec, and held at 25,000 lb.
gauge load for 5 min. Samples were then rapidly transferred to
a cooling press and held at 25,000 lb. gauge load for 5 min.
Some of the lower melting samples were pressed at 100°C.

Portions of these films were placed on a glass slide and
covered with a cover glass. Samples were melted in an air oven
at the desired temperature, usually 150°C for the desired time,
usually 15 min and then rapidly transferred to a hot stage at

Current address: Institute of Polymer Science, University of
Akron, Akron, Ohio 44325.

70

constant temperature. The hot stage temperature was controlled by circulating liquid from a Haake NBS bath through the stage. Temperatures, measured by means of a thermocouple in the stage near the sample, were constant to 0.1°C or less. The growth of the spherulites that formed was observed using a Unitron polarizing microscope with crossed polaroids. Photographs were taken with the aid of an American Optical Co. Photomicrographic camera with a Polaroid Land camera back. Melting was followed using a heating rate of 0.5 to 1° per min. The slower rate was used in the vicinity of the melting temperature.

Dilatometry. Volume-temperature measurements and crystallization rate measurements were carried out in J-shaped dilatometers made from 1 mm Precision bore graduated capillary tubing with mercury as the confining liquid. The procedure followed was very similar to that described by Bekkedahl (1). Well-fused pellets of appropriate dimensions were pressed at 5 Ram force/lb. Hydraulic Pressure on the gauge and 25 to 120°C (usually 90°C). The pellets were cooled to 45-50°C at full pressure before removing from the mold. The sealed dilatometers containing the pellets were evacuated to about 10^{-5} mm Hg while heating at 125-35°C for about 3 hrs prior to filling with mercury.

For the rate studies, the prepared dilatometers were placed in a 150°C bath for about 30 min before transferring rapidly to a second bath at the crystallization temperature. Crystallization temperatures were controlled to ± 0.01 °C with the aid of a Dynapac-15 temperature controller. Higher temperatures of the melting bath and longer melting times were tried occasionally. These did not change the observed rates for any of the samples studied. All rates are reported in terms of the time, $t_{\frac{1}{2}}$, for half the total change in height to occur. Whenever the value of $t_{\frac{1}{2}}$ was less than about 10 min, we were not able to determine an exact value because crystallization began before thermal equilibrium was achieved.

Melting temperatures after isothermal crystallization were obtained in the same bath using heating rates of 0.3°C per min and observing the change in height with temperature which was measured with a calibrated mercury thermometer. Melting temperatures were taken as the temperature where the last traces of crystallinity disappeared.

Results

Description of Polymers.   A wide variety of crystalline poly-
epichlorohydrins were examined in this study.   Some typical
examples are given in Table 1.   All the polymers were prepared
from racemic monomer, but some of them were prepared using
initiators of the type previously reported to give partially opti-
cally active polymers (2-6). The polymers were shown to be iso-
tactic by comparison of the observed d-spacings with those re-
ported in the literature for crystalline isotactic polyepichloro-
hydrin (8, 9).   Also included in Table 1 for comparison are some
data on polypropylene oxides prepared with different initiators.

Spherulite Morphology.   Crystalline polyepichlorohydrin
readily forms spherulites on cooling from the melt.   As shown
in Figure 1, we have observed two kinds of spherulites.

a   b
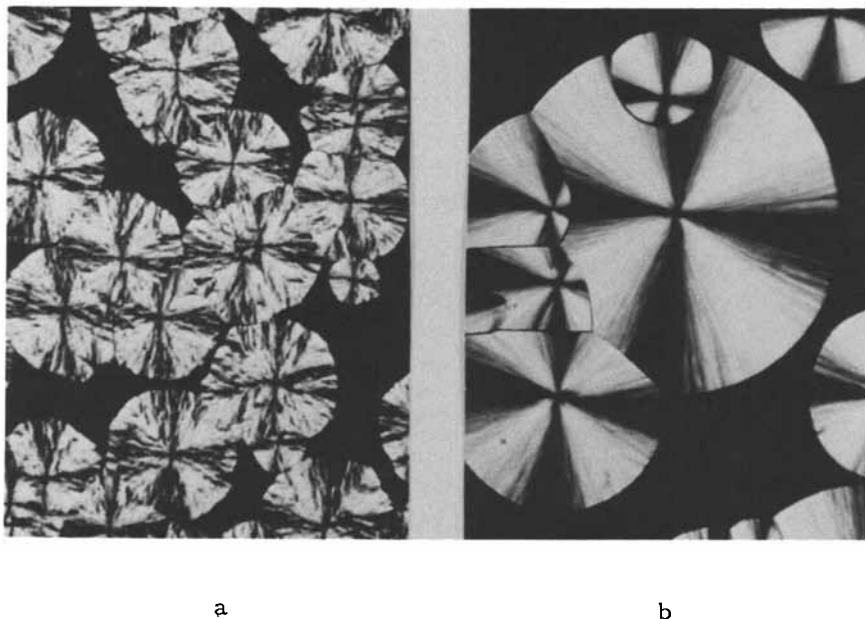
Figure 1.   Polyepichlorohydrin spherulites. Left: Type I spherulites from 329C after melting at 170°C and crystallizing at 50°C for 185 min. (128x). Right: Type II spherulites from 39A after melting at 150°C and crystallizing at 50°C for 222 min. (128x).

Table 1

Typical Crystalline Polyepichlorohydrins

Sample	Initiator[a]	$[\alpha]$ in M-Pyrol at 23°C	Ref
329C	A	0	--
100Z	A	0	--
162A	B	-2.36	--
2437	B	-2.80	--
2413	B	-9.75	--
2431	B	-10.1	--
Polymer from racemic propylene oxide	Diethyl zinc-d-borneol	Crystalline, 8.0[b], -9.3[c] Semicrystalline, 6.1b, -8[c] Amorphous, 4.9b, +1[c]	4
Polymer from *l*-propylene oxide	Potassium hydroxide	25 ± 5[b], -16 ± 5[c]	7
Polymer from *l*-propylene oxide	Ferric chloride	17 ± 5[b]	7

[a] A is a typical initiator for the preparation of non-optically active but crystalline polymers from racemic monomer. B are typical initiators for the preparation of optically active polymer from racemic monomer.

[b] Determined in chloroform at 20°C.

[c] Determined in benzene at 20°C.

Both have fibrillar structures but the structure of Type I is coarser than that of Type II. Occasionally rings are observed in Type II spherulites. Sometimes as shown in Figure 2 both types of texture are observed in a single spherulite.

When the spherulites were observed between crossed polaroids using a 1st order red plate in the usual 45° orientation, it was found that both types of spherulites are negatively birefringent. This is not surprising since negative spherulites have also been observed in polypropyleneoxide films (10). Nevertheless, the spherulites are not identical when viewed with the 1st order red plate. Type I is blue in the second and fourth quadrants and orange in the first and third. Type II is similar but the quadrants are separated by a red cross.
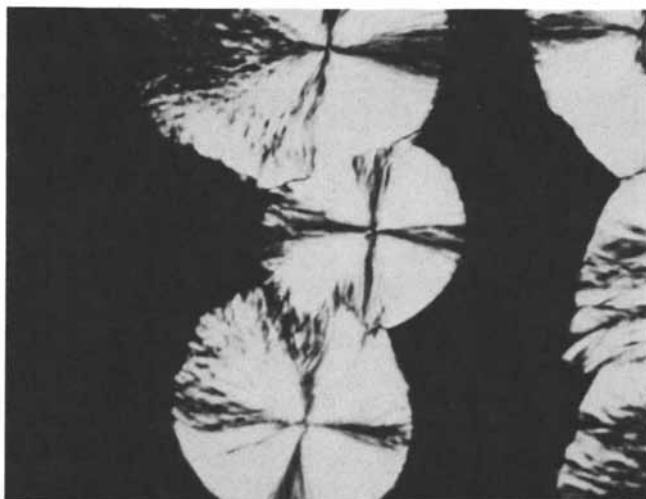
Figure 2. Type I and II spherulites both seen in the same spherulite, from 164A melted at 150°C and crystallized at 50°C for 168 min. (128x)

The type of spherulite that forms does not seem to be affected by the temperature at which the sample is melted or by the temperature of crystallization. We have observed the growth of spherulites of both types at 30, 50, and 60°C after melting at 150°C. Similar morphology was obtained from the same sample at all temperatures. However, as expected, the growth rate and

perfection of the spherulites are dependent on the temperature of
crystallization. Rates are slower and perfection is greater at
temperatures nearer to the polymer melting temperature. We
have been able to grow very large spherulites by crystallizing
for several days at 50°C.

The morphology does not seem to be affected by the tempera-
ture at which the sample is melted prior to crystallization. We
have crystallized at 50°C after melting at 130, 150, and 170°C.
The morphology obtained from the same sample was similar in
all cases. The main difference was that more small spherulites,
unresolvable at our usual magnification of 150x, formed after
melting at 130°C.

Melting Temperatures. The melting temperatures we ob-
serve microscopically are usually higher by a few degrees than
thoseobserved dilatometrically. Some typical results are given
in Table 2 and in Figures 3-5. This is not an unexpected result,
since polymer melting temperatures are very sensitive to the
rate of heating unless extremely slow heating rates, such as
0.5°C per day, are used. Also, the heat transfer in a dilatom-
eter and on a hot stage may be quite different. In addition,

<div align="center">Table 2</div>

<div align="center">Microscopic and Dilatometric Melting Temperatures
of Crystalline Polyepichlorohydrin</div>

Polymer	Microscopic T_m (°C)	Dilatometric T_m (°C)
329C	115-16	113
39A	119-20	115
164A	114 and 117	108.5 and 113
2413	------	115-17
2431	------	117.5
100Z	------	111

sample preparation and previous heat history can affect the
exact melting temperature observed (11). The important point
here is that two different melting temperatures have been ob-
served both microscopically and dilatometrically in the same
sample and in different samples. In some of the later experi-
ments, samples were held at temperatures between the higher
and lower melting temperatures for several hours to verify that
the higher melting polymer was not just slower to melt. Thus,
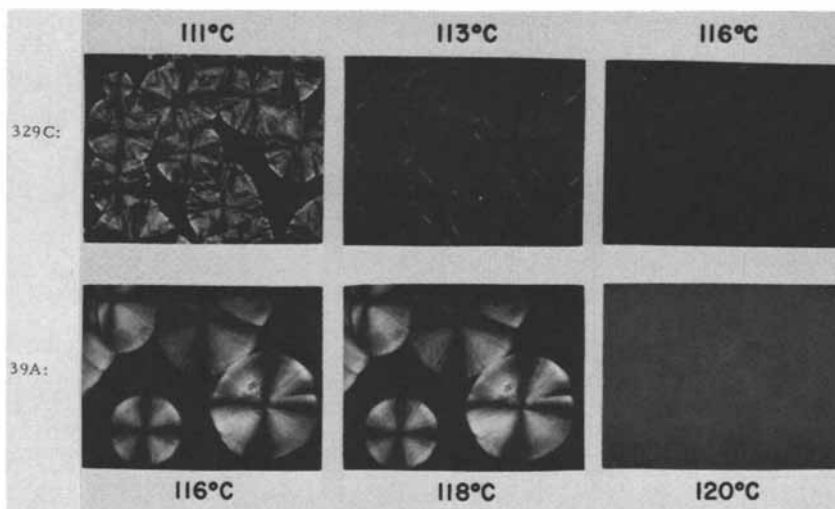there are two families of crystalline polyepichlorohydrins. As

Figure 3.   Melting of 329C and 39A after simultaneously melting at 150°C and crystallizing at 50°C on the same slide
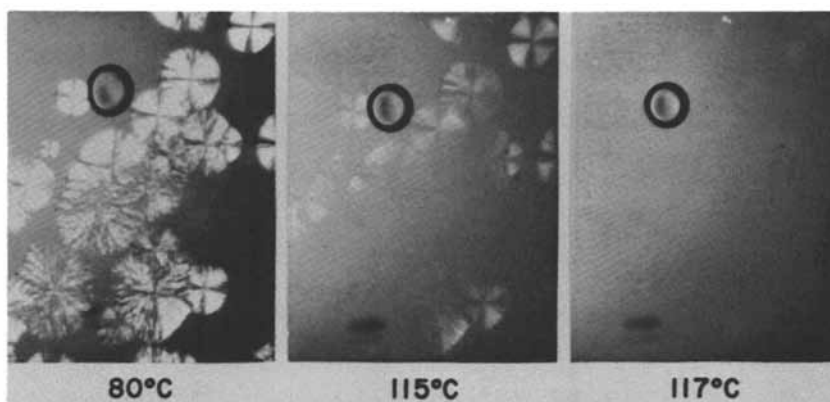

Figure 4.   Melting of spherulites of 164A. At 80°C both Type I and Type II spherulites are visible. By 115°C Type I spherulites are melted. Type II spherulites disappear by 117°C (83x).
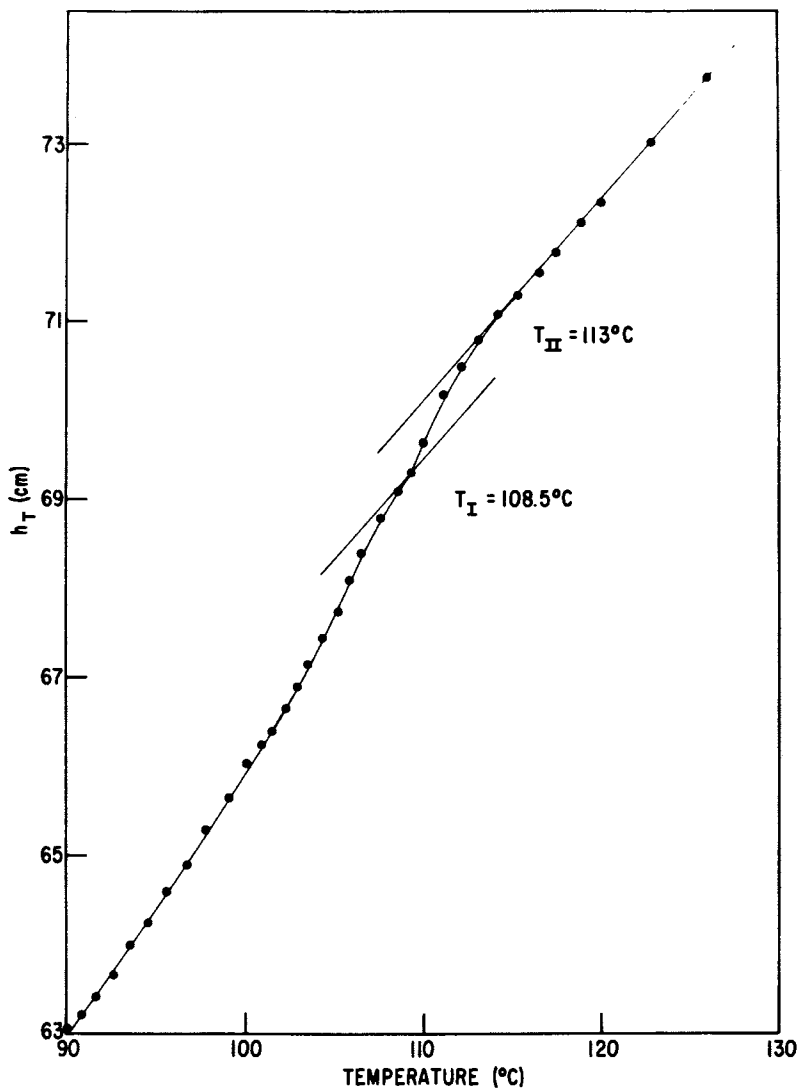
Figure 5.   *Dilatometric melting curve of 164A. Two inflections suggest two different melting temperatures.*

will be discussed below these two families can be related to the
stereoregularity of the polymers.

Crystallization Rates.   We determined growth rates of the
spherulites microscopically, but only examined the rates of
nucleation qualitatively for reasons that will emerge below.
Overall rates of crystallization were determined dilatometrical-
ly.

Nucleation of Spherulites.   We have examined the rates of
crystallization of the two kinds of spherulites microscopically in
order to obtain further evidence to aid in understanding the
differences observed.   We found that different kinds of nucleation
apparently occurred in different samples.   Some samples gave
spherulites of uniform size suggesting instantaneous, hetero-
geneous nucleation.   Other samples gave spherulites of variable
size such as would be expected from sparodic, homogeneous
nucleation.   Only these latter samples were used in the compari-
son made below in determinations of overall rates of crystalli-
zation.   The number of nuclei that appear in the field of view
also varies considerably from sample to sample and even from
area to area in the same sample.   Nevertheless, throughout
our studies it appears that spherulites form more readily from
Type II spherulites, that is, from more optically active polymer.

Growth Rates of Spherulites.   As shown in Figure 6, both
types of spherulites grow in the typical fashion observed many
times for spherulites: namely, linearly with time.   In the par-
ticular examples illustrated it was not possible to follow the
growth of 39A for as long as 329C was studied because impinge-
ment occurred sooner.   The fact that a single straight line can
be drawn for both types is fortuitous in as much as the particu-
lar spherulites examined happened to have the same diameter
at the same initial time.   But it is significant that the growth
rates determined from the slope of the line do not appear to be
different.   Both are of the order of 1.5 microns per minute.
If either type grows faster, the data in Figure 6 suggests that
Type II spherulites grow faster.

Overall Rates of Crystallization.   We divided our studies of
overall rates of crystallization into two areas: reproducibility
studies and determination of the temperature of maximum rate
of crystallization.

1. Reproducibility. As stated above, observations of the
overall rate of crystallization of crystalline polyepichlorohydrins
turned out to be a particularly sensitive was of characterizing
polyepichlorohydrins. Thus, we have taken special care to
check the reproducibility of our dilatometric observations of
overall rates. We have carried out three different kinds of anal-
ysis to check reproducibility. First, we showed that the data
from any given dilatometer were superimposable over the whole
range on repeated runs at the same temperature. This was true
for both "slow" and "fast" crystallizing polymers. Second, we
demonstrated that two different samples of the same polymer in
two different dilatometers gave reproducibility of $t_{\frac{1}{2}}$ measure-
ments over the whole temperature range studied. Finally, we
showed that good superposition is observed on shifting curves
obtained at different crystallization temperatures. Such repro-
ducibility is typical of dilatometric results on crystalline poly-
mers in general ($\underline{11}$). From these studies we conclude that
crystalline polyepichlorohydrin crystallizes in a normal repro-
ducible manner. The variations reported below are due to
differences in the polymers.
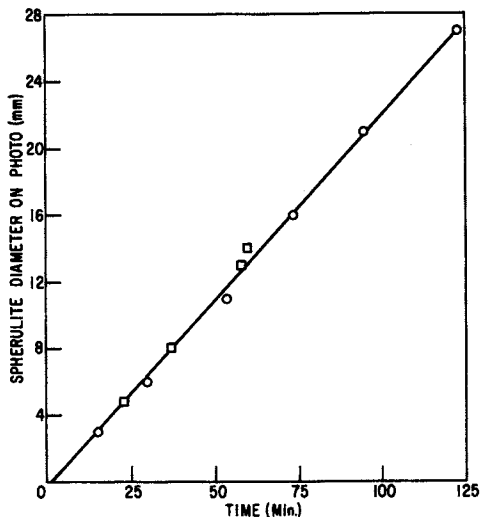
*Figure 6. Comparison of spherulite growth
rates at 50°C after melting at 150°C. ○ = Type
I spherulites from 329C. □ = Type II spher-
ulites from 39A.*

2.   Determination of the maximum rate of crystallization.
The rate of crystallization of any given polymer is very sensitive
to the temperature at which the measurement is carried out (11).
It goes through a maximum at a fairly well-defined temperature.
Above that temperature, as the melting temperature is approach-
ed, the rate of nucleation is lower and lower and the overall rate
decreases.   Below that temperature as the glass transition temp-
erature is approached, the melt becomes increasingly viscous,
the rate of diffusion of the polymer chains decreases, and a slow-
er overall crystallization rate is obtained.   Therefore, in order
to make meaningful comparisons of polymers prepared under
different conditions it was necessary to determine the effect of
temperature on the crystallization rate of epichlorohydrin.   We
have examined the rate of crystallization of well over 200 differ-
ent polyepichlorohydrins at at least three different temperatures.
Some of our more thorough studies are illustrated in Figure 7.
As the figure illustrates, the maximum rate of crystallization
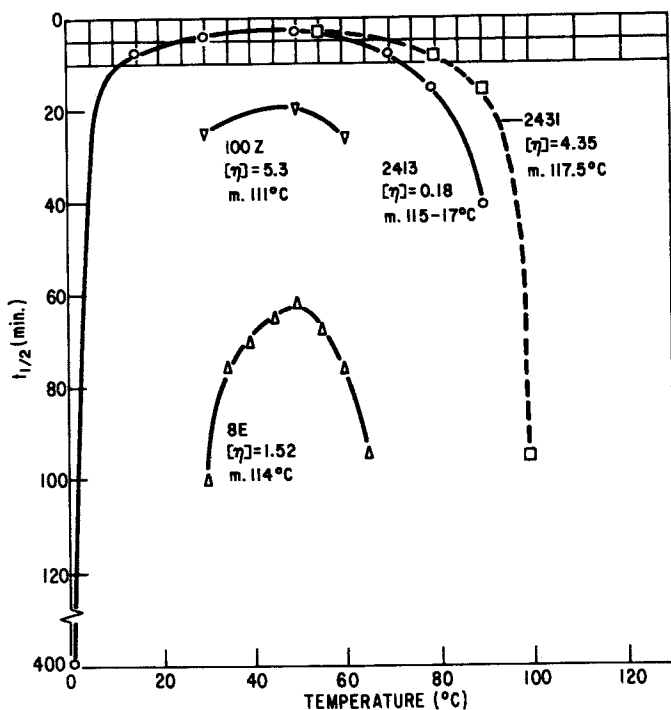
Figure 7.   Effect of temperature on the crystallization rate of poly-
epichlorohydrin

(lowest $t_\frac{1}{2}$) occurs at about 50°C.

   There are several interesting and unusual features about crystallization rates of polyepichlorohydrin illustrated in Figure 7. Evidently, there are not one or even two polyepichlorohydrins. Instead there is a whole family of crystalline polyepichlorohydrins. There are the "slowly crystallizing" members of the family like 8E. These polymers have a relatively sharp maximum and an intermediate melting temperature. They crystallize too slowly and have too narrow a processing range to be useful for, say, molded articles. There are the members with an "intermediate" rate of crystallization like 100Z. These polymers surprisingly have a somewhat lower melting temperature. They too have a rather sharp maximum in the rate versus temperature curve and would not be expected to process well over a very broad range. Finally, there are the "fast crystallizing" members, illustrated by 2413 and 2431. These polymers have the highest melting temperatures we have observed so far and a broad maximum in rate versus temperature curve that suggests a broad processing range. The "fast crystallizing" polymers also have the highest optical rotations that we observed. They crystallize in the form of Type II spherulites. We have studied many examples of each type of polymer.

   From the curves and the intrinsic viscosities given for the polymers, it appears that in the range studied, intrinsic viscosity does not have an important effect on crystallization rate. An apparent anomaly illustrated by the data in Figure 7 is the relationship or rather lack of relationship between the observed rate and the melting temperature. Usually a lower melting temperature corresponds to greater structural irregularity and slower crystallization rate (11). In this case 329C has a lower melting temperature than 8E and yet crystallizes much more rapidly. These observations are discussed below and an explanation is given.

   3. Overall crystallization rate of blends of "fast" and "slow" crystallizing polymers. We obtained further evidence that the greater ease of nucleation of optically active polymer into Type II spherulites is responsible for the observed increase in crystallization rate by studying solution blends of 2413 and a nonoptically active polyepichlorohydrin. We found that addition of only 6% of 2413 reduced the $t_\frac{1}{2}$ at 50°C of the "slow" polymer from 32 min to less than 10 min.

Discussion and Conclusions

Polymerization of monomers like epichlorohydrin, $\overline{OCH_2 \underset{*}{C}H-}$ (CH₂Cl), leads to polymers which theoretically can have many different isomers. As a result of the very elegant work of Price and coworkers (12) and of Vandenberg (13) in their mechanistic studies of the ring opening polymerization of epoxides, the task of analyzing these polymers is somewhat simplified. For example, head-to-head, tail-to-tail, and head-to-tail polymers are all theoretically possible, but only head-to-tail need to be considered for the following reasons. We know that polymerization occurs by ring opening in which the bond between oxygen and the carbon labelled with an asterisk (the asymmetric carbon atom) is broken. Furthermore, we know from studies with optically active propyleneoxide that polymerization occurs by inversion at the asymmetric carbon and that no racemization occurs on polymerization. We also know that even when optically active monomer is used, some amorphous polymer is produced. Price and coworkers (7) have found that these irregularities are largely, if not entirely units of head-to-head, tail-to-tail structure formed as a result of some reaction involving cleavage of the bond corresponding to the CH₂-O bond in epichlorohydrin. In addition we know that all crystalline polyepoxides known to date are isotactic. Syndiotactic polyethers remain a product of the future.

Although similar studies have not been reported for polyepichlorohydrin, there is no reason to expect any differences in mechanism of polymerization for this epoxide. It can be assumed that polymerization leading to crystalline polymer occurs predominantly by inversion at the asymmetric carbon atom and results in head-to-tail placement of the monomer. Mainly isotactic polymer will be formed. Our studies and previous work have born this out (8, 9, 14, 15).

The results of this study further reveal that the crystalline polyepichlorohydrin we have studied consists of isotactic sequences that can crystallize in the form of two different kinds of spherulites. We have shown that the two kinds of spherulites can cocrystallize. At present our educated guess is that all the polymers we have examined contain either Type I or a mixture of Type I and Type II spherulites in varying proportions. The polymers that crystallize most rapidly and that have the highest melting temperatures have some optical activity and their films contain predominantly Type II spherulites. We conclude that the Type II spherulites are obtained from optically active polymer sequences. We do not mean to imply that all sequences in these

polymers have the same comformation. We merely wish to
suggest that enough of an excess of one enantiomer has polymer-
ized to give a measurable rotation and that the overall structure
of these polymers is more regular. We suggest that Type I
spherulites are obtained from racemic polymer that shows little
or no optical rotation.

It is unfortunate from a theoretical point of view that our
conclusions cannot be definitely related to the degree of optical
activity in the polymer. To accomplish this we would need to
prepare polymer of known and variable amounts of optical rota-
tion, preferably from optically active monomer. This we have
not done. However, we believe that our results are sufficiently
conclusive even without this comparison. Polymers of lower
melting temperature can crystallize more rapidly than those
having a higher melting temperature because they are structur-
ally and morphologically different. Racemic polymer crystal-
lizes in the form of Type I spherulites. As long as the polymer
has a sufficiently low concentration of atactic sequences, fairly
rapid crystallization can occur. However, the rate will be slow-
er than that of polymers that lead to Type II spherulites. The
free energy barrier to nucleation of Type II spherulites seems to
be lower. Polymer containing some optically active sequences
crystallize most rapidly primarily because the rate of nucleation
is greater. An increased rate of nucleation combined with the
demonstrated potential of cocrystallization of Type I and Type II
spherulites also provides an explanation for the usefulness of
"fast" crystallizing polyepichlorohydrin in increasing the rate
of crystallization of "slow" crystallizing polyepichlorohydrin.

In fact, there is a direct parallel to some of our findings
reported in the case of crystalline polypropyleneoxide, which
is structurally the same as polyepichlorohydrin except that the
chlorine atom on the pendant methylene substituent is replaced by
a hydrogen atom. Two kinds of spherulites have been observed
in crystalline polypropyleneoxide (14). The two were not shown
to cocrystallize.

Acknowledgement

Summary

    The purposes of this study were to determine what chemical
and physical structures are present in polyepichlorohydrin and
to correlate these structures with the crystallization rates ob-
served microscopically and dilatometrically. Crystallization
rates were shown to be an extremely sensitive way of character-
izing these polymers. For example, the study revealed that the
crystalline polyepichlorohydrins examined consisted of isotactic
sequences that can crystallize as two different kinds of spheru-
lites, arbitrarily called Type I and Type II. The two types can
cocrystallize. The polymers that crystallize most rapidly and
that have the highest melting temperature have some optical
activity. Their films contain predominantly Type II spherulites.
Polymers that contain Type I spherulites melt lower and show
little or no optical activity. These polymers are racemic
mixtures.

Literature Cited

1. Bekkedahl, N., J. Research Nat'l. Bur. Standards, (1949),
    43, 145.
2. Tsuruta, T., Inoue, S., Yoshida, N., and Furukawa, J.,
    Makromol. Chem., (1962), 53, 215.
3. Tsuruta, T., Inoue, S. Yoshida, N., and Furukawa, J.,
    (1962), 55, 230.
4. Inoue, S., Tsuruta, T., and Yoshida, N., Makromol. Chem.,
    (1964), 79, 34.
5. Tsuruta, T., Inoue, S., Ishimori, M., and Yoshida, N.,
    J. Polym. Sci., C, (1963), (No. 4), 267.
6. Tsuruta, T., Macromolecular Reviews, J. Polym. Sci., D,
    (1972), 179.
7. Price, C. C., and Osgan, M., J. Am. Chem. Soc., (1956),
    78, 4787.
8. Kambara, S. and Takahashi, A., Makromol. Chem., (1963),
    63, 89.
9. Richards, J. R., Ph. D. Thesis, University of Pennsylvania,
    1961, Part III, University Microfilms, 61-3547.
10. Magill, J. H., Makromol. Chem., (1965), 86, 283.
11. Mandelkern, L., "Crystallization of Polymers," McGraw-
    Hill Book Co., New York, N. Y., 1964.
12. Price, C. C., and Spector, R., J. Am. Chem. Soc., (1965)
    87, 2069.
13. Vandenberg, E. J., J. Polym. Sci., A-1, (1969), 7, 525.

14. Perego, G., and Cesari, M., Makromol. Chem., (1970),
    133, 133.
15. Hughes, L. J., Dangieri, T. J., Watros, R. G., and Alling,
    L. J., Polymer Preprints, (1968), 9, 1126.

6

X-ray Structural Analysis of Crystalline Polymers

RICHARD J. CELLA* and ROBERT E. HUGHES

Department of Chemistry, Cornell University, Ithaca, N. Y. 14853

The determination of the atomic structure of crystalline polymers by wide angle X-ray diffraction techniques presents formidable problems which cannot conveniently be treated by the conventional methods of structure analysis. Consequently, existing methods need to be modified and new approaches to the problem developed to extract the maximum amount of structural information from the available experimental data. The nature of the problems encountered will be discussed in this paper, together with a description of methods that have been utilized to overcome them. A subsequent paper will deal with the applications of these methods to the determination of the molecular structure of several crystalline polyethers.

Characteristically, crystals composed of long chain molecules provide much less diffraction data than do single crystals of low molecular weight substances, and often this data is of very poor quality. This is a direct consequence of the limited long range order exhibited by crystalline polymers; small crystallite size, imperfect crystallite orientation, structural defects, and the presence of a non-crystalline component in the sample all contribute to the rapid attenuation of the available data.

The first of these deficiencies, the limited long range three dimensional order, is the single most important factor involved in creating the difficulties encountered in the structural analysis of macromolecular materials. The great length of the polymer chains and the concomitant possibilities for chain entanglements prohibit the molecules from ordering themselves

*E. I. du Pont de Nemours and Company, Inc., Wilmington, Delaware 19898

over an extended region with a high degree of regularity. Furthermore, the individual molecules themselves are not perfectly regular, and often contain intrinsic structural defects such as steric inversions of asymmetric sites, chain branches, and crosslinks. Such defects do not necessarily prevent the chain from becoming incorporated into a crystalline domain; oftentimes a molecule containing a minor structural imperfection will manage to pack reasonably well into the structure, thereby enlarging the crystalline domain but at the same time destroying the perfect regularity of the assemblage.

Another type of packing defect occurs when a "multi-state" structure is possible. This happens when each successive chain may enter the crystallite in any of several spatially different conformations. Thus, if a chain may be accommodated into the crystal lattice in either an "up" or a "down" position a two-state structure will result; if a side group may assume any of three different angular positions in the solid phase, then a three-state structure is possible. These defects may occur sporadically with low probability or they may occur randomly each time the opportunity presents itself. In the latter case it is likely that a statistical distribution of several different models will have to be invoked in order to obtain satisfactory agreement to the experimental data.

Each of the structural defects described will tend to attenuate the intensity of the diffracted beam at higher scattering angles, and a situation is soon reached in which the scattered beam is of lower intensity than the background scattering. This fall-off of the data at higher scattering angles is similar to that caused by thermal motion and atomic scattering, but these phenomena also occur in non-polymeric systems and can be corrected for rather easily.

The cylindrically symmetric distribution of crystallites about the fiber axis also leads to a decrease in the quantity of data obtainable, although for an entirely different reason. The rotational character of the diffraction pattern causes all lattice plans whose reciprocal lattice points have the same ξ and ζ coordinates to diffract into the same point in space, irrespective of the value of their angular reciprocal lattice coordinate ($\underline{1}$). This leads to an overlapping of reflections which would otherwise be distinguishable were it not for the cylindrical symmetry of the polymeric fiber. Thus, in many instances two or more independent reflections produce only one observable diffraction maximum.

Isotactic poly(propylene oxide), PPO, provides a numerical example of the above considerations. Using copper K_α radiation, this polymer should in principle generate approximately 400 unique reflections (regardless of whether or not their intensities are large enough to be measurable above background scattering) out to a resolution of 0.77 Å. In practice, an actual fiber of PPO yielded data out to only 0.97 Å, thereby reducing the potential number of data to 178 reflections; for this purpose, each allowable reflection contributing to an overlapping group of reflections is counted separately, and a reflection is counted whether or not it is of sufficient intensity to be detectable. When the rotational symmetry of the fiber specimen is taken into consideration and overlapping reflections are counted as one observation only 94 observations are to be expected. Of these, only 60 are of sufficient intensity to be experimentally measurable above the background scattering. This example dramatically illustrates that at best less than 25% of the theoretically allowable data may be observed, and of these less than two-thirds actually are observed. Furthermore, it should be emphasized that isotactic PPO is a polymer which yields a relatively large amount of data, and many examples could be quoted in which an even smaller fraction of the data is actually obtained.

The poor quality of the data obtained is a consequence of the imperfect alignment of the crystalline domains with respect to the fiber axis of the sample. The crystallites are not perfectly uniaxially oriented, and this misorientation causes the reflections from polymeric substances to appear as elongated arcs rather than as sharp, well defined spots. Measuring the total, or integrated, intensity of these arcs proves to be extremely difficult, and even the simpler task of determining the peak intensity is subject to large error (2). Furthermore, all crystalline polymers contain a certain amount of non-crystalline material which produces only diffuse scattering and has the effect of increasing the background level, thereby rendering even more difficult the process of measuring intensities. These two factors taken together, therefore, are responsible for the poor quality of the data when compared with the accuracy achieved in single crystal analyses.

The characteristic features of polymer structures described above were discussed at some length because they are almost wholly responsible for the difficulties encountered in the structural analysis of these materials. Many of the powerful methods existent for single

crystal studies are inadequate when dealing with such
a limited amount of data, and the poor quality of the
data merely serves to intensify the problem. Thus,
techniques such as direct methods, Patterson synthesis,
or isomorphous replacement are not applicable to poly-
mer crystal structure analyses, and resort must be made
to trial and error methods to select a reasonable
starting structure which must subsequently be refined.

    The standard technique for refining a proposed
structure is a least squares analysis in which the
structural parameters are systematically varied so as
to produce the best agreement between the calculated
diffraction pattern and the experimental data. When
applied to the determination of polymer structures,
however, this method suffers from two deficiencies.
The first of these is that a least squares refinement
will converge to the nearest minimum in the multi-
dimensional parameter space, and unless the proposed
starting model is quite close to the correct structure
this will not be the global minimum. Thus, the least
squares approach will often converge to an incorrect
structure.

    The second shortcoming of the least squares method
lies in the poor data to parameter ratio generally
encountered in polymer structures. Typically, the
number of parameters to be refined in a polymeric
structure is of the same order of magnitude as that
found in small molecule structures, yet there is much
less data with which to work. Consequently, if one
independently refines the atomic positional coordinates
in addition to scale factors and thermal parameters the
results will be statistically meaningless. Thus, for
these types of structures it would be beneficial to
possess computational methods which do not allow all of
the atomic coordinates to vary independently, but
rather which couples them in a meaningful way to reduce
the number of parameters involved.

    The preceding discussion has described the inade-
quacy of standard crystallographic methods when applied
to the determination of polymer structures. The lack
of an analytical method of phase determination makes
the solution of these structures a matter of trial and
error; there is no alternative but to postulate various
models and compare the theoretically calculated inten-
sities to those actually observed. It would be useful,
therefore, to develop computational techniques whereby
physically realistic models may be systematically gen-
erated and evaluated in a straightforward, efficient
manner. The problem divides itself naturally into two
distinct parts: (1) the calculation of geometrically

and energetically allowable structures, and (2) the
refinement of these structures to produce the best
agreement to the available X-ray data.

Geometric Considerations

     It is not possible to rely solely on geometric
arguments to determine a polymer structure; ultimately,
recourse must be made to variational methods. Geomet-
ric constraints, however, are extremely useful in
eliminating from consideration vast numbers of physi-
cally unreasonable structures, thereby reducing the
number of trial models which need to be investigated.
A survey of the many substances whose molecular struc-
tures have been established indicates that certain
structural features, namely bond lengths and bond
angles, assume values which are essentially constant in
any series of related compounds. On the other extreme,
the internal rotation angles about single bonds are
free to assume a wide range of values, and in most
cases it is not possible a priori to assign values to
these parameters with any degree of certainty (the
relative invariance of some molecular parameters in
relation to others is of course a direct consequence of
the energetics involved in effecting changes in their
values, but the problem is best treated from a purely
geometric point of view). Thus, to a good approxima-
tion, it is possible to assume values for the bond
lengths and bond angles and to use these values in the
geometrical determination of the internal rotation
angles. Because of the small amount of diffraction
data available this practice is universally followed in
polymer studies, and it is necessary in order to reduce
the analysis to manageable proportions. If the data
allows, it will be possible to vary these values
slightly at a later stage in the structural determina-
tion.

     Consider a linear polymer molecule whose skeletal
atoms are numbered 0, 1, ..., N, and represented by C_0,
C_1, ..., C_N, successively from one end of the chain to
the other. Let $\vec{r}_i$ represent the vector from C_{i-1} to C_i
and let ϕ_i represent the supplement of the angle
between $\vec{r}_i$ and $\vec{r}_{i+1}$. The angle τ_i between the two
planes determined by $\vec{r}_{i-1}$ and $\vec{r}_i$, and $\vec{r}_i$ and $\vec{r}_{i+1}$,
respectively, is measured from the cis position in the
direction of clockwise rotation of $\vec{r}_{i+1}$, facing in the
direction of $\vec{r}_i$.

     The chain skeleton of a helix with two backbone
atoms in the repeating unit may be completely described
by specifying the two types of bond lengths, $b_1 =$

$|\vec{r}_1| = |\vec{r}_3| = \ldots = |\vec{r}_i| = \ldots$ and $b_2 = |\vec{r}_2| = |\vec{r}_4| =$
$\ldots = |\vec{r}_{i+1}| = \ldots$, the two types of bond angles $\phi_1 =$
$\phi_3 = \ldots = \phi_i = \ldots$ and $\phi_2 = \phi_4 = \ldots = \phi_{i+1} = \ldots$, and
the two types of dihedral angles $\tau_1 = \tau_3 = \ldots = \tau_1 =$
$\ldots$ and $\tau_2 = \tau_4 = \ldots \tau_{i+1} = \ldots$. Alternatively, the
helical conformation is uniquely determined by specify-
ing the bond lengths, the bond angles, the rotational
angle about the helix axis, θ (unit twist), and the
translational distance along the helix axis per repeat
unit, d (unit translation); there is only one set of
dihedral angles, τ_1 and τ_2, compatible with these six
quantities.

Similarly, the skeletal conformation of a three
atom helix is uniquely determined by specifying the
following quantities: $b_1 = |\vec{r}_1| = \ldots = |\vec{r}_i| = \ldots$,
$b_2 = |\vec{r}_2| = \ldots = |\vec{r}_{i+1}| = \ldots$, $b_3 = |\vec{r}_3| = \ldots =$
$|\vec{r}_{i+2}| = \ldots$, $\phi_1 = \ldots = \phi_i = \ldots$, $\phi_2 = \ldots$, $\phi_{i+1} =$
$\ldots$, $\phi_3 = \ldots = \phi_{i+2} = \ldots$, $\tau_1 = \ldots = \tau_i = \ldots$, $\tau_2 =$
$\ldots = \tau_{i+1} = \ldots$, and $\tau_3 = \ldots = \tau_{i+2} = \ldots$. In this
case, however, a knowledge of the bond lengths, bond
angles, θ and d is insufficient to determine a unique
triad $\{\tau_1, \tau_2, \tau_3\}$ which is consistent with the given
geometric constraints. One of the three dihedral
angles (usually chosen to be τ_2) must be specified as
an independent variable, and for a given value of this
angle the values of the other two dihedral angles are
unique.

Various relationships have been published giving
θ and d as functions of the bond lengths, bond angles
and dihedral angles for helices containing as many as
six backbone atoms in the repeating unit (3-8). While
useful for calculating the unit twist and unit repeat
for a particular helical model, these relationships are
of limited use in structural analysis for θ and d are
usually known quantities, while little or nothing is
known about the dihedral angles. Cognizant of this,
Nagai and Kobayashi have derived complex analytical
expressions explicitly giving the rotational angles as
functions of the other helical parameters (9). In the
case of a three atom helix these formulas specify τ_1
and τ_3 as functions of the bond lengths, bond angles,
θ, d and τ_2.

A computer program, DIHED, was written which would
solve the necessary matrix equations and calculate all
allowable helical conformations consistent with the
imposed stereochemical constraints. Given bond lengths,
bond angles, θ and d, the program systematically varies
τ_2 over any preselected range and calculates the corre-
sponding values of τ_1 and τ_3; the coordinates of the
helical backbone are computed in cylindrical and

Cartesian coordinates. Several examples of the program
output are shown graphically in Figure I. Each curve
is the locus of all possible dihedral angles, $\{\tau_1, \tau_2,$
$\tau_3\}$, for the highly symmetric three atom helix with
$b_1 = b_2 = b_3 = 1.54$ Å, $\phi_1 = \phi_2 = \phi_3 = 109.5°$, and $\underline{d} =$
3.60 Å; the curves correspond to $\theta = 180°$, $120°$, and
$90°$. The values of τ_1 and τ_3 are read as the intersec-
tions of the curve with a vertical line drawn through
a given value of τ_2. Thus, for the 4_1 helix, $\{\tau_2 =$
$140°$, τ_1 (or τ_3) = $161°$, τ_3 (or τ_1) = $126°\}$ is a solu-
tion of the geometric problem. The right and left hand
extremes of the curve (i.e., $\tau_2 = 121°$ or $162°$) repre-
sent those conformations for which $\tau_1 = \tau_3$. For τ_2
greater than $162°$ or less than $121°$ no solutions exist
and these regions of the space may be excluded from
further consideration.
        It is apparent that such an analysis when used in
conjunction with chemically reasonable values of the
b_i's and ϕ_i's can prove extremely useful. Although no
unique helical conformation results, the number of
possibilities to be investigated is drastically reduced.

Energetic Considerations

        The above geometric arguments are based on non-
interacting point atoms; by introducing the side chain
substituents and replacing the point atoms by real
atoms it becomes possible to use energy considerations
to further limit the number of plausible models (10-14).
Energy calculations may be conducted at various levels
of sophistication ranging from hard sphere atoms with
square well potentials to "soft" atoms using a more
realistic potential function. Furthermore, one may
include torsional and vibrational energies, polar
interactions, hydrogen bonding and various other terms
in the calculation.
        In this study, an elegant energy minimization com-
puter program, PACK, was employed to calculate the
total packing energies of the structures under investi-
gation. The program, belonging to Professor H.
Scheraga, calculates the total energy of an assemblage
of molecules by taking into account the following con-
tributions to the total energy of the system:
        (a) non-bonded interactions
        (b) polar interactions
        (c) torsional barriers
        (d) hydrogen bonding
        (e) bond angle bending and bond stretching

In addition, the program may be used to generate an
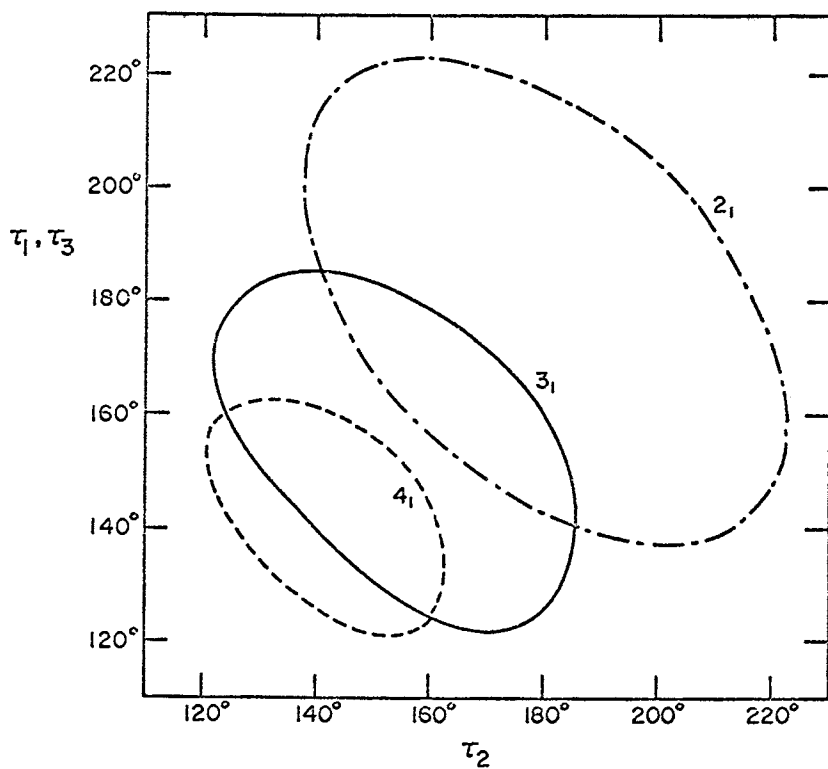
Figure 1.   Dihedral angles τ_1 and τ_3 as a function of τ_2 for a hypothetical three-atom helix

energy contour map as a function of any two structural parameters. Although a comprehensive discussion of this program is beyond the scope of this paper, items (a) and (b) listed above require further explanation.

The program uses a "6-12" potential to calculate the non-bonded atomic interactions. The pairwise potential energy, $U(r)$, is given as a function of the internuclear distance, $\underline{r}$, by:

$$U(r) = \epsilon_0 \left(\frac{r}{r_0}\right)^{12} - 2\,\epsilon_0 \left(\frac{r}{r_0}\right)^{6}$$

where r_0 is the equilibrium internuclear distance and ϵ_0 is the interaction energy at r_0. The values of ϵ_0 and r_0 to be used for a given atom pair are determined empirically by studying established structures and fitting the energetically minimized structure to the actual structure by varying ϵ_0 and r_0.

Polar interactions may be included either by using a monopole approximation, which replaces polar bonds by point charges on the bonded atoms and then uses a Coulombic potential, or by the more involved treatment of del Re (15-16). The latter method uses a semi-empirical quantum mechanical approach to distribute partial charges throughout the molecule; it then uses a Coulombic potential to calculate the energies of various charge pairs.

When applied to the determination of crystal structures the program first generates the coordinates of the entire structural array in accordance with the given space group. It then calculates the packing energy by including all pairwise interactions (both polar and non-bonded), including any desired contributions from specific terms such as torsional barriers. The structure is changed by varying any predetermined molecular or structural parameters and the energy is recalculated. By proceeding in this manner the program selects the structure which is of lowest energy using the given degrees of freedom. Even though the absolute energies calculated may not be exact, the relative energies are extremely useful in determining favorable structures.

By applying energy calculations to those structures which are geometrically allowable it is possible to reduce the number of probable structures to manageable proportions. In general, two or more structures will remain which are both energetically and geometrically reasonable and the distinction among them must be made on the basis of the X-ray data. If successful, however, the utilization of geometric and energetic constraints will generate trial structures which are

quite close to the actual structure, thereby insuring
the efficiency of the structural refinement process.

Structural Refinement

An extremely versatile computer program, POLYMIN,
which is designed specifically for the structural
refinement of crystalline polymers has been developed.
It incorporates several features not found in standard
refinement programs and thereby eliminates many of the
difficulties encountered in their use. The main advan-
tages of the program are that it:

(a)   uses line search rather than least squares
        minimization
(b)   maintains geometric and stereochemical
        constraints during the refinement
(c)   utilizes overlapping and unobserved data
        in the refinement process.

By using a line search minimizer rather than
least squares the program does not require that the
structure to be refined be close to the correct struc-
ture in order to insure convergence. Unlike a least
squares treatment, the line search refinement will not
of necessity converge to the nearest minimum, and thus
it has a higher probability of finding the global
minimum. The quantity being minimized, however, is the
same as that being minimized in the least squares
approach:

$$\Phi = \sum_m w_m [I_o(m) - I_c(m)]^2 = \sum_m w_m [\Delta I(m)]^2$$

with

w_m = statistical weight of the mth observation = $1/\sigma_m^2$

σ_m = standard deviation of the mth observation

$I_o(m)$ = corrected observed intensity of the mth observation

$I_c(m)$ = calculated intensity of the mth observation

The main advantage of using this program, however,
is that it enables a refinement to be carried out sub-
ject to geometric constraints. By varying atomic
coordinates a least squares procedure simultaneously
changes bond lengths, bond angles, and dihedral angles.
As stated previously, the minimal amount of data
obtainable from polymeric structures makes it desirable
to fix the bond lengths and bond angles during the
course of a structural determination in addition to the
helical parameters θ and d. Consequently, while a
least squares refinement treats the atomic positions as

independent parameters, the line search refinement
program couples the movement of the atoms, thereby
preserving the geometrical nature of the problem.
POLYMIN has the ability to refine a structure using any
or all of the following parameters:
    (a)   scale factors
    (b)   rigid body rotations and translations
    (c)   isotropic thermal parameters (individual or
          overall)
    (d)   bond lengths
    (e)   bond angles
    (f)   dihedral angles
    (g)   atomic multiplying factors
During the course of a refinement the parameters (a),
(b), (c), and (f) would normally be varied; if the
data/parameter ratio is favorable it would be possible
to refine using (d) and (e) as additional variables.
The atomic multiplying factors, (g), are useful for
studying multi-state systems, where it is desirable to
determine the relative abundances of each of several
different models.

    The program is extremely well suited for the
determination of polymer structures in its treatment of
unobserved and overlapping data. Standard least
squares treatments assume that only one reflection con-
tributes to any given observation; due to the cylindri-
cal symmetry of fiber diffraction patterns a great many
of the observations are actually superpositions of two
or more reflections. Under these circumstances the
observed intensity must be compared to the sum of the
contributing calculated intensities. Thus, if $\underline{q}$ inde-
pendent reflections contribute to the $\underline{m}^{th}$ observation,
then

$$I_c(m) = \sum_q I_c^q(m)$$

and

$$\Delta I(m) = I_o(m) - \sum_q I_c^q(m)$$

where $I_c^q(m)$ is the calculated intensity of the qth
reflection contributing to the $\underline{m}^{th}$ observation.

    The treatment of unobserved data is of necessity
different from that given to observed data. For these
data there is only a threshold intensity with which to
compare the calculated value, and it becomes necessary
to define a number, $\underline{f}$, such that $fI_o(m)$ is the most
probable value of the observed intensity, where $I_o(m)$
is now the minimum intensity which the $\underline{m}^{th}$ observation
would have to display in order to be detectable above
background scattering (it has been shown that $\underline{f} = 0.33$

for a centrosymmetric space group). If the calculated
intensity is lower than the threshold value then the
agreement is considered to be perfect and the contribu-
tion to the least squares residue, Φ, is taken to be
zero. If, however, the calculated intensity is larger
than the threshold value then Φ is incremented by the
amount $w_m[I_c(m) - fI_o(m)]^2$. Thus, intensities which
are larger than the observable threshold values are
used in driving the refinement to the correct structure.
     It has become customary in X-ray crystallography
to describe the agreement between the observed and
calculated structure factors by using the residual
index, R_F, defined by

$$R_F = \frac{\sum_n | \, |F_o(n)| - |F_c(n)| \, |}{\sum_n |F_o(n)|}$$

where $\underline{n}$ is the total number of reflections (not the
number of observations!). For purposes of computing R_F
POLYMIN divides $I_o(m)$ up into $\underline{q}$ parts in the ratio of
the contributing calculated intensities. By taking the
square root of these "observed" and calculated inten-
sities $|F_o(n)|$ and $|F_c(n)|$ respectively are obtained
and used in the calculation of R_F. The terms contribu-
ting to the numerator and denominator of the residual
index are as follows:
     (1) For observed reflections $||F_o(n)| - |F_c(n)||$ is
added to the numerator and $|F_o(n)|$ is added to the
denominator.
     (2) For unobservable reflections for which
$|F_o(n)| \geq |F_c(n)|$ the agreement is taken to be exact and
nothing is added to either the numerator or the denomi-
nator of R_F. These reflections are omitted from the
calculation because their inclusion could result in a
misleadingly low value for R_F.
     (3) For unobservable reflections for which
$|F_o(n)| < |F_c(n)|$ the numerator is incremented by
$||F_c(n)| - f^{\frac{1}{2}}|F_o(n)||$ and the denominator is incre-
mented by $f^{\frac{1}{2}}|F_o(n)|$.
     The calculation of R_F in this fashion, while
slightly artificial, leads to values for the residual
index which can be meaningfully compared to those
values found in the literature. When used in conjunc-
tion with the large body of crystallographic knowledge
available this number provides a useful criterion with
which to assess the correctness of the structure. By
convention, R_F is normally calculated using only
observable reflections and it should be pointed out
that adherence to items (2) and (3) above will produce
a value of R_F which will be at best equal to that

TABLE I

Contributions to the Least Squares Residue and Residual Index

	Contribution to Φ	Contribution to R_F	
		Numerator	Denominator
Observable Reflections	$= w_m[I_o(m) - \sum_q I_c^q(m)]^2$	$= ||F_o(n)| - |F_c(n)||$	$= |F_o(n)|$
Unobservable Reflections	$= w_m[I_o(m) - f^2\sum_q I_c^q(m)]$ if $\sum_q I_c^q(m) > I_o(m)$ $= 0$ if $\sum_q I_c^q(m) \leq I_o(m)$	$= ||F_c(n)| - f^{\frac{1}{2}}|F_o(n)||$ if $|F_c(n)| > |F_o(n)|$ $= 0$ if $|F_c(n)| \leq |F_o(n)|$	$= f^{\frac{1}{2}}|F_o(n)|$ if $|F_c(n)| > |F_o(n)|$ $= 0$ if $|F_c(n)| \leq |F_o(n)|$

calculated in the usual way and will most likely be slightly larger. It was felt, however, that the unobserved reflections are of sufficient importance to demand their inclusion into R_m when the calculated structure factors are larger than the threshold values. In other words, any structural model which predicts intensity values above the threshold intensity for very many of the unobserved data must of necessity be incorrect. In single crystal work, where thousands of reflections are measurable, this criterion is unnecessary, since any structure which predicts the observable data will very likely also predict the unobservable data. In analysis involving only a limited number of data, however, this may not be the case and such missing data can then give positive structural information.

Conclusion

This paper has described in very general terms the unique problems encountered in the determination of the molecular packing in polymeric crystals. Standard crystallographic procedures lose their utility when dealing with such problems, and additional information, such as stereochemical constraints and packing energies, should be brought to bear in the problem. Finally, a method of structural refinement which is especially suited to polymeric structures should be employed in place of classical least squares methods. A subsequent paper will deal with the application of these principles and techniques to the determination of the crystal structures of several crystalline polyethers.

Acknowledgment

Literature Cited

1.   Buerger, M., "X-Ray Crystallography," John Wiley
     and Sons, Inc., New York, N.Y. (1962).
2.   Cella, R. J., Lee, B., and Hughes, R. E., Acta
     Cryst., (1970), A26, (6).
3.   Miyazawa, T., J. Polym. Sci., (1961), 55, 215.
4.   Hughes, R. E. and Lauer, J. L., J. Chem. Phys.,
     (1959), 30 (5), 1165.
5.   McCullough, R., Polymer Letters, (1965), 3, 509.

6.   Shimanouski, T. and Mizushima, S., J. Chem. Phys.,
     (1955), 23 (4), 707.
7.   Sugeta, H. and Miyazawa, T., Biopolymers, (1967),
     5, 673.
8.   Kijima, H., Sato, T., Tsuboi, M., and Wada, A.,
     Bull. Chem. Soc. Jap., (1967), 40, 2544.
9.   Nagai, K. and Kobayashi, M., J. Chem. Phys.,
     (1962), 36 (5), 1268.
10. Nemethy, G. and Scheraga, H., Biopolymers, (1965),
     3, 155.
11. Scott, R. A. and Scheraga, H., J. Chem. Phys.,
     (1966), 45, 2091.
12. Ooi, T., Scott, R., Vanderkooi, G., and Scheraga,
     H., J. Chem. Phys., (1967), 46, 4410.
13. DeSantis, P., Giglio, E., Liquori, A., and
     Ripamonti, A., J. Polym. Sci., (1963), 1383.
14. Liquori, A., J. Polym. Sci., (1966), Part C, No.
     12, 209.
15. Del Re, G., Theor. Chim. Acta, (1963), 1, 188.
16. Del Re, G., Rev. Mod. Phys., (1963), 34, 604.

Coordination Polymerization of Trimethylene Oxide

E. J. VANDENBERG and A. E. ROBINSON*

Research Center, Hercules Inc., Wilmington, Del. 19899

INTRODUCTION

General

The polymerization of oxetanes with cationic catalysts has been studied by many investigators.[1][2] Rose[3], in particular, first reported the homopolymerization of the parent compound, trimethylene oxide (TMO), with a Lewis acid catalyst, boron trifluoride. The use of coordination catalysts to polymerize oxetanes has been reported in the patent literature by Vandenberg.[4] In this work, Vandenberg polymerized oxetanes with the aluminum trialkyl-water-acetylacetone coordination catalyst (referred to as chelate catalyst) that he discovered for epoxide polymerization[5]. This paper describes the homo- and co-polymerization of TMO with these coordination catalysts. Specific TMO copolymers, particularly with unsaturated epoxides such as allyl glycidyl ether (AGE), are shown to provide the basis for a new family of polyether elastomers. These new elastomers are compared with the related propylene oxide-allyl glycidyl ether (PO-AGE) copolymer elastomers. The historical development and general characteristics of polyether elastomers and, in particular, the propylene oxide elastomers, are reviewed below.

Early Polyether Elastomer Studies

Charles C. Price played a pioneering role in the polyether elastomer field[6]. In 1948, as reported in his 1961 Chemist article, Price recognized that an oxygen chain atom would contribute greatly to chain flexibility and thus enhance elastomeric behavior, particularly since such polyethers should have low

101

cohesive energy between chains. At that time, he suggested that
poly(propylene oxide) should be a superior elastomer but unfor-
tunately soon found that the known methods of polymerizing pro-
pylene oxide gave only low polymers, not the desired high polymer.
However, he quickly devised a simple way around this impasse,
i.e., the polyurethane approach, which consisted of making a pro-
pylene oxide adduct of a polyol and then reacting this polyfunc-
tional polyether with a diisocyanate to give a polyether urethane
network. This approach to polyether elastomers was protected by a
U.S. patent[7] which recently received the Creative Invention
Award of the American Chemical Society. Although these polyether-
urethane elastomers proved to be of tremendous value in foam
rubber, the more conventional polyether elastomer based on a
cross-linkable high polymer remained unavailable. The latter
required the development of new catalyst systems for polymerizing
propylene oxide.

      The first improved catalyst for polymerizing PO to high
polymer was the iron catalyst of Pruitt and Baggett[8], i.e., the
simple reaction product of ferric chloride and propylene oxide.
Price and Osgan[9] recognized that this iron catalyst involved a
new polymerization mechanism--coordination polymerization--in
which the propylene oxide coordinates with the iron atom before
insertion into the propagating polymer chain. Price and Osgan
also discovered a new coordination catalyst for polymerizing
propylene oxide to high polymer, i.e., the aluminum isopropoxide-
zinc chloride catalyst system[10]. In subsequent work with this
coordination catalyst, Price described the copolymerization of PO
with an unsaturated epoxide, such as butadiene monoxide[11].

      In the same time period of Price's work, Hill, Bailey and
Fitzpatrick of Union Carbide Corporation developed some improved
catalysts for polymerizing ethylene oxide to high polymer[12].
These new catalysts included improvements on the very early sys-
tems of Staudinger, i.e., strontium, calcium, and zinc oxides and
carbonates[13], as well as some new, even better, systems based on
calcium alkoxides[14] and amides[15][16]. Bailey used the latter
systems in 1958 to make water-soluble ethylene oxide-unsaturated
epoxide copolymers[17]. Vulcanizates of these copolymers were
very water sensitive and thus not very useful in the conventional
elastomer area.

      In 1957, Vandenberg discovered some especially effective
coordination catalysts for polymerizing epoxides to high poly-
mers. Some of these new catalysts were the reaction products of
organo-compounds of aluminum, zinc, and magnesium with water[18].
An especially versatile system was the combination of organo-
aluminums with water and acetyl acetone. These new catalysts
were much better than earlier epoxide catalysts, giving generally
higher rates at lower temperatures, higher molecular weight, and
broader utility.

      As a result of finding these superior new catalysts,
Vandenberg was able to make many new high polymers from epox-

ides[5][18], including a wide spectrum of new polyether elastomers. Some of these new polyether elastomers have been commercialized, such as the epichlorohydrin elastomers available from Hercules Incorporated under the trademark HERCLOR®and from B. F. Goodrich Chemical Co. a licensee of Hercules Incorporated, under the trademark HYDRIN. Very early in this work, Vandenberg also made high molecular weight, largely amorphous propylene oxide-unsaturated epoxide copolymers and recognized in unpublished studies with A. E. Robinson their potential value as improved elastomers. Subsequently, Gruber et al.[19], of General Tire, published detailed properties of similar propylene oxide-unsaturated epoxide copolymer elastomers. Vandenberg also filed two patent applications on these copolymers. As a result of patent interferences involving the Hercules applications, a Carbide patent, and a General Tire application, the last a Price application, and extensive subsequent litigation, Vandenberg was awarded priority. Two patents have issued covering these unsaturated copolymers as new compositions of matter[20][21]. This new type of polyether elastomer is commercially available from Hercules Incorporated under the trademark PAREL®. PAREL elastomer is a sulfur-curable copolymer of propylene oxide and allyl glycidyl ether.

Some of the key properties of PAREL elastomer vulcanizates are summarized in Table I. They have excellent low temperature properties; excellent dynamic properties, which are much like those of natural rubber; good ozone resistance; and good heat-aging resistance. This interesting combination of properties is leading to substantial specialty markets in such applications as automotive engine mounts. Vulcanization and stabilization studies on PAREL elastomer, as well as additional specific properties of PAREL elastomer, are reported in this book by Boss.

The work described above for PO copolymers has been extended to the homo- and co-polymers of oxetanes, particularly TMO, and are reported in this paper.

Table I

KEY PROPERTIES OF PAREL ELASTOMER VULCANIZATES

- Excellent low temperature properties

- Excellent dynamic properties (like natural rubber)

- Good ozone resistance

- Good heat aging resistance

EXPERIMENTAL

Polymerization Studies

General. Reagents and general procedures for making

catalysts, for running polymerizations and for characterizing polymers were the same as described previously[5] unless otherwise noted. The chelate catalysts were prepared by the general procedure previously given for this catalyst[5]. The unmodified $Et_3Al-0.5$ H_2O catalyst was made by this same procedure, in the solvent noted in Table III, by omitting the acetyl acetone.

Monomers. Commercial, polymerization grade monomers were used as received. The sources were: ethylene oxide (EO), propylene oxide (PO), and epichlorohydrin (ECH) from Union Carbide Corp.; allyl glycidyl ether (AGE) from Shell Chemical Corp.; butadiene monoxide (BMO) from PPG Industries, Inc. (no longer commercially available); and 3,3-bis(chloromethyl) oxetane (BCMO) from Hercules Incorporated (no longer commercially available). The other monomers described below were finally purified by fractionation in a 25-50 plate column at a 25:1 reflux ratio.

Trimethylene oxide (TMO) was obtained from Farchan Research Labs, was freed of water by azeotropic distillation with diethyl ether and then fractionated (b.p. 48°C., n_D^{30} 1.3870).

3,3-Bis(allyloxymethyl) oxetane (BAMO) was prepared by adding BCMO (31.0 g., 0.2 mole) over 2 hrs. to a mixture of allyl alcohol (23.2 g., 0.40 mole) and NaOH (16.0 g., 0.4 mole) in dimethyl sulfoxide (100 ml.) at 50°C. After the mixture was heated for an additional 2 hrs. at 50°C., water was added, and the water-insoluble fraction recovered, dried, and fractionated (b.p. 118°/10 mm., n_D^{30} 1.4538).

3,3-Dimethyloxetane was prepared from neopentylglycol by the procedure of Schmoyer and Case[22]. The fractionated product had: b.p. 81°C., n_D^{30} 1.3921.

Polymer Isolation. The procedures used for the runs in Tables II and III are given below. Unless otherwise noted, products were dried at 80°C. in vacuo (0.4 mm.).

Procedure A. Ether was added and then the product was washed twice with 3% HCl (15 min. to 1 hr. stir per wash), and then with water until neutral. The ether-insoluble (if any) was collected, washed twice with ether and once with 0.05% Santonox in ether and dried as the ether-insoluble fraction. The ether-soluble was stabilized with 0.5% Santonox (based on total solids), the ether stripped off, and the polymer dried. In Run 7, Table III, the ether-soluble was stabilized with 1% phenyl β-naphthyl amine.

Procedure B. Excess n-heptane (4-6 vols.) was added and the heptane-insoluble polymer was collected, washed once with heptane, washed once with 0.5% HCl in CH_3OH, washed neutral with CH_3OH, washed with 0.1% Santonox in CH_3OH, and then dried. Run 5, which was used in the vulcanization studies, was stabilized with 1% phenyl β-naphthyl amine.

Procedure C. Product precipitated with 4 vols. of n-heptane (ether in Run 3, Table II). The insoluble was collected, washed with n-heptane (or ether, if used initially), washed with 1% HCl in anhydrous ethanol, washed neutral with CH_3OH, washed with 0.4% Santonox in CH_3OH and dried. In Run 2, Table II, the heptane-insoluble was not HCl washed but instead washed with 0.1% Santonox in heptane and dried. This product was then further separated by tumbling 1-gram in 40 ml. of H_2O overnight and then collecting the water-insoluble, washing with H_2O, and drying. The water-soluble was recovered by stripping off the water and drying.

Procedure D. Excess ether was added, the ether-insoluble fraction was collected, washed with ether, washed with 0.5% HCl in 80-20 ether-methanol, washed neutral with 80-20 ether-methanol, washed with 0.4% Santonox in ether, and then dried in vacuo at 50°C.

Polymer Characterization. Inherent viscosity was determined under the following conditions: TMO-ECH copolymer, 0.1%, α-chloronaphthalene, 100°C.; other TMO and DMO homo and copolymers 0.1%, $CHCl_3$, 25°C.; TMO-PO-AGE terpolymer and PO-BCMO copolymer, 0.1%, benzene, 25°C.; BCMO homopolymer, 1.0%, cyclohexanone, 50°C.

Unsaturated copolymers were analyzed for the unsaturated comonomer by Kemp Bromine No. (in $CHCl_3$)[21] after correcting for the Bromine No. of the antioxidant (Santonox, 125 and phenyl β-naphthyl amine, 143). Chlorine-containing comonomers were determined by a chlorine analysis. The composition of the TMO-EO copolymers was determined by C and H analysis. The PO content of the TMO-PO-AGE terpolymer was determined by infrared analysis.

The relative reactivity of monomers in copolymerization was calculated from the following equation based on ideal copolymerization.

$$r_1 = \frac{\ln \dfrac{[M_1]_o}{[M_1]_t}}{\ln \dfrac{[M_2]_o}{[M_2]_t}}$$

where r_1 is the reactivity ratio of monomer 1 relative to monomer 2, $[M_1]_o$ and $[M_2]_o$ are the initial monomer concentrations of monomers 1 and 2, and $[M_1]_t$ and $[M_2]_t$ are the monomer concentrations at time t during the copolymerization.

Vulcanization Studies

Vulzanizates were prepared by conventional milling and compounding at 100°F. followed by press curing according to the formula in Table IV unless otherwise noted. The HAF carbon black was Philblack O (N-330) of Phillips Petroleum Co. A cure rate study is given in Figure 1. Gel/swell data (wt. %) were deter-

mined in cyclohexanone after 4 hours at 80°C. Tests used to
evaluate vulcanizates were as follows:

Test	ASTM
Tensile	D412 (miniature, 2" Die C dumbbell)
Tear	D624 (miniature Die C)
Hardness	D676
Bashore resilience	D2632
Yerzley oscillograph	D945
Torsional rigidity	D1043
Heat Build-up	D623
Oven aging	D573
Solvent Resistance	D1460

Table IV

VULCANIZATION FORMULA

Elastomer	100
HAF Black	50
ZnO	5
Stearic Acid	1
Sulfur	2
Benzothiazyl disulfide	1
Tetramethyl thiuram disulfide	2

Cured 30 min. at 310°F.
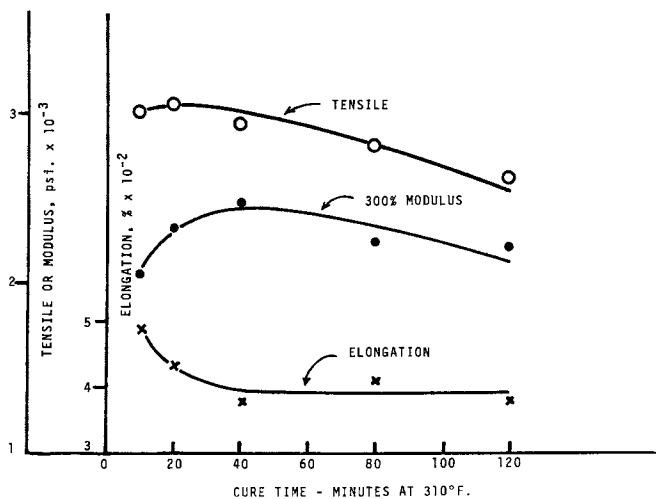
Figure 1. Effect of cure time on properties of TMO–AGE
elastomer

RESULTS AND DISCUSSION

Polymerization Studies.

TMO homopolymerization. The Et_3Al-$0.5H_2O$-1.0 acetylacetone catalyst polymerized TMO at 65°C. in heptane diluent to a high conversion of a very high molecular weight polymer ($n_{inh} = 12$), which was tough, rubbery, and crystalline, with a 40°C. melting point (Table II). The polymer was insoluble in n-heptane and methanol but soluble in benzene and chloroform. This homopolymer is apparently similar to that prepared by Rose[3] with BF_3 catalyst except that the present product is of much higher molecular weight and a little higher melting. Rose obtained an n_{inh} of 1.3 at 50°C. and 2.9 at -80°C. with a melting point of 35°C.

The polymerization of TMO is to be compared with that of PO since the monomers and polymers are isomeric (Eqs. 1 and 2)

$$\text{TMO} \longrightarrow (-CH_2CH_2CH_2-O-)_n \qquad \text{Eq. 1}$$

$$\text{PO} \longrightarrow (-CH_2CH_2-O-)_n \qquad \text{Eq. 2}$$
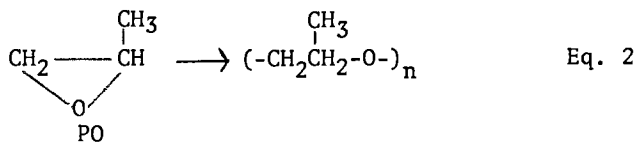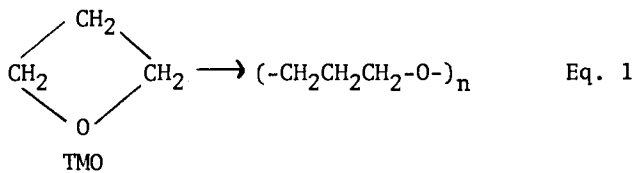
On the basis of our prior work on PO polymerization, with this same chelate catalyst[5], TMO polymerizes about 10 times more slowly than PO does under the same conditions. Also, the TMO homopolymer is much less soluble than poly(propylene oxide), since the latter polymer is soluble in heptane and methanol, both non-solvents for poly(trimethylene oxide). The TMO homopolymer is, of course, crystalline because of its very regular structure. On the other hand, the poly(propylene oxide) prepared with the chelate catalyst is largely amorphous because of tacticity and head-to-tail variations in structure which are not possible in poly(trimethylene oxide).

This TMO polymerization with the chelate catalyst no doubt involves coordinate propagation and is the first such case of coordinate propagation of an oxetane. Heretofore, oxetanes have been cationically polymerized. There are several reasons for concluding that this chelate catalyst system is a coordination polymerization. First, the very high molecular weight obtained at elevated temperature with a low rate is characteristic of coordination polymerization rather than of cationic polymerization. Also, Vandenberg's work on the cis- and trans-2,3-epoxy-

Table II

Polymerization of TMO with Et$_3$Al-0.5 H$_2$O-Acetyl Acetone Catalyst (a)

No.	Comonomer Name	%	Diluent Name	ml.	Catalyst Acetyl Acetone per Al	mmoles (Al Basis)	Time hrs.	Temp. °C.	Total % Conv.	Isolated Polymer Procedure	Fraction	% Conv.	η inh.	% Co-monomer
1	-	0	n-heptane	92	1.0	8	19	65	85	A	Ether-insol.(b)	67	12	
2	EO	20	Toluene	92	0.5	4	12	30	13	C	Water-insol.(c) Water-sol. (c)	1.4 12	11.0 6.5	44 8
3	ECH	50	Toluene	42	1.0	4	7.5	65	19	C	Ether-insol.(d) Ether-sol., Heptane-insol.(e)	5.6 10	3.3 1.0	12 55
4	AGE	3	n-heptane	92	1.0	8	.7	65	27	D	Ether-insol.(d)	23	8.1	12.6
5	AGE	5.6(f)	n-heptane	82	1.0	8	14	65	-	B	Heptane & CH$_3$OH-insol.(e)	71	15.4	4.4
6	BMO	9.4	"	82	1.0	8	14	65	-	B	"	89	13.5	6.5
7	PO AGE	45(g) 5(g)	n-heptane	92	0.5	4	10	65	54	A	Heptane-insol.(h) Heptane-sol.(i)	28 20	5.3 4.1	PO AGE 58 10.0 60 9.3

(a) Based on 10 g. total monomer. See Experimental for isolation procedure. TMO = trimethylene oxide, EO = ethylene oxide, ECH = epichlorohydrin, AGE = allyl glycidyl ether, BMO = butadiene monoxide, and PO = propylene oxide.

(b) Very strong, tough, orientable rubber. Crystalline by x-ray (m.p. = 40°C.). Insoluble in H$_2$O, n-heptane and CH$_3$OH. Soluble in benzene and chloroform.

(c) Isolated from initial heptane and methanol-insoluble product.

(d) Largely amorphous and rubbery.

(e) Amorphous and rubbery.

(f) 20% of total comonomer added initially, remainder added in 6 equal portions at 2-hr. intervals.

(g) Added in 5 equal portions at 2-hr. intervals.

(h) Tough, amorphous rubber

(i) Tacky rubber.

Table III

Polymerization of Oxetanes with Et_3Al-0.5 H_2O Catalyst (a)

No.	Monomer Name	%	Diluent Name	ml.	Catalyst(b) mmoles	Time hrs.	Temp. °C.	Total % Conv.	Isolated Polymer Procedure	Fraction	% Conv.	η_{inh}	% Co-monomer
1	TMO	100	Toluene	48	4	0.25 2.3	65	49 78	B	Heptane and CH_3OH-insol.	66	5.5	
2	TMO	100	Toluene	48	4	0.5 2.0 23	30	29 47 78	B	"	65	5.3	
3	TMO BAMO	94 6	Toluene	83	4	2	30	51	B	Heptane-and CH_3OH-insol.	27	2.7	6.7
4	BCMO	100	Toluene	42	2	6	50		C	Heptane- and CH_3OH-insol.	94	0.29	
5	BCMO	100	"	50	2 (c)	19	30	60	C	"	60	3.3	
6	DMO	100	n-heptane	48	4	42	0	100(d)	A	Total polymer (e)	99	1.5	
7	DMO BAMO	90 10	n-heptane	32	4	0.08	0	92	A	Total polymer (f)	92	1.3	11.7
8	PO BCMO	80 20	"	40	4 (g)	5	30	27	A	Total polymer	27	5.2	0.7

(a) Based on 10-g. total monomer. See Experimental for isolation details. TMO = trimethylene oxide; DMO = 3,3-dimethyl oxetane; BAMO = 3,3-bis (allyl oxymethyl)oxetane.
(b) Unless otherwise noted, catalyst prepared in n-heptane with 3 moles of diethyl ether per aluminum.
(c) Ether omitted from catalyst preparation.
(d) Most of polymerization occurred in a few minutes.
(e) Initially a tacky rubber after drying at 80°C. which slowly crystallized to a hard solid of ca. 50°C. m.p.; heptane-soluble.
(f) Low crystallinity [poly(3,3-dimethyl oxetane) pattern]; heptane-soluble.
(g) Et_3Al-0.5 H_2O-0.5 acetyl acetone catalyst.

butanes clearly established that the chelate catalyst operates by
a coordination mechanism and does not give cationic polymeriza-
tion[5]. It is perhaps surprising that TMO polymerizes ten times
more slowly than PO, since it is a stronger base than PO by about
4 orders of magnitude[24] and thus it should coordinate much more
readily with a metal. One explanation for the more facile poly-
merization of PO is that the greater ring strain in PO, compared
with that in TMO, greatly facilitates the ring opening propagation
step with PO and more than compensates for its lower coordination
tendency because of its lower base strength.

TMO polymerizes much faster (about ten-fold) with the Et_3Al-
$0.5H_2O$ catalyst (Table III) and still gives fairly high molecular
weight homopolymer. In this case, based on Vandenberg's prior
work with the 2,3-epoxybutanes, the polymerization could be either
cationic or coordination, or both. The cationic route would be
expected to be faster. Also, the lower steric hindrance at
propagation sites with the unmodified organoaluminum-H_2O should
also permit more facile coordination and thus faster coordination
polymerization. The increased Lewis acid character of propagation
sites with the unmodified catalyst could also enhance the coordin-
ation step and thus propagation.

TMO Copolymerization With Saturated Epoxides. Copolymerizing
TMO with ethylene oxide (EO) in an 80:20 weight ratio with the
chelate catalyst gave a water-soluble product (90% of the total)
which contained only 8% TMO (Run 2, Table II). On the basis of an
ideal copolymerization, the EO is estimated to enter the copolymer
in this fraction approximately 70 times more readily than does the
TMO. This result confirms that alkylene oxides polymerize much
more readily than oxetanes with the chelate catalyst. A small
amount (10% of the Total) of a water-insoluble copolymer contain-
ing 44% TMO was obtained. This result indicates that the chelate
catalyst contains some sites which give more favorable copolymer-
ization. One possible explanation is that the unfavorable copoly-
merization of TMO at the major sites is due to steric hindrance
which reduces the ability of TMO to coordinate at this site.
Based on this hypothesis, less hindered sites would be more favor-
able for copolymerization. An alternate but unlikely possibility
is that there are a limited number of cationic sites in the
chelate catalyst and that these give some copolymer by a more
favorable cationic propagation mechanism.

The copolymerization of TMO and epichlorohydrin (ECH) with
the chelate catalyst and a 50:50 weight ratio charge is more
favorable (Run 3, Table II); again, two fractions, both rubbery
in nature, were obtained which differed in solubility and com-
position. Thus, the chelate catalyst again appears to contain at
least two different copolymerization sites. It is significant
that these two monomers, which probably have similar steric re-
quirements, do copolymerize better, thus adding credence to the
earlier proposal that steric restrictions at certain sites affect

copolymerization. Of course, this result is also evidence for a
coordination polymerization.

TMO Copolymerization With Unsaturated Epoxides and Oxetanes.
The low conversion copolymerization of TMO and allyl glycidyl
ether (AGE) with the chelate catalyst and a 97:3 weight ratio
charge gave a rubbery, largely amorphous, high molecular weight
copolymer product which contained about 13% AGE (Run 4, Table II).
On the basis of an ideal copolymerization, the AGE enters the
copolymer about 14 times more readily than TMO does. This result
is to be contrasted with the ideal PO-AGE copolymerization, with
this same catalyst, in which the copolymer has the same composi-
tion as the initial monomer charge. To compare the elastomer
behavior of this TMO elastomer with a comparable PO-AGE elastomer,
a procedure was developed for making larger samples of relatively
uniform TMO-AGE copolymers containing about 4% AGE (Run 5, Table
II). Thus, the copolymerization was begun with all the TMO in
the initial charge along with 20% of the total AGE used. As the
polymerization proceeded, additional AGE was added as indicated
in Table II. In this way, a high conversion to heptane- and
methanol-insoluble, amorphous copolymer containing 4.4% AGE was
obtained. On the basis of the sulfur vulcanizate data that is
presented in the vulcanizate property data section, this product
appears to be relatively uniform. However, this procedure and
perhaps even the catalyst may not be optimal and some degree of
nonuniformity may still persist.
    A copolymer of TMO with butadiene monoxide (BMO) was also
made by using the same procedure as in the large sample method
for TMO-AGE (Run 6, Table II). Since BMO gives ideal copolymer-
ization with PO, as does AGE, with the chelate catalyst, it was
assumed that the system which worked with TMO-AGE would work with
TMO-BMO.
    A terpolymer of TMO-PO-AGE was also made by the same general
procedure used in the large scale TMO-AGE work (Run 7, Table II).
The terpolymer was isolated in two fractions of similar composi-
tion (ca. 60% PO and 10% AGE), but different solubility, and
different molecular weight. The highest molecular weight frac-
tion was heptane-insoluble, confirming that TMO units contribute
substantial heptane-insolubility.
    TMO was also copolymerized with an unsaturated oxetane, 3,3-
bis(allyloxymethyl)oxetane (BAMO) (Run 3, Table III). This work
was done with the $Et_3Al-0.5H_2O$ catalyst. This copolymerization
appears to be a nearly perfect one.

Polymerization of Other Oxetanes. The cationic polymeriza-
tion of 3,3-disubstituted oxetanes, especially 3,3-bis(chloro-
methyl)oxetane (BCMO), has been widely studied[1][2]. A few
experiments with this type of oxetane using the $Et_3Al-0.5H_2O$
catalyst are given in Table III. BCMO polymerizes readily with
this catalyst to give high molecular weight polymer, n_{inh} 3.0, at

30°C., provided there is no ether in the catalyst system (Run 5, Table III). However, with ether present (Run 4, Table III), the molecular weight is greatly reduced as indicated by the 0.3 inherent viscosity. The large effect of ether indicates that the Et_3Al-$0.5H_2O$ catalyst is behaving here as a cationic catalyst with ether acting as a chain transfer agent. The molecular weight without ether is, however, very high for an ordinary cationic catalyst with BCMO at these temperatures. Usually lower temperatures are required to obtain high molecular weight polymer from BCMO with Lewis acid type catalysts[1].

Some experiments on the polymerization of BCMO with the chelate catalyst are recorded in the patent literature[4]. In this work, high molecular weight polymer (η_{inh} up to 4.3) was obtained at very high temperatures (200-250°C.) in a continuous, bulk polymerization method. These data indicate that the chelate catalyst polymerizes BCMO by a coordination mechanism. Presumably the very high temperature works well because of the relatively low basicity of BCMO[24].

The copolymerization of PO with BCMO using the chelate catalyst (Run 8, Table III) at 30°C. indicates that the PO enters the copolymers about thirtyfold more readily than does BCMO, based on ideal copolymerization. This result is similar to our findings on the copolymerization of TMO with ethylene oxide. Similar explanations no doubt apply.

3,3-Dimethyloxetane (DMO) polymerizes very rapidly at 0°C. with Et_3Al-0.5 H_2O catalyst to a high molecular weight, (η_{inh}, 1.6), low melting (ca. 50°C.), crystalline polymer (Run 6, Table III). This polymerization is apparently cationic, on the basis of the very rapid polymerization. The small amount of ether in the catalyst does not have a large chain transfer effect, as with BCMO, presumably because of the much higher base strength of DMO compared with BCMO and ether.

DMO was copolymerized with BAMO (Run 7, Table III). Because of the very rapid polymerization, it was difficult to obtain a low conversion and to assess the copolymerization behavior of this monomer pair. However, vulcanizate properties on this product (Table III) were good, indicating a relatively uniform copolymer and thus a favorable copolymerization.

Vulcanizate Studies

The various unsaturated copolymers were vulcanized with the sulfur-accelator system given in Table IV.

TMO-AGE Elastomers. The sulfur vulcanizate of the 96-4 TMO-AGE copolymer had high tensile, modulus, and tear strength at 23°C. at a good elongation level (Table V). The hot tensile properties at 100°C. are somewhat lower but still good. Crystallinity and/or crystallization on stretching could enhance tensile properties at 23°C.; apparently this is not the case, since the hot tensile results, which could not involve crystallinity

effects, are in line with the usual effect of increased temper-
ature on tensile properties. The properties obtained in these
studies are affected only slightly by increasing the cure time
fourfold over the optimum used (Fig. 1).

Table V

VULCANIZATE PROPERTIES OF TMO-AGE ELASTOMER

	23°C.	100°C.
Tensile strength, psi.	3190	1800
300% modulus, psi.	2590	1515
Elongation at break, %	400	225
Break set, %	20	0
Hardness, A2	82	82
Tear Strength, p./i.	345	230
Resilience, Bashore, %	65	
Yerzley Dynamic Data		
Modulus, psi.	6555	
Resilience, %	67	
Frequency, Hz	7.5	
Kinetic Energy, in.-lb./cu.in.	31.7	
Heat Build-up, °F.	27	
Tg., °C.	-75	
Vol. % Swell		
(5 days at 60°C.)		
Toluene	315	
H_2O	0	

The TMO-AGE copolymer vulcanizate also has excellent resil-
ience, low heat build-up, and a low Tg of -75°C. (Table V).
Volume % swell in toluene is high but water-swell is low. Al-
though not measured, we would expect, based on the heptane-
insolubility of the amorphous 96-4 TMO-AGE copolymer, that oil
resistance of TMO-AGE copolymer would be fairly good. The
methanol-insolubility of the amorphous TMO-AGE copolymer also
suggests that it should have resistance to polar solvents.
     The gum vulcanization properties of the TMO-AGE copolymer
(Table VI) are low. These data are further evidence that the
excellent tensile properties observed for the black-filled TMO-
AGE vulcanizates is not due to crystallinity or crystallizability.
The 91% gel result does support our conclusion that the TMO-AGE
copolymer is reasonably uniform.
     Air aging for 48 hours at 100°C. does not greatly affect the
room temperature properties of the TMO-AGE vulcanizate (Table
VII). These conditions would seriously degrade the properties of
natural rubber and thus clearly show that TMO elastomers, like PO
elastomers, are superior in heat aging to natural rubber. Unfor-
tunately we did not make an extended air aging study on the TMO
vulcanizate to determine its long term oxidation resistance. One

would expect, however, that the lack of tertiary hydrogens in the
TMO chain unit would be a favorable factor.

Table VI

GUM VULCANIZATE PROPERTIES OF TMO-AGE ELASTOMER

Tensile strength, psi.	515
300% Modulus, psi.	260
Elongation at break, %	515
Break set, %	10
Hardness, A2	48
Tear strength, p/i	80
Gel/swell, %/%	91/520

Table VII

EFFECT OF AIR AGING ON TMO-AGE VULCANIZATE(a)

	hrs. at 100°C.	
	0	48
Tensile strength, psi.	3190	3380
200% Modulus, psi.	2590	2630
Elongation at break	400	290
Break set, %	20	10
Hardness, A2	82	70

(a) Stabilized with 1% phenyl β-naphthylamine.

Torsional rigidity versus temperature data for the TMO-AGE
vulcanizate and a comparable PO-AGE vulcanizate are given in
Figure 2. The increase in modulus for the TMO vulcanizate from
0 to -60° obviously is due to a low temperature crystallization
of this copolymer. Other samples did not exhibit this crystal-
lization problem. The data do indicate that the TMO and PO elas-
tomers have about the same Tg at about -75°C.

The low temperature crystallization problem of the TMO elas-
tomer can no doubt be eliminated in a variety of ways, such as
preparing a more uniform copolymer, adding a plasticizer such as
an aromatic oil, and/or altering the composition of the copolymer.

An approach to altering the TMO-AGE copolymer composition
would be to make a terpolymer containing PO as described pre-
viously. Vulcanizate data are given on the PO-TMO-AGE elastomers
in Table VIII. The properties are fair but indicate that the
vulcanizates are overcured. The AGE level was evidently too high
for the cure system used. The results do confirm the preparation
of the desired terpolymer and indicate that this approach is
feasible.
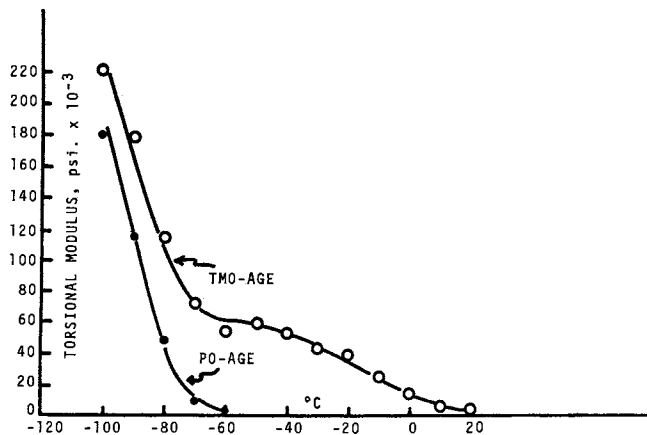
Figure 2.   Torsional rigidity vs. temperature for TMO and PO elastomers

Other Oxetane Elastomers. The TMO-butadiene monoxide (BMO) copolymer elastomer (Run 6, Table II) containing 6.5% BMO gave inferior properties (Table VIII) to the TMO-AGE elastomer with 4.4% AGE described in the previous section. Actually the properties were even slightly inferior to a 98-2 TMO-AGE copolymer vulcanizate (Table VIII). Thus AGE appears about three times more effective (on a weight basis) in conferring sulfur vulcanizability than BMO. On a molar basis, the difference is even greater, i.e., AGE is five times more effective. This same difference between BMO and AGE was previously observed on comparing PO-BMO elastomer with PO-AGE elastomer.

Bis(3,3-allyloxymethyl)oxetane (BAMO), on the other hand, appears to have about the same order of effectiveness for conferring sulfur curability to a TMO elastomer as does AGE (on an equal double-bond content basis).

The 88:12 DMO:BAMO elastomer gave only fair properties since it was substantially overcured with the high level of BAMO used (Table VIII). The low heat-build-up does indicate that this elastomer is inherently a good one.

CONCLUSIONS

The first polymerization of an oxetane, trimethylene oxide, by coordination polymerization has been described. Copolymers of TMO with epoxides were readily made. Such copolymers provide an interesting family of new elastomers. One such elastomer, the TMO-AGE copolymer, was investigated in some detail and found to have a desirable combination of properties. Such TMO elastomers,

Table VIII

Vulcanizate Properties of Various Oxetane Elastomers

Elastomer (a)		% Gel	% Swell	Tensile psi.	300% Modulus psi.	Elongation	Heat Build-up @ 212°F.
Name	Composition						
PO-TMO-AGE, heptane-insol.	58-32-10	-	-	2040	695 (c)	225	
" " " -sol.	60-31-9	-	-	2030	930 (c)	200	
TMO-BMO	93.5-6.5	94	625	2090	1155	535	
TMO-AGE	98-2 (b)	93	820	3010	1035	770	
TMO-BAMO	93.3-6.7	100	270	3280	3250	305	
DMO-BAMO	88-12	99	390	1985	-	210	14

(a) Products described in Tables II and III unless otherwise noted.

(b) Prepared by the same procedure described in Run 5, Table II, using 2.6% total AGE in the charge. n_{inh} = 16.6.

(c) 100% modulus.

like the PO elastomers, are excellent rubbers with low Tg and high
resilience. Also, the TMO elastomers give good tensile and tear
properties and should have at least fair oil resistance. Although
abrasion resistance data has not been obtained, we would expect
the good tensile and tear properties of the TMO vulcanizates to
favor good abrasion resistance. There appear to be two main dis-
advantages of the TMO elastomers; first, the low temperature
crystallization problem which can no doubt be easily corrected.
Second, and more important, there is no current economic source
of TMO. For example, trimethylene glycol, a possible precursor,
sells for about $4/lb. in volume. Thus the development of this
interesting family of elastomers based on TMO must await the
development of a low cost route to this monomer.

Acknowledgment

Summary

The first coordination polymerization of an oxetane, tri-
methylene oxide (TMO), occurs readily, much like propylene oxide
(PO), with the Et_3Al-H_2O-acetyl acetone catalyst at 65°C., to give
high molecular weight polymer (n_{inh} up to 12). TMO copolymerizes
with epoxides with this coordination catalyst. For example, TMO
copolymerized well with allyl glycidyl ether (AGE) which was about
seven times more reactive than TMO, in contrast to the PO-AGE
copolymerization in which both monomers are of equal reactivity.
A 96-4 TMO-AGE copolymer prepared under conditions to make it rea-
sonably uniform gave an interesting sulfur-curable elastomer.
Preliminary vulcanizate data on this elastomer show good tensile
and tear properties, a low Tg (-75°C.), high resilience, and good
heat resistance. Further development of this family of interest-
ing elastomers requires a lower cost route to TMO. Copolymeriz-
ations of TMO with other epoxides and oxetanes as well as the
polymerization of other oxetanes are also described.

Literature Cited

1. Boardman, H., Encyl. of Chem. Tech., 2nd Supplement, (1960),
   655.

2. Dreyfuss, P. and Dreyfuss, M. P., "Polymerization of 1,3
   Epoxides" in "Ring Opening Polymerization" (K. C. Frisch and
   S. L. Reegen, eds.), Marcel Dekker, Inc., New York, 1969,
   Chap. 2-2.

3. Rose, J. B., J. Chem. Soc. <u>1956</u>, 542, 546.

4. Vandenberg, E. J. (to Hercules Incorporated), U.S. Pat. 3,205,183 (1965).

5. Vandenberg, E. J., J. Polym. Sci., Al, (1969), <u>7</u>, 525.

6. Price, C. C., Chemist (1961), <u>38</u>, 131.

7. Price, C. C., (assigned to University of Notre Dame), U.S. Pat. 2,866,774 (1958).

8. Pruitt, M. E. and Baggett, J. M., (to Dow Chemical Co.), U.S. Pat. 2,706,181 (1955).

9. Price, C. C. and Osgan, M., J. Amer. Chem. Soc. (1956), <u>78</u>, 4787.

10. Osgan, M. and Price, C. C., J. Polym. Sci., (1959), <u>34</u>, 153.

11. Price, C. C., (to General Tire and Rubber Co.), Br. Pat. 893,275 (1962).

12. Hill, F. N., Bailey, Jr., F. E., and Fitzpatrick, J. T., Ind. Eng. Chem., (1958), <u>50</u>, 5.

13. Staudinger, H. and Lohmann, H., Ann. Chem. (1933), <u>505</u>, 41.

14. Bailey, Jr., F. E., Hill, F. N., and Fitzpatrick, J. T., (to Union Carbide Corp.) U.S. Pat. 3,100,750 (1963).

15. Bailey, Jr., F. E., Hill, F. N., and Fitzpatrick, J. T., (to Union Carbide Corp.) U.S. Pat. 2,969,402 (1961).

16. Bailey, Jr., F. E., Hill, F. N., and Fitzpatrick, J. T., (to Union Carbide Corp.) U.S. Pat. 3,062,755 (1962).

17. Bailey, Jr., F. E., (to Union Carbide Corp.) U.S. Pat. 3,031,439 (1962).

18. Vandenberg, E. J., J. Polym. Sci. (1960), <u>47</u>, 486.

19. Gruber, E. E., Meyer, D. A., Swart, G. H., and Weinstock, K. U., Ind. Eng. Chem. Prod. Res. Develop. (1964), <u>3</u>(3), 194.

20. Vandenberg, E. J. (to Hercules Incorporated), U.S. Pat. 3,728,320 (1973).

21. Vandenberg, E. J. (to Hercules Incorporated), U.S. Pat. 3,728,321 (1973).

22. Schmoyer, L. F. and Case, L. C., Nature (1960), <u>187</u>, 592.

23. Kemp, A. R. and Mueller, G. S., Ind. Eng. Chem. Anal. Ed. (1934), <u>6</u>, 52.

24. Yamashita, Y., Tsuda, T., Okada, M., and Iwatsuki, S., J. Polym. Sci., A1, (1966), <u>4</u>, 2121.

8

Vulcanization and Stabilization Studies on Propylene Oxide Rubber

C. R. BOSS

Research Center, Hercules Inc., Wilmington, Del. 19899

Parel® elastomer is made by copolymerizing propylene oxide with a small amount of allyl glycidyl ether. Typical samples have reduced specific viscosities (RSV) between 4 and 12, indicating molecular weights of the order of a million. The unsaturation contributed by the allyl glycidyl ether monomer units provides sites for sulfur cross-linking. Vulcanization can be effected with combinations of sulfur and sulfur donors as used for other unsaturated rubbers. A typical vulcanization formulation is given in Table 1. Peroxides are ineffective for curing this elastomer since they tend to degrade rather than cross-link it. When Parel elastomer is cured with the formulation shown, for the recommended 30 minutes at 160°C., the properties given in Table 2 are obtained.

This paper will summarize some of the studies leading to selection of a number of the components of this vulcanization formulation and to determination of the advantageous properties of the vulcanized products.

Vulcanization

Sulfur cure systems are well known to be complex in their reactions and in the types of cross-links they produce[1][2]. There is general agreement that if sulfur alone is used to vulcanize a rubber, most of the cross-links will have more than two sulfur atoms in them[1]. These polysulfides are less stable than monosulfides or disulfides. This phenomenon has been examined in some vulcanized elastomers by using chemical probes, which modify or break only certain kinds of cross-links[3][4][5]. Parel elastomer is more difficult to study in this fashion than styrene-butadiene rubber (SBR) or natural rubber because many of these chemical reagents also react with the C-O bonds of the polyether.

® Registered trademark of Hercules Incorporated

However, triphenylphosphine is a reagent which can be utilized advantageously. It reduces polysulfides to disulfides[6], but does not break the polymer chains in Parel elastomer. To determine the types of cross-links which are produced in representative cure systems, two samples of vulcanized Parel elastomer were prepared. One was cured with sulfur alone, and the other with the formulation shown in Table 1. The samples were then treated with triphenylphosphine in benzene. The results of continuous stress relaxation measurements run on the products at 150°C. are shown in Figure 1. The stabilizers were extracted by the benzene used in the triphenylphosphine treatment so subsequent tests in air could not be compared with previous test results. Therefore, all of these stress relaxation measurements were made in nitrogen.
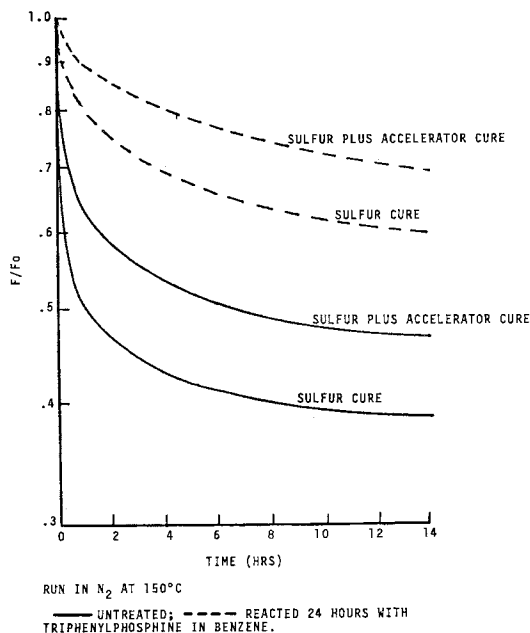
Figure 1. Effect of polysulfides on the stress relaxation of vulcanized Parel elastomer

Both of the unextracted samples suffer from a rapid initial loss of modulus, but the sample cured with sulfur has a considerably more severe loss. After the cross-links were converted from

TABLE 1

TYPICAL VULCANIZATION FORMULATION FOR PAREL ELASTOMER

100	PAREL ELASTOMER
50	HAF BLACK
1.0	STEARIC ACID
1.5	NICKEL DIBUTYLDITHIOCARBAMATE
5.0	ZNIC OXIDE
1.5	TETRAMETHYLTHIURAM MONOSULFIDE
1.5	MERCAPTOBENZOTHIAZOLE
1.25	SULFUR

TABLE 2

TYPICAL PHYSICAL PROPERTIES OF VULCANIZED PAREL ELASTOMER

100% MODULUS	465 P.S.I.
300% MODULUS	1740 P.S.I.
TENSILE STRENGTH	2075 P.S.I.
ELONGATION	375 %
HARDNESS (SHORE A)	68
BAYSHORE RESILIENCE	48 %

polysulfides to disulfides, both samples had a much smaller loss of modulus in the first few hours of test. These stress relaxation results show that polysulfides are weaker than disulfides. Lal has shown that reduction of polysulfides to disulfides does not interfere with the tensile properties of natural rubber[7]. We did not determine whether this was true for the Parel elastomer.

The sulfur content of these samples was determined after treatment with benzene alone and after treatment with triphenyl-phosphine in benzene. The samples lost about 1/3 of their sulfur in the benzene. About half of this loss (about 1/6 of the total amount of sulfur) could be attributed to loss of nickel dibutyl-dithiocarbonate (NBC), the stabilizer. When these samples were treated with triphenylphosphine in benzene, the sample cured with an accelerator lost about 50% of its original sulfur. The one cured with sulfur alone lost 90% of its original sulfur. Thus, we have further evidence that both cure systems result in polysulfide cross-links, but they represent a smaller percentage of the total when an accelerator is used.

Stabilization and Hydroperoxide Decomposers

When properly compounded, vulcanized Parel elastomer is quite stable in hot air. Nickel dibutyldithiocarbamate (NBC) has been found to be a very effective stabilizer for this rubber. Results of aging a standard formulation in a 150°C. air oven are shown in Table 3. The hardness results are given as a change (in points) from the original value, while the percentage of the original value is given for the other properties. During the first three days of aging, the 100% modulus and hardness were higher than the original values, while the elongation was lower. These changes are probably due to additional cross-linking. Then the rubber gradually softened and lost strength. After a week, the vulcanized elastomer lost only about 10% of its 100% modulus, less than one-third of its tensile strength, and softened very little; the rubber was still quite serviceable. After 10 days under these test conditions, the elastomer deteriorated considerably. These heat aging tests show that properly compounded Parel elastomer vulcanizates are outstanding in high temperature oxidation resistance.

TABLE 3

CHANGE OF PROPERTIES OF PAREL ELASTOMER AGED IN AIR AT 150°C.

| DAYS | % OF ORIGINAL | | | CHANGE IN HARDNESS |
	100% MOD.	T.S.	ELONG.	
1	130	95	65	+4
3	145	75	60	+3
7	90	70	65	-2
10	60	30	55	-7

Figure 2 compares the effectiveness of two stabilizers in Parel elastomer. Since the elastomer contains an in-process antioxidant, only a hydroperoxide decomposer was added. The superiority of NBC in maintaining the physical properties of Parel elastomer is obvious.
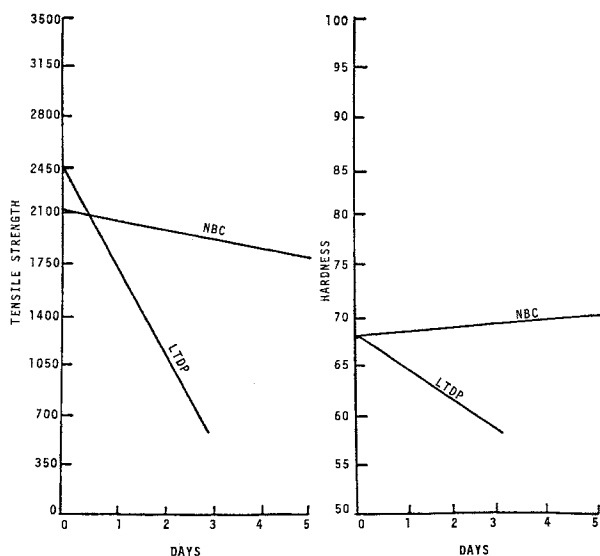
Figure 2. Effect of stabilizer on vulcanized Parel elastomer aged at 150°C

A model system has been used to explain the effectiveness of dithiocarbamates as hydroperoxide decomposers. Table 4 summarizes results of decomposing t-butyl hydroperoxide (TBHP) with dithiocarbamates or dilaurylthiodipropionate (LTDP). The dithiocarbamates were tested at room temperature and at 60°C., while the experiment with LTDP was run at 100°C.

LTDP is an effective hydroperoxide decomposer and is often used for this purpose in polypropylene and other polymers. It decomposes hydroperoxides catalytically and quickly at 100-150°C., but not at room temperature[8]. Each mole of NBC reacts with about 6 moles of hydroperoxide in 15 minutes at 25°C. The zinc compound requires several hours at 25° or about 20 minutes at 60°C. to effectively decompose TBHP.

Undoubtedly more important than the rate of decomposition of hydroperoxides is the type of product obtained. Table 5 lists the major products obtained by completely decomposing TBHP with various sulfur compounds. With nickel and zinc dithiocarbamates

TABLE 4

DECOMPOSITION OF TBHP BY SULFUR COMPOUNDS

TIME (MIN)	TBHP CONCENTRATION (MOLAR)				
	NBC (25°)	ZEC (25°)	NBC (60°)	ZEC (60°)	LTDP (100°)
0	0.205	0.203	0.201	0.201	0.188
15	0.060	-	0.020	0.188	0.162
30	0.030	0.198	0.016	0.075	0.108
60	0.029	0.195	0.014	0.026	0.014
180	0.019	0.179	-	-	-

ALL SOLUTIONS INITIALLY 0.02M STALILIZER

NBC= nickel dibutyldithiocarbamate
ZEC= zinc diethyldithiocarbamate
LTDP= dilaurylthiodipropionate
TBHP= t-butyl hydroperoxide

TABLE 5

PRODUCTS OF TBHP DECOMPOSITION

STABILIZER	$\left[\dfrac{TBHP}{S}\right]_0$	% TBHP TO	
		TBA	DTBP
NBC	5	70	5
ZBC	4	80	5
LTDP	5	0	40
$(C_4H_9S)_2$	5	0	40
SO_2	1D	0	90

TBA= t-butanol

DTBP= di-t-butylperoxide

most of the hydroperoxide went to the alcohol, and only a small
amount to the peroxide; LTDP formed the peroxide from TBHP, but
not the alcohol. About half of the TBHP was unaccounted for, but
neither methanol nor acetone was detected.

    The products formed from TBHP may explain why LTDP does not
work well in Parel elastomer. The peroxides formed in polyethers
would not be stable, so their decomposition would cause continu-
ation of the oxidative chain reaction.

Heat Aging Comparison with Other Elastomers

    Parel elastomer, natural rubber, and neoprene, compounded
with standard recommended formulas for each, were heat aged in a
125°C. forced draft oven. Figure 3 is a plot of the change in
tensile strength and hardness of the vulcanized Parel and neoprene
elastomers. Neoprene maintained its properties for 3 days, but
after a week at 125°C., it was quite hard and brittle. Results
with natural rubber are not included in the figure because it
failed so quickly at 125°C. It was seriously deteriorated in
about 3 days at 100°C.
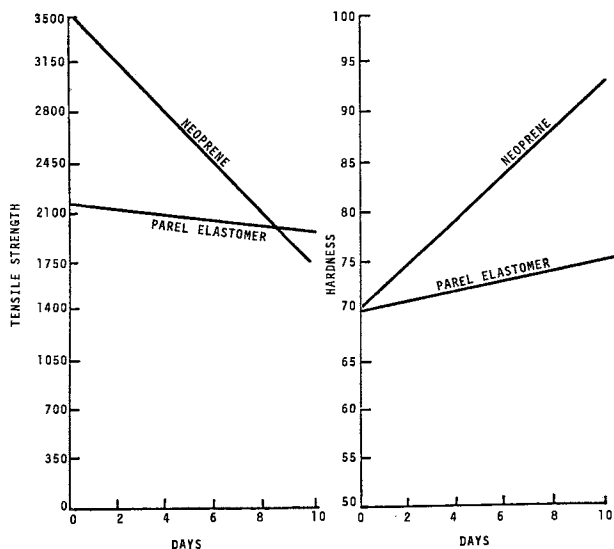
*Figure 3. Physical properties of Parel and neoprene elasto-
mers aged at 125°C*

    Compression set is the inability of rubber to return to its
original size after being squeezed. Standard tests usually com-
press the vulcanized rubber to 75% of its original size for 1 or

3 days at 70°, 100°, or 125°C. Figure 4 is a plot of the compres-
sion set of vulcanized Parel elastomer tested for up to 7 days at
temperatures from 70° to 150°C. While rather high compression set
was attained initially there was not much change as the time and
temperature increased. For example, there was nearly 50% set
after 1 day at 100°, but still less than 70% after a week at
150°C. The results obtained at 125° and 150°C. are within experi-
mental error of each other.
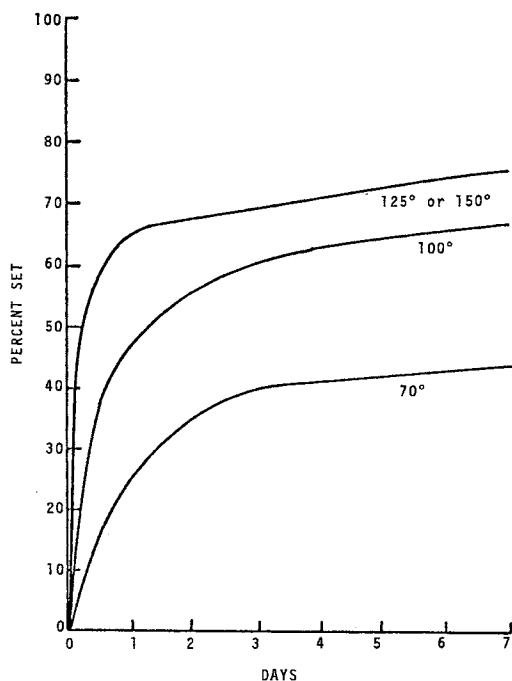
*Figure 4. Effect of time and temperature on the
compression set of vulcanized Parel elastomer*

Figures 5 and 6 compare the compression set of vulcanized
Parel, natural rubber, and neoprene elastomers at 100° and 150°C.,
respectively. At 100°C., the compression set of Parel elastomer
is within experimental error of that of natural rubber; neoprene
is clearly superior. When the compression set test was run for a
long time at 150°C. (Figure 7), Parel elastomer was the best of
these three rubbers. Natural rubber had 100% compression set
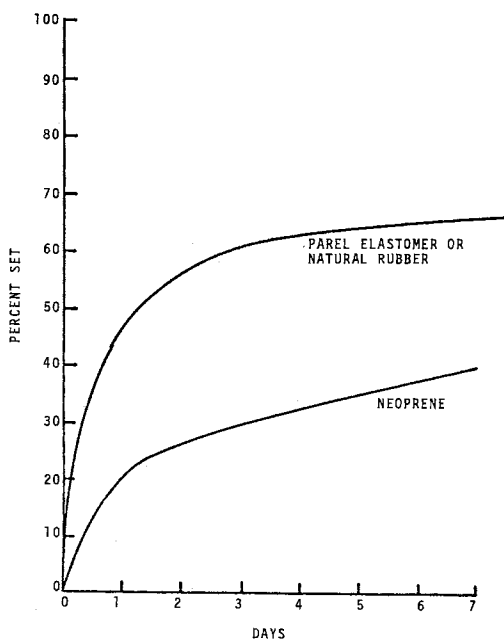
Figure 5. Compression set at 100°C

within three days, probably as a result of oxidative degradation.
Neoprene had a lower compression set than the Parel elastomer vul-
canizate for about five days, but then it became worse.

Stress relaxation measurements were made on cured Parel and
neoprene elastomers. The samples were held at 25% elongation in
our tests. This technique measures chain or cross-link scission,
but does not show the effect of any recombination or additional
curing that occurs. Such new bonds would be load-bearing if the
sample were pulled further as happens in an intermittent run where
the sample is extended for a few seconds, then returned to its
original length for about 10 minutes. Since the sample spends
about 95% of its time in the relaxed state, new bonds are load-
bearing the next time the sample is elongated. Many rubbers
undergo a rapid loss of modulus in continuous experiments, but not
in intermittent runs. At 70°C. natural rubber underwent less
rapid initial loss than Parel elastomer or neoprene. Since oxida-
tive degradation is not significant in 10-20 hours at 70°C.,
natural rubber was superior to Parel elastomer or neoprene in this
test. At 100°C., however, the oxidative chain scission or natural
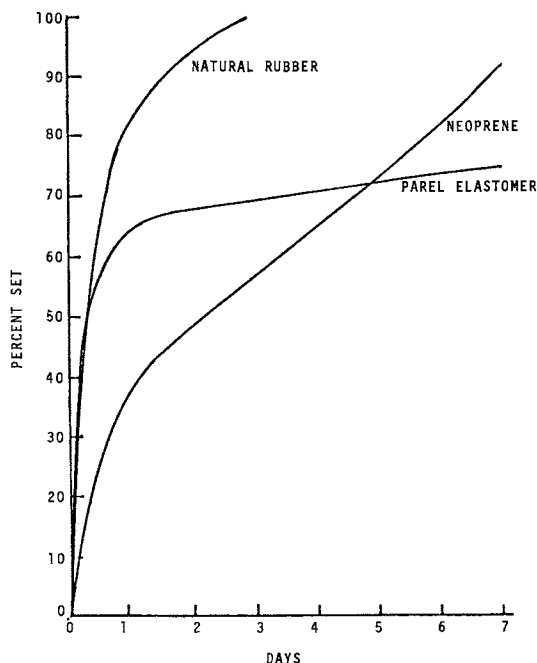
Figure 6.   Compression set at 150°C

rubber was much more rapid than that of either of the synthetic rubbers. Therefore, its modulus dropped rapidly after a few hours.

Figure 7 shows stress relaxation results with Parel elastomer and neoprene at 125°C.; their rates of chain scission are similar. In this test, neoprene maintained a larger fraction of its initial modulus than the vulcanized Parel elastomer. However, Figure 8 shows stress relaxation results with these two rubbers at 150°C. Under these conditions, the greater oxidative stability of the Parel elastomer is more significant than its somewhat greater loss of modulus in the first few hours of test.

Dynamic Properties

The dynamic properties of typical formulations of Parel elastomer, neoprene, nitrile, and natural rubber were measured from -55°C. to +80°C. using a vibrating reed apparatus. These
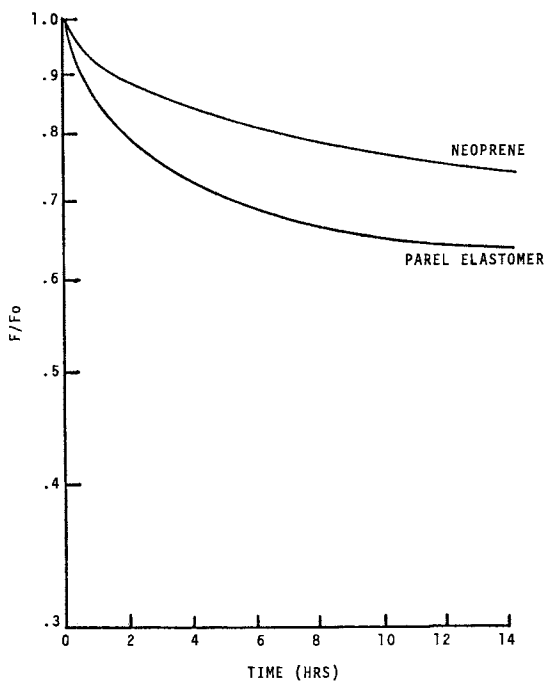
Figure 7.   Stress relaxation at 125°C

measurements were made at a frequency of about 500 hertz at
temperatures below the glass transition, and at about 30 hertz at
higher temperatures. The dynamic modulus of the four rubbers is
plotted against temperature in Figure 9. Although the samples
were strained less than 0.5%, dynamic modulus results are calcu-
lated by extrapolating to 100% strain. Therefore, dynamic tests
gave higher modulus values than static tests. The glass transi-
tion temperatures are very obvious, as shown by the rapid changes
in modulus. They varied from about -55°C. for Parel elastomer to
about 0°C. for neoprene. In many applications, the region of
importance is from about -25° to +40°C. The dynamic modulus of
these four rubbers changed little as the temperature was increased
above 30°C. At well below room temperature, the dynamic modulus
of Parel elastomer and natural rubber remained desirably constant.
The other two rubbers are so close to their glass transition
temperatures that the properties of articles prepared from them
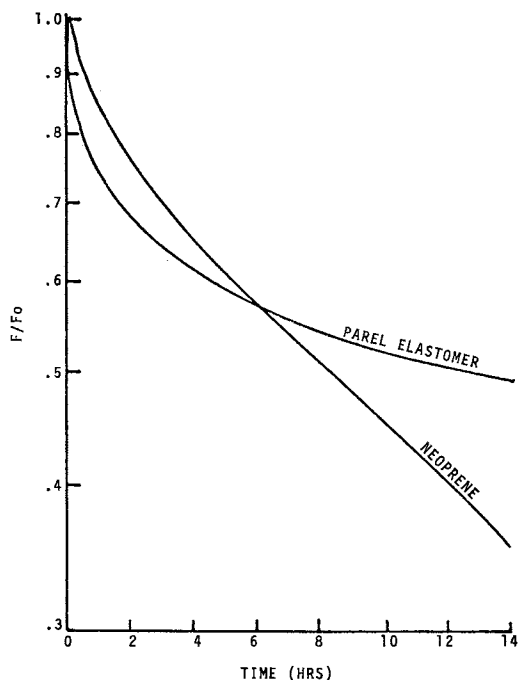
Figure 8.   Stress relaxation at 150°C

would vary considerably at temperatures encountered in the winter.
Decreasing the level of carbon black or adding plasticizer shifted
these curves to lower modulus values, and adding plasticizers
lowered the Tg. However, plasticizers can be lost by extraction
or volatility, and so should be selected to avoid such loss.

In a rubber, there is a time lag between an applied stress
and the resulting strain. In a dynamic test, the stress is ap-
plied in a sinusoidal fashion so this delay can be treated as a
phase angle - delta. Dynamic results are often given as the
tangent of delta. Tan δ is a measure of the ratio of energy
absorbed to energy put in per cycle. Heat buildup in a flexing
rubber is dependent upon the energy required to strain the sample
(the dynamic modulus), and on tan δ, which is a measure of the
fraction of this energy retained by the sample as heat. Small
values are desirable where heat buildup may be a problem, while
larger values mean the material will absorb a larger fraction of
vibrational energy.

Tan δ of Parel elastomer vulcanizates and of three other
rubbers is plotted against temperature in Figure 10; these data
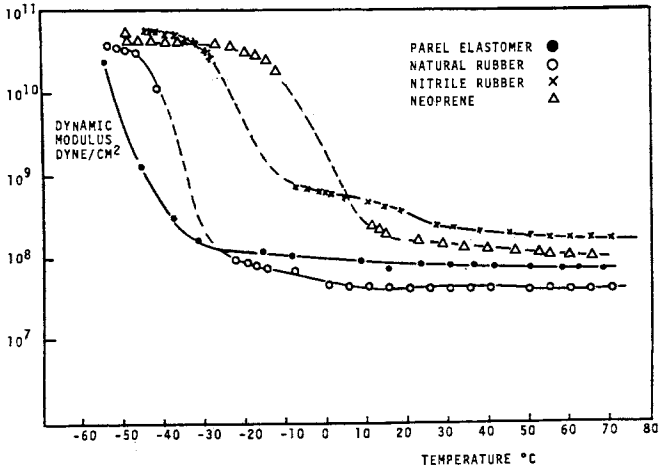
Figure 9. Dynamic modulus vs. temperature
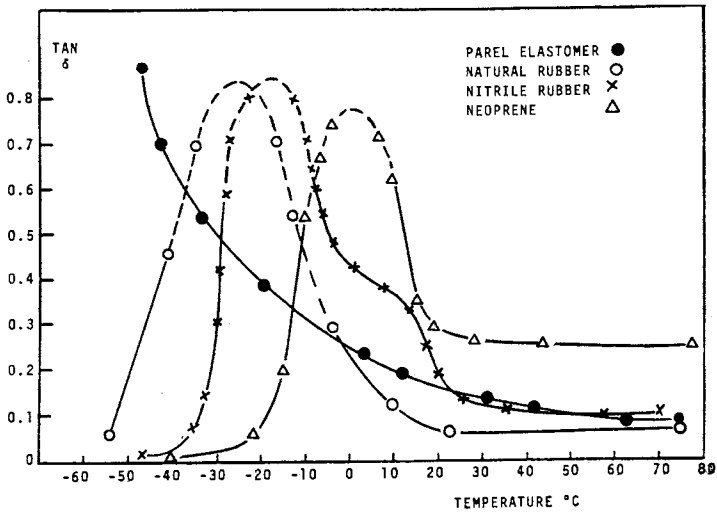
Figure 10. Tan δ vs. temperature

also were obtained on a vibrating reed apparatus. Parel elastomer
gave more constant values above approximately -20°C. than the
other rubbers. The large change in tan δ below room temperature
for the other rubbers means that they will have variable proper-
ties when exposed to outdoor winter conditions.

Summary

        Parel elastomer, a copolymer of propylene oxide and allyl
glycidyl ether, has a combination of properties that make it very
useful in many rubber applications. It can be vulcanized with a
conventional mixture of sulfur and accelerators. The cured
elastomer has a low glass transition temperature (approximately
-55° to -60°C.), and the excellent dynamic properties of natural
rubber. It can be made very stable to high temperature oxidative
degradation, and is better than neoprene in this respect, when
NBC is added as a stabilizer.

Experimental

        Rubber samples were Banbury mixed with final sheeting (and
curatives added) on a 6-inch x 12-inch two-roll mill. All samples
were press cured.
        The formulations for the various compounds contained the
following ingredients (based on parts per hundred of rubber)
and were added in the order given:

Parel elastomer - 1.0 Stearic acid, 50. HAF black (N-330), 1.5
                  Nickel dibutyldithiocarbamate (NBC), 5.0 ZnO,
                  1.5 Tetramethylthiuram monosulfide (TMTM), 1.5
                  mercaptobenzathiazole (MBT), 1.25 Sulfur.
                  Cured 30 minutes at 160°C.

Neoprene W   - 0.5 Stearic acid, 60. HAF-LS black (N-326),
                  5.0 ZnO, 4.0 Maglite D Bar, 2.0 Agerite Gel,
                  0.5 Thiate E.
                  Cured 35 minutes at 154°C.

Natural Rubber   - 2.0 Stearic acid, 35. SRF black (N-770), 1.0
                  Agerite Stalite S, 0.8, N-oxydiethylene benzo-
                  thiazole-2-sulfenamide, 2.0 Reogen, 2.5 Sulfur
                  Cured 30 minutes at 143°C.

Nitrile (Hycar 1042) - 1.0 Stearic acid, 40. HAF black (N-330),
                  1.0 Agerite Resin D, 5.0 ZnO, 1.5 TMTM, 1.5 MBT,
                  1.5 Sulfur.
                  Cured 30 minutes at 160°C.

The vibrating reed equipment used in this work utilized the general principles presented by Robinson[9]. The "reed" was a piece of rubber about 2 mm. x 6.3 mm. x 50 mm. hanging vertically and clamped at the upper end. The lower end was driven magnetically by two fixed coils and a small (about 40 mg.) iron wire clipped about the lower end of the reed. A small correction for the presence of this wire was made according to a method suggested by Forsman[10]. Driving current was supplied by a stable audio oscillator; however, frequency was measured by a Beckmann internal timer. Amplitude of the reed motion was sensed by a light beam and photocell. Values of the dynamic modulus (E*) and tangent of the loss angle (tan δ) were calculated according to the formulas of Wapman and Forsman[11].

Decomposition of t-butylhydroperoxide (TBHP) was carried out by first mixing the TBHP with solvent. The stabilizer was weighed into a tube and the TBHP solution added. A magnetic stir bar was put into the tube and the tube was capped, filled with nitrogen, and put into an oil bath. Samples of the mixture were titrated at intervals by the $NaI-Na_2S_2O_3$ technique. Some runs were made overnight to decompose all of the hydroperoxide. The products were determined by gas chromatography (GC) and infrared spectroscopy. The GC column was a 12 ft. x 6 mm. glass column with silicone grease on Chromasorb W. The column temperature was 90°C.

One-half sized ASTM dumbbells of rubber (~85 mils thick) were aged in a forced draft air oven. Their tensile properties were measured on a Model LACC Scott Tester, at 20 inches/min. Compression set tests were made on buttons 0.5 inch thick and 0.75 inch in diameter. They were compressed 25%, according to ASTM D-395 method B.

Stress relaxation measurements were made on strips of rubber, approximately 2" x 1/2" x 15 mils. They were clamped into an apparatus that fits into a well in a silicone oil bath. The bottom clamp was fixed and the top clamp had a rod connected to a strain gauge. The sample was warmed for 20 minutes in a stream of helium, then it was elongated 25% and tested in air or N_2. The strain gauge converted the force to an electrical signal which was fed into a recorder.

Literature Cited

1. Alliger, G. and I. J. Sjothun, "Vulcanization of Elastomers" Reinhold Publishing Co., New York, 1964.

2. Bateman, L., "The Chemistry and Physics of Rubber-Like Substances" John Wiley and Sons, New York, 1963.

3. Saville, B. and A. A. Watson, Rubber Chem. and Technol. (1967) 40, 100.

4.   Skinner, T. D., ibid. (1972) 45, 182.

5.   Baldwin, F. P., ibid. (1972) 45, 1348.

6.   Moore, C. G., B. R. Trego and J. R. Dunn, J. Appl. Poly. Sci. (1964) 8, 723.

7.   Lal, J., Rubber Chem. and Technol. (1970) 43, 664.

8.   Chien, J. C. W. and C. R. Boss, J. Poly. Sci. A-1 (1972) 10, 1579.

9.   Robinson, D. W. J., Soc. Inst. (1965) 32, 2.

10. Forsman, W. C., private communication.

11. Wapman, P. G. and W. C. Forsman, Trans. Soc. Rheology (1971) 15, 603.

9

Irregular Structures in Polyepichlorohydrin

K. E. STELLER

Hercules Inc., Wilmington, Del. 19899

Introduction

Information concerning the microstructure of a polymer is essential for elucidation of the polymerization mechanism. The polymerization of substituted epoxides such as propylene oxide is particularly interesting. This monomer is unsymmetrical, and polymerization can proceed by attack at either the head or the tail end. If both types of ring openings occur in the propagation step, head-to-tail, head-to-head, and tail-to-tail linkages appear in the polymer chain [eq.(1)].

$$
\begin{array}{ll}
\overset{CH_3}{\underset{H}{-O-C-CH_2-O-}}\overset{CH_3}{\underset{H}{C-CH_2-O-}} & \text{HEAD-TO-TAIL UNIT} \\
& \text{ISOTACTIC (dd and } \ell\ell)
\end{array}
$$

$$
\begin{array}{ll}
\overset{CH_3}{\underset{H}{-O-C-CH_2-O-}}\overset{H}{\underset{CH_3}{C-CH_2-O-}} & \text{HEAD-TO-TAIL UNIT} \\
& \text{SYNDIOTACTIC (d}\ell \text{ and } \ell d)
\end{array}
$$

$$
\begin{array}{ll}
\overset{CH_3}{\underset{H}{-O-CH_2-C-O-}}\overset{H(CH_3)}{\underset{CH_3(H)}{C-CH_2-O-}} & \text{HEAD-TO-HEAD UNIT} \\
& \text{(d}\ell \text{ and } \ell d \text{ or dd and } \ell\ell)
\end{array}
$$

$$
\begin{array}{lll}
\overset{CH_3}{\underset{H}{-O-C-CH_2-O-CH_2-}}\overset{H(CH_3)}{\underset{CH_3(H)}{C-O-}} & \text{TAIL-TO-TAIL UNIT} & \\
& \text{(d}\ell \text{ and } \ell d \text{ or dd and } \ell\ell) & (1)
\end{array}
$$

TAIL   HEAD
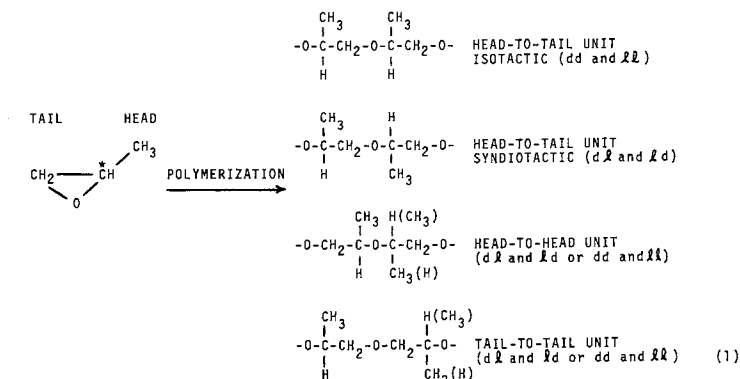
POLYMERIZATION $\longrightarrow$

Hercules Research Center Contribution Number 1646

136

In addition to this structural problem, there is also a stereochemical problem. Unlike vinyl monomers or α-olefins, propylene oxide has an asymmetric carbon atom before polymerization. Thus, it is possible to obtain optically active polymers if the polymerization proceeds with either complete retention or complete inversion at the asymmetric center. Four different dimer units in the main chain are therefore possible [eq.(1)].

It is common knowledge that the microstructure of a polymer has a profound influence on many of its properties. In fact, there have been several such effects observed with poly-(propylene oxide). In 1959, Madorsky and Straus reported that isotactic poly(propylene oxide) is somewhat more stable than the atactic polymer (1). Aggarwal and coworkers showed that the melting point of crystalline poly(propylene oxide) could be related to the sequence length of isotactic units in the polymer (2). Furthermore, Oguni and coworkers showed that the existence of tail-to-tail linkages in poly(propylene oxide) disturbed crystallization of the polymer and thereby depressed its melting point (3).

In polyether research, however, Dr. Charles C. Price was perhaps the first to recognize the influence of polymer microstructure on the resultant physical properties. In 1956, he reported the formation of crystalline, low molecular weight, optically-active polymer from ℓ-propylene oxide by potassium hydroxide-catalyzed polymerization [eq.(2)].

$$
\underset{\ell}{\overset{\overset{\displaystyle CH_3}{\diagup}}{CH_2 \!-\!\!\!-\!\!\!- \overset{*}{C}H}} \quad \xrightarrow{\text{KOH}} \quad \text{CRYSTALLINE, OPTICALLY ACTIVE POLYMER (low M.W.)}
$$

$$
\underset{\ell \qquad \ell \qquad \ell \qquad \ell}{-CH_2\!-\!\overset{\overset{\displaystyle CH_3}{|}}{CH}\!-\!O\!-\!CH_2\!-\!\overset{\overset{\displaystyle CH_3}{|}}{CH}\!-\!O\!-\!CH_2\!-\!\overset{\overset{\displaystyle CH_3}{|}}{CH}\!-\!O\!-\!CH_2\!-\!\overset{\overset{\displaystyle CH_3}{|}}{CH}\!-\!O\!-} \qquad (2)
$$

<div align="center">ISOTACTIC</div>
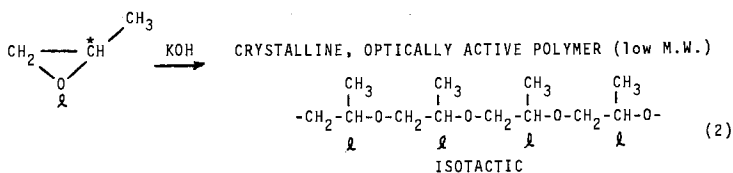
This product was in sharp contrast to the liquid polymer of the same molecular weight produced from racemic monomer under the same conditions [eq.(3)].

$$
\underset{d,\ell}{\overset{\overset{\displaystyle CH_3}{\diagup}}{CH_2 \!-\!\!\!-\!\!\!- CH}} \quad \xrightarrow{\text{KOH}} \quad \text{LIQUID POLYMER (SAME M.W. AS EQ. 2)}
$$

$$
-CH_2\!-\!\overset{\overset{\displaystyle CH_3}{|}}{CH}\!-\!O\!-\!CH_2\!-\!\overset{|}{\underset{\underset{\displaystyle CH_3}{|}}{CH}}\!-\!O\!-\!CH_2\!-\!\overset{|}{\underset{\underset{\displaystyle CH_3}{|}}{CH}}\!-\!O\!-\!CH_2\!-\!\overset{\overset{\displaystyle CH_3}{|}}{CH}\!-\!O\!- \qquad (3)
$$

<div align="center">ℓ   d   d   ℓ</div>

<div align="center">ATACTIC</div>
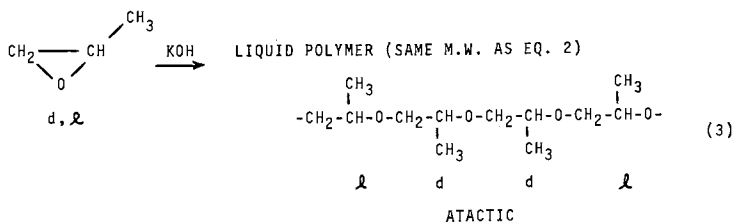
He concluded that this remarkable difference in physical proper-
ties resulted from identical configuration of all the asymmetric
centers in the crystalline polymer. The liquid polymer from
racemic monomer, on the other hand, was evidently a stereorandom
atactic polymer (4). Both polymers were later shown to be formed
almost exclusively by head-to-tail polymerization. Vandenberg,
Price, and others later showed that addition of each epoxide unit
to the polymer chain occurs with inversion of configuration at
the carbon atom where ring opening occurs. The asymmetry in this
case is not disturbed, however, because the bond between the
oxygen and the asymmetric carbon is never broken.

    Dr. Price also showed that ferric chloride-catalyzed polym-
erization of either ℓ- or dℓ-propylene oxide gave polymeric
material which could be separated into amorphous, intermediate
molecular weight and crystalline, high molecular weight fractions
[eqs. (4) and (5)].

A. CRYSTALLINE, OPTICALLY ACTIVE POLYMER
   (HIGH M.W.)

                        AND

B. AMORPHOUS, LESS OPTICALLY ACTIVE POLYMER
   (INTERMEDIATE M.W.)   (4)

C. SAME AS A BUT OPTICALLY INACTIVE

                        AND

D. SAME AS B BUT OPTICALLY INACTIVE
                                                      (5)
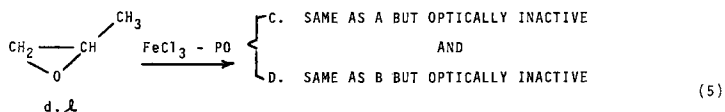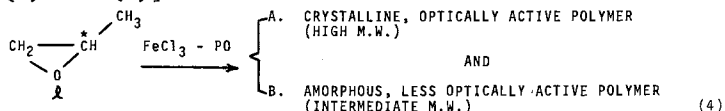
    There was no detectable difference between the products
from the optically active and racemic monomers except for optical
activity (4). He later demonstrated that the amorphous fractions
of poly(propylene oxide) from optically active monomer contained
head-to-head sequences (5) and (6). The formation of head-to-
head sequences requires normal head-to-tail opening followed by
an abnormal head-to-head attack [eq. (6)].

HEAD-TO-TAIL

HEAD-TO-HEAD

(6)

m= METAL ATOMS OF CATALYST SPECIES
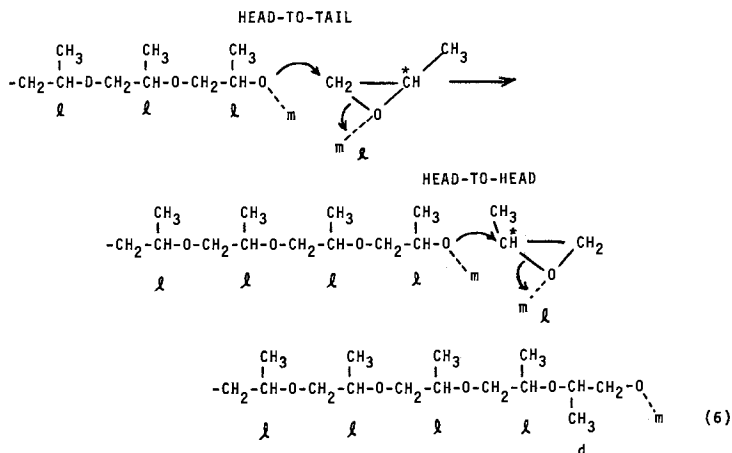
Since the carbon atom undergoing ring opening in the latter case
is the asymmetric carbon, inversion of configuration occurred
each time a unit inserted head-to-head. The resultant optical
activity was therefore less.

Dr. Price explained that the formation of any crystalline
polymer at all from racemic monomer must be due to asymmetric
catalytic sites. These sites exhibit highly preferential reacti-
vity for propylene oxide of one particular configuration. Thus,
he was one of the first to recognize that defects in the catalyst
or the existence of several different catalytic sites can pro-
foundly affect the resultant polymer microstructure.

When Hercules entered the specialty rubber business in 1968
with its two HERCLOR® epichlorohydrin elastomers (Table I),
very little was known about their structure. As indicated pre-
viously, it should be possible to change the microstructure by
altering the catalyst system and in this way optimize the balance
of properties.

TABLE I - HERCULES EPICHLOROHYDRIN ELASTOMERS

	HERCLOR H ELASTOMER	HERCLOR C ELASTOMER
STRUCTURE	$-(CH_2-CH-O)_n$ | CH_2Cl	$-(CH_2-CH-O-CH_2-CH_2-O)_n$ | CH_2Cl
EPICHLOROHYDRIN, MOLE %	100	50
ETHYLENE OXIDE, MOLE %	0	50
CHLORINE, %	38.4	26.0
SPECIFIC GRAVITY	1.36	1.27
Tg, °F. (by DTA)	-15	-49

We first set out to determine the microstructure of the epi-
chlorohydrin homopolymer, HERCLOR H elastomer. Since epichloro-
hydrin, like propylene oxide, is unsymmetrical and contains an
asymmetric carbon atom, the polymer chain could contain the same
four types of chain units as shown previously for poly(propylene
oxide). Our approach to determining the amounts of irregular
head-to-head and tail-to-tail structures consisted of replacing
all the chlorines in polyepichlorohydrin with hydrogens. Since
the dechlorination reaction does not involve the asymmetric
center, the resultant poly(propylene oxide) should have the same
configuration around each asymmetric carbon as the original poly-
epichlorohydrin. The resultant poly(propylene oxide) could then
be cleaved to dimer units according to a procedure developed by
Vandenberg (7).

Experimental

Dechlorination of Polyepichlorohydrin. Polyepichlorohydrin
(5.0 g., 54 mmoles Cl) was transferred to a dry 28-oz. beverage
bottle in a nitrogen-filled glove bag. The polymer was dissolved

in 150 ml. of distilled, dried tetrahydrofuran and treated with
fresh lithium aluminum hydride [LAH] (5.13 g., 135 mmoles) which
was weighed and transferred in the glove bag. The mixture was
stirred 50 hours at 50°C. and quenched with about 900 mmoles of
water in tetrahydrofuran solution. The resultant poly(propylene
oxide) was isolated by filtration and evaporation of the solvent
in vacuo.

Cleavage of Poly(propylene oxide). The dechlorinated polymer
(0.157 g., 2.7 mmoles of propylene oxide units) was dissolved in
benzene in a dry 4-inch polymerization tube. n-Butyllithium (1.5
mmoles) was added and the solution was tumbled for 18 hours at
25°C. and stirred 4 hours at 90°C. before being shortstopped with
distilled ethyl alcohol and cooled. Vandenberg's procedure (7)
was greatly simplified by neutralization of the cleavage mixtures
while they were still in the polymerization tubes by micro-poten-
tiometric titration with a standardized solution of HCl in ethyl
alcohol. Neutralization was followed by injection of internal
standard and centrifugation to yield clear samples for direct gas
chromatographic analysis.

Gas Chromatographic Analysis of Cleavage Mixtures. The above
samples were analyzed directly by gas chromatography using 5%
(w/w) Carbowax 1000 on 100/110 mesh Anakrom SD as the packing in
a 12 ft. x 1/4 in. O.D. borosilicate glass column at 150°C.
Samples were injected directly into the glass column to avoid any
contact with metal. An internal standard (methyl p-toluate) and
flame ionization detection were also employed.

Carbon-13 NMR Analysis of Polyepichlorohydrin. Natural-
abundance carbon-13 NMR spectra at 22.6 MHz were measured in
benzene at 70°C. with proton noise decoupling, using a Bruker
HFX-10 spectrometer equipped with a Nicolet 1085 Fourier trans-
form spectroscopy accessory.

Results and Discussion

HERCLOR H elastomer was readily dechlorinated by treatment
with excess lithium aluminum hydride [LAH] (2.5 moles/mole of Cl)
in tetrahydrofuran at 50°C. Unreacted hydride was quenched with
water, and the polymer samples were isolated for chlorine
analyses. The observed pseudo-first-order rate constant for the
disappearance of chlorine was found to be 1.9×10^{-4} min.$^{-1}$ under
these conditions (Fig. 1).
Polymers were isolated in about 99% yield after treatment for
50 hours at 50°C. Although they contained less than 0.3% of the
original chlorine, they were not otherwise seriously changed. The
weight average molecular weights were found to be about 0.5
million. If no cleavage whatsoever occurred, the molecular weight
should decrease from 1.7 million to 1.1 million due simply to the
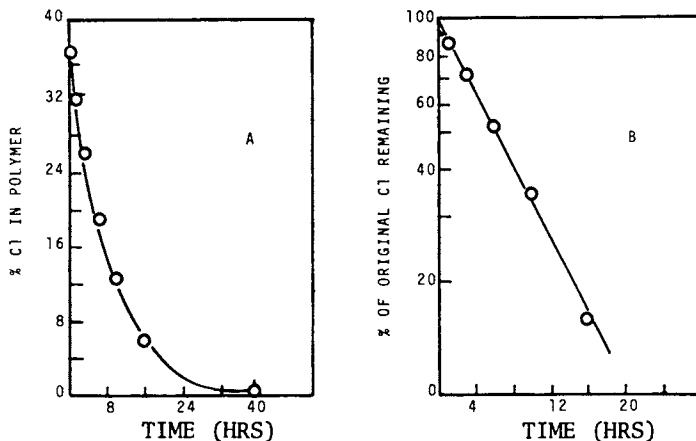
Figure 1. Linear (A) and semi-log (B) plots showing dechlorination of HERCLOR H elastomer with lithium aluminum hydride (2.5 moles/ mole Cl) in tetrahydrofuran at 50°C

replacement of chlorine with hydrogen. The additional decrease in molecular weight occurred when the polymer - either polyepichloro- hydrin or poly(propylene oxide) - was simply dissolved and re- isolated under the experimental conditions. No additional de- crease in molecular weight was observed when the poly(propylene oxide) was treated with LAH for 50 hours at 50°C.

Since HERCLOR H elastomer could be converted quantitatively to poly(propylene oxide), the microstructure could be determined by using the method developed by Vandenberg for poly(propylene oxide) (7). This method consists of cleavage with n-butyllithium and analysis of the resultant dipropylene glycol fraction for the various different structural isomers (Fig. 2). The relative amounts of the various types of dipropylene glycols indicate the relative numbers of head-to-head and tail-to-tail linkages in the original polymer.

Initial GC analyses of the cleavage mixtures were not repro- ducible, due to poor resolution and tailing of the dipropylene glycol GC peaks until Carbowax 1000 on an inert support such as Anakrom SD was used as the packing in a glass column. Figure 3 shows the excellent resolution eventually obtained with authentic samples of the dipropylene glycols. The two diastereoisomeric forms of the diprimary isomer were resolvable on the GC. The amounts due to each of the two peaks were summed to give the total diprimary (or head-to-head) content.

The results shown in Table II clearly indicate that typical HERCLOR H elastomer has a very regular structure with 97-99% head-to-tail attachment of monomer units. The chromatogram of a typical cleavage mixture (Figure 4) further emphasizes the lack of any significant number of the irregular head-to-head or tail- to-tail dimers.

| DIPROPYLENE GLYCOL STRUCTURE | TYPE OF DIMER UNIT IN ORIGINAL POLYMER |

$$CH_3 \quad\quad CH_3$$
$$HO-C-CH_2-O-C-CH_2-OH \quad\quad \text{HEAD-TO-TAIL}$$
$$H \quad\quad\quad H$$

MIXED PRIMARY-SECONDARY GLYCOL, 2d ℓ PAIRS
(erythro and threo)

$$CH_3 \ CH_3$$
$$HO-CH_2-C-O-C-CH_2-OH \quad\quad \text{HEAD-TO-HEAD}$$
$$H \ \ H$$

DIPRIMARY GLYCOL, MESO AND RACEMIC

$$CH_3 \quad\quad CH_3$$
$$HO-C-CH_2-O-CH_2-C-OH \quad\quad \text{TAIL-TO-TAIL}$$
$$H \quad\quad\quad H$$

DISECONDARY GLYCOL, MESO AND RACEMIC
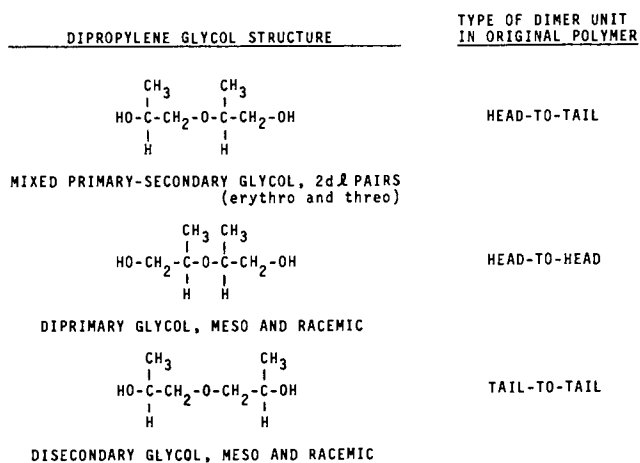
Figure 2. Dipropylene glycols resulting from n-butyllithium cleavage of poly(propylene oxide)

TABLE II

RESULTS FROM CLEAVAGE OF DECHLORINATED HERCLOR H ELASTOMER

SAMPLE OF DECHLORINATED HERCLOR H ELASTOMER	% OF TOTAL DIPROPYLENE GLYCOLS			% OF ORIGINAL POLYMER	
	DISECONDARY DIMER	MIXED DIMER	DIPRIMARY DIMER	PROPYLENE GLYCOL	DIPROPYLENE GLYCOLS
A	1.6	96.7	1.6	6.0	15.8
B	0.7	99.3	D	6.3	12.5
B	0.7	99.3	0	6.1	12.4
B	0.7	99.3	0	6.2	12.7

Of course, the mixture of dipropylene glycols obtained after dechlorination and cleavage of HERCLOR H elastomer is representative of the original structure only if the following conditions hold true. First, the dechlorination of HERCLOR H elastomer with LAH does not alter the structure of the backbone; second, the cleavage is completely random; and third, all the dipropylene glycols are equally resistant to further degradation. Our effort to verify these conditions is summarized in Table III. A sample of poly(propylene oxide) made with a catalyst different from that used for HERCLOR H elastomer was treated with LAH (2.5 mmoles/mmole of propylene oxide) for 50 hours at 50°C. The resultant polymer was isolated and cleaved by the normal procedures. Other samples of the same poly(propylene oxide) were cleaved directly for varying lengths of time. The following observations are apparent from the data:

I.   SOLVENT
II. PROPYLENE GLYCOL
III. INTERNAL STANDARD (METHYL p-TOLUATE)
IV. DISECONDARY DIPROPYLENE GLYCOL
V.   MIXED DIPROPYLENE GLYCOL
VI. DIPRIMARY II DIPROPYLENE GLYCOL
VII. DIPRIMARY I DIPROPYLENE GLYCOL
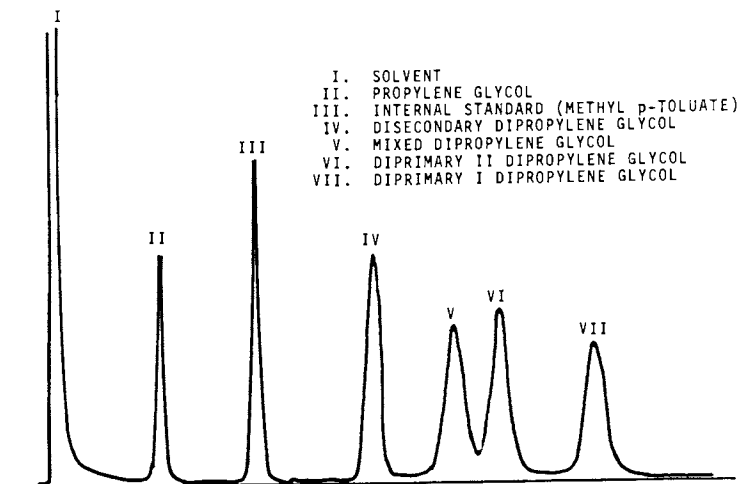
Figure 3.   Gas chromatogram showing resolution of the dipropylene glycols

I.   SOLVENT
II. PROPYLENE GLYCOL
III. INTERNAL STANDARD (METHYL p-TOLUATE)
IV. DISECONOARY DIPROPYLENE GLYCOL
V.   MIXED DIPROPYLENE GLYCOL
VI. DIPRIMARY II DIPROPYLENE GLYCOL POSITION
VII. DIPRIMARY I DIPROPYLENE GLYCOL POSITION
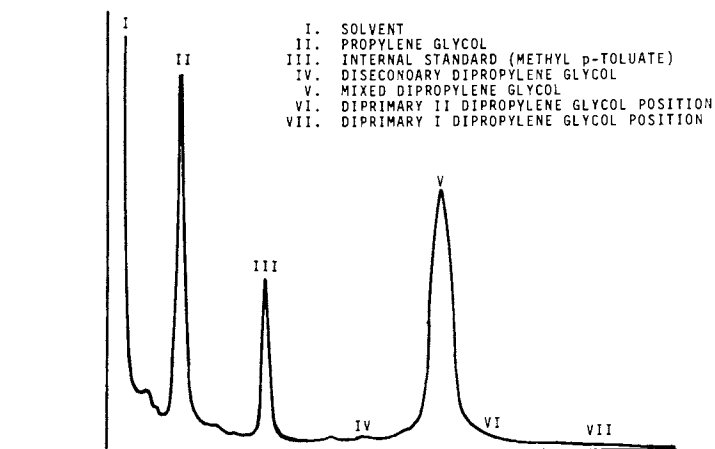
Figure 4.   Gas chromatogram of cleavage mixture from dechlorinated HERCLOR H elastomer

TABLE III

EFFECT OF LAH TREATMENT AND EXTENT OF CLEAVAGE

LAH TREATMENT*	CLEAVAGE TIME		% OF DIPROPYLENE GLYCOLS		% OF ORIGINAL POLYMER	
	HOURS AT 25°C	HOURS AT 90°C	HEAD-TO-TAIL DIMER	IRREGULAR DIMERS	PROPYLENE GLYCOL	DIPROPYLENE GLYCOLS
YES	18	4	63.4	36.6	8.1	13.2
YES	18	4	61.2	38.8	7.4	13.5
NO	4	0	61.0	39.0	5.6	11.5
NO	10	0	64.0	36.0	5.6	10.8
NO	18	0	63.4	36.6	6.3	11.6
NO	18	1	63.5	36.5	5.6	11.9
NO	18	4	60.5	39.5	5.6	12.4

*STIRRED 50 HOURS AT 50°C. WITH 2.5 LAH/C_3H_6O UNIT BEFORE ISOLATION AND CLEAVAGE WITH n-BUTYLLITHIUM.

(1) The relative amounts of the dipropylene glycols formed
    were nearly identical whether or not the polymer was
    treated with LAH. Thus, LAH treatment under the con-
    ditions used caused no isomerization of the polyether
    backbone.

(2) The relative amounts of the dipropylene glycols formed
    remained constant and were independent of time. If
    cleavage were a nonrandom process, the ratios of dimers
    formed at low levels of cleavage should be different
    from the ratios observed after complete cleavage. Al-
    though no data were obtained at <u>very</u> low levels of
    cleavage (cleavage was much more rapid than expected),
    the data are consistent with a nondiscriminatory
    cleavage process.

(3) The stabilities of the dipropylene glycols under the
    cleavage conditions appeared to be very similar and
    there was no indication that any of the dimers degraded
    further.

Further confirmation of the uniformly head-to-tail structure
of HERCLOR H elastomer was obtained from its carbon-13 NMR
spectrum. Since no literature spectra of polyepichlorohydrin were
available for comparison, the carbon-13 NMR spectra of the poly-
(propylene oxide) resulting from dechlorination with LAH were also
examined. Published spectra of poly(propylene oxide) with
detailed peak assignments are available.

Oguni and co-workers have examined the carbon-13 NMR spectra
of crystalline poly(propylene oxide) and of amorphous poly-
(propylene oxide) made with a base catalyst (8). They made the
peak assignments shown in Figure 5. The spectrum of the crystal-
line polymer contained three peaks at 17.33, 73.98, and 75.98 ppm.
downfield from tetramethylsilane. These were identified as aris-
ing from methyl, methylene, and methine carbons, respectively.

The spectrum of amorphous poly(propylene oxide) contained
three peaks in the methine carbon region with an observed peak
area ratio of 25:50:25, and two main peaks in the methylene carbon
region with an observed peak area ratio of 50:50. Since it is
known that poly(propylene oxide) made with base catalysts is atac-
tic and contains practically no head-to-head or tail-to-tail link-
ages, it was reasonable to assign the two methylene peaks to equal
amounts of isotactic and syndiotactic dyads and the three methine
carbon peaks to isotactic, heterotactic, and syndiotactic triads.
Thus, the two peaks observed at 73.98 and 75.98 ppm. in the spec-
trum of the crystalline isotactic polymer were assigned to iso-
tactic dyad and triad, respectively. These assignments lead
naturally to those of syndiotactic dyad (73.71 ppm.), syndio-
tactic triad (75.78 ppm.), and heterotactic triad (75.90 ppm.).
These assignments were recently confirmed by other workers (9).

Figure 6 shows the much more complicated NMR spectrum of a
sample of poly(propylene oxide) known to contain abnormal head-to-
head and tail-to-tail linkages. Thirteen partially resolved peaks
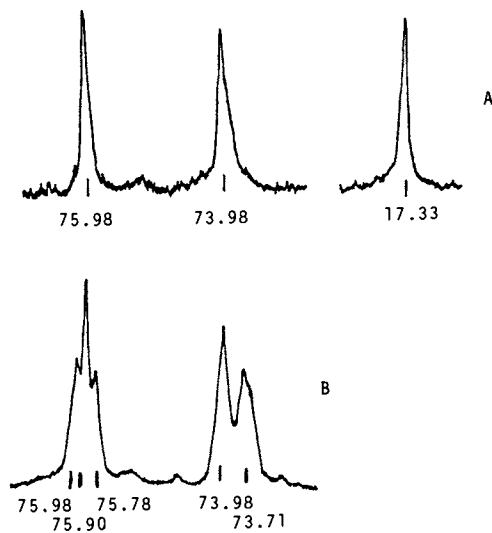
Macromolecules

*Figure 5.   Carbon-13 NMR spectra of (A) crys-
talline poly(propylene oxide) and (B) amorphous
poly(propylene oxide) made with t-BuOK catalyst
(8)*
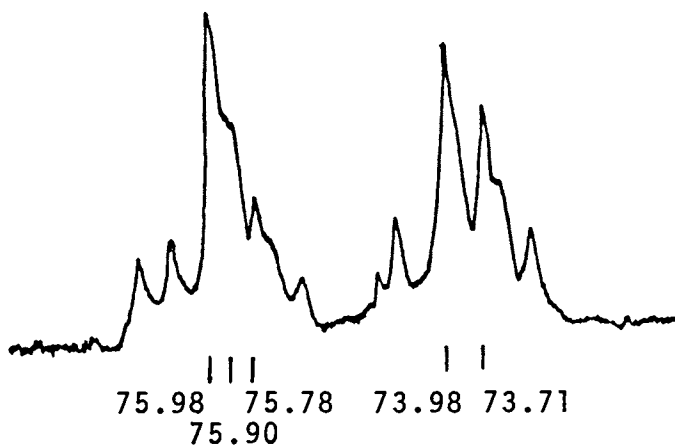
Macromolecules

*Figure 6.   Carbon-13 NMR spectrum of amorphous poly(propylene
oxide) made with an Al(C₂H₅)₃–H₂O (1:1) catalyst. This polymer is
known to contain head-to-head and tail-to-tail linkages (8).*

were observed in the spectrum of this particular sample (<u>8</u>).

The carbon-13 NMR spectra of HERCLOR H elastomer and the poly(propylene oxide) we obtained by dechlorination with LAH are shown in Figure 7. The spectrum of the dechlorinated product is seen to resemble very closely that of poly(propylene oxide) made with the base catalyst and contains no noticeable peaks due to structural imperfections. The two major peaks* in the methylene carbon region at 73.94 and 73.65 ppm. are in the ratio of 55 to 45. These were assigned to isotactic and syndiotactic dyads which were observed at 73.98 and 73.71 by Oguni and co-workers. The slight change in chemical shift is within the experimental error of the procedure, especially considering the broad peaks obtained by Oguni. Thus, it seems reasonable that the two peaks at 70.17 and 70.00 ppm. (peak area ratio approximately 58 to 42) in the spectrum of HERCLOR H elastomer can also be assigned to isotactic and syndiotactic dyads. It is also apparent that the methine peaks in the spectrum of HERCLOR H elastomer are not sufficiently resolved to permit measurement of the relative concentrations of the various triad structures. Thus, to obtain information about the triad structures in polyepichlorohydrin, it must first be dechlorinated to poly(propylene oxide).
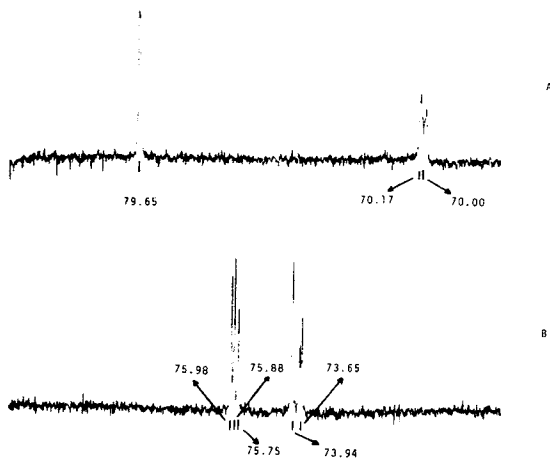
Figure 7. Carbon-13 NMR spectra of (A) HER-CLOR H elastomer and (B) the poly(propylene oxide) obtained by dechlorination with LAH

---

*The resolution was so good that the 73.65 ppm. peak was parti-ally resolved into two peaks. Thus, it might be possible to see variations due to triad structures in this region also.

The assignment of the 70.17 ppm. peak to isotactic dyads in
polyepichlorohydrin was confirmed by observing the spectrum of
crystalline material prepared by a published procedure (10).
Figure 8 shows the carbon-13 NMR spectra of crystalline poly-
epichlorohydrin and the poly(propylene oxide) it yielded by de-
chlorination with LAH. The poly(propylene oxide) was also highly
crystalline (m.p. 64°C. by DTA) and its carbon-13 NMR spectrum
corresponds closely to that reported for the isotactic polymer.
Thus, the single methylene peak at about 70.2 ppm. in the spectrum
of crystalline polyepichlorohydrin is due to isotactic dyads. The
poor resolution in this spectrum is due to low solubility of the
crystalline polymer in the benzene solvent. No trace of the peaks
due to polyepichlorohydrin are observable in the spectra of the
poly(propylene oxide) obtained by dechlorination. In addition,
the number of observable peaks does not increase as a result of
the LAH treatment. This is further evidence that the dechlorin-
ation reaction results in smooth replacement of Cl with H without
otherwise altering the structure of the polymer.
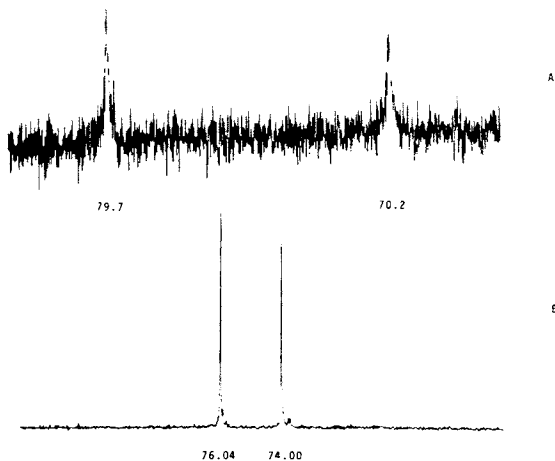
*Figure 8.   Carbon-13 NMR spectra of (A) crys-
talline polyepichlorohydrin and (B) the poly(pro-
pylene oxide) obtained by dechlorination with
LAH*

Summary

A procedure has been described for the determination of
irregular head-to-head and tail-to-tail linkages in polyepichloro-
hydrin. This procedure involves dechlorination of the polymer
with lithium aluminum hydride, cleavage of the resultant poly-
(propylene oxide) with n-butyllithium, and analysis by gas chroma-
tography to determine the relative amounts of the respective
dipropylene glycols.

The dechlorination reaction was shown to result in smooth replacement of chlorine with hydrogen without otherwise altering the structure of the polymer. The cleavage reaction was shown to be random and the dipropylene glycols to be equally resistant to further degradation. Thus, the relative amounts of the diprimary and disecondary dipropylene glycols formed are identical to the number of head-to-head and tail-to-tail units in the original polymer.

HERCLOR H epichlorohydrin elastomer was found by this procedure to have a very uniform structure with more than 97% head-to-tail monomer placements. This structure was confirmed by examination of the carbon-13 NMR spectra of HERCLOR H elastomer and of the poly(propylene oxide) obtained by dechlorination with LAH.

Acknowledgment

Literature Cited

1. Madorsky, S. L. and S. Straus, J. Poly. Sci. (1959), 36, 183.
2. Aggarwal, S. L., L. Marker, W. L. Kollar, and R. Geroch, Advan. Chem. Ser. (1966), 52, 88.
3. Oguni, N., S. Watanabe, M. Maki, and H. Tani, Macromolecules (1973), 6(2), 195.
4. Price, C. C. and M. Osgan, J. Amer. Chem. Soc. (1956), 78, 4787.
5. Price, C. C., R. Spector, and A. L. Tumolo, J. Poly. Sci. A-1 (1967), 5, 407.
6. Price, C. C., M. K. Akkapeddi, B. T. DeBona, and B. C. Furie, J. Amer. Chem. Soc. (1972), 94(11), 3964.
7. Vandenberg, E. J., J. Poly. Sci. A-1 (1969), 7, 525.
8. Oguni, N., K. Lee, and H. Tani, Macromolecules (1972), 5(6), 819.
9. Uryu, T., H. Shimazu, and K. Matsuzaki, J. Poly. Sci. B (1973), 11, 275.
10. Vandenberg, E. J., Macromolecular Syntheses (1972), 4, 49.

10

Cationic Polymerization of Cyclic Ethers Initiated by Superacid Esters

TAKEO SAEGUSA and SHIRO KOBAYASHI

Department of Synthetic Chemistry, Faculty of Engineering, Kyoto University, Kyoto 606, Japan

Introduction

Superacids are more acidic than 100% sulfuric acid, the most frequently used strong acid solvent (1,2). With this respect fluorosulfuric, chlorosufuric, and trifluoromethanesulfonic acids are familiar among superacids (3). 2,4,6-Trinitrobenzenesulfonic acid is also a superacid since it forms a stable trialkyl oxonium salt (4). Superacid esters have long been known, e.g., ethyl chlorosulfate was prepared more than a century ago (5). However, little attention has been paid on the reaction of superacid esters (6) until recently Alder et al., have reported that methyl and ethyl fluorosulfates are very effective alkylating agents for nitrogen and/or oxygen containing compounds (7). We have found that methyl and ethyl esters of fluorosulfuric and chlorosulfuric acids are good initiators for the cationic ring-opening polymerization of tetrahydrofuran (THF), oxetane, 2-oxazoline, and propylene oxide (8). At almost the same time Smith and Hubin have reported semi-quantitative studies of the THF polymerization initiated by superacid derivatives including methyl trifluoro-methanesulfonate (9,10). Very recently we have performed kinetic studies of the ring-opening polymerization of cyclic ethers initiated with superacid esters (3,11-14). The esters employed were ethyl fluorosulfate (EtOSO$_2$F), chlorosulfate (EtOSO$_2$Cl), tri-fluoromethanesulfonate (EtOSO$_2$CF$_3$, "triflate" EtOTf), and 2,4,6-trinitrobenzenesulfonate ("trinitate" EtOTn) ; cyclic ether monomers being THF and 3,3-bis(chloromethyl) oxetane (BCMO). Kinetic analyses were carried out by means of our "phenoxyl end-capping" method (15,16) as well as of ^{1}H and ^{19}F nmr spectroscopy. These methods allowed the direct determination of the concentration of the propagating species [P*]. Thus, we have disclosed new findings which are characteristic to the superacid ester-initiated systems of the THF and BCMO polymerizations (11,12). The present article describes these results (3,11,12). Cationic ring-opening polymerizations of cyclic ethers initiated with typical Lewis acid catalysts (conventional initiators) have

recently been reviewed by us (15,16).

Polymerization of THF

Kinetics of the THF Polymerization by Phenoxyl End-Capping
Method (3). In determining [P*] during the THF polymerization
initiated by superacid esters the phenoxyl end-capping procedure
is shown in Scheme 1. The reaction of sodium phenoxide with the
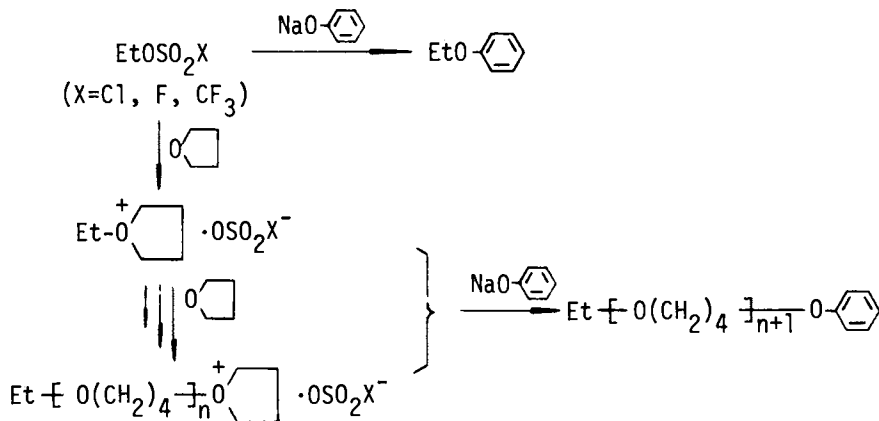
Scheme 1

propagating species and with the unreacted initiator should
quantitatively produce the polymer phenyl ether and phenetole,
respectively. The quantitativeness of the reaction between
sodium phenoxide and the propagating cyclic oxonium has been
established in the previous studies by using Lewis acid catalysts
(17,18). Therefore, the reactions of sodium phonoxide with
superacid esters of $EtOSO_2F$ and $EtOSO_2Cl$ were examined (Table I).
From the results shown in Table I Reaction 1 has been regarded
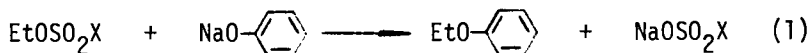
as quantitative (3). This indicates that the phenoxyl end-
capping method can be used for the kinetic analysis of the THF
polymerization by superacid ester initiators as in the case of
$Et_3O^+BF_4^-$ initiator system (19).
     The initiation reaction can be formulated as
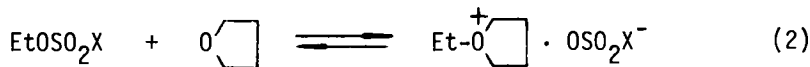
On the basis of an S_N2 mechanism the rate equation of initiation
is given by

Table I.   Reactions of $EtOSO_2X$ (X=F and Cl) with Sodium
           Phenoxide at Room Temperature

$EtOSO_2X$[a] (mmol)	X	$NaOC_6H_5$[b] (mmol)	Reaction Time (min)	Yield[c] (%)
0.99	F	4.0	10	96
0.59	F	2.9	30	95
1.15	Cl	3.5	5	93

a) Solution in 3 ml of THF.   b) Solution in 6 ml of THF.

c) Based on $EtOSO_2X$.   Determined by UV analysis.

                              Bull. Chem. Soc. Japan (3).

$$- \frac{d[I]}{dt} = k_i [I] [M] \tag{3}$$

Integration of Equation 3 gave

$$\ln \frac{[I]_0}{[I]_t} = k_i \int_0^t [M]dt \tag{4}$$

where k_i is the rate constant of initiation.
     It has already been established that the propagation of the
cationic polymerization of THF is expressed by

$$\sim\sim O \overset{+}{\Box} \cdot A^- \ + \ O\Box \ \underset{}{\overset{k_p}{\rightleftharpoons}} \ \sim\sim O(CH_2)_4\text{-}\overset{+}{O}\Box \cdot A^- \tag{5}$$
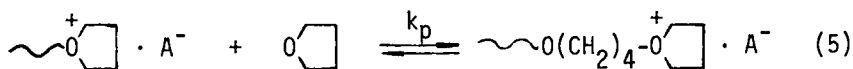
According to a bimolecular mechanism the rate equation of
propagation is given by

$$- \frac{d[M]}{dt} = k_p[P*] \left\{ [M] - [M]e \right\} \tag{6}$$

where [M] and [M]e represent the instantaneous and equilibrium
monomer concentrations, respectively, and k_p is the rate constant
of propagation.   Integration of Equation 6 leads to

$$\ln \frac{[M]t_1 - [M]e}{[M]_{t_2} - [M]e} = k_p \int_{t_1}^{t_2} [P*]dt \tag{7}$$

     Figure 1 shows the [P*] - time (curve A) and monomer
conversion - time (curve B) relationships in the THF polymerizat-

ion initiated by $EtOSO_2F$ in CH_2Cl_2 at 0°C. After 20 hr, [P*]
reached to 63% of the feed concentration of the initiator. The
presence of the induction period (curve B) indicates a slow
initiation followed by a fast propagation. Plots of Equations 4
and 7 were made on the basis of the data of curves A and B,
respectively. In both cases straight lines passing through the
origin were obtained, the slopes of which gave values of
$k_i = 0.33 \times 10^{-5}$ 1/mol·sec and $k_p = 0.66 \times 10^{-3}$ 1/mol·sec,
respectively. Table II lists the kinetic data of three superacid
ester initiators as well as of an oxonium species of $Et_3O^+ \cdot BF_4^-$.

Table II.   Kinetic Data of the THF Polymerization with Superacid
            Ester Initiators in CH_2Cl_2 Solution

	$EtOSO_2F$	$EtOSO_2Cl$	$EtOSO_2CF_3$	$Et_3\overset{+}{O}BF_4^-$ [a]
Initiation				
$k_i \times 10^5$ at 0°C (1/mol·sec)	0.33	0.38	0.80	6.1 [b]
$\Delta H_i^{\ddagger}$ (kcal/mol)	13.5	12.8	10.5	16.4
$\Delta S_i^{\ddagger}$ (e.u.)	−34	−37	−44	−16
Propagation				
$k_p \times 10^3$ at 0°C (1/mol·sec)	0.66	1.4	1.7	3.7
$\Delta H_p^{\ddagger}$ (kcal/mol)	13.0	11.8	11.6	12
$\Delta S_p^{\ddagger}$ (e.u.)	−26	−28	−29	−26

a) Taken from (15, 16, 19, 20).

b) Data at 2.5°C (20).   Bull. Chem. Soc. Japan (3).

    The initiation is a dipole-dipole reaction to produce an
oxonium ion (Equation 2). The k_i values of superacid esters are
1/20 – 1/10 of that of $Et_3O^+BF_4^-$ and at least 2×10^2 times smaller
than the k_p values in the superacid ester systems. The activation
parameters exhibited relatively low $\Delta H_i^{\ddagger}$ (favorable) and $\Delta S_i^{\ddagger}$
(unfavorable) values. This tendency has often been observed in
dipole-dipole S_N2 reactions producing ionic species, e.g., the
Menschutkin reaction (21) and the oxonium formation reaction from
superacid esters and tetrahydropyran (Reaction 8) (22).

$$ROSO_2X \quad + \quad O\langle\hexagon\rangle \quad \rightleftharpoons \quad R-\overset{+}{O}\langle\hexagon\rangle \cdot OSO_2X^- \qquad (8)$$
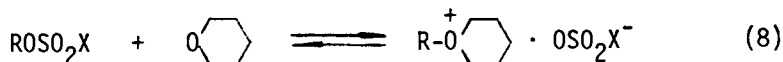
The k_p value of $EtOSO_2F$ is extremely small, e.g., about 1/6 of that of $Et_3\overset{+}{O}BF_4^-$ initiator. The k_p values of $EtOSO_2Cl$ and $EtOSO_2CF_3$ are between those of $EtOSO_2F$ and $Et_3O^+BF_4^-$. Since the activation parameters of the propagation are very close to those of $Et_3O^+BF_4^-$, it is reasonable to conclude that the propagation initiated by $EtOSO_2X$ proceeds mainly via an oxonium mechanism (Equation 5).

Kinetics of the $EtOSO_2CF_3$-Initiated Polymerization of THF by ^{1}H and [19]F Nmr Spectroscopy. It has been pointed out in several studies (3, 9, 10, 23) that in the THF polymerization by a super-acid ester initiator, e.g., $EtOSO_2CF_3$, the propagating chain end may be in the equilibrium of the oxonium (I) – ester (II) species (Equation 9). Our previous study showed that kinetics of the THF

$$\sim\sim\overset{+}{O}\square \cdot OSO_2CF_3^- \quad \overset{K}{\rightleftharpoons} \quad \sim\sim\sim O(CH_2)_4OSO_2CF_3 \qquad (9)$$

$$\text{I} \hspace{5.5cm} \text{II}$$
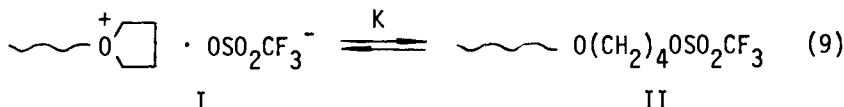
polymerization initiated with superacid esters could be carried out by ^{1}H nmr spectroscopy alone (3). However, it was very difficult to verify directly the equilibrium of Equation 9 due to the limitation of the sensitibity and resolution of ^{1}H nmr spectroscopy. We disclosed that ^{19}F nmr spectroscopy is very powerful to abserve directry both the oxonium counteranion $OSO_2CF_3^-$ (I) and ester species $\sim\sim CH_2OSO_2CF_3$ (II).

[19]F nmr spectroscopy (11). Figure 2 shows the ^{19}F nmr spectrum of the THF polymerization system initiated by $EtOSO_2CF_3$ in CCl_4 after 48 min at 13°C. The molar ratio of THF to initiator was 5 : 1. Peak A at δ -2.52 (in ppm relative to the external standard of CF_3CO_2H capillary) is assigned to the initiator $EtOSO_2CF_3$. Peak B at δ +0.46 is due to the oxonium counteranion of I ($OSO_2CF_3^-$) of the propagating species. Finally, peak C at δ -2.80 is reasonably ascribed to the ester species of II ($\sim\sim CH_2OSO_2CF_3$). No other peaks were detected during a kinetic run. Thus, the ^{19}F nmr spectroscopy provides with a new method for the direct determination of the instantaneous concentrations of initiator and the oxonium and ester species of propagation.

Figure 3 shows the variations of ($[O^+] + [E]$) (curve A) and $[O^+]$ (curve B) as a function of time under the polymerization conditions of Figure 2, where $[O^+]$ and $[E]$ denote the concentrations of the oxonium (I) and ester (II) species, respectively. At the end of the kinetic run (after 76 min) 28% of the charged initiator has been reacted. The molar ratio of $[O^+]$ to $[E]$ reached to a constant value of 46 : 54 at a latter stage of

polymerization (after about 30 min). This indicates that the
equilibrium of Equation 9 is actually present in the THF poly-
merization initiated with $EtOSO_2CF_3$.

Similarly the THF polymerization was monitored by ^{19}F nmr
spectroscopy in other four solvents. In $CHCl_3$, CH_2Cl_2, and
benzene solvents the fractions of $[O^+]$ were 85, 89, and 75% at
0°C, respectively, after the equilibrium was reached. In nitro-
benzene, however, the [E] fraction was very small, e.g., below
2% at 0°C throughout the polymerization.

<u>Kinetics.</u> Based on the above nmr results the follwing
reactions will explain the course of the THF polymerization
initiated with $EtOSO_2CF_3$ (EtOTf).

Initiation

$$EtOTf \;+\; O\!\!\diagdown\!\!\square \;\xrightarrow{k_i}\; Et\text{-}\overset{+}{O}\!\!\diagdown\!\!\square \cdot OTf^- \;\rightleftharpoons\; EtO(CH_2)_4OTf \qquad (10)$$

Propagation

$$\sim\!\!\sim\!\!\overset{+}{O}\!\!\diagdown\!\!\square \cdot OTf^- \;+\; O\!\!\diagdown\!\!\square \;\xrightarrow{k_{p(i)}}\; \sim\!\!\sim O(CH_2)_4\text{-}\overset{+}{O}\!\!\diagdown\!\!\square \cdot OTf^-$$

$$\rightleftharpoons \;\sim\!\!\sim\!\!\left[O(CH_2)_4\right]_2 OTf \qquad (11)$$

and

$$\sim\!\!\sim O(CH_2)_4 OTf \;+\; O\!\!\diagdown\!\!\square \;\xrightarrow{k_{p(e)}}\; \sim\!\!\sim O(CH_2)_4\text{-}\overset{+}{O}\!\!\diagdown\!\!\square \cdot OTf^-$$

$$\rightleftharpoons \;\sim\!\!\sim\!\!\left[O(CH_2)_4\right]_2 OTf \qquad (12)$$
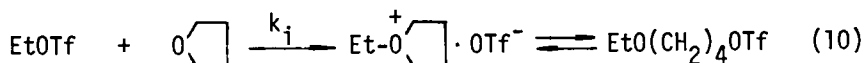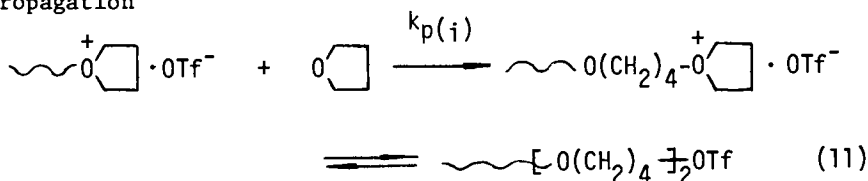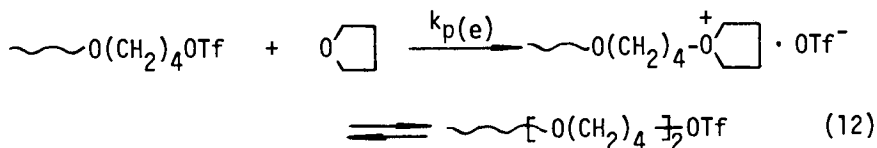
The integrated form of the rate equation of propagation is
expressed as

$$\ln \frac{[M]_o - [M]_e}{[M]_t - [M]_e} = k_{p(ap)} \int_0^t [P^*]dt \qquad (13)$$

where $k_{p(ap)}$ is the apparent rate constant of propagation and $[P^*]$
represents the total concentration of the propagating species,
e.g.,

$$[P^*] = [O^+] \;+\; [E] \qquad (14)$$

The ester species (II) is not dead, but is thought to be
inherently capable of propagation (Equation 12), since the ester
species EtOTf initiates the THF polymerization. $[P^*]$ was equal
to the amount of the reacted initiator. Therefore, the following
relationship is derived
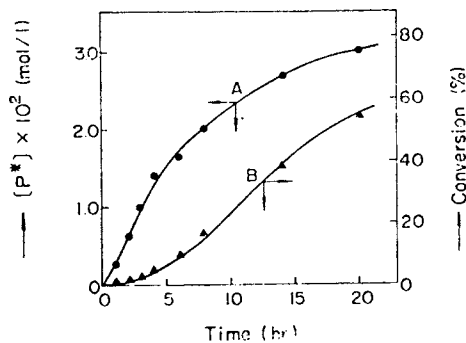
Bulletin of the Chemical Society of Japan

Figure 1. Polymerization of THF by EtOSO₂F at 0°C. [P]–time (curve A) and monomer conversion–time (curve B) relationships: [I]o = 4. 8 × 10⁻² mol/l., [M]o = 9.8 mol/l. in CH₂Cl₂ solution (3).*
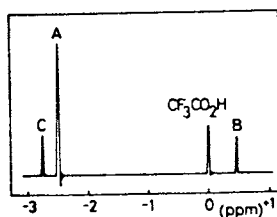
Macromolecules

Figure 2. ¹⁹F nmr spectrum of the THF polymerization mixture by EtOSO₂CF₃ initiator in CCl₄ after 48 min at 13°C (11)
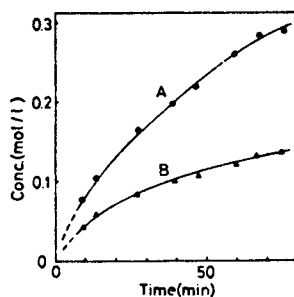
Macromolecules

Figure 3. Polymerization of THF with EtOSO₂CF₃ monitored by ¹⁹F nmr spectroscopy in CCl₄ at 13°C. Relationships of ([O·] + [E])–time (curve A) and of [O·]–time (curve B): [M]o = 5.30 mol/l., [I]o = 1.05 mol/l. (11).

$$k_{p(ap)} = k_{p(i)} \cdot X_i + k_{p(e)} \cdot X_e \tag{15}$$

where $k_{p(i)}$ and $k_{p(e)}$ are the rate constants of propagation due respectively to the oxonium ion (I) and ester (II) species, and X_i and X_e are the molar fractions of $[O^+]$ and $[E]$, respectively, i.e., $X_i + X_e = 1$. It is reasonable to assume that the magnitude of $k_{p(e)}$ is at least smaller than that of k_i which was about 140-280 times smaller than that of $k_{p(i)}$ (Tables III and IV), i.e., $k_{p(i)} \gg k_{p(e)}$. Furthermore, X_e was not so large, i.e., below 0.55 in all cases (Tables III and IV). Therefore, Equation 15 becomes

$$k_{p(ap)} \simeq k_{p(i)} \cdot X_i \tag{16}$$

Consequently, Equation 13 is converted to

$$\ln \frac{[M]_0 - [M]_e}{[M]_t - [M]_e} = k_{p(i)} \int_0^t [O^+] \, dt \tag{17}$$

The integrated values of $[P*]$ in Equation 13 and $[O^+]$ in Equation 17 were obtained by graphical integration on curves A and B in Figure 3, respectively. The monomer conversion was followed by ^{1}H nmr spectroscopy (3) under the same reaction conditions as Figure 3. Thus, plots of Equations 13 and 17 could be made as shown in Figure 4 (A) and (B), whose slopes gave values of $k_{p(ap)} = 1.6 \times 10^{-3}$ and $k_{p(i)} = 3.6 \times 10^{-3}$ 1/mol·sec at 13°C in CCl_4. Similarly the $k_{p(ap)}$ and $k_{p(i)}$ values were determined at 0 and 25°C (Table III). It is interesting to note that the $[O^+]$ fraction was not changed at the reaction temperatures

Table III. Rate Constants, Activation Parameters, and the $[O^+]$ Fraction in the THF Polymerization by $EtOSO_2CF_3$ Initiator in CCl_4 [a)]

Temp (°C)	$k_i \times 10^5$ (1/mol·sec)	$k_{p(ap)} \times 10^3$ (1/mol·sec)	$k_{p(i)} \times 10^3$ (1/mol·sec)	$[O^+]$ fraction (%) [b)]
0	0.80	0.84	2.2	45
13	2.1	1.6	3.6	46
25	3.9	3.0	5.7	47
$\Delta H^{\ddagger}$ (kcal/mol)	20	16	13	
$\Delta S^{\ddagger}$ (e.u.)	-5	-12	-24	

a) $[M]_0 = 5.30$ mol/1, $[I]_0 = 1.05$ mol/1.

b) After the equilibrium was reached.

of 0, 13, and 25°C, after the equilibrium of Equation 9 has been reached.

The results of similar kinetics in other four solvents are shown in Table IV. The k_i values were increased with an increase

Table IV. Rate Constants and the [O+] Fraction in the THF Polymerization by EtOSO$_2$CF$_3$ Initiator in Five Solvents at 0°C a)

Solvent	(ε) b)	ε of the mixture c)	$k_i \times 10^5$ (1/mol·sec)	$k_p(ap) \times 10^3$ (1/mol·sec)	$k_p(i) \times 10^3$ (1/mol·sec)	[O+] fraction d) (%)
CCl$_4$	2.24	4.5	0.80	0.84	2.2	45
C$_6$H$_6$	2.28	4.5	1.1	1.7	2.7	75
CHCl$_3$	4.81	6.0	1.1	1.8	2.2	85
CH$_2$Cl$_2$	8.93	8.3	1.2	1.7	2.0	89
C$_6$H$_5$NO$_2$	34.8	23.4	3.1	4.4	4.4	>98

a) $[M]_0 = 5.30$ mol/1, $[I]_0 = 1.05$ mol/1.

b) Dielectric constant.

c) Calculated by assuming the molar additivity in the dielectric constant value of solvent and THF. ε of THF = 7.58.

d) At equilibrium.

Macromolecules (11).

of polarity of the mixture. This phenomenon is very familiar with dipole-dipole S_N2 reactions to produce ionic species such as

the Menschutkin reaction (21) and Equation 8 (22).

In CCl_4 the value of $k_{p(ap)}$ was 2.6 times smaller than that of $k_{p(i)}$. In a highly polar solvent of nitrobenzene, however, both the $k_{p(ap)}$ and $k_{p(i)}$ values were identical since the $[O^+]$ fraction was higher than 98% throughout the kinetic run. It should be noted that the k_p values in Table II correspond to the $k_{p(ap)}$ values because the phenoxyl end-capping method gives $[P^*]$ as the total propagating species, i.e., $[O^+]$ + $[E]$ = $[P^*]$. Therefore, it is quite reasonable that both values of k_p (Table II) and $k_{p(ap)}$ (Table IV) were 1.7×10^{-3} 1/mol·sec at 0°C in CH_2Cl_2.

More interestingly, the $k_{p(i)}$ values did not vary so much in five solvents, being in a narrow range of $2.0 - 4.4 \times 10^{-3}$ 1/mol·sec at 0°C, notwithstanding a big change of the dielectric constant of the system. The reason may be explained as follows. The propagating chain-end probably consists of three kinds of species, i.e., the free ion (Ia), ion-pair (Ib), and ester (II) species, respectively. This is very reasonable since Sangster and

$$\sim\!\!\sim\!\!O \underset{(Ia)}{\overset{+}{\diagup\!\!\!\square}} +\ OSO_2CF_3^- \rightleftharpoons \sim\!\!\sim\!\!O \overset{+}{\diagup\!\!\!\square} \cdot OSO_2CF_3^-$$
$$\underset{(Ib)}{}$$

$$\rightleftharpoons \sim\!\!\sim\!\!\sim\!\!O(CH_2)_4OSO_2CF_3$$
$$(II)$$

$$(18)$$
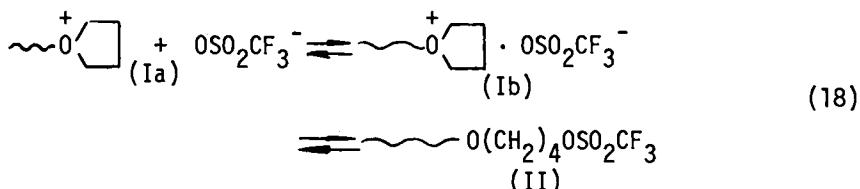
Worsfold have recently reported that two kinds of the oxonium propagating species, the free ion and the ion-pair, were involved in the THF polymerization initiated by $Et_3O^+BF_4^-$. Each of both species exhibited a different rate constant of propagation (24). In Equation 18 the combined concentration of Ia and Ib corresponds to the $[O^+]$ value. It is likely, therefore, that the change of the solvent brings about the variation not only in the $[O^+]/[E]$ ratio but also in the Ia/Ib ratio in the $[O^+]$ fraction. In addition the rate constants of propagation due to Ia and Ib may be varied with the change of the solvent.

The above results are quite compatible with the proposed mechanism (Reactions 10-12). All the processes of the THF polymerization by $EtOSO_2CF_3$ initiator can be given by Scheme 2. In the scheme the interconversion between I and II was a faster process than propagation, i.e., the equilibrium of Equation 9 was attained during the polymerization. The $k_{p(e)}$ value was estimated to be very small compared with the $k_{p(i)}$ value. The ester type species (II) is not dead, but is inherently able to react with THF to produce oxonium species. In this sense we propose to denote II as a "sleeping" species. In the THF polymerization, the so-called "dormant" species (III) is known, which is produced by a chain-transfer of the propagating oxonium to polymer alkyl ether (15, 16 25). The acyclic oxonium (III) is also not a dead species, and can regenerate a cyclic oxonium ion by the reaction with THF.

$$EtOSO_2CF_3 \xrightarrow[\underset{O\square}{}]{k_i} Et\text{-}\overset{+}{O}\square \cdot OTf^- \xrightleftharpoons[]{K} EtO(CH_2)_4OTf$$

$$k_p(i) \Big\downarrow \, O\square$$

$$k_p(e)$$

$$O\square$$

$$EtO(CH_2)_4\text{-}\overset{+}{O}\square \cdot OTf^- \xrightleftharpoons[]{K} Et\text{-}\!\!\!\left[O(CH_2)_4\right]\!\!\!\underset{2}{}OTf$$

$$k_p(i) \Big\downarrow\!\!\Big\downarrow\!\!\Big\downarrow \, O\square \qquad\qquad k_p(e)$$

$$O\square$$

$$Et\text{-}\!\!\!\left[O(CH_2)_4\right]\!\!\!\underset{n}{} \overset{+}{O}\square \cdot OTf^- \xrightleftharpoons[]{K} Et\text{-}\!\!\!\left[O(CH_2)_4\right]\!\!\!\underset{n+1}{}OTf$$

<p align="center">Scheme 2.</p>

$$P_1\!\sim\!\!\!\sim\!\overset{+}{O}\square \;+\; O\!\!<_{P_3}^{P_2} \longrightarrow P_1\!\sim\!\!\!\sim\!\overset{+}{O}(CH_2)_4O\!\!<_{P_3}^{P_2}$$

<p align="center">III</p>
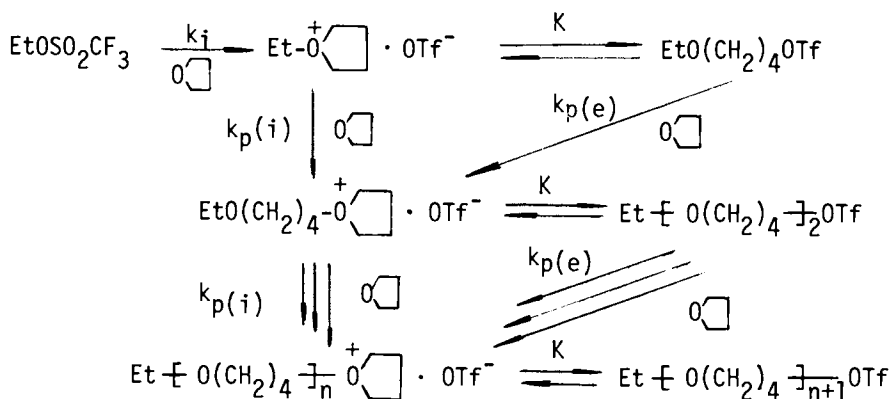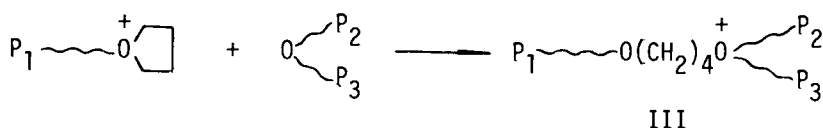
However, III should be distingushed from a "sleeping" species (II) in a sense that II can awake into a cyclic oxonium ion of the propagating species (I) not only by the intermolecular reaction with THF but also by the intramolecular cyclization of the so-called back-biting reaction.

Effects of the counteranion on rate constants of propagation $(k_{p(i)})$ [13]. It is worth while to mention the effect of the counter-anion on $k_{p(i)}$ in the THF polymerization. There are several data available until now. Table V lists the rate constants of propagation due to the oxonium species $(k_{p(i)})$ by various initiators, all of which were recently determined in our laboratory. It was once thought that the value of $k_{p(i)}$ was not changed depending on the nature of the counteranion [23, 26]. However, the $k_{p(i)}$ values in Table IV clearly indicate that a wide variety of counteranions brings about the change of the $k_{p(i)}$ value significantly. Such change in $k_{p(i)}$ values is probably due to the change of the fraction of free ions and ion-pairs in the propagating species.

Polymerization of BCMO [12]

Kinetics of the $EtOSO_2CF_3$-Initiated Polymerization of BCMO. The polymerization was monitored by ^{1}H nmr spectroscopy. Figure 5 shows an example of the ^{1}H nmr spectrum of the reaction system. The molar feed ratio of BCMO to $EtOSO_2CF_3$ was 6 : 1. Figure 5 shows a ^{1}H nmr spectrum at a reaction time of 180 min at 63°C in

Table V.   Rate Constants of Propagation ($k_{p(i)}$) by Various
          Initiators at 0°C

Initiator	$k_{p(i)} \times 10^3$	Method[e-g]	Ref.
EtOSO$_2$F	0.8[c]	e	3
EtOSO$_2$Cl	1.5[c]	e	3
EtOSO$_2$CF$_3$	2.0[c]	e, f	3, 11
EtOTn[a]	0.70[c]	e	13
Et$_3$O$^+$BF$_4^-$	3.7[c]	g	19
BF$_3$-ECH[b]	4.1[c]	g	18
BF$_3$-ECH[b]	4.6[d]	g	18
SnCl$_4$-ECH[b]	6.7[d]	g	18
AlEtCl$_2$	7.8[d]	g	18

a) Ethyl 2,4,6-trinitrobenzenesulfonate.
b) ECH : epichlorohydrin as a promotor.
c) Solution polymerization in CH$_2$Cl$_2$.
d) Bulk polymerization.   e) By ^{1}H nmr spectroscopy.
f) By ^{19}F nmr spectroscopy. g) By phenoxyl end-capping method.

$$\underset{\text{IV}}{\text{EtOCH}_2\overset{\overset{\text{CH}_2\text{Cl}}{|}}{\underset{\underset{\text{CH}_2\text{Cl}}{|}}{\text{C}}}\text{CH}_2\text{OSO}_2\text{CF}_3}$$

$$\underset{\text{V} \ (n\geqq 2)}{\text{Et}(\text{OCH}_2\overset{\overset{\text{CH}_2\text{Cl}}{|}}{\underset{\underset{\text{CH}_2\text{Cl}}{|}}{\text{C}}}\text{CH}_2)_{\overline{n-1}}\text{OCH}_2\overset{\overset{\text{CH}_2\text{Cl}}{|}}{\underset{\underset{\text{CH}_2\text{Cl}}{|}}{\text{C}}}\text{CH}_2\text{OSO}_2\text{CF}_3}$$
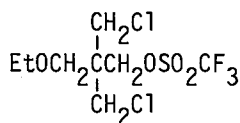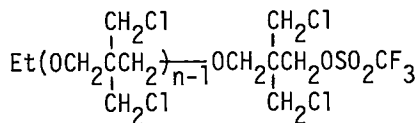
nitrobenzene solvent. Characteristic peaks are A_1 (δ 4.80) and
A_n (δ 4.83), which are assigned to α-methylene protons (2H) of
-OSO$_2$CF$_3$ group in ester type species IV and V, respectively.
Other peaks' assignments may be found in Figure 5. These results
indicate that the propagating species of the BCMO polymerization
is ester type species given by IV and V.
      An authentic compound of IV was prepared by the reaction of
EtOSO$_2$CF$_3$ with BCMO and isolated by distillation in vacuo, bp,
45-46°C (0.04 mmHg). The chemical shift of the methylene protons
α to -OSO$_2$CF$_3$ group of the compound is identical with that of
A_1 peak of the polymerization mixture. In addition, oligomer of
V was prepared to assign peak An. The average degree of poly-
merization of the isolated oligomer V was n=2.30. The oligomer
did not contain IV at all, and hence showed no signal correspond-
ing to A_1. Instead, the α-methylene signal in V appeared at
δ 4.83, being identical with the chemical shift of peak An. Thus
the kinetic analyses could be performed by means of ^{1}H nmr
spectroscopy.

The following scheme of reactions will explain the course of the BCMO polymerization.

Initiation

$$EtOTf + O\diamondsuit\begin{smallmatrix}CH_2Cl\\CH_2Cl\end{smallmatrix} \xrightarrow[\text{slow}]{k_i} \left[Et\overset{+}{-}O\diamondsuit\begin{smallmatrix}CH_2Cl\\CH_2Cl\end{smallmatrix} \cdot OTf\right]$$

VI

$$\xrightarrow[\text{fast}]{} EtOCH_2\underset{\overset{|}{CH_2Cl}}{\overset{\overset{\displaystyle CH_2Cl}{|}}{C}}CH_2OTf \qquad (19)$$

IV $(P_1{}^*)$

Propagation

$$EtOCH_2\underset{\overset{|}{CH_2Cl}}{\overset{\overset{\displaystyle CH_2Cl}{|}}{C}}CH_2OTf + O\diamondsuit\begin{smallmatrix}CH_2Cl\\CH_2Cl\end{smallmatrix} \xrightarrow[\text{slow}]{k_{p1}}$$

$$\left[EtOCH_2\underset{\overset{|}{CH_2Cl}}{\overset{\overset{\displaystyle CH_2Cl}{|}}{C}}CH_2\overset{+}{-}O\diamondsuit\begin{smallmatrix}CH_2Cl\\CH_2Cl\end{smallmatrix} \cdot OTf\right] \xrightarrow[\text{fast}]{} Et\left(OCH_2\underset{\overset{|}{CH_2Cl}}{\overset{\overset{\displaystyle CH_2Cl}{|}}{C}}CH_2\right)_2 OTf \quad (20)$$

VII   VIII $(P_2{}^*)$

Generally

$$Et\left(OCH_2\underset{\overset{|}{CH_2Cl}}{\overset{\overset{\displaystyle CH_2Cl}{|}}{C}}CH_2\right)_n OTf + O\diamondsuit\begin{smallmatrix}CH_2Cl\\CH_2Cl\end{smallmatrix} \xrightarrow{k_{pn}} Et\left(OCH_2\underset{\overset{|}{CH_2Cl}}{\overset{\overset{\displaystyle CH_2Cl}{|}}{C}}CH_2\right)_{n+1} OTf \quad (21)$$

IX (P_n*) X $(P_{n+1}*)$

In the above reactions, 19–21, oxonium species VI, and VII may be involved as intermediates. However, these intermediates are not stable under reaction conditions and rearrange very rapidly to the stable ester species IV and VIII, respectively.

The rate constant of initiation (k_i) was obtained by Equation 4. After the complete reaction of initiator, the consumption rate of the first propagating species P_1* is given by

$$- \frac{d[P_1*]}{dt} = k_{p1}[P_1*][M] \qquad (22)$$

where k_{p_1} is the rate constant of the first propagation.   Therefore, k_{p_1} was calculated according to

$$\ln \frac{[P_1^*]t_1}{[P_1^*]t_2} = k_{p_1} \int_{t_1}^{t_2} [M]dt \qquad (23)$$

where the value of $[P_1^*]t_1/[P_1^*]t_2$ was obtained by the integration of peaks A_1 and A_n.

In the above scheme, IV is the smallest propagating species. Therefore, kinetics of the polymerization by IV as an initiator was also carried out at elevated temperatures. In this case, the rate of polymerization by IV is given by

$$-\frac{d[M]}{dt} = k_{p_1}[P_1^*][M] + [M] \sum_{n=2} k_{p_n}[P_n^*] \qquad (24)$$

The total amount of $[P_1^*]$ and $[P_n^*]$ was found to be equal to the initial concentration of IV throughout the kinetic run, i.e., $[P_1^*] + [P_n^*]_{n\geq2} = [IV]_0$.   On the assumption that $k_{p_2}=k_{p_3}=\cdots\cdots=k_{p_n}$ integration of Equation 24 gives

$$\ln \frac{[M]t_1}{[M]t_2} = k_{p_1} \int_{t_1}^{t_2}[P_1^*]dt + k_{p_n} \int_{t_1}^{t_2}[P_n^*]dt \qquad (25)$$

therefore

$$\ln \frac{[M]t_1}{[M]t_2} - k_{p_1} \int_{t_1}^{t_2}[P_1^*]dt = k_{p_n} \int_{t_1}^{t_2}[P_n^*]dt \qquad (26)$$

At 128°C in nitrobenzene a linear plot of Equation 23 gave a value of $k_{p_1}=1.8 \times 10^{-4}$ 1/mol·sec.   Then, a plot of Equation 26 was made (Figure 6), which is consist of two straight lines, A and B, of different slopes.   The plot in Figure 6 is taken to indicate $k_{p_2} > k_{p_3} \simeq k_{p_4}$.   The straight line A was utilized to calculate k_{p_2} since its period corresponds to the stage of the monomer consumption of the second to third propagation step.   Thus, k_{p_2} was obtained as $k_{p_2}=5.7 \times 10^{-5}$ 1/mol·sec at 128°C.   From the slope of line B the rate constant was obtained as $k_{p_3}=k_{p_4}=k_{p_n}=2.5 \times 10^{-5}$ 1/mol·sec at 128°C.   At a higher temperature of 137°C k_{p_n} was found to be constant from n=3 to at least n=5.   These results are summarized in Table VI.

Reaction Mechanism.   The above data are quite compatible with the reaction mechanism of 19-21.   The ester type propagating species were actually observed directly by nmr spectroscopy during the kinetic run.   In addition, the first propagating species IV

Macromolecules
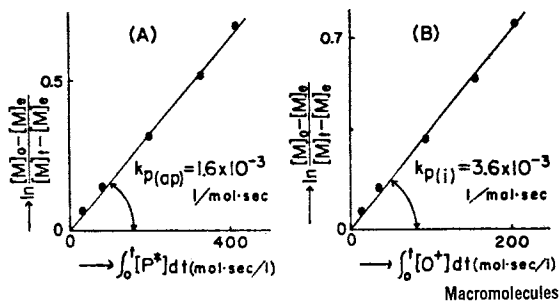
Figure 4. Plots of Equation 13 (A) and of Equation 17 (B) in the THF polymerization by EtOSO$_2$CF$_3$ in CCl$_4$ at 13°C: [M]o = 5.30 mol/l., [I]o = 1.05 mol/l., [M]e = 2.3 mol/l. (11)

Bulletin of the Chemical Society of Japan
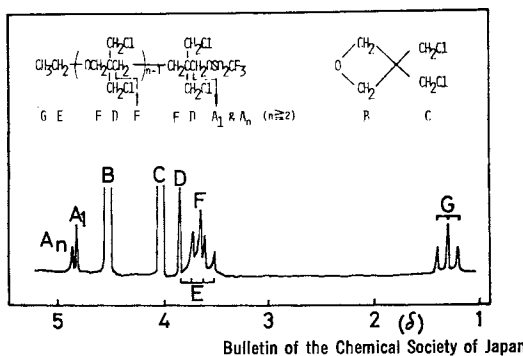
Figure 5. ^{1}H nmr spectrum of BCMO polymerization mixture by EtOSO$_2$CF$_3$ in nitrobenzene after 180 min at 63°C (12)
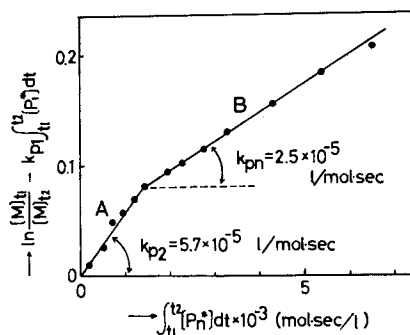
Bulletin of the Chemical Society of Japan

Figure 6. Plots of Equation 25 in BCMO polymerization initiated by IV in nitrobenzene at 128°C: [M]o = 3.5 mol/l., [IV]o = 0.45 mol/l. (12)

Table VI.   Rate Constants and Activation Parameters in the BCMO
            Polymerization in Nitrobenzene[a]

Temp. (°C)	$k_i \times 10^3$ (1/mol sec)	$k_{p_1} \times 10^5$ (1/mol·sec)	$k_{p_2} \times 10^5$ (1/mol·sec)	$k_{p_n} \times 10^5$ (1/mol·sec)
90[b]	4.2[d]	3.7		
119[c]		10	3.5	1.5
128[c]		18	5.7	2.5
128[c]		17	6.0	2.8
137[c]		~30	8.0	4.0
$\Delta H^{\ddagger}$ (kcal/mol)	12.5	13	13	14
$\Delta S^{\ddagger}$ (e. u.)	-36	-45	-46	-45

a) $[M]_o = 3.50-3.90$ mol/l, $[I]_o = 0.37-0.56$ mol/l.

b) $EtOSO_2CF_3$ initiator.

c) IV as an initiator.

d) Extrapolated value.   Bull. Chem. Soc. Japan   (12).

was isolated by vacuum distillation, which induced the BCMO poly-
merization directly from the first propagation.

It is an important findings that the rate of propagation
varied depending on the degree of polymerization, i.e.,
$k_{p_1} > k_{p_2} > k_{p_3} = k_{p_n}$ (n≧3). These values were successfully
determined since P_1^* and P_n^* (n≧2) were directly observed by nmr
spectroscopy. The difference in k_p is due to different electro-
philic reactivity of alkyl groups toward BCMO monomer when n=1,
2, and ≧3 in V. The bulkier the alkyl chain the less the
reactivity bacame.

Activation parameters (Table VI) also support the mechanism
19-21. They are characterized by a general feature of activation
parameters of S_N2 reaction between two neutral molecules to
produce an ionic species, i.e., combination of low $\Delta H^{\ddagger}$ value
(favorable for rate) and low $\Delta S^{\ddagger}$ value (unfavorable) is seen in
every process. This tendency is already noted in Reaction 8.

The magnitude of k_{p_1} is about one-hundredth of that of k_i.
The small k_{p_1} value is ascribed to the lower $\Delta S^{\ddagger}$ value; $\Delta H^{\ddagger}$
being the same in both cases. The rate difference between
initiation and the first propagation is due to the different
reactivity between CH_3CH_2- and $EtOCH_2C(CH_2Cl)_2CH_2-$ groups attached
to $-OSO_2CF_3$. A similar result was reported by Buncel and

Millington (27) in the hydrolysis of primary alkyl chlorosulfates
(XI) in 85.3% aq. dioxane, in which the rate of ethyl group (XIa)

$$ROSO_2Cl$$

(XIa)   R=CH_3CH_2

(XIb)   R=$(CH_3)_3CCH_2$
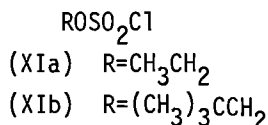
was 4.2×10^2 times as high as that of neopentyl group (XIb).

The transition state of the BCMO polymerization by $EtOSO_2CF_3$
is probably formulated as XII, in which two neutral molecules of

XII   R=CH_3 or
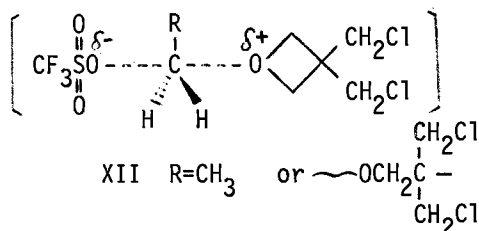
ester species (electrophile) and BCMO monomer (nucleophile) are
polarized. It is generally accepted that the polymerization of
oxetanes initiated by typical Lewis acids proceeds via an S_N2
reaction between the propagating oxonium and monomer (16, 25).
In this case the transition state is given by XIII.
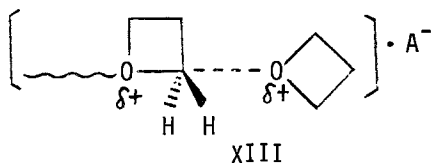
XIII

The mechanistic difference of these two cases is well recognized
by the observation that the transition state XII differs much
from XIII since going from the initial to transition state the
charge is developed at XII whereas it is despersed at XIII. This
was further supported by the examination of the solvent effect on
the rate of BCMO polymerization (12).

Conclusion

New findings specific to the THF and BCMO polymerizations
initiated by superacid esters are described. In the THF
polymerization the oxonium (I) and ester (II) species of the
propagating end were involved in equilibration, which were direct-
ly observed by ^{19}F nmr spectroscopy. Thus, $k_p(ap)$ and $k_p(i)$ were
separately determined, in which the contribution of the
propagation due to the ester species (II) was estimated to be very
small. In the BCMO polymerization, however, the ester species
(IV and V) were actually the propagating chain-ends. This provides

a new concept of the mechanism in the cationic ring-opening poly-
merization of cyclic ethers, i.e., the polymerization via the
ester type (covalent) propagating species. The other examples of
the covalent propagating species ever known are seen in the
polymerization of cyclic imino ethers ; alkyl iodides being the
stable propagating species (28).

"Literature Cited"

1. Gillespie, R. J., Accounts Chem. Res. (1968) 1, 202.
2. Gillespie, R. J., Peel, T. E., Adv. Phys. Org. Chem. (1971)
    9, 1.
3. Kobayashi, S., Danda, H., Saegusa, T., Bull. Chem. Soc. Japan
    (1973) 46, 3214.
4. Pettitt, D. J., Helmkamp, G. K., J. Org. Chem. (1964) 29,
    2702.
5. Muller, M., Ber. (1873) 6, 227.
6. Kobayashi, S., Yuki Gosei Kagaku Kyokai Shi (J. Syn. Org. Chem.
    Japan) (1973) 31, 935.
7. Ahmed, M. G., Alder, R. W., James, G. H., Sinnott, M. L.,
    Whiting, M. C., Chem. Commun. (1968) 1533.
8. Saegusa, T., Kobayashi, S., Presented at the 21st Annual
    Meeting of the Society of Polymer Science, Japan, May 1972.
9. Smith, S., Hubin, A. J., "Polymer Preprint" (1972) 13, 66.
10. Smith, S., Hubin, A. J., J. Macromol. Sci. Chem. (1973) A7,
    1399.
11. Kobayashi, S., Danda, H., Saegusa, T., Macromolecules (1974)
    7, 415.
12. Kobayashi, S., Danda, H., Saegusa, T., Bull. Chem. Soc. Japan
    (1974) 47 (No. 11), in press.
13. Kobayashi, S., Nakagawa, T., Danda, H., Saegusa, T. Bull. Chem.
    Soc. Japan, submitted.
14. Kobayashi, S., Morikawa, K., Saegusa, T., to be reported.
15. Saegusa, T., J. Macromol. Sci. Chem. (1972) A6, 997.
16. Saegusa, T., Kobayashi, S., Prog. Polymer Sci. Japan (1973) 6,
    107.
17. Saegusa, T., Matsumoto, S., J. Polymer Sci. Part A-1 (1968) 6,
    1559.
18. Saegusa, T., Matsumoto, S., Macromolecules (1968) 1, 442.
19. Saegusa, T., Matsumoto, S., J. Macromol. Sci. Chem. (1970) A4,
    873.
20. Saegusa, T., Kimura, Y., Fujii, H., Kobayashi, S.,
    Macromolecules (1973) 6, 657.
21. Wiberg, K., "Physical Organic Chemistry", p.379, John-Wiley &
    Sons, Inc., New York, 1966.
22. Kobayashi, S., Ashida, T., Saegusa, T., Bull. Chem. Soc. Japan
    (1974) 47, 1233.
23. Matyjaszewski, K., Kubisa, P., Penczek, S., Presented at the
    International Symposium on Cationic Polymerization, September,
    1973, Rouen, France.

24. Sangster, J. M., Worsfold, D. J., Macromolecules (1972) $\underline{5}$, 229.
25. Dreyfuss, P., Dreyfuss, M. P., "Ring-Opening Polymerization"
    Frisch, K. C., Reegen, S. L., Eds., Chapter 2, Marcel Dekker,
    New York, 1969.
26. Dreyfuss, P., Dreyfuss, M. P., Adv. Chem. Ser. (1969) $\underline{91}$, 335.
27. Bunsel, E., Millington, J. P., Can. J. Chem. (1965) $\underline{43}$, 556.
28. Saegusa, T., Makromol. Chem. (1974) $\underline{175}$, 1199.

11

Brominated Poly(Phenylene Oxide)s. I. Polymerization of Mono-, Di- and Tribromo-2,6-Dimethylphenol

DWAIN M. WHITE and HOWARD J. KLOPFER

General Electric Research and Development Center, Schenectady, N. Y. 12301

The introduction of halogen atoms onto the aromatic rings of the backbone of poly(phenylene oxide)s is of interest because of the effects the halogen can have on the flammability and on the solution and thermal properties of the polymer. This paper describes poly(2,6-dimethyl-1,4-phenylene oxide)s which contain monobromo and dibromo repeating units and have bromine contents ranging from approximately 5 to over 50 wt. %. The general approach for the introduction of the bromine was via synthesis of polymers utilizing di- and tribromophenols as monomers and comonomers. A second method, the direct bromination of poly-(phenylene oxide)s in solution, and the properties of the brominated polymers are described in the following paper.

Polymerization of 3,4-dibromo-2,5-dimethylphenol (I) provided a route to polymer in which the bromine was only on the aromatic rings and not on the methyl groups (reaction 1). The reaction was found to proceed under conditions similar to the reaction described by Staffin and Price[1] for the polymerization of 4-bromo-2,6-dimethylphenol, III (reaction 2). Poly(3-bromo-

169
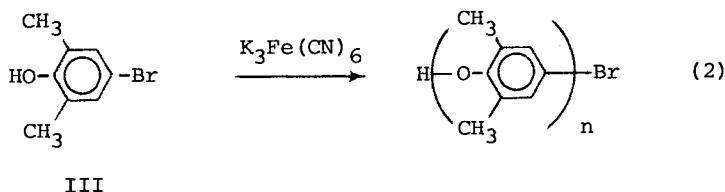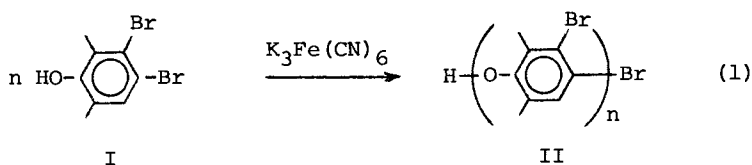
2,6-dimethyl-1,4-phenylene oxide), II, was formed in quantitative
yield and with high molecular weight (intrinsic viscosities in
chloroform were as high as 0.91 dl/g and correspond to molecular
weights up to $\overline{M}_n$ ca. 1.5 x 10^5). [1]H nmr and elemental analyses
confirmed the presence of one bromine atom per repeating unit.
The nmr analyses (both ^{1}H nmr and ^{13}C nmr) also showed that the
displacement of bromine had only occurred at C-4, i.e., the
repeating unit was indeed the moiety shown in structure II. The
infrared spectrum of the polymer was consistent with structure II
except in one respect. In addition to a weak hydroxyl absorption
at the normal end group frequency for unbrominated polymer
(3610 cm^{-1} in CS[2]), there was a slightly weaker absorption at
3525 cm^{-1}. Both absorptions were more intense in lower molecular
weight polymers and absent in acetylated samples.
     One characteristic of 2,6-disubstituted polyphenylene oxides
is the tendency to redistribute with phenols when heated in the
presence of an initiator.[2-4] The polymers are converted to low
molecular weight oligomers terminated at the non-phenolic end of
the molecule with the aryl ether derived from the phenol. The
application of this redistribution reaction to II (reaction 3) is
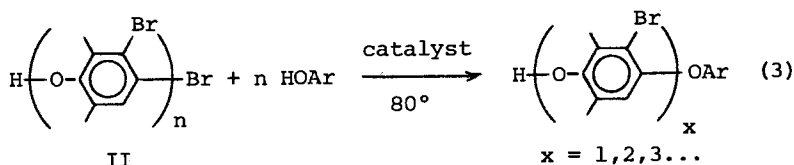
summarized in Table I. With unbrominated polymer, the combination
of the initiator 3,3',5,5'-tetramethyl-4,4'-diphenoquinone (TMDQ)
and either phenol or VII at 80° (the milder reaction conditions
cited in Table I) normally causes extensive redistribution and,
as a result, low yields of recovered polymer. Since, in contrast,
the yields with II were high at 80°, more forcing conditions
(3,3',5,5'-tetraphenyl-4,4'-diphenoquinone, TPDQ, and 4-chloro-
phenol in chlorobenzene at 130°) may have been needed to compen-
sate for the higher oxidation potential of the phenolic end group
caused by the bromine atom. Even at 130°, only the lower
molecular weight polymer underwent a moderate amount of reaction.
The results indicate that redistribution reactions proceed at
slower rates in II than in unbrominated polymer. The terminal
phenolic end group is required for redistribution to proceed.
Possibly the 3525 cm^{-1} hydroxyl group may represent a second type
of end group which is less reactive toward redistribution.
     When polymerization reaction (1) was applied to 3,4,5-tri-
bromo-2,6-dimethylphenol, IV, an intractable product was produced
which corresponded to low molecular weight homopolymer V on the
basis of yield, elemental analysis and infrared spectrum.
Similar intractable products arise from exhaustive bromination of
unbrominated polymer under forcing conditions (see the following

TABLE I

Redistribution of Phenols with II

[η] of Initial Polymer (dl/g)	Initiator	Phenol	Reaction Temperature	Yield of Recovered Polymer (%)
0.35	TMDQ	VII	80	75
0.35	TPDQ	p-chloro-phenol	130	55
0.91	TMDQ	phenol	80	86
0.91	TPDQ	p-chloro-phenol	130	83

paper). Soluble products were obtained, however, by copolymeri-
zation of IV with I even when the ratio of IV to I was as high as
2:1. The products were copolymers which contained the 3,4-
dibromo- and the 3-bromo-2,6-dimethyl-1,4-phenylene oxide
repeating units, structure VI. The ^{13}C nmr spectrum of VI was
consistent with a random copolymer structure.[5] Attempts to
prepare random copolymers from either I or IV with monomer III
were unsuccessful because III polymerized at a much faster rate
than did either I or IV.

Phenols I and IV were copolymerized with 2,6-dimethylphenol
VII, however, by employing oxidative coupling conditions. This
was possible since the conditions for polymerization of I and IV
bear a similarity to the oxidative coupling conditions for VII
(a cuprous halide/amine catalyst; reaction 4).[6-8] Polymerization

of 4-bromo-2,6-dimethylphenol requires at least a stoichiometric
quantity of a base and a catalytic amount of an oxidizing agent.[1]

We found that when using the catalyst system for reaction (4),
the amine (in sufficient excess) functioned as base and the
copper/amine complex functioned as initiator for reaction (1) as
well as catalyzing oxidative coupling. This result differs from
the report by Blanchard and coworkers[9] in which reaction (2)
could not be initiated by a copper/amine (pyridine) catalyst. The
suggested route for reaction is similar to the proposed route for
reaction (2)[1] and involves coupling between a phenoxy radical and
a monomer anion:
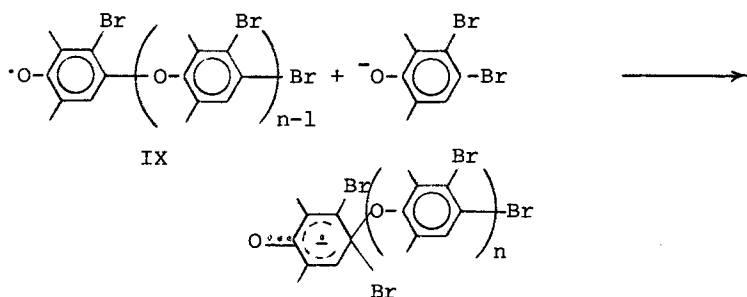
whereas reaction (4) involves dimerization of polymer radicals:[10]
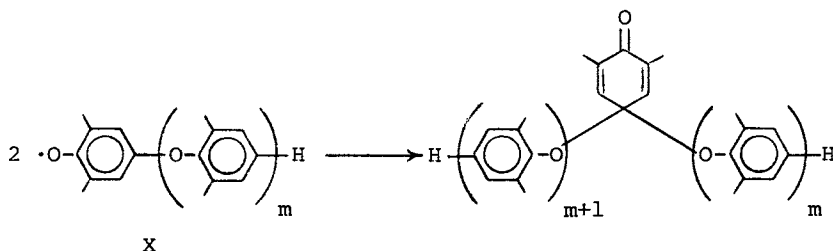
Due to the similarity of the intermediate polymer radicals, cross-
coupling reactions should occur when reactions (1) and (4) are
run simultaneously; for example:

and

$$X \quad + \quad {}^-O-\langle\bigcirc\rangle-Br \quad \longrightarrow \quad O^{\prime\prime\prime}\langle\bigcirc\rangle\left(O-\langle\bigcirc\rangle\right)_{m+1}H$$

Br
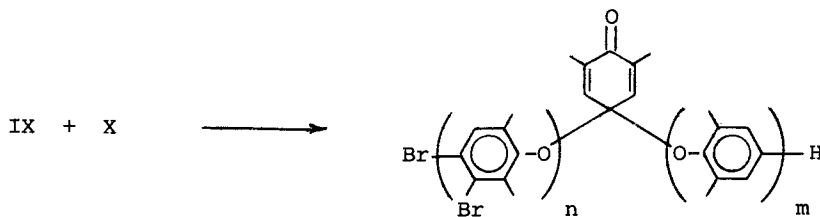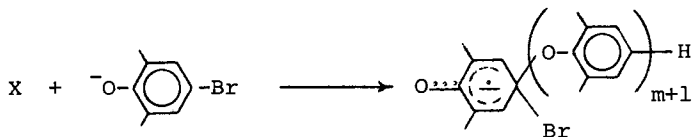
Additional steps in the reaction sequence involve the normal redistribution reactions[10] and loss of halide anion eventually leading to high polymers. With monomers I and VII, extensive crosscoupling reactions would produce random copolymers. [1]H nmr and ^{13}C nmr spectra suggested that copolymers did form, and that they were random (i.e., the general structure was XI where x and y are 0, 1, 2....). Polymer XI was identical to the product that

XI   XII
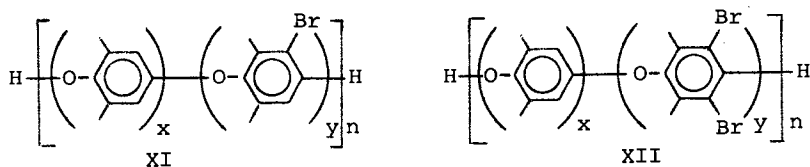
resulted from the direct bromination of polymer VIII under mild conditions (see following paper). The product from IV and VII had structure XII. This product does not arise from the direct bromination of VIII since the introduction of a second bromine atom onto a repeating unit does not occur until almost all of the rings have been monobrominated.

Copolymer XI was also prepared from a mixture of I and VII with lead dioxide serving as oxidant for VII and initiator for I.

Polymer II (a sample with [η] 0.35 dl/g) was used as a phenol for copolymerization with 2,6-dimethylphenol. The physical properties of the product (intrinsic viscosities as high as 0.68 dl/g; no fractionation of VIII during methylene chloride complexation;[11] no long range nmr effects) suggested a block copolymer structure for the product. Since it is likely that polymer II did not redistribute under the mild conditions of polymerization (Table I shows little equilibration with monomer even at 80°), polymer II was functioning as a monofunctional component which did not readily co-equilibrate with the other oligomers. Polymer II can be viewed as a chain stopper for reaction (4) and the product can be represented by structure XIII. Colorless, hazy
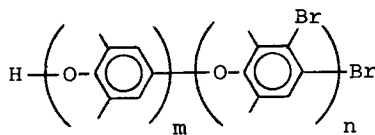
XIII

films resulted after solution casting of a polymer which was composed of equal molar quantities of each type of repeating unit. With an initial 2:1 ratio of VII to C_8H_7OBr units, films of the product were homogeneous.

The ^{1}H nmr spectra of the bromopolymers are summarized in Table II. Both short range and longer range effects of bromine were found on both the aryl and methyl protons.

TABLE II

Chemical Shifts for Protons in the Polymer Segment
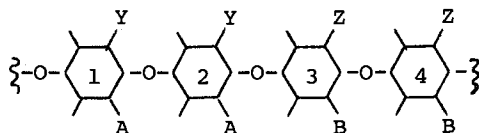
		Chemical Shift (δ)[a]			
Polymer		Aryl H with a		Methyl H with an	
Structure	Br Location	m-H	m-Br	o-H	o-Br
VIII	None	6.50		2.08	
II	Y,Z		6.07	2.00	2.32
XI	Y	6.40	6.12	2.08 (3 & 4)	2.35
				2.02 (1 & 2)	
XII	A,Y	6.42(4)		2.07(4)	2.30(1)
		6.30(3)		1.93(3)	2.23(2)
VI	A,Y,Z		6.02(4)	1.98	2.20
			5.83(3)		

(a) Number in parenthesis specifies the ring on which the H or methyl is located.

When an aromatic proton was oriented meta to a bromine in the same ring, the resonance was shifted upfield 0.4 ppm.[12] An additional upfield shift was noted when a bromine atom in one ring shielded an aryl proton on the adjacent ring ortho to the bromine. The effect was pronounced (ranging from 0.1 to 0.3 ppm)

in polymers containing the dibromo unit since one of the two
bromine atoms on each ring always had to lie directly above the
adjacent ring due to steric effects. For polymer VI both the
long and short range effects were possible and the peak for the
proton at location B on ring 3 (Table II) was shifted upfield 0.7
ppm relative to the aryl proton in VIII.

    The methyl protons were affected in several ways by bromine.
The methyl peaks were shifted upfield (0.1 ppm) by shielding
bromines of adjacent dibrominated rings. In addition, a bromine
in the same ring shifted an ortho methyl downfield (0.2 to 0.3
ppm) and shifted a para methyl upfield (<0.1 ppm). This latter
effect accounted for the two methyl peaks between 2.0 and 2.1 ppm
in polymer XI.

    The pronounced upfield shift of the dibrominated adjacent
ring allowed an estimation of the distribution of repeating units
in copolymers VI and XII since the characteristic peak only
occurred when the dibromo ring preceded the other type of ring.
The relative intensities of shifted and unshifted peaks for all
samples indicated a random distribution.

Acknowledgements

Experimental

    All viscosities were measured in chloroform at 25°. The
mono-, di- and tribromodimethylphenols[13] were prepared by the
direct bromination of 2,6-dimethylphenol. Elemental analyses of
the polymers were consistent with the suggested structures; nmr
data are reported in Table II (run in CDCl$_3$ vs. TMS).

    Preparation of II. Aqueous potassium ferricyanide (0.329 g,
0.001 m) was added dropwise over a 27 minute period to a vigor-
ously stirred mixture of a solution of 3,4-dibromo-2,6-dimethyl-
phenol (I) (2.80 g, 0.01 m) in 150 ml benzene and 150 ml aq. 2%
solution of potassium hydroxide at 25° under a nitrogen atmos-
phere. After 170 minutes, the benzene layer was separated and
washed with 10% hydrochloric acid and then with water. The
solution was added dropwise to 500 ml methanol. The polymer was
filtered off, washed with methanol, and dried 20 hours at 25° and
12 Torr. Weight: 2.0 g (100% yield). Intrinsic viscosity:
0.91 dl/g (CHCl$_3$ at 25°). Tg 292°; no transitions indicative of
T$_m$ or T$_{crys}$ were noted by differential scanning calorimetry.
    The copolymerizations of mixtures of 4-bromophenols were run
in an identical manner. In one instance of the homopolymeriza-
tion of I, the ferricyanide was added at once. The polymer had
an intrinsic viscosity of 0.35 dl/g. The polymer was useful for
the synthesis of block copolymers (see below).

Copolymerization of VII and I. A solution of VII (4.88 g, 0.04 m) and I (2.80 g, 0.01 m) in 50 ml benzene was added to a stirred (Vibromixer) oxygenated solution of cuprous bromide (0.072 g, 0.0005 m) and dibutylamine (2.58 g, 0.02 m) in 50 ml benzene at 25° (stirred water bath). After 10 minutes, the temperature rose to 38.5°, then slowly decreased. After 120 minutes, the solution was added dropwise to 750 ml methanol containing 5 ml hydrochloric acid. The polymer was filtered off, washed with methanol and dried. Weight: 6.54 g (96% yield). Intrinsic viscosity: 0.51 dl/g. The polymer could be cast from chloroform solution to form a clear, transparent flexible film. The nmr spectrum and elemental analysis indicated a 4:1 ratio of poly(phenylene oxide) units to poly(monobromophenylene oxide) units.

A similar procedure was used for the other polymerizations of VII and either I or IV. In some cases, the bromophenol concentration differed substantially and the dibutylamine concentration was changed proportionately.

Block Copolymers of II and VII. A solution of polymer II (intrinsic viscosity 0.35 dl/g, 1.99 g, 0.01 m repeating units) and 2,6-xylenol (1.22 g, 0.01 m) in benzene was added to an oxygenated, stirred (Vibromixer) solution of cuprous bromide (0.0144 g, 0.0001 m) and dibutylamine (0.258 g, 0.002 m) in benzene (total volume of 64 ml). After 70 minutes, the polymer was isolated in the manner of the previous example. Weight: 3.02 g (94% yield). Intrinsic viscosity: 0.50 dl/g (CHCl₃). A cast film (from chloroform) was flexible and slightly hazy.

The same procedure was used to prepare a block copolymer from a 2:1 ratio of VII to II. The high molecular weight product (intrinsic viscosity: 0.68 dl/g) was isolated in 91% yield and could be cast from chloroform into flexible, transparent films.

Lead Dioxide Oxidations. A slurry of VII (2.44 g, 0.02 m), I (1.40 g, 0.005 m) and 20 g lead dioxide in 100 ml benzene was stirred at 25°. After 55 minutes, the mixture was filtered through Filter Cell (which was then washed with benzene) and precipitated by adding to methanol. After washing and drying, the polymer weighed 2.6 g (76% yield) and could be cast from chloroform to form a transparent, flexible film. The nmr spectrum was consistent with the 4:1 monomer ratio.

With a 9:1 ratio of VII to I, the polymer was isolated in 83% yield and formed a flexible transparent film. The higher yield in this case was probably due to extensive washing with hot benzene to remove the polymer from the lead salt residue.

Summary

Highly brominated poly(2,6-dimethyl-1,4-phenylene oxide)s have been prepared by polymerization of bromophenols and by

copolymerization of bromophenols and 2,6-dimethylphenol. 3,4-Dibromo-2,6-dimethylphenol (I) has been homopolymerized to form poly(3-bromo-2,6-dimethyl-1,4-phenylene oxide) (II):

I   II
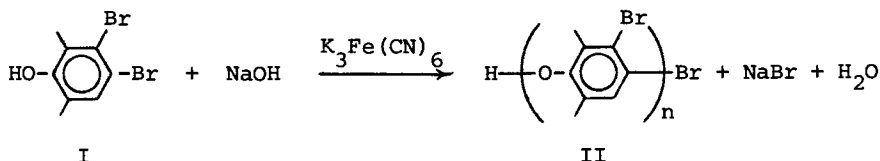
and copolymerized with 3,4,5-tribromo-2,6-dimethylphenol to form a random copolymer with mono- and dibromo repeating units. Both bromophenols have been copolymerized with 2,6-dimethylphenol under oxidative coupling conditions to form copolymers with unbrominated repeating units and either mono- or dibromo repeating units. Co-oxidation of polymer II and 2,6-dimethylphenol produced predominantly a block copolymer. The block structure was supported by spectral and chemical evidence (e.g., the very slow rate of redistribution of II with phenols) and fractionation data.

Spectral analysis of the copolymers of bromophenols and of bromophenols and 2,6-dimethylphenol indicated random copolymer structures. [1]H nmr spectra of the copolymers displayed long range effects in which bromine atoms caused pronounced upfield shifts on aryl protons in adjacent rings.

Literature Cited

1. Staffin, G. C. and Price, C. C., J. Am. Chem. Soc. (1960), 82, 3632.
2. White, D. M., J. Org. Chem. (1960), 34, 297.
3. White, D. M., J. Polymer Sci. A-1 (1971), 9, 663.
4. White, D. M. and Klopfer, H. J., ibid. (1972), 10, 1565.
5. The ^{13}C nmr spectra of the polymers were complex and will be described in detail elsewhere.
6. Hay, A. S., Blanchard, H. S., Endres, G. F., and Eustance, J. W., J. Am. Chem. Soc. (1959), 81, 6335.
7. Hay, A. S., U.S. Patent 3,306,874 (February 28, 1967).
8. Hay, A. S., U.S. Patent 3,306,875 (February 28, 1967).
9. Blanchard, H. S., Finkbeiner, H. L. and Russell, G. A., J. Polymer Sci. (1962), 58, 469.
10. Hay, A. S., Advances in Polymer Sci. (1967), 4, 496.
11. Factor, A., Heinsohn, G. E. and Vogt, L. H., Polymer Letters (1969), 7, 205.
12. A similar shift (0.35 ppm) was found in 3-bromo-2,6-dimethyl-4(2,6-dimethylphenoxy)phenol; Hamilton, S. B. and Blanchard, H. S., J. Org. Chem. (1970), 35, 3348.
13. Auwers, K. and Markovitz, T., Chem. Berichte (1908), 41, 2332.

12

Brominated Poly(Phenylene Oxide)s. II. Bromination of Poly(2,6-Dimethyl-1,4-Phenylene Oxide)

DWAIN M. WHITE and CHARLES M. ORLANDO

General Electric Research and Development Center, Schenectady, N. Y. 12301

The preparation of bromine-containing polyphenylene oxides by modification of Price's[1] polymerization of bromophenols was described in the preceding paper. An alternate route to these polymers is the direct bromination of polyphenylene oxides. The bromination of poly(2,6-dimethyl-1,4-phenylene oxide)[2-5] I, to prepare II, III and IV and combinations of the repeating units in I and III and in III and IV is described in this paper. The properties of these products are compared with the corresponding polymers derived from polymerizations of bromophenols.
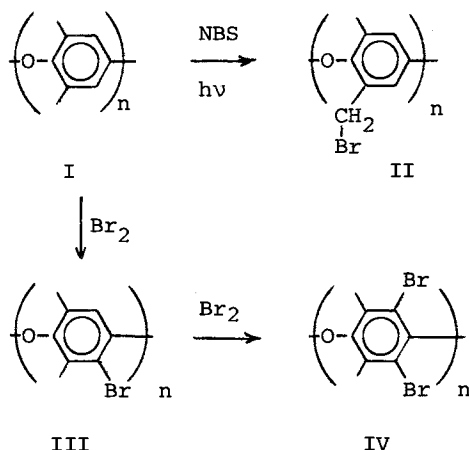
The introduction of a single bromine atom onto the aromatic ring and/or onto the methyl group of I has been investigated. In our laboratory, Hall[6] found that 0.5 mole bromine per mole of repeating unit of I at 15° in chloroform under ionic conditions introduced one bromine per two repeating units. Recently, Cabasso et al[7] investigated several routes to II and III. Free radical conditions (e.g., N-bromosuccinimide (NBS) and light)

afforded methyl bromination while ionic conditions led to as much as one aryl bromine per ring. The introduction of two bromine atoms onto a single aromatic ring of I has not been reported. We have found that the introduction of more than one bromine to form units such as in IV did occur when the bromination was carried out at high bromine concentrations. Furthermore, the reaction conditions which favored the formation of dibrominated rings over mono-brominated rings were found to be very concentration dependent. Under mild conditions (15°, dilute solution in trichloroethylene) and with one mole of bromine per repeating unit I, the product contained 0.9 Br/unit and had predominantly structure III. With excess bromine, the value could be raised readily to 1.0 Br/unit but did not exceed 1.1 Br/unit even at relatively high solution concentrations (2.4 g I added to 6 g Br_2 in 4 ml chloroform) or at 80° with Lewis acid catalysts. Dibromo units were formed with either I or III as starting materials when very high bromine concentrations were used (2.4 g I, 9 g Br_2, 4 ml $CHCl_3$). The bromine contents of these polymers usually contained between 1.6 and 1.85 Br/unit. Above this bromine level the products were partially insoluble. In an extreme case, the addition of I to liquid bromine produced an almost completely insoluble solid which corresponds to the homopolymer IV.

The nmr and ir spectra of the products from direct bromination showed that only ring bromination had occurred and that there was no methyl group bromination. The spectra were almost identical to the spectra of the corresponding homopolymers and copolymers from combinations of 2,6-dimethylphenol, 3,4-dibromo-2,6-dimethylphenol and 3,4,5-tribromo-2,6-dimethylphenol. A detailed description of the spectra of these brominated polymers is presented in the preceding paper.

The conversion of I to III and IV by the direct bromination of I resulted in a decrease in intrinsic viscosity of the polymer. Since the introduction of bromine increased the unit molecular weight of the polymer without affecting the length of the unit and since the intrinsic viscosity measurement was based on weight percent concentrations, an increase in repeating unit weight resulted in a proportional decrease in molar concentration of polymer. The actual decrease in viscosity was compared with the estimated decrease based on the change in repeating unit weight due to bromination (Table I). Bromination in dilute solution produced no abnormal variation in viscosity while bromination at higher bromine concentrations resulted in a decrease in viscosity which was as much as 30% greater than expected. Chain cleavage reactions involving hydrogen bromide may have contributed to the additional decrease.

Methyl brominated polymers (II) were prepared for comparison with the ring brominated materials. Under the conditions used (NBS, light, CCl_4 at reflux, 3 hrs) with 0.5 mole NBS/repeating unit, the product contained 0.41 Br/unit by bromine analysis. A four hour reaction with 1.0 NBS/unit introduced 0.88 Br/unit.

TABLE I

Decrease in Intrinsic Viscosity Upon Ring Bromination

Br/Unit	Bromine Concentration	Intrinsic Viscosity (dl/g)	
		Found	Calculated
0 (initial polymer)		0.50	
0.66	Dilute	0.41	0.39
1.1	Dilute	0.35	0.34
1.1	Concentrated	0.29	0.34
1.6	Concentrated	0.20	0.30
1.7	Concentrated	0.21	0.29

[1]H nmr spectra showed no ring bromination. The intrinsic viscosities had decreased from an initial 0.49 dl/g to 0.39 dl/g for the sample with 0.41 Br/unit and to 0.29 dl/g for 0.88 Br/unit. These decreases were greater than for the ring brominated polymers which had been prepared under mild conditions (Table I) and suggest the likelihood of a chain cleavage reaction occurring during the photo-catalyzed bromination.

The effects of introduction of bromine on the properties of the polymer are shown in Tables II and III. The glass transition temperature, Tg, was measured by thermal optical analysis,[8] TOA, and/or differential scanning calorimetry, DSC (Table II). The Tg was raised by introducing bromine onto the aromatic rings and lowered by introducing bromine onto the methyl groups. The values of Tg for polymer III (ca. 290°) were similar whether the polymer was prepared from bromination of I or from the polymerization of 3,4-dibromo-2,6-xylenol. The slightly higher value observed for polymer III from the bromo displacement reaction probably was due to the higher molecular weight. Further introduction of bromine onto the single remaining sites on the rings did not appear to change the value of Tg appreciably even when as much as 85% of the rings were dibromo units. Above the 1.85 Br/unit level no transitions were discernible by DSC. Since these polymers were insoluble, films could not be prepared for TOA measurements.

The effect of the presence of aryl bromo units on the Tg of the polyphenylene oxide was approximately the same for both the mono- and dibromo- moieties. Thus when two copolymers contained the same weight percentage of bromine but one contained mono-bromo units and the other contained dibromo units, the former (with twice as many bromo repeating units) had the higher Tg.

TABLE II

Glass Transition Temperatures Measured by Thermal Optical
Analysis[8] and Differential Scanning Calorimetry

Polymer Source[a]	% Br	Br/Unit	Tg DSC	Tg TOA
I	0	0	214	221
I + Br$_2$	30.1	0.65	250	238
	37.1	0.88		280
	41.6	1.06	285	
	53.1	1.69		290
	55.5	1.85		293
I + NBS	19.6	0.37	201	
	21.5	0.41	197	
	38.4	0.92	190	
DBX (homopolymer)	40.2	1.00	289	292
DBX + X	10.0	0.17	234	
TBX + X	5.4	0.08	222	
	9.3	0.16	223	221
	12.2	0.22	223	
	30.7	0.67	237	248
	32.4	0.70	242	

(a) Abbreviations: DBX = 3,4-dibromo-2,6-xylenol; TBX = 3,4,5-
   tribromo-2,6-xylenol; X = 2,6-xylenol. Polymers from DBX
   and TBX are described in the preceding paper.

The oxygen index[9] (Table III) was, in general, proportional to the bromine content of the polymer and appeared to be relatively unaffected by the structure of the polymer.

TABLE III

Oxygen Indices[9] of Bromo Polymers

% Br	Polymer Source	Oxygen Index
0	Polymer I	28
5	TBX + X	37
10	TBX + X	36
30	I + Br$_2$	42
40	I + Br$_2$	52
42	I + Br$_2$	55

Experimental

All viscosities were measured in chloroform at 25°C. Bromine contents were based on elemental analyses for C, H and Br and were corroborated by ^{1}H nmr. Tg values are averages for the second and third scans on a Perkin-Elmer DSC-2 differential scanning calorimeter (40°/min). In several cases, particularly when the DSC transitions were very weak, the Tg was measured by thermo-optical analysis (TOA).[8]

Bromination of I. Poly(2,6-dimethyl-1,4-phenylene oxide)[2-5] (2.4 g, 0.02 m repeating units; intrinsic viscosity 0.5 dl/g) was added over a 5 minute period to a solution of bromine (9 g, 0.056 m) in 4 ml chloroform, while the mixture was stirred vigorously. The temperature rose from 25° to 35° during the addition, then gradually dropped to 25°. After two hours, 50 ml chloroform was added and the solution was added dropwise to 500 ml methanol. The precipitated polymer was washed with methanol and dried. Weight: 4.7 g. The nmr spectrum was characteristic of a structure with 1.6 aryl Br/unit. The polymer could be case to form a flexible, clear film.

With less bromine (6 g) in the above procedure, the polymeric product contained 1.1 Br/unit. With a two-stage bromination (2.4 g polymer added to 4.5 g bromine in 4 ml chloroform over a 5 minute period followed by the addition of 4.5 g bromine), there was less loss of bromine due to vaporization and the polymeric products contained from 1.7 to 1.85 Br/unit.

Brominations of I in dilute solution (10%) were carried out at 10 to 25° in trichloroethylene. With 0.6 to 1.0 moles Br_2 per repeating unit, ring bromination was nearly quantitative. With $FeBr_3$ or $AlCl_3$ (5 wt % based on I) and temperatures ranging from 25° to 80° and 2.0 moles Br_2 per repeating unit, only up to 1.1 Br/unit was found.

Bromination of II. To a solution of III (2 g, 1 Br/unit) in 2 ml chloroform was added bromine (3 g, pure liquid) with stirring over a 5 minute period. After 2 hours, 20 ml chloroform was added, nitrogen was passed through the mixture to remove unreacted bromine and residual HBr. The solution was filtered to remove a tan solid, 0.75 g when dry, and then added dropwise to methanol. The precipitated polymer, when washed and dried, weighed 1.75 g, 1.7 Br/unit.

Addition of I to Pure Bromine. Poly(2,6-dimethyl-1,4-phenylene oxide) (1.5 g, intrinsic viscosity 0.49 dl/g) was slowly added to a flask containing 15 ml of bromine. The polymer dissolved immediately, HBr was vigorously evolved and the reaction mixture became viscous. The reaction mixture was stirred for 30 minutes and the excess bromine was evaporated with a nitrogen stream. The residue was suspended in 50 ml of benzene, filtered, thoroughly washed with methanol and dried under vacuum. The brominated product (3.2 g) was insoluble in acetone, benzene, acetonitrile, chlorobenzene, chloroform, hot DMF and hot DMSO.

Preparation of II. To a solution of poly(2,6-dimethyl-1,4-phenylene oxide-) (48 g, 0.40 m repeating units, intrinsic viscosity 0.49 dl/g) in 500 ml carbon tetrachloride at reflux was added N-bromosuccinimide (35.6 g, 0.20 m) over a ten minute period while the solution was irradiated with a 150 watt flood lamp at a distance of 10 cm. After three hours the mixture was filtered to remove crystals of succinimide. The filtrate was added to 1000 ml methanol which was being stirred vigorously in a blender. After filtering, the polymer was stirred in methanol, filtered and dried. Weight: 59.6 g, 0.41 Br/unit. Intrinsic viscosity: 0.39 dl/g. For a similar reaction with an irradiation time of one hour, the polymer contained 0.37 Br/unit.

With twice as much NBS (71.2 g) and a four hour reaction time, the product weighed 78 g and contained 0.88 Br/unit. Intrinsic viscosity: 0.29 dl/g. [1]H nmr ($CDCl_3$ vs. TMS): δ 1.88 (CH_3), 4.35 (CH_2Br), 6.48 and 6.67 (Ar H's).

Summary

Direct bromination of poly(2,6-dimethyl-1,4-phenylene oxide) (I) at high bromine concentrations introduced two bromine atoms onto the aryl rings of a majority of the repeating units while at lower concentrations mainly monobromo units were formed. No

bromination of the methyl groups was observed. Polymers with an
average of 1.8 bromine atoms per repeating unit or lower were
soluble in liquids such as chloroform and benzene. The homo-
polymer, poly(3,5-dibromo-2,6-dimethylphenylene-1,4-oxide), an
insoluble solid, was prepared by addition of I to liquid bromine.
Free radical bromination with N-bromosuccinimide (NBS) introduced
bromine onto the methyl groups exclusively. The intrinsic
viscosities of the polymers decreased upon both methyl and aryl
bromination. Chain cleavage during bromination did not occur
under mild ionic bromination conditions, but was detectable at
higher bromine concentrations and with NBS. Spectral, flam-
mability and thermal properties of the polymers from direct
bromination and the polymers from bromophenol polymerization
were similar.

Literature Cited

1. Staffin, G. C. and Price, C. C., J. Am. Chem. Soc. (1960),
    82, 3632.
2. Hay, A. S., Blanchard, H. S., Endres, G. F., and Eustance,
    J. W., J. Am. Chem. Soc. (1959), 81, 6335.
3. Hay, A. S., U.S. Patent 3,306,874 (February 28, 1967).
4. Hay, A. S., U.S. Patent 3,306,875 (February 28, 1967).
5. Hay, A. S., Adv. Polymer Sci. (1967), 4, 496.
6. Hall, W. L., personal communication.
7. Cabasso, I., Jagur-Grodzinski, J. and Vofsi, D., personal
    communication from Dr. Cabasso.
8. Kovacs, A. J. and Hobbs, S. Y., J. Applied Polymer Sci. (1972)
    16, 301.
9. Fenimore, C. P. and Martin, F. J., Mod. Plast. (1966), 44,
    141; ASTM D-2863.

Polyperfluoroalkylene Ethers as High-Temperature Sealants

R. W. ROSSER and J. A. PARKER
Ames Research Center, NASA, Moffett Field, Calif. 94035

R. J. DePASQUALE and E. C. STUMP JR.
PCR Inc., Gainesville, Fla. 32601

Although the objective of this paper is to honor Dr. Price for his contributions to polyether chemistry, our interests take a tangential course in that we deal with polyperfluoroalkylene ethers. After reviewing some of the literature to point out limitations in fluoroether synthesis, we discuss current work that is designed to alleviate deficiencies in obtaining high molecular weights and then give our projections on some of the challenges for future work in this area.
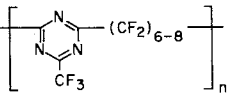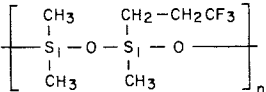
Figure 1 reflects Dr. Price's work on propylene oxide polymerization. You will recall that the base catalyzed, room temperature polymerization of propylene oxide shown in the first equation led to only low molecular weight dihydroxy terminated species (1). The second equation shows that a ferric chloride-propylene oxide complex (2) at 80° C yielded polymers of very high molecular weights. Both amorphous and crystalline polymers were isolated from this experiment. In other studies (3), Dr. Price utilized a variety of complexes such as aluminum isopropoxide-zinc chloride, which also produced high molecular weight polyethers. As a result of some of Dr. Price's important discoveries in high molecular weight polyethers, a whole spectrum of commercially significant materials has been developed. As an example, the chain extension of polyethers with diisocyanate has led to a host of polyurethane applications.

These achievements prompted us to consider the possibility of building long-chain perfluoroalkylene ethers that would yield a combination of properties for severe environmental applications that would not be possible with any other polymer system. Our goal, then, was to obtain high molecular weight elastomers that have good low-temperature mechanical properties, high thermal stability, and high chemical resistance, while maintaining sufficient flexibility over a wide temperature range. It should be mentioned here that, until now, perfluoroether synthesis has been limited by inadequate molecular weights. Perhaps more research in catalysis will overcome this problem and open another important door, as Dr. Price and others have done with the

propylene oxide polymerization.

Table 1 shows a list of fluoro-elastomers. The unusual resistance of highly fluorinated materials to high temperatures, oxidation, and a variety of organic solvents has been known since Plunkett's discovery of Teflon in 1938. Efforts since then have

TABLE 1.
FLUORINATED POLYMERS

FLUOROCARBON BACKBONE	CONTINUED SERVICE TEMPERATURE, °C	Tg,°C	CROSS-LINK
$+CH_2-CF_2-CF_2-\overset{\overset{CF_3}{\mid}}{CF}+_n$	200	-10	DIAMINE
$-(CF_2-CF_2)_n-$	270	127	—
$+\overset{\overset{OCF_3}{\mid}}{CF}-CF_2-CF_2-CF_2+_n$	250	-12	C_6F_5 OR CN
(triazine ring)—$(CF_2)_{6-8}$—, CF_3	260	-10	CN
ETHER BACKBONE			
$+\overset{\overset{CF_3}{\mid}}{N}-O-CF_2-CF_2+_n$	180	-50	PENDANT COOH
$\left[-\overset{\overset{CH_3}{\mid}}{\underset{\underset{CH_3}{\mid}}{Si}}-O-\overset{\overset{CH_2-CH_2CF_3}{\mid}}{\underset{\underset{CH_3}{\mid}}{Si}}-O-\right]_n$	220	-65	VINYL-SILANE

centered on the synthesis of partially and completely fluorinated polymers designed to retain the thermo-oxidative and chemical stability of polytetrafluoroethylene, while adding elastomeric character, low-temperature flexibility, processability, etc. Note that the high glass transistion temperature of Teflon is lowered by going to a Viton system (4). However, Viton's limitations of chemical and solvent resistance and service life at higher temperatures are a result of the presence of C-H bonds singularly and alternating -CF-CH- bonds cooperatively leading to hydrogen fluoride elimination. In the cases of Viton, fluorocarbon triazine (4), and a new duPont elastomer (4)

(ECD 006), the glass transition temperatures are near −10° C, with an increase in thermal stability of ECD 006 chiefly because of its perfluorocarbon backbone. Materials at the top of the table basically have a Teflon backbone, which appears to limit their usefulness for very low temperature applications.

It can be readily seen that only by incorporating ether backbones can one design materials that will maintain flexibility below −30° C. For example, the nitroso rubber has a T_g of −50° C, but its high-temperature stability is limited. The fluorosilicone comes nearest to meeting the requirements of a high-temperature sealant. It has excellent low- and high-temperature properties, but it tends to undergo reversion and has low tear strength. Because these materials still fall somewhat short of anticipated requirements, let us turn our attention to the perfluoroalkylene ethers and examine their potentialities.

Before we discuss our efforts to prepare long-chain fluoroethers that have difunctional termination, let us briefly consider some of the fluoroether work in the literature. Although much work has been done with tetrafluoroethylene oxide, it is quite unstable and therefore difficult to handle experimentally. Consequently, efforts have been centered on hexafluoropropylene oxide polymerization.

The mechanism of hexafluoropropylene oxide polymerization is shown in Figure 2. Hexafluoropropylene oxide is first prepared by treating hexafluoropropylene with hydrogen peroxide in the presence of base. Charcoal and fluoride ion have both been used as catalysts, but the fluoride ion is the preferred nucleophile. Ring-opening attack is apparently at the most hindered carbon atom, and the resulting n-perfluoropropoxide ion reacts with more hexafluoropropylene oxide to give equilibrium mixtures of alkoxide and acid fluoride (5). Anionic polymerization of hexafluoropropylene oxide is reported to behave like a "living polymer." Continued chain growth is achieved by using a solvating system of glymes for emulsion. Polymers up to 4000 molecular weight were synthesized, but, by using hexafluoropropylene diluent to minimize viscosity buildup, the molecular weight could be increased somewhat. The resulting polymers are liquids that yield only monofunctional materials that are incapable of either chain-extension or cross-linking. This is in marked contrast to the aliphatic series of polyethers, which have dihydroxy termination and thus can be further modified.

Figure 3 reflects stabilization or end-capping of the reactive acyl fluoride end group, which may be carried out in several ways as shown. Antimony fluoride adds a fluorine atom to the chain while eliminating carbon monoxide (5). Base treatment of the acyl fluoride gives rise to an additional hydrogen atom, and irradiation approximately doubles the molecular weight with the elimination of two gas species. This last mechanism is utilized in our work. The materials shown in
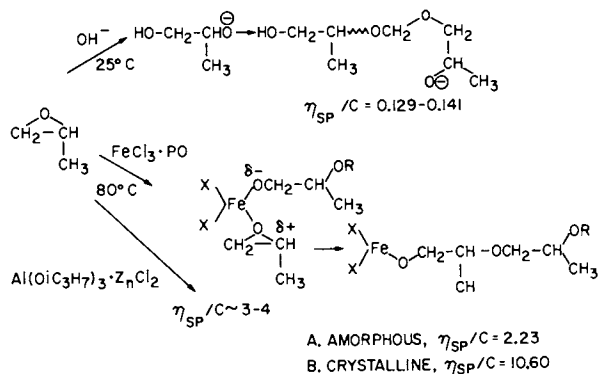
Figure 1.   Propylene oxide polymers
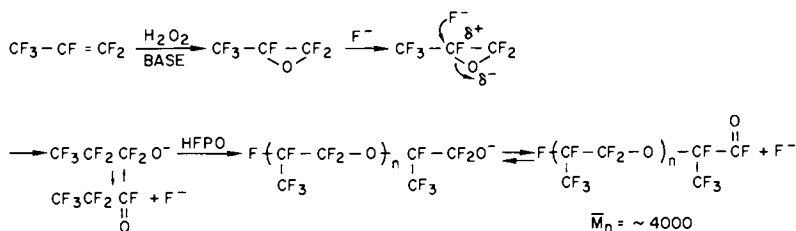
Figure 2.   Hexafluoropropylene oxide polymerization
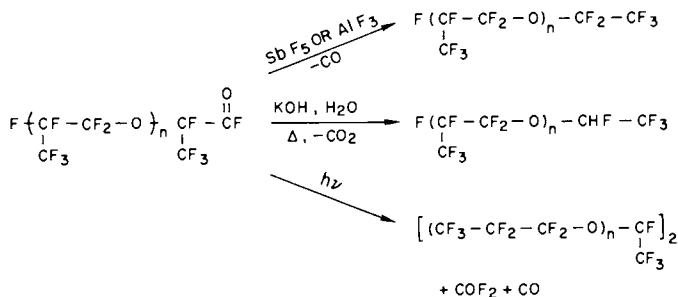
Figure 3.   Krytox fluids—end capping

Figure 3 have found commercial use as polymerization solvents
and inert hydraulic fluids. Note that these uses reflect the
molecular weight limitations which preclude their consideration
for high-temperature sealant applications.

Figure 4 depicts recent efforts by European workers (6). In
this case, hexafluoropropylene oxide is not isolated, but
hexafluoropropylene is irradiated with oxygen directly. In the
gas phase, hexafluoropropylene yields acyl fluorides of low
molecular weights, and in the liquid phase, it produces peroxides
of up to 7000 molecular weight, as shown in line 2. Even though
we have an initially high average molecular weight, the peroxides
are not stable. The chains are stabilized by heat or radiation,
which first destroys the peroxide, and then they are treated with
elemental fluorine to end-cap the polymer. Unfortunately, this
process effects a lowering of the molecular weight and results in
a polymer that is inadequate for a sealant application.

Figure 5 shows a series of reactions designed to yield
difunctional or multifunctional oligomers. The diiodide shown
on line 1 was irradiated to give an oil of low molecular weight.
Line 2 describes the irradiation of perfluoro-oxydipropionyl
fluoride (POPF) in FC-75 solution which gives a difunctional acid
fluoride terminated poly(perfluorotetramethylene oxide) (7) at
an $\bar{M}_n$ of 1000 or more. Investigators turned their attention
to end-group modification by forming dialcohols and dinitriles
from the low molecular weight polyfunctional acyl fluorides.
Elastomers were made through chain extension reactions of the
dialcohols with diisocyanates to give polyurethanes (7);
triazines were prepared by analogous routes. However, urethanes
have limited thermal stability, and, although triazines are
adequate thermally, the fluoroether chains between aromatic
groups are too short to allow a T_g that is adequate for low-
temperature compliance applications.

Figure 6 indicates attempts to build elastomeric properties
into a polymer by incorporating a fluoroether chain into a
polyimide system (8). Line 1 shows an aryl diamine polymer
intermediate prepared in a lengthy series of synthesis steps
from a perfluoroalkylene ether dicarboxylic acid. The polymer
is prepared from the reaction of the diamine with perfluoro-
hexamethylene-bis(phthalic anhydride). As expected, the polymer
had excellent thermal stability, but, again, its low-temperature
properties were deficient. For example, when X + y = 0, the
T_g was 130° C; when x + y = 1, the T_g was 110° C; and when
x + y = 3, the T_g was 80° C. With this system, we are unable
to achieve requisite chain flexibility because of a preponderance
of rigid aromatic groups that inhibit elasticity and cause a
raising of the T_g beyond practical limits for our intended
purpose as a sealant material. The fluoroether segment is
simply too short to yield a useful low-temperature elastomer.
If a high molecular weight difunctional fluoroether had been
synthesized by some unique catalyst system, many of the problems

$$CF_3 - CF = CF_2 + O_2 \xrightarrow[\text{GAS PHASE}]{h\nu} CF_3 - O(CF_2 - O)_n\, CF_2\, \overset{\overset{O}{\|}}{CF}$$

$$CF_3 - CF = CF_2 + O_2 \xrightarrow[\text{LIQUID PHASE}]{h\nu} -O(C_3F_6O)_n - (C_3F_6 - O - O)_m -$$

$$\overline{M}_n \text{ UP TO 7000}$$

$$\xrightarrow{\Delta \text{ OR } h\nu} -O(C_3F_6O)_n - \overset{\overset{O}{\|}}{CF} \xrightarrow[\text{STABILIZES}]{F_2} \left(O - \underset{\underset{CF_3}{|}}{CF} - CF_2\, OF \right) \longrightarrow \left(O - \underset{\underset{CF_3}{|}}{CF} \right)_n + CF_2O$$

$$\text{LUBRICANT}$$

Figure 4.   Fomblin fluids

$$I\, CF_2\, CF_2\, O - CF_2\, CF_2 - I \xrightarrow{h\nu} \left(CF_2\, CF_2\, CF_2\, CF_2\, O \right)_{\overline{n}}\ \text{OILS}$$

$$\overset{\overset{O}{\|}}{FC} - CF_2 - CF_2 - O - CF_2\, CF_2 - \overset{\overset{O}{\|}}{CF} \xrightarrow{h\nu} \overset{\overset{O}{\|}}{FC} \left(CF_2\, CF_2\, O - CF_2\, CF_2 \right)_n \overset{\overset{O}{\|}}{CF}\ \ \overline{M}_n > 1000$$

$$\xrightarrow{} \begin{array}{l} \text{DIACIDS} \\ \text{DIALCOHOLS} \xrightarrow{\text{NCO}} \text{POLYURETHANES} \\ \text{DINITRILES} \xrightarrow{\text{NH}_3} \text{POLYTRIAZINE} \end{array}$$

Figure 5.   Polyether through photolysis

$$H_2N - \cdots O \left[CF_2 - \underset{\underset{CF_3}{|}}{CF} - O \right]_x (CF_2)_5 \left[O - \underset{\underset{CF_3}{|}}{CF} - CF_2 \right]_y O - \cdots NH_2 \; + \; \text{(dianhydride)}$$

$$x + y = 3$$

$$\xrightarrow[-H_2O]{\Delta} \left(\cdots O \left[CF_2 - \underset{\underset{CF_3}{|}}{CF} - O \right]_x (CF_2)_5 \left[O - \underset{\underset{CF_3}{|}}{CF} - CF_2 \right]_y O - \cdots \text{(imide)}(CF_2)_6\text{(imide)} \right)_n$$

Figure 6.   Imide-linked perfluoroalkylene ether

in the above systems would be obviated. Other investigators have also prepared difunctional fluoroether nitriles, notably through the use of tetrafluoroethylene oxide (9).

We at NASA reopened the question of learning to chain extend these fluoroether systems in consort with scientists at PCR Inc. The objective was to prepare long-chain difunctional polyperfluoroethers and investigate chain extension mechanisms, as well as to convert these materials to stable cross-linked polymers for sealant applications. The nitrile, acetylene, and isocyanate groups were considered. Each of these is capable of both trimerization reactions *and* dipolar cycloadditions. From this base line, one could then evoke both chain extension and cross-linking with a variety of reaction schemes.

One can see in Figure 7 that we are still using a fluoride ion catalyst as in the original work on hexafluoropropylene oxide polymerization. Our procedure differs from the earlier work in that we emphasize the synthesis of difunctional materials. Reasonably high molecular weight diacid fluorides were prepared by the co-oligomerization of hexafluoroglutaryl fluoride and HFPO initiated by CsF in tetraglyme. The reaction consists of converting hexafluoroglutaryl fluoride to a perfluoroalkoxy anion, which then reacts with HFPO to afford the desired diacid fluorides. HFPO was gradually added and the progress of product appearance was monitored by GLC. The fluorocarbon layer was carefully distilled and samples of 60% $m + n = 5$ (7-EDAF) ether diacid fluoride and 30% $m + n = 6$ (8-EDAF) were obtained as well as various other fractions containing diacid fluoride mixtures. Photolytic dimerization of 7-EDAF with a 450 W Hanovia lamp for 650 hours at reflux gave an 89% conversion of starting material to 7-EDAF dimer, bp 224-235°C/1 mm. As the dimer formed in the vapor phase, it precipitated on the walls of the vessel.

In Figure 8, conversion of acyl fluorides to dinitriles where $m + n = 6$ (8-EDAF) and also the dimer of $m + n = 5$ (7-EDAF dimer) gave us two molecular weights for additional study. The conversion procedure calls for the use of ammonia in Freon 113 followed by distillation from P_2O_5. This presents the background for the work reported below. It was hypothesized that by using long-chain polyether dinitriles from triazine precursors, the resulting materials would be useful as sealants.

The 8-EDAF dinitrile and the 7-EDAF dimer dinitrile previously prepared were polymerized in separate experiments to three-dimensional matrixed polytriazines by treating them with catalytic amounts of ammonia at 225° C. These polymers were gel-like materials which maintained the shape of the tubes from which they were prepared. They possessed excellent thermal properties but were deficient in mechanical properties.

We then turned our attention to alternate chain extension and cross-linking reactions to overcome the obvious molecular weight deficiencies. The first series of reactions utilize unsaturated functionalities as extension points. Nitrile was

Figure 7.   Preparation of long-chain perfluoroether

Figure 8.   Cross-linked triazine

chosen as the principal dipolarophile to study, but any
unsaturated system such as acetylene might be utilized.
Difunctional nitriles were mixed with reactive dipolar,
difunctional nitrile oxide moieties, as shown on line 1 of
Figure 9. Thus, long-chain fluoroether dinitriles combine
conveniently with terephthalonitrile,N,N'-dioxide in a 1,3-dipolar
cycloaddition to yield poly (1,2,4-oxadiazolyl fluoroether), a
five-membered ring heterocycle-fluoroether system. Polymerization
was followed by disappearance of nitrile oxide (2300 cm^{-1}) and
nitrile (2220 cm^{-1}) infrared absorptions. New bands appeared
at 1560 and 915 cm^{-1}, presumably owing to the 1,2,4-oxadiazole
structure. That we have significantly increased the molecular
weight is demonstrated by the result that the 8-EDAF dinitrile/
TPNO reaction gave a light-yellow "snappy" rubber of considerable
strength and elasticity. It must be kept in mind that diacety-
lenes can also react with nitrile oxides to form isoxazoles.
On line 2, we have another 1,3-dipole, a nitrile imine, which
will react with nitriles to give poly 1,2,4-triazoles. Finally,
on line 3, we show a reaction scheme for synthesizing poly
(1,3,4-oxadiazolyl fluoroethers). These same pathways may be
used for achieving stable cross-links, as will be shown presently.

Let us briefly examine the fluoroether polymers which have
been synthesized. From Figure 10, it can be seen that both
structures are essentially long fluoroether chains separated
by thermally stable anchor points. These "hard domains" are
expected to improve high-temperature mechanical properties, as
well as provide cross-link sites and molecular weight control.
You will recall that our goal was to reduce the number of
branch points in the fluoroether system by more effective chain
extension of the original fluoroether. With the photolytic
dimerization, we have probably reached the upper molecular
weight limits with fluoride ion catalysis. However, we have
demonstrated that, by increasing the molecular weight of the
fluoroether backbone to 3000 through this awkward process, it
is possible to obtain a T_g (-50° C) consistent with the chain
extension that was required.

One of the possibilities for overcoming the disadvantages
of low molecular weights in current state-of-the-art perfluoro-
ether systems is to increase the weights by the use of poly-
functionality. Figure 11 shows perfluoro 1,5-hexadiene dioxide,
which is currently being copolymerized in the HFPO
co-oligomerization scheme. This, then, provides us with the
opportunity of securing high branch functionalities in linear
polyfluoroethers. Therefore, lower extents of reaction with
respect to the nitrile group may now become reasonable in
terms of achieving a well-vulcanized, effectively cross-linked
elastomer for a sealant application. In addition, we are
addressing ourselves to a similar mechanism through the cross-
linking agent (trifunctional nitrile) which contains a branch
point as well.

$$R_f = \text{PERFLUOROALKYLENE ETHER}$$

Figure 9.   Chain extension reactions

Figure 10.   Heterocyclic-perfluoroalkylene ether copolymers

1. INCORPORATE

INTO FLUOROETHER SYNTHESIS

2. INCORPORATE

INTO TRIMERIZATION OF FLUOROETHER
DINITRILE
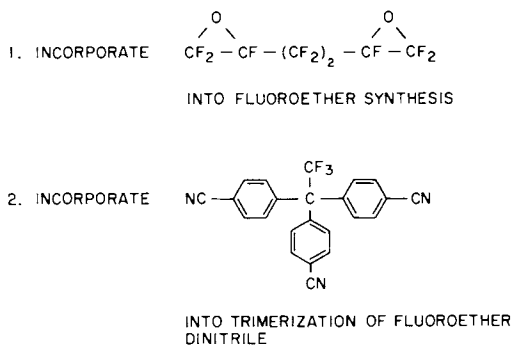
Figure 11.   Polyfunctionality

A totally different approach to enhancing the linearity
of the fluoroethers is based on the preparation of poly(imidoyl
amidine). In the first step of Figure 12, the dinitrile is
first converted to an amidine which is isolated and purified.
More dinitrile is then added to the amidine to give a *linear*
poly(imidoyl amidine). Ring closure to triazine can be
accomplished with an acid fluoride or an anhydride. For example,
a low-molecular weight, linear poly(imidoyl amidine) derived from
8-EDAF dinitrile was prepared and converted to the polytriazine
by $(CF_3CO)_2O$ treatment.

In preliminary experiments, the corresponding triazine was
prepared with pendant $-(CF_2)_3CN$ groups by partial treatment of
the poly(imidoyl amidine) with $(N\equiv CCF_2CF_2CF_2CO)_2O$. Mole-ratios
of 85:15 and 70:30 of $(CF_3CO)_2O$: $[NC(CF_2)_3CO]_2O$, respectively,
were used. Volatiles were removed, and the residues were
viscous liquids which contained both CN and triazine bands in
the infrared. It is significant that, in a straight trimerization
of perfluorosebacoylnitrile to triazine, a hard plastic with a
T_g of 110° C results. However, by evoking the stepwise linear
growth of poly(imidoyl amidine) a substantial lowering of the
T_g was reported.

Thus, we can take advantage of the chemistry learned in
chain extensions shown in the previous figures and introduce
pendant groups to cross-link with a 1,3-dipolar cycloaddition of
nitrile oxide to either nitrile or acetylene; this gives us a
low-temperature curing mechanism, as shown in Figure 13. One
can also visualize, although it is not shown, a trimerization
of the pendant nitrile by using a catalyst such as tetraphenyl
tin to give a cross-linked system where three chains are tied
together.

Another approach is shown in Figure 14. Here, we have an
aryl ether cross-link resulting from a p-fluoroaromatic pendant
group which undergoes facile nucleophilic substitution with the
dipotassium salt of hexafluoroacetone bisphenol. Of course,
n is much greater than m and can be controlled by altering
stoichiometry.

It has been documented (10) that polytriazines derived from
perfluoroaliphatic dinitriles are tough and, in some cases,
brittle. Thus, it is conceivable that, by mixing a fluoro-
aliphatic dinitrile with a long-chain fluoroether dinitrile and
subsequently polymerizing to a polytriazine, the resulting
material would display properties intermediate between the
polytriazines derived from homopolymerization of the nitriles.
This approach is currently under investigation. Various ratios
of 7-EDAF dimer dinitrile and perfluorosebaconitrile have been
polymerized with catalytic quantities of ammonia at 225° C.
Preliminary results are shown in Figure 15 which clearly
demonstrates the principle stated.

In summary, we believe the long-chain perfluoroether
polymers afford excellent opportunities for application in the
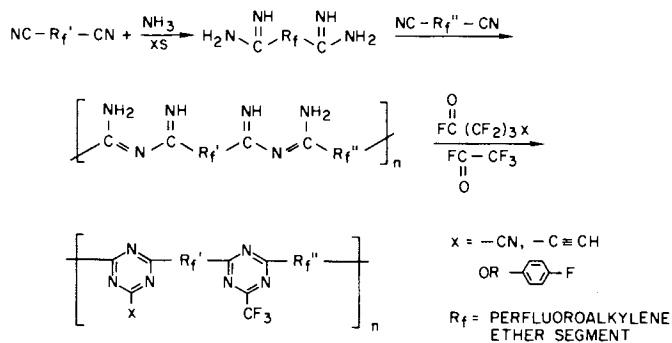
Figure 12. *Chain extension—polyimidoyl amidine*
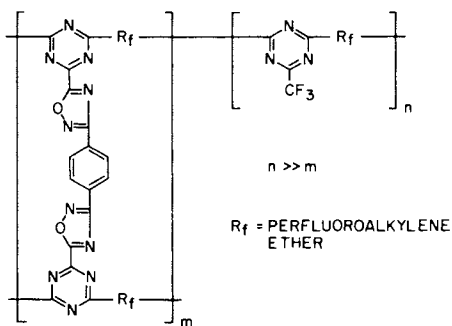
Figure 13. *Heterocyclic cross-link*
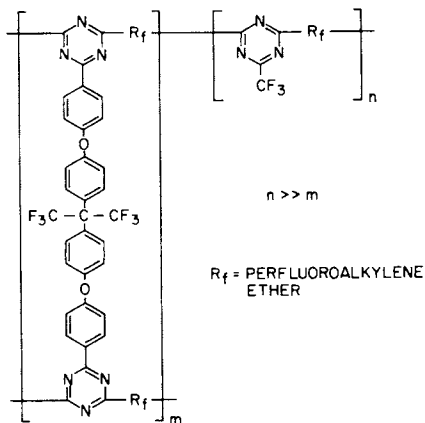
Figure 14. Aryl ether cross-link

RATIO $\dfrac{\text{FLUOROETHER CHAIN}}{\text{FLUOROALIPHATIC CHAIN}}$, BY WEIGHT
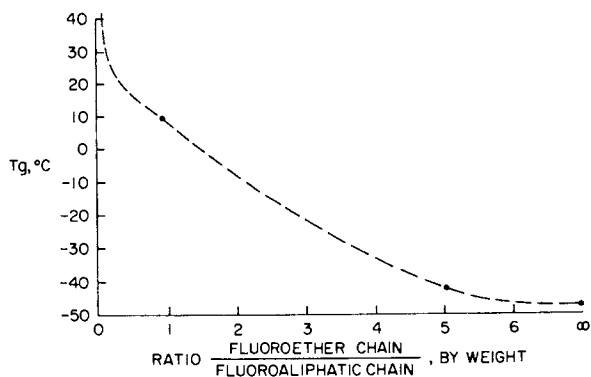
Figure 15. Effect of copolymer ratios on T_g

area of high-temperature elastomers and, in particular, as a
supersonic fuel tank sealant. The accomplishments to date
clearly point out the importance of obtaining both low- and
high-temperature properties that have sufficient molecular
weight to achieve mechanical form. The deficiencies in applying
a 1:1 application of Dr. Price's mechanism in achieving high
molecular weights have yet to be overcome in these systems.
However, we believe the increasing use of fluoroethers for
other applications will lead to simplification of the chemistry
that is involved in attaining high molecular weight polymers.

Literature Cited

1. St. Pierre, L. E. and Price, C. C.: *J. Amer. Chem. Soc.*
    (1956) <u>78</u>, *3432*.

2. Price, C. C. and Osgan, M.: *ibid* (1956) <u>78</u>, 4790.

3. Osgan, M. and Price, C. C.: *J. Polym. Sci.* (1959) <u>34</u>.
    p. 153, Nottingham Symposium.

4. Arnold, R. G., Barney, A. L. and Thompson, D. C.: *Rubber
    Chemistry and Technology* (July 1973) <u>46</u>, 646.

5. Eleuterio, H. S.: *J. Macromol Sci. - Chem.* (1972) <u>A6(6)</u>,
    1027.

6. Sianesi, D., Pasetti, A., Fontanelli, R., Bernardi, G. C.
    and Caporiccio, G.: *La Chimica E L'Industria* (1973)
    <u>55(2)</u>, 208.

7. Zollinger, J. L., Throckmorton, J. R., Ting, S. T. and
    Mitsch, R. A.: "Polymers in Space Research," C. L. Segal,
    ed., p. 409, Marcel Decker Inc., N. Y., 1970.

8. Webster, J. A., NASA Report, NAS-8-21401, (Monsanto Res.
    Corp., Ohio), Mar 1972.

9. Fritz, C. A. and Warnell, J. L.: U.S. Pat. 3,317,484
    (1967).

10. Dorfman, E., Emerson, W. E. and Lemper, A. I.: *Rubber
    Chemistry & Technology* (1966) <u>39</u>, 1175.

INDEX

201